Università degli Studi di Cagliari

DOTTORATO DI RICERCA IN

SCIENZE DELLA VITA, DELL'AMBIENTE E DEL FARMACO

Ciclo XXXI

Endocannabinoid System Modulation By Natural Products From Ancient Medicinal Plants

CHIM/08

Presentata da: Marta Collu

Coordinatore Dottorato: Prof. Enzo Tramontano

Tutor: Dr. Laura Casu

Esame finale anno accademico 2017 – 2018

Tesi discussa nella sessione d'esame Gennaio 2019

University of Cagliari, Italy

DOCTORAL SCHOOL IN LIFE, ENVIRONMENTAL AND DRUG SCIENCES

XXXI Cycle

Endocannabinoid System Modulation By Natural Products From Ancient Medicinal Plants

CHIM/08

Presented by: Marta Collu

Doctoral School Coordinator: Prof. Enzo Tramontano

Tutor: Dr. Laura Casu

Final dissertation academic year 2017 – 2018

Thesis publicly defended on January 31st 2019

A zio Antioco

This work was supported by the International PhD Program in Life, Environmental and Drug Science – cycle XXXI – of the University of Cagliari (Italy). The study was conducted at the Department of Life, Environmental and Drug Science of the University of Cagliari (Italy) and at the Institute of Biochemistry and Molecular Medicine of the University of Bern (Switzerland) under the supervision of:

Dr. Laura Casu, PhD
Assistant Professor in Pharmaceutical Chemistry
University of Cagliari - Faculty of Biology and Pharmacy
Department of Life and Environmental Sciences - Unit of Drug Sciences
Via Ospedale 72
09124 Cagliari, Italy
Phone: 0039 070 675 86 79/86 81
Email: lcasu@unica.it

Prof. Jürg Gertsch, MSc, Dr. sc. nat. ETH
Deputy Director Institute of Biochemistry and Molecular Medicine (IBMM)
National Centre of Competence in Research TransCure
Bühlstrasse 28, University of Bern
CH-3012 Bern, Switzerland
Phone: 0041 (0)31 631 41 24
Email: juerg.gertsch@ibmm.unibe.ch

This PhD project has been made possible thanks to the contribution of **Prof. Marco Leonti** (Department of Biomedical Science, University of Cagliari, Italy) and the "*MedPlant*" EU project entitled "*Herbal drugs in European tradition. A phylogenetic, chemosensory and neuropharmacological approach*".

AKNOWLEDGEMENTS

Behind a PhD there is the participation of several people who contribute, professionally and privately, to its achievement. For that, I would like to express my deepest thanks to those people who took part to this experience with me.

Prima di tutto il ringraziamento piu' grande va alla mia famiglia, per avermi sempre sostenuto e incoragiato nei miei percorsi accademici e non solo. Quello che sono oggi lo devo a voi, ai vostri sacrifici e al vostro amore. Anche con la distanza degli ultimi anni, non mi avete mai fatto sentire sola. Grazie a mia sorella Sara, per essere sempre un punto di riferimento per me e per i consigli utili alla realizzazione di questo lavoro. Purtroppo quest'anno chi ha sempre gioito per i miei traguardi non potrà essere presente per condividere anche questo. Il mio pensiero va a te zio Antioco, sono sicura che anche questa volta saresti felice per me.

I would like to specially thank my supervisor Laura Casu for giving me the opportunity of doing this PhD, for her advices and inputs and for the nice scientific and personal discussions we always had during these years. Also, I would like to thank Marco Leonti for his invaluable scientific support and help, especially in the final stage of my PhD.

During the first years of PhD spent at the University of Cagliari, some people left a special memory and I would like to thank them. In particular, I would like to mention Matthias Geck, Annesha Sil and Rina Štrajn for our amazing dinners, scientific discussions and for all the good times we spent together. Also, I would like to thank Benedetta Fois for the helpful scientific exchanges we had and wish her good luck for her PhD.

Then, I would like to thank Jürg Gertsch for giving me the opportunity of working in his team. During the time spent with the team, I have grown professionally and personally and I have received priceless advices that I will always keep in mind for my future.
In particular, a special thank goes to Sara Calarco, Margherita Lapillo and Sandra Glasmacher for their invaluable help, for the interesting exchange of ideas and for the nice time we spent together in the lab. I would like also to thank Andrea Chicca and Ines Reynoso for their useful advices.

Talking about Bern, I cannot forget to deeply thank my "Bernese family". Many thanks to Sara, Giuseppe, Margherita, Vanessa, Sandra and Silvia. With our movie evenings, dinners and all the nice moment we spent together you made me feel at home. In you, I found real friends who have contributed to make this experience amazing and unforgettable.

Then, I would like to thank my “Sardinian family”. Even if during the last years the different pathways we chose spread us around Italy and Europe, you never make me feel alone.
Especially, I would like to mention Francesca Magari. We chose different countries, but we decided to follow the same pathway and we shared the same contrasting feelings that characterize a PhD. Continue with the determination and the passion for science you always had and good luck for your PhD.

I would like to thank the researchers and technicians of the University of Cagliari and the University of Bern who helped and contributed to the realization of this project. In particular, a sincere thank you goes to Roberto Maxia for teaching me the nuclear magnetic resonance spectroscopy with patience, professionalism and always good humour, to Daniele Pellegata for helping in the mass spectrometry measurements and to Simona Distinto for the molecular docking studies.

And then, I would like to deeply thank José Cruz, not only for your constant presence, but also because in this work there is your contribution. Thanks for all your help, advices and encouragement, it meant a lot for me. You are a good scientist, I wish you a successful career and I hope to be with you to celebrate it. Muito obrigada!

ABSTRACT

Herbal drugs have been important for the treatment of multiple pathological conditions since ancient times. A multitude of historical texts document the importance of plant-based therapies, but the therapeutic effectiveness of many described applications remains questionable. Concomitantly, the pharmacological properties and the associated chemistry of many herbal drugs described in ancient texts remain poorly studied. The development of modern pharmacology and analytical tools in the past century has led to the discovery of a plethora of novel plant-derived compounds and propelled advancements in medicine and pharmacology. The identification of (-)-*trans*-Δ^9-tetrahydrocannabinol (THC) as the active principle of *Cannabis sativa* L., triggered research activities conductive to the elucidation of the endocannabinoid system (ECS). The ECS is a major modulatory system involved in a variety of physiological functions including the regulation of appetite, pain perception, memory, mood, and the modulation of inflammation and immune responses. A deregulation of the ECS is commonly associated with pathological conditions such as mood disorders, pain, inflammation, and neurodegenerative and immune diseases. Therefore, identifying target specific agonists, antagonists and inhibitors constitutes a promising strategy to tackle these conditions. The inhibition of fatty acid amide hydrolase (FAAH), the major enzyme involved in the termination of endocannabinoid signalling via the degradation of the endocannabinoid anandamide (AEA), represents a pharmacological strategy to treat conditions such as anxiety, depression or metabolic disorders. Besides the main cannabinoid type-1 (CB_1) receptors, activation of cannabinoid type-2 (CB_2) receptors represents as well an interesting pharmacological approach to treat diverse disorders such as diabetes, and neurodegenerative and immune diseases.

Therefore, the main aim of this doctoral thesis was to identify and characterize plant-derived compounds able to target and modulate specific components of the ECS. As a starting point to address this objective, a plant extract library of drug samples mainly associated with the herbal drugs described in Dioscorides' *De Materia Medica* (*DMM*; *ex* Matthioli, 1568) was built up. The extracts were tested for *in vitro* inhibition of FAAH and affinity towards CB_2 receptors. In addition, as an indication of non-specific cytotoxicity, their antiproliferative activity was evaluated. For the screened extracts, the possible relationship between investigated bioactivity and plant phylogeny was first questioned. From the results of the FAAH inhibition screening, it emerged that extracts with significant FAAH inhibitory activity are phylogenetically clustered, as they are associated preponderantly with herbal drugs derived from the Fabaceae family. Isoflavonoids and prenylated derivatives, secondary metabolites commonly produced in Fabaceae, were proposed as potential FAAH inhibitors. Among the isoflavonoids tested, the prenylated luteone and neobavaisoflavone proved to be highly potent, selective, competitive and reversible FAAH inhibitors at the nanomolar range. In addition, preliminary results from the screening of the extract library

towards CB_2 receptors suggested the identification of sesquiterpene coumarins as a new class of CB_2 receptor ligands at the low micromolar range.

In conclusion, in this thesis project we have identified two classes of natural products showing *in vitro* pharmacological interaction with the ECS. Moreover, the compounds may prove promising scaffolds for the development of new therapeutic agents with anti-inflammatory, anti-nociceptive, anxiolytic, anti-diabetic or immunomodulatory activities.

SINTESI

Fin dall'antichità le piante medicinali hanno avuto grande importanza nel trattamento di molteplici condizioni patologiche. L' importanza delle terapie a base di piante medcinali è documenta in molteplici testi storici, ma l'efficacia terapeutica di molte delle applicazioni descritte rimane discutibile. Allo stesso tempo, le proprietà farmacologiche e la caratterizzazione fitochimica di molte delle piante medicinali descritte in tali testi antichi rimangono poco studiate. Lo sviluppo della farmacologia moderna e di moderni strumenti analitici nel secolo scorso hanno portato alla scoperta di una moltitudine di nuovi composti di origine vegetale e hanno favorito il progresso in campo medico e farmacologico. L'identificazione del (-)-*trans*-Δ^9-tetraidrocannabinolo (THC) come principio attivo della *C. sativa* L., ha stimolato attività di ricerca che hanno portato alla delucidazione del Sistema Endocannabinoide (ECS). L'ECS è un importante sistema modulatorio coinvolto in una varietà di funzioni fisiologiche che comprendono regolazione dell'appetito, percezione del dolore, umore, memoria e regolazione di risposte infiammatorie e immunitarie. Una disregolazione dell'ECS è comunemente associata all'insorgenza di condizioni patologiche, quali disturbi dell'umore, dolore, infiammazione e malattie neurodegenerative e immunitarie. Pertanto, l'identificazione di agonisti, antagonisti e inibitori specifici per questo target costituisce una promettente strategia volta a contrastare queste condizioni. L'inibizione dell'enzima fatty acid amide hydrolase (FAAH), principale enzima coinvolto nella terminazione del segnale degli endocannabinoidi attraverso la degradazione dell'endocannabinoide anandamide (AEA), rappresenta una strategia farmacologica utile al trattamento di condizioni quali ansia, depressione o disturbi metabolici. Oltre al principale recettore cannabinoide di tipo 1 (CB_1), l'attivazione dei recettori cannabinoidi di tipo 2 (CB_2), rappresenta un interessante approccio farmacologico per il trattamento di diversi disturbi come diabete e malattie neurodegenerative e immunitarie.

Pertanto, lo scopo principale di questa tesi di dottorato è stato quello di caratterizzare composti di origine vegetale in grado di mirare e modulare componenti specifici dell'ECS. Per raggiungere questo obiettivo, come punto di partenza è stata realizzata una libreria di estratti principalmente associata alle piante medicinali descritte nel testo di Dioscoride *De Materia Medica* (*DMM*; ex Matthioli, 1568). Gli estratti sono stati testati per l'inibizione *in vitro* dell'enzima FAAH e per l'affinità *in vitro* verso i recettori CB_2. In aggiunta, è stata valutata anche la loro attività antiproliferativa, come indice di citotossicità non specifica. Per gli estratti sottoposti a screening, è stata analizzata prima di tutto la possibile relazione tra attività biologica investigata e la filogenia delle piante associate Dai risultati dello screening sull'inibizione della FAAH, si evince che estratti con significativa attività inibitoria sono filogeneticamente correlati, in quanto tale attività è associata prevalentemente a piante medicinali appartenenti alla famiglia delle Fabaceae. Isoflavonoidi e corrispondenti derivati prenilati, metaboliti secondari comunemente prodotti

nelle Fabaceae, sono stati proposti come potenziali FAAH inibitori. Tra gli isoflavonoidi testati, i prenilati luteone e neobavaisoflavone si sono rivelati potenti, selettivi, competitivi e reversibili FAAH inibitori, con concentrazioni nel range del nanomolare. Inoltre, i risultati preliminari dello screening degli estratti della libreria sui recettori CB_2 hanno suggerito l'identificazione di cumarine sesquiterpeniche come nuova classe di ligandi dei recettori CB_2 con un'affinità nel basso range micromolare.

In conclusione, in questo progetto di tesi sono state identificate due classi di composti naturali che mostrano un'interazione farmacologica con l'ECS *in vitro*. Tali composti possono rivelarsi promettenti scaffolds per lo sviluppo di nuovi agenti terapeutici con attività antinfiammatoria, antinocicettiva, ansiolitica, antidiabetica o immomodulatoria.

TABLE OF CONTENTS

LIST OF ABBREVIATIONS

2-AG	2-arachidonoylglycerol
2-OG	2-oleoylglycerol
5-HT3	Serotonin-type 3 receptors
AA	Arachidonic acid
ABHD12	α/β-hydrolase 12
ABHD4	α,β-hydrolase 4
ABHD6	α/β-hydrolase 6
AC	Adenylate cyclase
ACN	Acetonitrile
AEA	Arachidonoylethanolamine; anandamide
AM1241	2-iodo-5-nitrophenyl-[1-[(1-methylpiperidin-2-yl)methyl]indol-3-yl]methanone
AM251	1-(2,4-dichlorophenyl)-5-(4-iodophenyl)-4-methyl-*N*-(1-piperidyl)pyrazole-3-carboxamide
AM3506	5-(4-Hydroxyphenyl)pentanesulfonylfluoride
AM404	*N*-arachidonoylaminophenol
AM630	1-[2-(morpholin-4-yl)ethyl]-2-methyl-3-(4-methoxybenzoyl)-6-iodoindole
AT	*N*-acyl transferase
BBB	Brain-blood barrier
BCA	Bicinchoninic acid
BSA	Bovine serum albumin
cAMP	Cyclic adenosine monophosphate
CB_1	Cannabinoid (receptors) type-1
CB_2	Cannabinoid (receptors) type-2
CBR	Cannabinoid receptor
CHO-K_1	Chinese hamster ovary cells
CNS	Central nervous system

COX-2	Cyclooxygenase-2
CP55,940	3-(2-hydroxy-4-(1,1-dimethylheptyl)phenyl)-4-(3-hydroxypropyl) cyclohexanol
DAG	Diacylglycerol
DAGL	Diacylglycerol lipase
DCM	Dichloromethane
DMM	De Materia Medica
DMSO	Dimethylsulfoxide
ECS	Endocannabinoid system
ECs	Endocannabinoids
EDTA	Ethylenediaminetetracetic acid
EMT	Endocannabinoids membrane transporter
EtOAc	Ethyl acetate
EtOH	Ethanol
FA	Formic acid
FAAH	Fatty acid amide hydrolase
FAB	Fatty acid binding protein
FABP5	Fatty acid binding protein P5
FBS	Fetal bovine serum
GABA	γ-aminobutyric acid
GDE1	Glycorophosphodiesterase 1
GDP	Guanosine diphosphate
GPCR	G protein-coupled receptor
GTP	Guanosine-5'-tryphosphate
Hex	Hexane
Hsp70	Heat-shock protein 70
HU-210	1,1-dimethylheptyl-7-hydroxy-delta(6)-tetrahydrocannabinol
IC_{50}	Half maximal inhibitory concentration

IS	Internal Standard
JEA	Juniperonoylethanolamine
JuA	Juniperonic acid
JWH-015	2-methyl-1-propyl-1H-indol-3-yl)-1-naphthalenylmethanone
JZL184	4-nitrophenyl-4-[bis(1,3-benzodioxol-5-yl)-hydroxymethyl]piperidine-1-carboxylate
Ki	Inhibition constant (dissociation constant)
LC	Liquid chromatography
LEA	*N*-linoleoylethanolamine
LY-2183240	5-biphenyl-4-ylmethyl-tetrazole-1-carboxylic acid dimethylamide
MAGL	Monoacylglycerol lipase
MAP	Methoxy arachidonyl phosphonate
MeOH	Methanol
MS	Mass Spectrometry
MTT	3-(4,5-dimethylthiazol-2-yl)-2,5-diphenyltetrazolium bromide
NADA	*N*-arachidonoyl-dopamine
NAEs	*N*-acylethanolamines
NAPE	*N*-acyl-phosphatidylethanolamine
NAPE-PLD	NAPE Phospholipase D
NAraPE	*N*-arachidonoyl-phosphatidylethanolamine
NBP	NAE binding protein
NP-LC	Normal phase liquid chromatography
NP-VLC	Normal phase vacuum liquid chromatography
OEA	*N*-oleoylethanolamine
OL-135	7-phenyl-1-[5-(pyridin-2-yl)-1,3-oxazol-2-yl]heptan-1-one
OMDM-1	*N*-[1-(4-hydroxyphenyl)-2-hydroxyethyl]oleamide
OMDM-2	*N*-[1-hydroxy-3-(4-hydroxyphenyl)propan-2-yl]octadec-9-enamide
pAEA	Phospho-*N*-arachidonoylethanolamine

PAL2	Phenylalanine ammonia lyase 2
PBS	Phosphate-buffered saline
PE	phosphatidylethanolamine
PEA	*N*-palmitoylethanolamine
PEI	Polyethylenimine
PGH2	Prostaglandin H2
PKA	Protein kinase A
PLA2	Phospholipase A2
PLC	Phospholipase C
PPARs	Peroxisome proliferator-activated receptors
PTPN22	Protein tyrosine phosphatase N22
R-(+)-WIN 55,212-2	2,3-dihydro-5-methyl-3((4-morpholinyl)methyl) pyrrolo(1,2,3,-de)-1,4-benzoxazin-6-yl)-1-naphthalenyl methanone
RMSD	Root-mean-square-deviation
RP-SPE	Reverse Phase Solid phase extraction
SAR	Structure-activity relationship
SDS	Sodium dodecyl sulphate
SHIP1	Phosphatidylinositol-3,4,5-trisphosphate 5-phosphatase 1
SPE	Solid phase extraction
SR141716A	5-(4-chlorophenyl)-1-(2,4-dichlorophenyl)-4-methyl-*N*-(piperidin-1-yl)-1H-pyrazole-3-carboxamide; rimonabant
ST-4070	1-biphenyl-4-ylethenyl piperidine-1-carboxylate
TFA	Trifluoroacetic acid
THC	(-)-trans-Δ^9-tetrahydrocannabinol
THL	Tetrahydrolipstatin
TLC	Thin-layer chromatography
TRPV1	Transient receptor potential vanilloid 1
U937	Human monocytic leukaemia cells
UCM707	*N*-(3-furylmethyl)eicosa-5,8,11,14-eicosatetraenamide

URB597	3-(3-carbamoylphenyl)phenyl]*N*-cyclohexylcarbamate
VDM11	N-(4-Hydroxy-2-methylphenyl)-5,8,11,14-eicosatetraenamide
VLC	Vacuum liquid chromatography
WOBE437	*N*-(3,4-dimethoxyphenyl) ethyl amide
WWL70	4'-carbamoylbiphenyl-4-yl methyl(3-(pyridin-4-yl)benzyl)carbamate

LIST OF FIGURES

LIST OF TABLES

CHAPTER 1 – GENERAL INTRODUCTION

1.1 Medicinal plants and natural products: from historical uses to contemporary therapeutic applications

Plants have always been important in human life, as a source for food or in popular and traditional medicines. Biological diversity is associated with chemical diversity and represents a proven source for drug discovery. The discovery and the identification of bioactive plant-derived products have propelled advancements in medicine and pharmacology. Some of the most noteworthy examples are represented by the cardiotonic glycoside digoxin (*Digitalis lanata*), the anti-cancer drugs paclitaxel (*Taxus brevifolia*) and camptothecin (*Camptotheca acuminata*), the salicylic acid (*Salix* sp.), as well as the active principle of *Cannabis sativa* THC (Gaoni and Mechoulam, 1964, Hollman, 1996, Wall and Wani, 1996, Cragg, 1998), which disclosed a new, challenging and exciting area of pharmacological research. Declining physical activity, changing dietary habits and growing life expectancy in the developed world is associated with an epidemiological increase in age-related chronic life-style diseases such as cancers, type II diabetes, cardiovascular diseases and neurodegenerative disorders, as well as chronic inflammatory autoimmune diseases. This changing epidemiological pattern has led to a growing demand for new effective and safe drugs, able to tackle multifactorial diseases. This situation led to renewed interest in the pharmacological study of plants used as medicines as well as efforts in the isolation and characterisation of their bioactive secondary metabolites (Leonti and Verpoorte, 2017). A plethora of new natural products has been discovered and some of them revolutionized the treatment of life-threatening diseases (Cragg et al., 1997, Cragg and Newman, 2013, Newman and Cragg, 2016). An often-pursued strategy in natural products drug discovery is using a set of metabolites presenting the same pharmacophore in order to study structure-activity relationships. This approach constitutes an interesting starting point for applying structural modifications in order to increase or ameliorate the pharmacological or pharmacokinetic profile of the lead compounds. The best-known example is probably the semi-synthetic anti-inflammatory drug acetylsalicylic acid, commercialized for the first time as Aspirin® by the Bayer in 1899.

Despite the successful identification of several plant-derived drugs, the huge effort dedicated to the discovery of new natural products was not always successful. Due to the fact, that natural product research is time consuming and costly, the big pharma industry lost interest in natural products. Therefore, as an alternative strategy, in their drug-discovery programmes, the pharmaceutical industry focused their attention more on synthetic and combinatorial chemistry (Floyd et al., 1999, MacCoss and Baillie, 2004). Natural product research was continuously pursued, however, as a niche of academic research efforts. An

analysis conducted by Newman and co-workers clearly shows the fundamental role and importance of natural products for drug discovery at large (Newman and Cragg, 2016) (Figure 1).

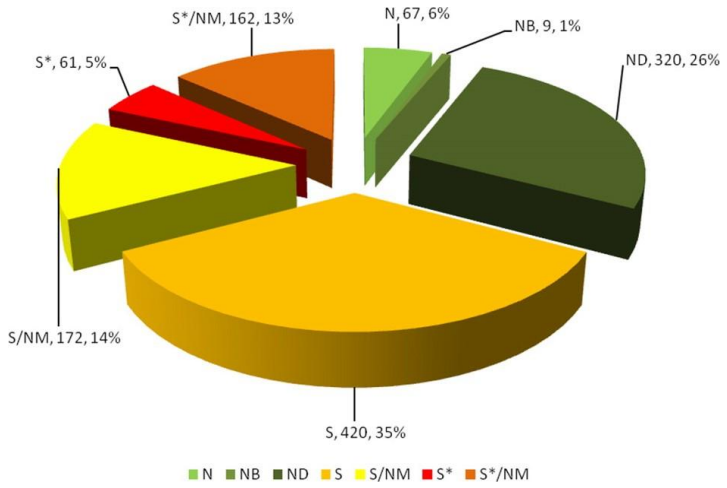

Figure 1. All small-molecule approved drugs 1981–2014s; *n*=1211. N=unaltered natural product, NB=botanical drug, ND=natural product derivative, S=synthetic drug, S/NM=synthetic drug mimic of natural product, S*=synthetic drug with a pharmacophore from natural product, S*/NM=synthetic drug with a pharmacophore mimic of a natural product. (From Newman and Cragg (2016)).

Therefore, the interest has again shifted back to pharmacological research with plant-derived compounds, but in a different and more rational approach than just the indiscriminate isolation and screening of natural products, moving the attention to smaller and focused libraries (Ramesha et al., 2011).

> "*The mass screening of plants in the search for new drugs is vastly expensive and inefficient. It would be cheaper and perhaps more productive to re-examine plant remedies described in ancient and medieval texts"* - Holland B.K. 1994

Societies have always given great importance to plants used as medicines and were interested in studying their effects on the human body and their possible uses in medicine and pharmacy. Ancient civilizations passed down their heritage of botanical and medical knowledge trough a multitude of manuscripts, which are considered to be essential sources for understanding ethnopharmacology and ethnomedicine, as well as for the development of the modern medicines and pharmacy (Leonti, 2011). The historical and ethnopharmacological analysis of therapeutic uses has been used as an approach for the identification of candidate herbal drugs for drug discovery (Buenz et al., 2004, Adams et al., 2007, Adams et al., 2009, Adams et al., 2011). Another interesting approach that has been followed is the validation of the link between traditional plant uses and contemporary therapeutic indications, trough diachronic and pharmacological studies (Giorgetti et al., 2007, Lardos et al., 2011, Adams et al., 2011, Valiakos et al., 2015).

Historical manuscripts such as the *Edwin Smith Papyrus* (Egypt, 17th century BCE), the *Corpus Hippocraticum* (Greece, 4th century BCE), the *De Materia Medica* (*DMM*) (Greece, 1st century CE) and the

Bower Manuscript (Kashmir, India, 6th century CE) represent some examples of texts containing the roots of the modern knowledge about herbal medicine and pharmacy. The *Edwin Smith Papyrus*, which takes its name from the American merchant Edwin Smith who bought it in 1862, is a text about medicinal practices in ancient Egypt, describing the treatment of injuries, fractures, wounds, dislocations and tumours. The *Bower Manuscript* is considered one of the oldest treatises of the traditional Indian medicine (Ayurveda). It was written in Sanskrit, probably by Buddhist monks, between the beginning and the middle of the 6th century CE (Sander, 1987, Hoernle, 2011, Leonti and Casu, 2014). The *Corpus Hippocraticum* is a comprehensive collection of medical and philosophical works associated to the Greek physician Hippocrates and his school, ranging from the 5th century BCE to the 2nd century CE. The Corpus contains lectures, case histories, researches, philosophical argumentations and hypotheses on various subjects in medicine. The *De Materia Medica* is a five-volume treatise on *materia medica* including herbs and herbal preparations written by the Greek physician Pedanios Dioscorides between 50 and 70 CE (Matthioli, 1568). The collection is considered one the most comprehensive guides on natural history and provided the basis for Western knowledge on *materia medica* for the following centuries.

The *DMM* consists of 800 monographies treating over 600 plant species, reporting plant names, botanical and pharmacological information, therapeutic uses, posology as well as formulations (Riddle, 1971, Riddle, 1980). Recently, a comprehensive quantitative survey of the herbal drugs described in the translation of the *DMM* by Pier Andrea Matthioli (Matthioli, 1568) (Figure 2) has been conducted by Staub and colleagues (2016).

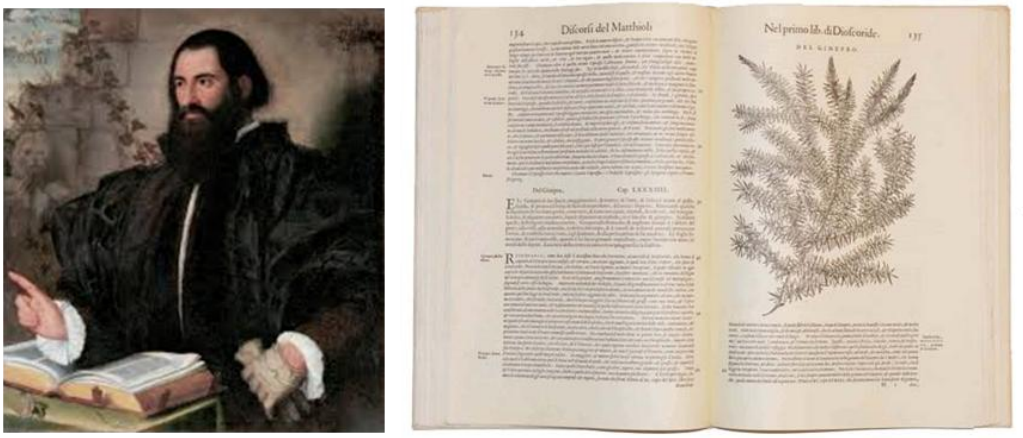

Figure 2. Pier Andrea Matthioli and the *De Materia Medica* translation. Facsimile version (1967-1970) of Pier Andrea Matthioli's Renaissance edition of Dioscorides' *De Materia Medica* from 1568.

In this quantitative analysis, 536 plant taxa associated with 5314 medical uses were recorded (Staub et al., 2016). The herbal drugs described by Dioscorides were obtained mostly from the Mediterranean area while a smaller number was imported from Africa, Near East and India. The work classified the therapeutic uses described in *DMM* into symptom and ailment defined categories. Categories

include for instance gastrointestinal uses (e.g. diarrhoea, abdominal pain and stomach ache, liver problems and nausea), dermatological uses (e.g. ulcers, wounds, tumours, skin inflammations and burns), gynecology (e.g. various uterine and vaginal conditions and control of the menstrual cycle) or neurology (e.g. epilepsy, fatigue, paralysis, melancholy and various pain conditions). As a result, the survey has identified several therapeutic, botanical and diachronic patterns. For instance, plants of the Apiaceae family were frequently cited for gastrointestinal uses and urology. Apiaceae exudates were often reported for neurology and musculoskeletal ailments, including species and taxa such as *Apium graveolens*, *Opopanax* sp., *Pimpinella anisum* and *Ferula* sp. Herbal drugs deriving from the Fabaceae family were the most frequently cited remedies for dermatology, including species such as *Pisum sativum*, *Lens culinaris*, *Trigonella foenum-graecum,* and *Glycyrrhiza* and *Lupinus* sp.

One of the objectives of this thesis project was to analyze and validate the traditional uses of the herbal drugs described in *DMM* with different approaches, including the molecular mechanisms of interaction with the ECS, main pharmacological target. Given the emerging role of the ECS and the broad spectrum of patho-physiological conditions for which it is relevant, the systematic screening aimed to identify active plant extracts and plant-derived compounds as starting points for drug discovery process. The extracts were analysed using phytochemical, pharmacological and phylogenetic approaches in order to describe and explain the observed biological activity. The phylogenetic approach is based on the assumption that plant metabolites are conserved during evolution and that related plant taxa have a higher probability to share specific metabolites and associated biological activities (Wink, 2003). This approach has been already used and tested previously for its possible application in drug discovery (Rønsted et al., 2008, Rønsted et al., 2012), in some cases successfully (Kingston, 2000, Ramesha et al., 2011).

Since this thesis project led to the identification of a number of medicinal plant extracts able to interact pharmacologically with the ECS, a brief introduction about the documented historical and traditional uses, the current therapeutic applications and the biologically active secondary metabolites of these herbal drugs is provided in the following section.

1.1.1 Fabaceae family

The Fabaceae (or Leguminosae) is a large family of flowering plants, including around 750 genera and more than 18’000 species with a worldwide distribution (Judd et al., 2002). Plants of this family are used as staple foods since millennia and their use is closely related to human evolution and agricultural practices. In fact, the family includes a number of important agricultural and food crops such as *Glycine max* (soybean), *Phaseolus* sp. (bean), *Pisum sativum* (pea), *Cicer arietinum* (chickpea), *Medicago sativa* (alfalfa), *Arachis hypogaea* (peanut), *Ceratonia siliqua* (carob)*, Lupinus* sp. (lupine) and *Glycyrrhiza* sp. (liquorice) (Graham and Vance, 2003). Figure 3 provides a representation of some of the cited plant species:

Figure 3. Plant species of the Fabaceae family. *Glycine max*, (B) *Lupinus angustifolius a*nd (C) *Glycyrrhiza glabra*.

Several studies reviewed the secondary metabolites present in Fabaceae (Southon, 1994, Wink, 2003, Wink and Mohamed, 2003, Wink, 2013). Since legumes can fix atmospheric nitrogen, nitrogen-containing secondary metabolites are widely produced. Among them, quinolizidine alkaloids, non-proteinous aminoacids and sulphur-containing compounds are typical classes of secondary metabolites of Fabaceae (Wink, 2003). The nitrogen-containing compounds often accumulate in seeds where they have a dual function: as defence compounds and as nitrogen storage compounds, which are later remobilized during germination and seedling development (Wink and Witte, 1984). Biologically active compounds such as flavonoids, terpenes and catechins are also widely distributed in species of this family, while isoflavonoids have a restricted distribution in the subfamily Faboideae and coumarins occur in only a few species, such as in *Psoralea* (Wink, 2013). Additionally, legumes such as lupine, fava bean, soybean and *Psoralea* sp. are an excellent dietary source of the anti-cancer, antioxidant and phytoestrogenic isoflavonoids genistein and daidzein (Kaufman et al., 1997).

Due to the presence of such a variety of bioactive secondary metabolites possessing a range of therapeutic and toxic properties, species of the Fabaceae family have a long tradition of use in herbal medicine. Of the various therapeutic uses of Fabaceae mentioned in *DMM* (treatment of ulcers, abscesses, animal bites, tumours and skin inflammation, as well as for gastrointestinal ailments and for gynecological problems) those applications related to women's ailments may be associated with the high content of phytoestrogenic compounds (Messina et al., 1994, Simons et al., 2011, Aisyah et al., 2016).

Among the Fabaceae, probably the most known for its traditional and historical uses is the liquorice (*Glycyrrhiza* sp.). The uses of liquorice are documented by ancient Greek and Egyptian societies as well as by Chinese and Ayurvedic medicine (Matthioli, 1568, Thyagarajan et al., 2002, Wujastyk, 2003, Fiore et al., 2005). *G. glabra* and *G. uralensis* were recommended for the treatments of wounds, skin lesions, ulcers, cough, respiratory problems, kidney pain, stomach inflammations, for diabetes and as diuretics (Matthioli, 1568, Dafni et al., 1984, Li et al., 2004, Fiore et al., 2005). Some of the traditional uses of liquorice find correspondence in the modern indications (Fiore et al., 2005, Hosseinzadeh and Nassiri-Asl, 2015). *Glycyrrhiza* extracts and derived secondary metabolites are used for their anti-microbial, anti-inflammatory and antioxidant activity (Hong et al., 2009, Kim et al., 2010, Kim et al., 2012, Wang et al., 2015), in the

treatment of respiratory and gastrointestinal problems (Nosalova et al., 2013, Asha et al., 2013, Jalilzadeh-Amin et al., 2015), skin diseases (Afnan et al., 2012) and diabetes and related disorders (Lee et al., 2010, Sen et al., 2011, Gaur et al., 2014). Effects on the central nervous system (CNS) are also reported (Dhingra et al., 2004, Cho et al., 2012, Mazzio et al., 2013).

All these pharmacological actions are mainly due to the presence of saponins, flavonoids, isoflavonoids and calchones. Notably, some of the mentioned therapeutic effects could be associated with an action mediated by the ECS, as will be discussed later.

1.1.2 *Ferula* species

Ferula is a genus of about 170 species of flowering plants of the Apiaceae family, native to the east Mediterranean region and central Asia. Species of this genus such as *F. gummosa*, and *F. persica* have been used in traditional medicine for the treatment of a wide range of ailments.

Ferula gummosa (Figure 4A), native to Iran, is known with the name *barijeh* and *galbanum oleo resin*, due to its milky white gum exudate produced by the roots (Mahboubi, 2016). In the Iranian traditional medicine, galbanum is used as an anti-spasmodic, expectorant, carminative, uterine tonic, memory enhancer and as anti-inflammatory agent (Zargari, 1989, Mahboubi, 2016). In the *DMM* galbanum finds applications against tooth pain, animal bites and respiratory problems, to induce delivery and menstruation and as anti-inflammatory (Matthioli, 1568). Galbanum can be also used as an antispasmodic agent for the treatment of diarrhoea (Sadraei et al., 2001) and as anti-inflammatory (Zarifkar et al., 2007). Some studies have reported cytotoxic and antiproliferative activity in cancer cell lines (Iranshahi et al., 2008, Iranshahi et al., 2010a) and some coumarins obtained from galbanum have been found to be acetylcholinesterase inhibitors, with possible applications in Alzheimer's disease (Adhami et al., 2014).

Ferula persica resin is known as *sagapenum* and the yellow translucent balsam obtained from the roots smells and resembles galbanum (Figure 4B). Similar to *F. gummosa*, also *F. persica* was prescribed by Dioscorides as an expectorant, anti-convulsant, against animal bites and for respiratory problems, to induce delivery and menstruation, as anti-inflammatory and for ophthalmic problems (Matthioli, 1568). The reported pharmacological properties of *F. persica* extracts and secondary metabolites include cytotoxic, antimicrobial, anti-inflammatory and anti-hypertensive effects (Esmaeili et al., 2012, Sattar and Iranshahi, 2017).

Figure 4. *Ferula gummosa* and *Ferula persica*. Detail of the plant and exudate obtained from the roots of *F. gummosa* (A) and *F. persica* (B).

The *Ferula* genus is particularly rich in terpenes/terpenoids, monoterpenes, sesquiterpenes, sesquiterpene coumarins and their glycosides (Abd El-Razek et al., 2001, Iranshahi et al., 2003a, Appendino et al., 2006, Iranshahi et al., 2010a, Nazari and Iranshahi, 2011, Jalali et al., 2011, Jalali et al., 2013). To a minor extent, sulphur-containing compounds can be found (Iranshahi et al., 2003b, Iranshahi et al., 2009b). Sesquiterpene coumarins are almost exclusively found in the genus *Ferula* and are responsible for a multitude of the reported biological activities (Nazari and Iranshahi, 2011).

1.1.3 *Tinospora cordifolia*

Tinospora cordifolia (Menispermaceae) is a large glabrous climbing shrub occurring in Jammu, Kashmir state to the south of India (Figure 5). Commonly named *gudûchi,* which in Sanskrit means “one which protects the entire body” or *amritâ* which means “immortality”, attributed to its ability to give vitality and longevity, is a widely used plant in the Ayurvedic system of medicine and its uses are also documented in the *Bower Manuscript* (AYUSH, 2001, Williamson, 2002, Hoernle, 2011).

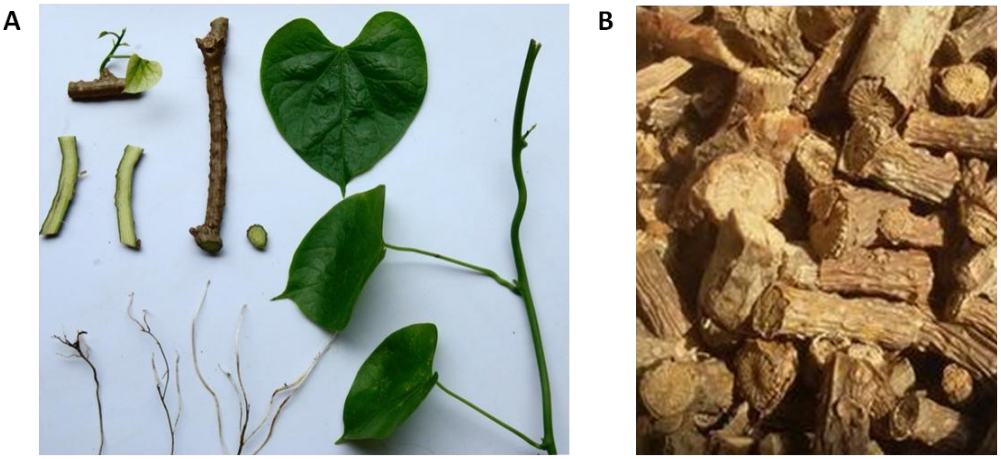

Figure 5. *Tinospora cordifolia* (*gudûchi*). Plant parts (A) and detail of the stems (B).

Traditionally, gudûchi was used in several herbal preparations to treat leprosy, asthma, fever, debility, skin infections, diabetes, diarrhoea and dysentery, to improve the immune system and body resistance against infections. *T. cordifolia* is mentioned in the Bower Manuscript as a component of two Amritâ formulations (Amritâ-Prâsa clarified butter and Amritâ oil), which are proposed to be related to the ancient gold-coloured exhilarating preparation called Soma. It has been proposed that protoberberine alkaloids of *T. cordifolia* contributed to the psychoactive metabolites responsible for the psychedelic and euphoric effects associated with its consumption (Leonti and Casu, 2014).

A variety of active components derived from the plant has been isolated from different plant parts, including stems, roots and aerial parts. Alkaloids such as berberine, palmatine, jatrorrhizine and magnoflorine have been isolated from roots and stems (Bisset and Nwaiwu, 1983, Sarma et al., 1995, Srinivasan et al., 2008, Kakkar et al., 2013). *T. cordifolia* is also rich in glycosides, such as cordifolioside A and B, tinosporaside, cordioside, cordifoliside A, B and C, palmatoside C and F (Khan et al., 1989, Gangan et al., 1994, Wazir et al., 1995, Maurya et al., 1996, Gangan et al., 1996). Terpenes include clerodane derivatives such as amritoside A, B, C and D and the sesquiterpenes tinocordifolioside and tinocordifolin (Maurya et al., 1997, Maurya and Handa, 1997, Maurya et al., 2004). Phenolic compounds are also present, such as syringing and tinoscorside D (Van Kiem et al., 2010). Steroids include β-sitosterol and γ-sitosterol (Singh et al., 2003, Upadhyay et al., 2010).

Several traditional uses of *T. cordifolia* have been validated through scientific studies and adequately reviewed (Upadhyay et al., 2010, Saha and Ghosh, 2012). Alone or in combination with other medicinal plants, *T. cordifolia* has been shown to enhance cognition, memory and concentration (Agarwal et al., 2002, Bairy et al., 2004, Mutalik and Mutalik, 2011), to exert anti-inflammatory and anti-rheumatic activity (Abiramasundari et al., 2012, Patgiri et al., 2014) as well as beneficial effects in case of cough and allergic rhinitis (Badar et al., 2005). Other noteworthy therapeutic effects include gastrointestinal and anti-ulcer activities in rat models (Bafna and Balaraman, 2005), anti-hyperglycemic activity and beneficial effects

in diabetic conditions (Gupta et al., 1967, Wadood et al., 1992, Stanely et al., 2000, Patel and Mishra, 2011). Moreover, immunomodulatory properties have been discussed (Maurya et al., 1996, Kapil and Sharma, 1997, Upadhyay et al., 2011, Sharma et al., 2012).

As documented in ancient manuscripts and shown in a multitude of studies, medicinal plants are able to exert a myriad of pharmacologic and therapeutic effects. The secondary metabolites directly responsible for such activities were in some cases identified and their mechanism of action elucidated. In other cases, the origin of their effects remains unknown. Some of the proposed pharmaco-therapeutic properties might be overhauled and revised considering the relevance and involvement of the ECS. The patho-physiological role and therapeutic potential of the ECS will be discussed in the following paragraphs.

1.2 The endocannabinoid system

The ECS is a lipid signalling network mainly constituted by two endogenous G-protein-coupled receptors (GPCR) namely CB_1 and CB_2 receptors, their main endogenous agonists AEA and 2-arachidonoylglycerol (2-AG) and the enzymatic machinery for their biosynthesis and degradation.

Although the early stage of the research on the ECS started in the twentieth century with the isolation and identification of some phytocannabinoids, the psychotropic effects of *Cannabis* species have been known for millennia, described as a state of relaxation, euphoria, and excitation and in some cases anxiety and paranoia (Hollister, 1986, Ameri, 1999, Mechoulam et al., 2014). *Cannabis* has been used across many cultures as a recreational drug and it was often associated to religious rituals and medicinal practices. In the traditional Chinese medicine, it was prescribed, together with other medicinal plants, for the treatment of various ailments. Roman and Greek societies described medical uses of *Cannabis*. In ancient India, it was a major component in religious and medicinal practices (Russo, 2007, Mechoulam et al., 2014). In 19th century, medical interest in the use of *Cannabis* began to grow in the West. The Irish physician William Brooke O'Shaughnessy can be considered the first who introduced the therapeutic use of *Cannabis* to Western medicine. He learnt from Indian natives the practices for the medicinal use of *Cannabis* and he tested *Cannabis*-based preparations first on animals and then on patients as sleeping aid, analgesic and anticonvulsant, and to treat disorders such as melancholia and migraines (O'Shaugnessy, 1841).

A growing interest on phytocannabinoids started with the isolation and identification of some components of *Cannabis* species in the 1940s. The first cannabinoid to be identified was the non-psychotropic component Cannabidiol, in 1940 (Jacob and Todd, 1940). Later on, the THC, the main component of *Cannabis* with psychotropic effects was isolated and identified (Gaoni and Mechoulam, 1964). At that time, its mechanism of action was still unknown and only more than twenty years after its characterization, its binding proteins were identified and cloned, namely CB_1 and CB_2 receptors (Matsuda et

al., 1990, Munro et al., 1993). After the discovery of a specific receptor for THC, its endogenous ligands, AEA and 2-AG, were isolated and identified (Devane et al., 1992, Mechoulam et al., 1995), opening the interest for a new area in the pharmacological research field.

Nowadays, it is known that the ECS is widespread in mammalian tissues and cells, in the central and peripheral nervous system, immune cells, bones, spleen, liver and gastrointestinal system. Even plant tissues possess an endocannabinoid signalling network very similar to the one present in mammals, suggesting a well conserved system in eukaryotic cells during evolution (Kim et al., 2013, Shrestha et al., 2006). In plants, it is responsible for functions such as regulation of seedlings grow and activation of defence responses in presence of elicitators. In mammals, it is involved in a variety of physiological processes including appetite, pain sensation, mood, memory, homeostatic regulation and modulation of neurotransmitter release, becoming a promising target for the development of novel therapeutic agents (Piomelli et al., 2000, Di Marzo and Petrosino, 2007, Di Marzo, 2009). The psychotropic effects of THC have limited its therapeutic use but several synthetic as well as phytocannabinoids beyond THC have shown promising therapeutic applications (Piomelli et al., 2000, Makriyannis et al., 2005, Sharma et al., 2015, Russo, 2016, Brindisi et al., 2018).

Since the present project was focused on the assessment of global medicinal plant libraries and potentially on the discovery of plant-derived molecules able to target the ECS, in the following paragraphs, the ECS components, the patho-physiological role and the therapeutic approaches will be discussed with particular emphasis to the modulation of the AEA signalling (hydrolysis and cellular uptake) and of the CB_2 receptors.

1.2.1 Cannabinoid receptors: distribution, mechanism of action and ligands

The THC binding site was identified for the first time in rat brain in 1988. Binding studies using the synthetic ligand [^{3}H]-CP55,940 revealed a very high affinity of the compound for the receptors (K_d=133 pM) (Devane et al., 1988). The binding was reversible and displaced by other cannabinoids such as THC and cannabidiol, providing a proof for the existence of the supposed receptor. In 1990 and 1993, CB_1 and CB_2 receptors, respectively were cloned (Matsuda et al., 1990, Munro et al., 1993). CB_1 and CB_2 receptors are 7 transmembrane GPCRs associated with proteins of the $G_{i/o}$ family, that upon activation, exert an inhibitory effect on the activity of adenylate cyclase (AC) (Howlett et al., 1988). CB_1 receptor mediates an inhibition of Q-type calcium channels and an activation of inward rectifying potassium channels. Except for the inability of CB_2 receptors to inhibit those ion channels, the CB_1 and CB_2 receptors display similar pharmacological and biochemical properties (Felder et al., 1995).

CB_1 receptors are abundantly expressed in the CNS. They are particularly highly expressed in cerebral cortex, hippocampus, basal ganglia, and cerebellum, in hypothalamus and spinal cord albeit to a

lesser extent (Matsuda et al., 1993, Howlett et al., 2002). More recently, they have been found in intracellular compartments such as mitochondria (Benard et al., 2012, Hebert-Chatelain et al., 2016). Despite being initially characterized in the CNS, CB_1 receptors were later found to be localized also peripherally in the gastrointestinal tract, in adipocytes, in the liver and in the kidneys (Pertwee et al., 1996, Pagotto et al., 2006, Tam et al., 2018). CB_1 receptors are also present in immune cells (Daaka et al., 1996, Sinha et al., 1998, Kaplan, 2013, Chiurchiu et al., 2016, Kleyer et al., 2012) .

CB_2 receptors are expressed mainly in immune cells, where they are responsible for a variety of modulatory functions, including immune suppression, induction of apoptosis and cell migration (Herring et al., 1998, Miller and Stella, 2008). They also have been found in the spleen, in the gastrointestinal system, in the CNS and in particular in microglia cells and more recently in pyramidal neurons in the hippocampus (Munro et al., 1993, Galiegue et al., 1995, Izzo, 2004, Stempel et al., 2016).

Tissues CB receptor expression and endocannabinoid levels change following physiological and pathological stimuli. In the brain at the synaptic level, endocannabinoids are produced “on demand” and they are released immediately after their production. The biosynthesis can be triggered by increased intracellular calcium following post-synaptic cell depolarization in response from presynaptic activity or mobilization of intracellular calcium (Di Marzo et al., 1994, Di Marzo and Petrosino, 2007). Through this mechanism, by acting on CB_1 receptors in presynaptic terminals, endocannabinoids mediate a retrograde modulatory action. As represented in Figure 6, the depolarization of the postsynaptic neuron following the binding of the neurotransmitter glutamate to its ionotropic and metabotropic receptors, triggers the biosynthesis and the release of endocannabinoids, which by diffusion or via a putative membrane transporter (ETM), are released in the synapse. After binding to cannabinoid receptors, $G_{i/o}$ protein activation will exert an inhibitory effect on AC cascade and a reduction of intracellular levels of Ca^{2+}. Inhibition of AC leads to a decreasing in the production of cyclic adenosine monophosphate (cAMP), which causes a reduction of the cAMP-dependent protein kinase A (PKA) activity and consequently dephosphorylation of the potassium channels. Increased K^+ efflux and reduced Ca^{2+} intracellular levels give cellular hyperpolarisation of the presynaptic terminal and thus reduce the neurotransmitter release.

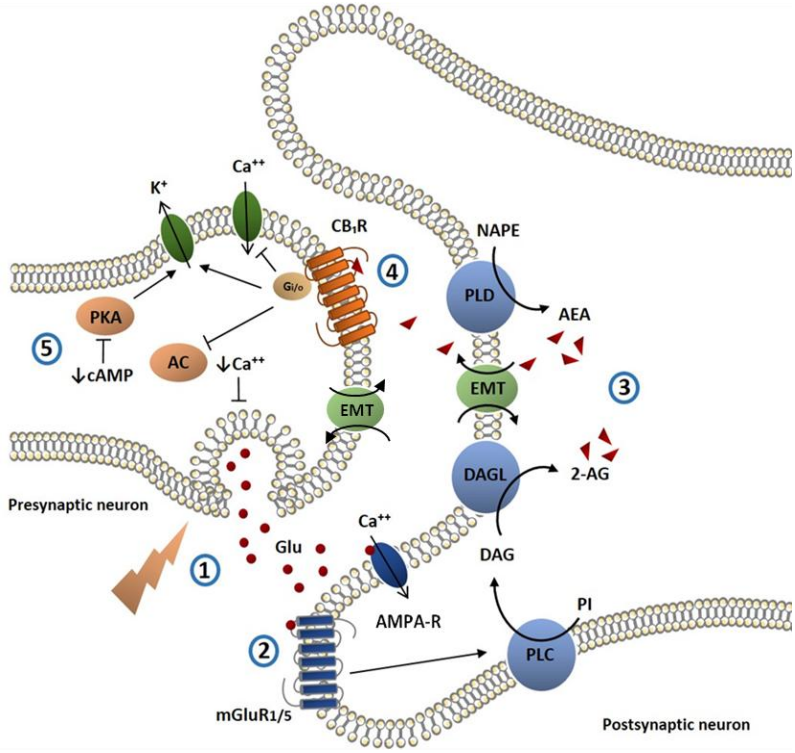

Figure 6. Endocannabinoids retrograde signalling in brain. A stimulus in the presynaptic neuron (1) leads to the release of neurotransmitters into the synapse (in this case a glutamatergic synapse is represented). The activation of the receptors in the postsynaptic neuron (2) triggers the biosynthesis of the endocannabinoids (AEA and/or 2-AG) (3), which are released in the synapse. The binding of the endocannabinoids to the CB receptors (4) leads to the activation of $G_{i/o}$ proteins, which determine an inhibition of the AC cascade (5). The resulting effect in the presynaptic neuron is hyperpolarisation and inhibition of neurotransmitter release. (Readapted from Nicolussi & Gertsch (2015)).

The resulting effect of the activation of CB receptors in the presynaptic neuron is a cellular inhibition. This retrograde activity has been shown to have neuroprotective effects, by preventing for instance cytotoxic effects of glutamate excitation in hippocampal neurons (Marsicano et al., 2003).

The two major endogenous ligands for cannabinoid receptors, the arachidonate-based lipids AEA and 2-AG (Figure 7), were discovered and identified only about forty years after the structural elucidation of THC (Devane et al., 1992, Mechoulam et al., 1995). AEA has high affinity for CB_1 receptors and is a partial agonist of CB_2 receptors, while 2-AG is a full agonist of both receptors even if with a lower affinity than those of AEA (Mechoulam et al., 1995).

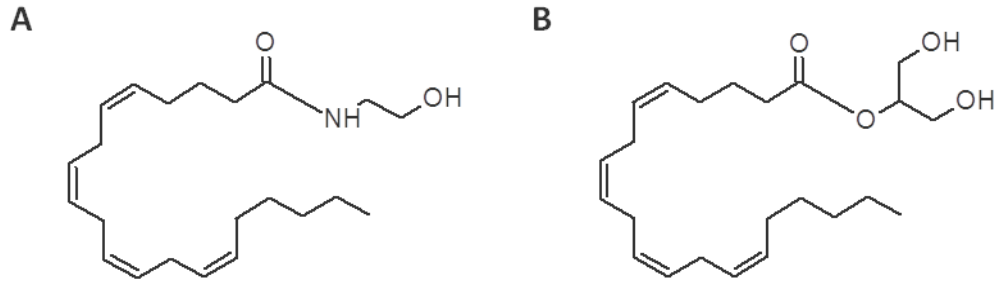

Figure 7. Major endocannabinoids AEA (A) and 2-AG (B).

Despite AEA and 2-AG, other natural and synthetic molecules act on CB receptors as agonists or antagonists/inverse agonists (Pertwee, 2005, Pertwee, 2008, Pertwee et al., 2010). The structure of some of them is represented in Figure 8. The "classical" CB_1/CB_2 agonists are dibenzopyran derivatives, either cannabis-derived (THC, Cannabidiol) or synthetic analogues, while "non-classical" agonists have different chemical structures. Some are closely related to the classical ones, i.e. CP55,940 and HU-210, which are bi or tricyclic analogues of THC. Others have a completely different structure, such as *R*-(+)-WIN55,212. Also the ligands HU-210, CP55,940 and *R*-(+)-WIN55,212 bind to both CB_1 and CB_2 receptors with approximately the same affinity (Felder et al., 1995). Despite synthetic ligands, also plant-derived compounds are CB receptors ligands. Natural CB_1 receptor ligands include falcarinol (*Daucus carota*), which is a covalent inverse agonist (Leonti et al., 2010), yangonin (*Piper methysticum*) (Ligresti et al., 2012), and salvinorin A (*Salvia divinorum*), which was shown to interact with the CB_1/*κ*-opioid receptor dimer (Fichna et al., 2012).

Because of the psychotropic effects mediated by CB_1 receptors activation, some CB_1 receptor ligands have limited uses. These side effects usually are not observed in the case of CB_2 receptor activation, which may represent an advantage in the development of therapeutic agents. For instance, the aminoalkylindole AM1241, which is a selective CB_2 receptor agonist, has shown therapeutic effects in neuropathic pain without the side effects typical of the CB_1 receptors activation (Ibrahim et al., 2003). Selective CB_2 receptor agonists have been also investigated for their benefits in arthritis and in obesity (Fukuda et al., 2014, Verty et al., 2015). Natural compounds as well display high affinity for CB_2 receptors and exert therapeutic properties deriving from their activation. The volatile sesquiterpene β-caryophyllene binds to CB_2 receptors with high affinity (K_i=155 nM in HEK293 cells) and exerts analgesic effects in mouse models of inflammation and neuropathic pain (Gertsch et al., 2008, Klauke et al., 2014). Some *N*-alkylamides from *Echinacea* preparations acts as full CB_2 receptor agonists in the nanomolar range and mediate the immunomodulatory effects of these medicinal plants (Raduner et al., 2006).

Although the enhancement of the endocannabinoid signalling mediates several therapeutic effects, its excessive activation can contribute to the progress of disorders and pathologic conditions as well. For instance, the activation of CB_1 receptors leads to increased appetite, decreased intestinal peristalsis, but an excessive activation can lead to obesity. Therefore, antagonism at these receptors can inverse these effects. The selective CB_1 antagonist SR141716A (rimonabant) was the first approved anti-obesity drug,

which binds with high affinity to CB_1 receptors and prevents or reverses the effect induced by agonists. The synthetic compound AM251 also displays higher affinity for CB_1 than CB_2 receptors and it showed antidepressant-like and anorectic effects in mice (Verty et al., 2015). Less attention has been dedicated to CB_2 antagonists/inverse agonists compared to the agonists. However, some CB_2 receptors antagonists may have therapeutic applications. For instance, AM630 has been shown to increase human osteoclast formations, necessary for regeneration and modelling of bone tissues, where a decreased CB_2 activation/expression is observed (Rossi et al., 2009, Whyte et al., 2012).

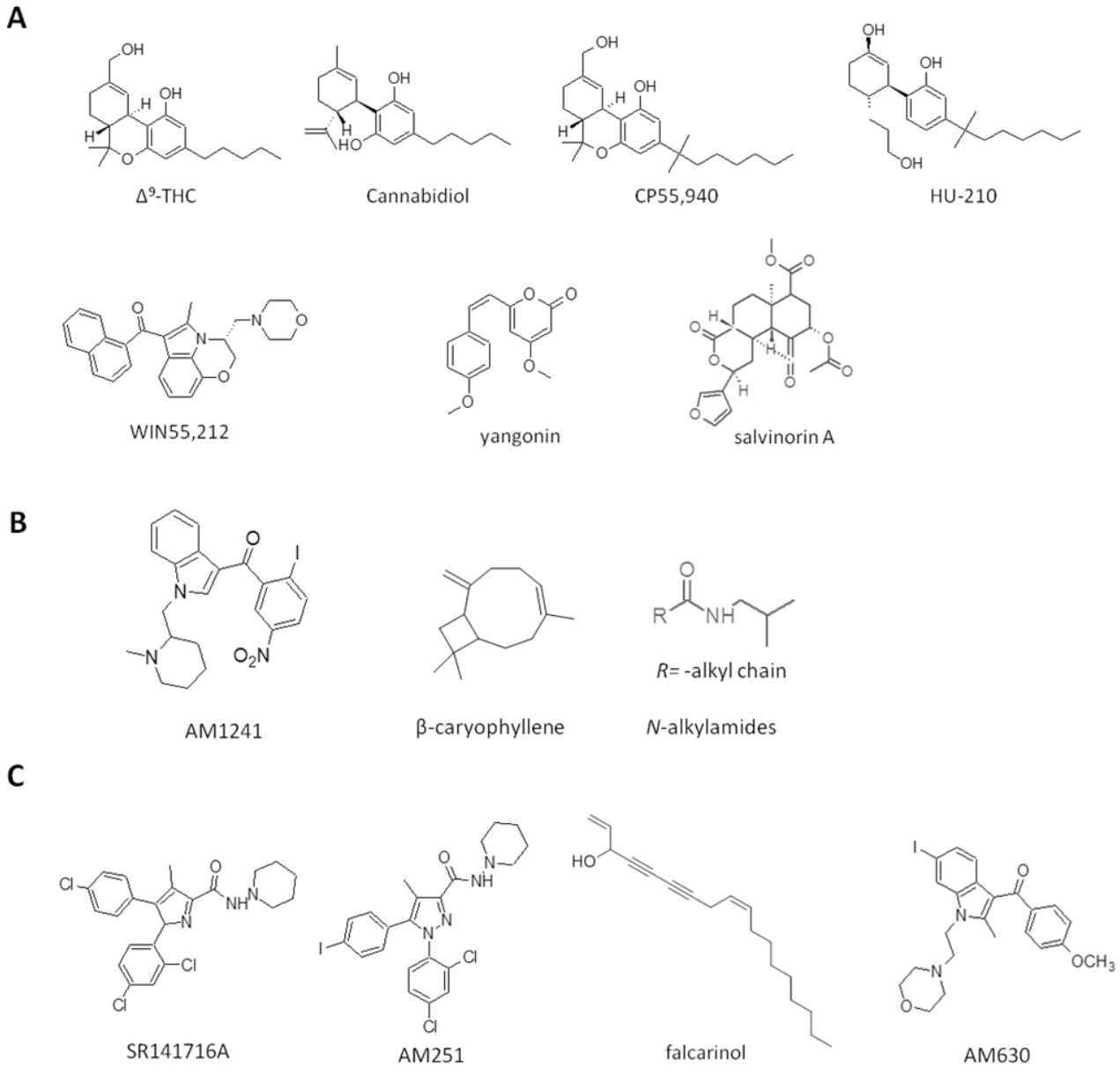

Figure 8. CB_1/CB_2 receptor agonists (A), selective CB_2 receptor agonists (B) and CB_1/CB_2 receptor antagonists/inverse agonists. (A) THC, Cannabidiol, CP55,940, HU-210 and *R*-(+)-WIN55,212 are both CB_1 and CB_2 receptor agonists, while yangonin only binds to CB_1 receptors and salvinorin A interacts with the CB_1/*κ*-opioid receptor dimer. (B) the aminoalkylindole AM1241, the sesquiterpene

β-caryophyllene and *N*-alkylamides are selective CB_2 receptor agonist. (C) SR141716A (rimonabant) and AM251 are selective CB_1 receptor antagonists, falcarinol is an inverse agonist at CB_1 receptor and AM630 is a selective CB_2 receptor antagonist.

More recently, some allosteric modulators of the endocannabinoid receptors have been identified. The endogenous compounds pregnenolone (Vallee et al., 2014) and the peptide pepcan-12 (Bauer et al., 2012) are CB_1 receptor negative allosteric modulators. Interestingly, pepcan-12 was also found to act as an efficient CB_2 receptor positive allosteric modulator, able to potentiate CP55,940 and 2-AG induced *h*CB_2 receptor signalling (Petrucci et al., 2017).

Additionally, other minor arachidonic acid (AA) derivatives have been identified as endocannabinoids: the CB_1 receptor-selective agonist 2-arachdonoyl-glyceryl ether (noladin ether) (Hanus et al., 2001), the CB_1 receptor antagonist *O*-arachidonoyl-ethanolamine (virodhamine) (Porter et al., 2002) and the TRPV1 activator *N*-arachidonoyl-dopamine (NADA) (Huang et al., 2002).

In the last two decades, numerous studies provided evidence that endocannabinoids can induce effects that are not mediate by the two classic CB_1 and CB_2 receptors. These CB_1/CB_2 receptors-independent actions include binding to ion channel or to other G-protein coupled receptors (Oz, 2006, Pertwee et al., 2010). For instance, AEA and WIN55,212-2 are able to inhibit serotonin type 3 ($5\text{-}HT_3$) receptors independently of cannabinoid receptors (Barann et al., 2002, Oz et al., 2002). AEA is a full agonist of the transient receptor potential vanilloid 1 (TRPV1) (Zygmunt et al., 1999, Smart et al., 2000). The orphan receptor GPR55 is activated by AEA and 2-AG, as well as by other natural and synthetic cannabinoids such as THC and CP55,940 (Ryberg et al., 2007) and by the CB receptor-inactive endogenous fatty acid amide *N*-palmitoylethanolamine (PEA). Although PEA does not bind to CB receptors, it is a substrate of the FAAH. AEA and 2-AG can directly inhibit glycine receptors in the hippocampus and modulate network activity (Lozovaya et al., 2005). Additionally, AEA, 2-AG, THC, PEA and *N*-oleoylethanolamine (OEA) are able to activate the peroxisome proliferator-activated receptors (PPARs) (Pertwee et al., 2010).

1.2.2 Biosynthesis of AEA and 2-AG

Unlike classical neurotransmitters, which are synthesized in the cytosol and stored in vesicles until an action potential causes their release, endocannabinoids are synthesized and released "on-demand" from membrane phospholipids containing AA following physiological or pathological stimuli, such as Ca^{2+} influx or cell depolarization (Di Marzo et al., 1994).

AEA, which belongs to the NAEs family, is mainly synthesized through an enzymatic hydrolysis of *N*-arachidonoyl-phosphatidylethanolamine precursors (NAraPE) by the action of an enzyme of the phospholipase family, selective for NAPEs (NAPE-PLD) (Schmid et al., 1983, Di Marzo et al., 1994, Schmid et al., 1996, Okamoto et al., 2009). NAPEs are synthesized by transferring an acyl group from membrane

phospholipids to the *N*-position of phosphatidylethanolamine (PE), reaction catalysed by an *N*-acyl transferase (AT).

Two other minor pathways are responsible for the biosynthesis of AEA (Sun et al., 2004). A Phospholipase A_2 (PLA_2) or an α,β-Hydrolase4 (ABHD4) hydrolyse NAarE into Lyso-NAraE, which is converted in AEA by a Lyso-PLD or first in glycerophospho-N-arachidonoylethanolamine (GP-NAraE) and then in AEA by a Glycerophosphodiesterase 1 (GDE1) (Simon and Cravatt, 2006). A third pathway involves the formation of phospho-*N*-arachidonoylethanolamine (pAEA) from the NAraPE precursor by a phospholipase C (PLC). Then, the Protein tyrosine phosphatase PTPN22 or the Phosphatidylinositol-3,4,5-trisphosphate 5-phosphatase 1 (SHIP1) generates AEA by dephosphorylation of pAEA (Liu et al., 2006).

In Figure 9, the three biosynthetic pathways of AEA are represented:

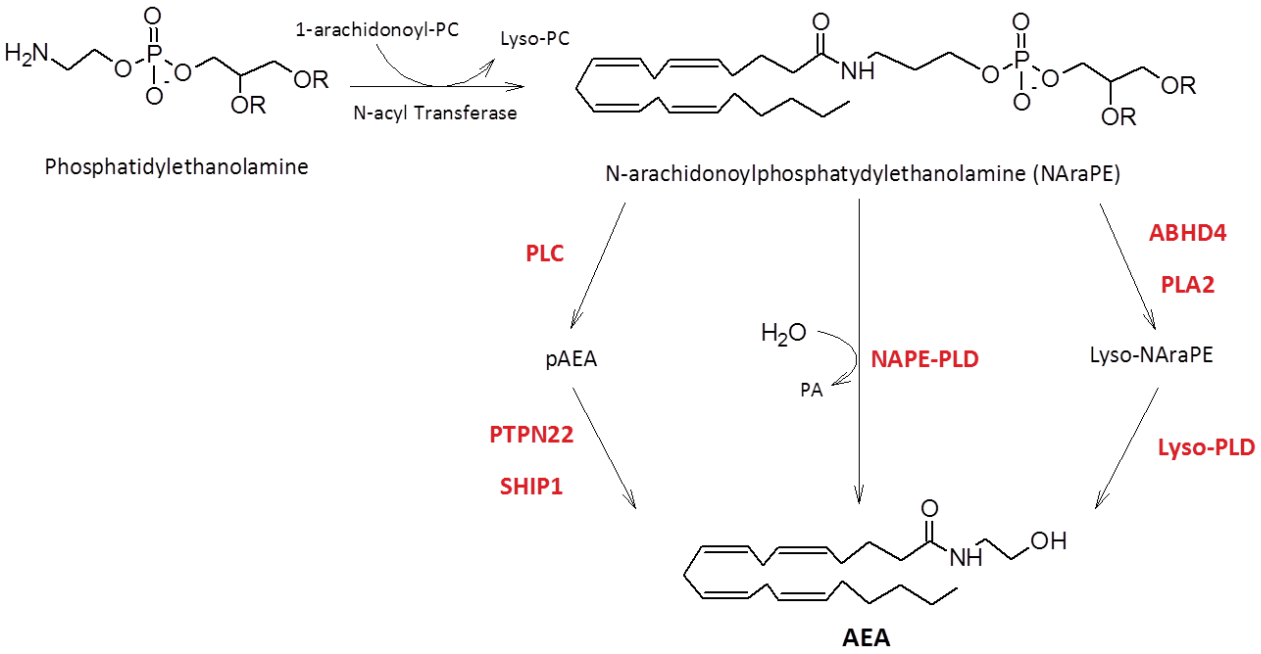

Figure 9. AEA biosynthesis pathways. AEA is biosynthesized from a *N*-acylphosphatidylethanolamine precursor containing AA (NaraPE). NAPE intermediate is obtained from reaction between the membrane phospholipid Phosphatidylethanolamine and 1-arachidonoyl-Phosphatidylcoline by the action of an *N*-acyl transferase. The main route involved an enzyme of the phospholipase D family, selective for NAPE (NAPE-PLD): NAPE-PLD catalyzes the hydrolysis of NAPE to obtain AEA and phosphatidic acid. A minor biosynthetic pathway involves a Phospholipase A2 (PLA2) or an α/β-Hydrolase4 (ABHD4), which hydrolyse NAraPE into Lyso-NAraPE, then converted in AEA by a Lyso-PLD. A third way involves the formation of phospho-N-arachidonoylethanolamine (pAEA) from NAraPE by the action of a phospholipase C (PLC). Then, the protein tyrosine phosphatase PTPN22 or the inositol 5' phosphatase (SHIP1) generates AEA by dephosphorylation of pAEA.

Despite AEA, 2-AG has other physiological functions than only the activation of CB receptors and its levels are physiologically higher than those of AEA (Baggelaar et al., 2018). Indeed, 2-AG is also the precursor or the product of several reactions that involve phosphoglycerides, as well as AA. It is synthesized

through several enzymatic pathways, mainly from the hydrolysis of diacylglycerol containing AA in the position 2 (DAGs), catalyzed by a DAG lipase (Bisogno et al., 1997, Bisogno et al., 2003, Bisogno et al., 2005). Figure 10 shows the main biosynthesis pathway for 2-AG:

Figure 10. Main 2-AG biosynthesis pathway. A diacylglycerol lipase (DAG-Lipase) catalyses the selective hydrolysis of the acyl group in the first position, giving the endocannabinoid 2-AG.

1.2.3 AEA transport

The reuptake of AEA is an essential step for the termination and the modulation of its signalling. Unlike the extensively characterized processes of biosynthesis and metabolism, the transport of AEA across the cell membrane remains unclear, although different hypotheses and models were proposed over the years (Fowler, 2013, Nicolussi and Gertsch, 2015).

Early investigations reported a link between the cellular transport of AEA and the enzymatic hydrolysis operated by FAAH (Di Marzo et al., 1994). Di Marzo and colleagues (1994) showed that transport of AEA inside the cell was rapid, selective, and temperature- and time-dependent. The uptake of AEA was then followed by its enzymatic hydrolysis into AA and ethanolamine. Thus, the first hypothesis for the transport of AEA proposed a model of simple diffusion across the plasma membrane, facilitated by the high lipophilicity of the molecule and by the hydrolytic activity of FAAH, which creates an inward concentration gradient (Day et al., 2001, Deutsch et al., 2001). Accordingly, FAAH inhibition should reduce the cellular reuptake of AEA. However, inhibition of the uptake of AEA was observed also in mouse neurons lacking FAAH (Fegley et al., 2004, Ligresti et al., 2004), suggesting that the hydrolysis of AEA was not the only factor regulating its uptake.

The first molecule synthesized to selectively inhibit the uptake of AEA was the *N*-arachidonoylaminophenol AM404. *In vitro* studies conducted in rat neurons and astrocytes showed that the compound was able to inhibit the AEA uptake with an IC_{50} in the low micromolar range (Beltramo et al., 1997). Later on, other AEA uptake inhibitors were synthesized, such as VDM11 (De Petrocellis et al., 2000), OMDM-1 and OMDM-2 (Ortar et al., 2003), and UCM707 (Lopez-Rodriguez et al., 2003). These molecules were first claimed to be selective over FAAH inhibition, but further studies demonstrated that in some assays conditions these compounds were also able to inhibit the AEA hydrolysis (Fowler et al., 2004, Vandevoorde and Fowler, 2005). Thus, although FAAH is not the only contributor to the uptake of AEA, the

enzyme is important to establish a driving force for the uptake, as it has been shown that inhibition of the enzyme leads to an inhibition of the uptake process.

Other models of AEA transport across the cells were proposed. Another proposed model was a carrier-mediated formation of caveolae and endocytosis of AEA. In this model, AEA binds first to a protein located within lipid rafts of the cellular membrane. After, a caveolae-mediated endocytosis leads to AEA cellular uptake (McFarland et al., 2004). With the identification of carrier proteins for AEA (Kaczocha et al., 2009, Oddi et al., 2009), an updated model of transport was proposed: by passive diffusion across the plasma membrane followed by a carrier-mediated intracellular transport, AEA can be relocated from different intracellular sites, such as degradation sites and target sites. Some proteins were proposed to be responsible of this transport, such as the fatty acid binding proteins (FABs), albumin and the heat-shock protein 70 (Hsp70). The identification of these proteins as potential carriers for AEA could explain the capability for such a lipophilic molecule to cross a hydrophilic medium like the cytosol (Kaczocha et al., 2009, Oddi et al., 2009).

Besides the progress in understanding the transport of AEA, one open question is whether there is a specific protein involved in AEA uptake across the membrane, a putative endocannabinoid membrane transporter (EMT) (Nicolussi and Gertsch, 2015). Several studies provided indirect evidence for the presence of the EMT. For instance, Ortega-Gutierrez and colleagues (2004) demonstrated that the uptake inhibitor UCM707 is still able to exert its inhibitory effect in FAAH (-/-) mice neurons, hypothesizing the participation of a specific protein in the uptake of AEA to which UCM707 is binding (Ortega-Gutierrez et al., 2004). In addition, Chicca and colleagues (2012) demonstrated that UCM707 and OMDM-2 are able to inhibit AEA uptake without binding to FABP5 (Chicca et al., 2012). Also the natural compound guineensine from *Piper nigrum* is a potent selective AEA uptake inhibitor which do not bind FABP5 or inhibit FAAH (Nicolussi et al., 2014b). More recently, it was shown that the natural product-derived *N*-(3,4-dimethoxyphenyl) ethyl amide (WOBE437) potently and selectively inhibits AEA uptake and exerts anxiolytic, anti-inflammatory, and analgesic effects in mice by increasing endocannabinoid levels. Furthermore, the WOBE437-derived diazirine-containing photoaffinity probe (RX-055) irreversibly blocks the membrane transport of both endocannabinoids. (Chicca et al., 2017, Reynoso-Moreno et al., 2018). Figure 11 shows the chemical structures of the above mentioned AEA uptake inhibitors.

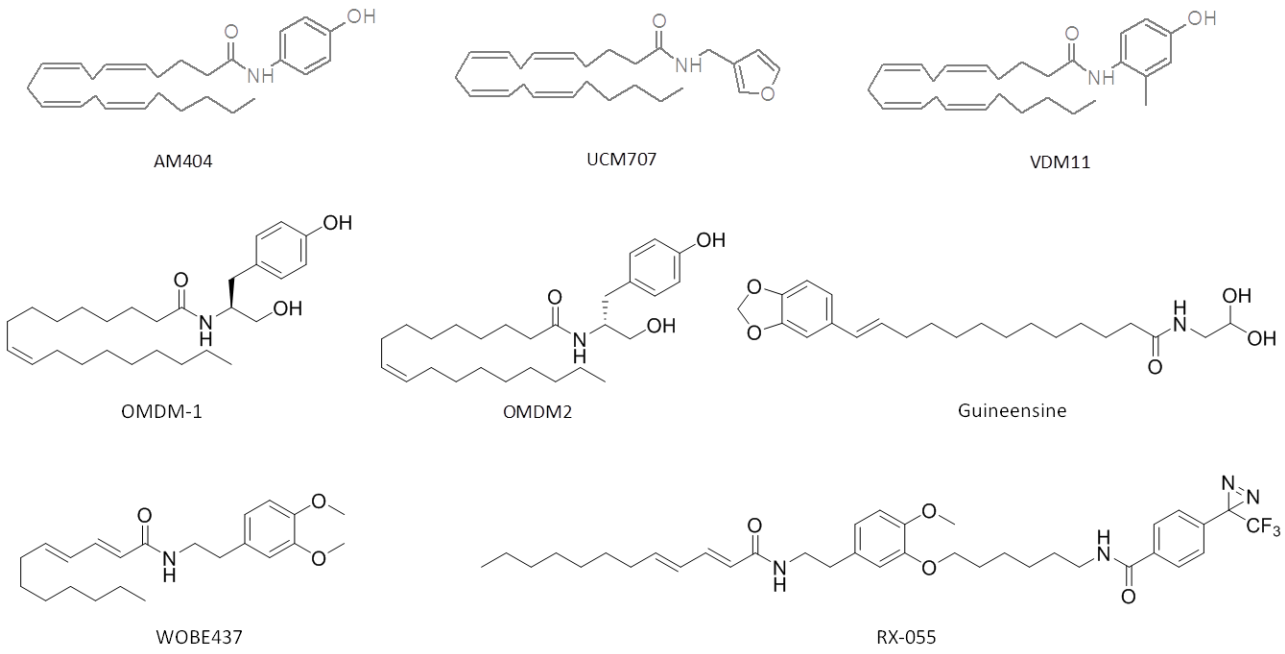

Figure 11. AEA uptake inhibitors.

Moreover, there is some evidence supporting a bidirectional transport of AEA across the cell membrane mediated by the EMT. Indeed, previous works demonstrated that AEA uptake inhibitors block AEA release, which unlike the reuptake, cannot be facilitated by FAAH (Ligresti et al., 2004, Chicca et al., 2012).

Altogether, the previous findings and the experimental data support a new model for the transport of endocannabinoids. In this model, AEA putatively binds first to a specific ETM to cross the lipid bilayer and enter the cell. Then, AEA binds to specific intracellular carrier proteins that will relocate it to different cell sites either to exert intracellular activity or to be simply degraded (Figure 12).

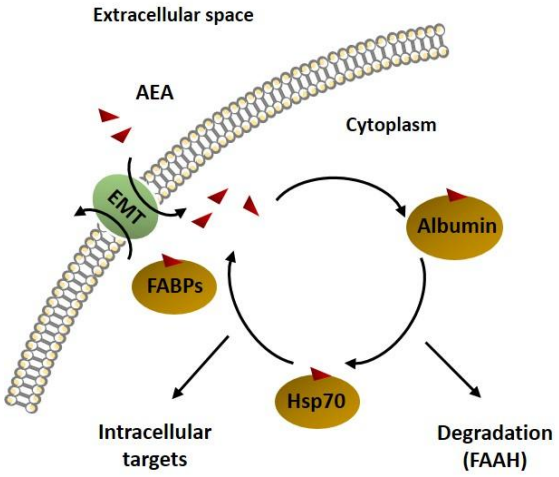

Figure 12. Possible mechanism of AEA transport across the cell. It includes a facilitated diffusion across the plasma membrane mediated by a putative ETM, followed by intracellular carrier mediated-transport. (Readapted from Nicolussi & Gertsch (2015)).

Although recent studies support the ETM theory (Chicca et al., 2012, Nicolussi et al., 2014b, Chicca et al., 2017, Reynoso-Moreno et al., 2018), the molecular identification of this transport protein is still missing. This identification thus would have a significant impact in the understanding of the endocannabinoids transport across the cell membrane.

1.2.4 Endocannabinoids degradation

Both AEA and 2-AG signalling is terminated via a combination of a cellular uptake process and an enzymatic hydrolysis. Figure 13 provides a schematic representation of the inactivation and transformation pathway of AEA and 2-AG at the synapse.

The major enzyme involved in the degradation of 2-AG is the monoacylglycerol lipase (MAGL) (Dinh et al., 2002, Makara et al., 2005). MAGL was originally purified and cloned from the adipocyte tissue (Karlsson et al., 1997) and it catalyzes the hydrolysis of the ester bond in the 2-AG producing AA and glycerol. Inhibition of MAGL by the selective inhibitor JZL184, results in the elevation of 2-AG levels in brain with cannabinoid-like behavioural effects in mice including analgesia, hypomotility, and hypothermia (Long et al., 2009). Two other enzymes of the serine hydrolase family with the typical α/β-hydrolase domain operate minor 2-AG hydrolysis: α/β-hydrolase 6 (ABHD6) and α/β-hydrolase 12 (ABHD12) (Blankman et al., 2007, Marrs et al., 2010, Savinainen et al., 2012). ABHD6 is inhibited by the carbamate WWL70, while the lipase/serine hydrolase inhibitor tetrahydrolipstatin (THL) is able to irreversibly inhibit ABHD12 (Li et al., 2007, Navia-Paldanius et al., 2012).

Cyclooxygenase-2 (COX-2) is responsible for oxidative reactions of both 2-AG and AEA, generating the prostaglandin H_2 (PGH_2), precursor of other prostaglandin, thromboxane and other biologically important molecules (Yu et al., 1997, Kozak et al., 2000).

The major enzyme responsible for the degradation of AEA is the serine hydrolase FAAH (Cravatt et al., 1996, Dinh et al., 2002). FAAH is an enzyme of broad substrate specificity able to hydrolyse a wide range of unsaturated, preferentially, and saturated fatty acid amides. The enzyme shows also esterase activity on 2-AG (Di Marzo et al., 1998, Boger et al., 2000). In 2006, Wei and colleagues reported the identification of a second fatty acid amide hydrolase (FAAH-2) (Wei et al., 2006). FAAH-2 shares 20% of sequence identity with the original FAAH enzyme, but distinct tissues distribution, substrate selectivity and inhibitor sensitivity profile. For instance, FAAH displays much higher affinity for AEA than FAAH-2, although also this enzyme contributes to its hydrolysis (Wei et al., 2006).

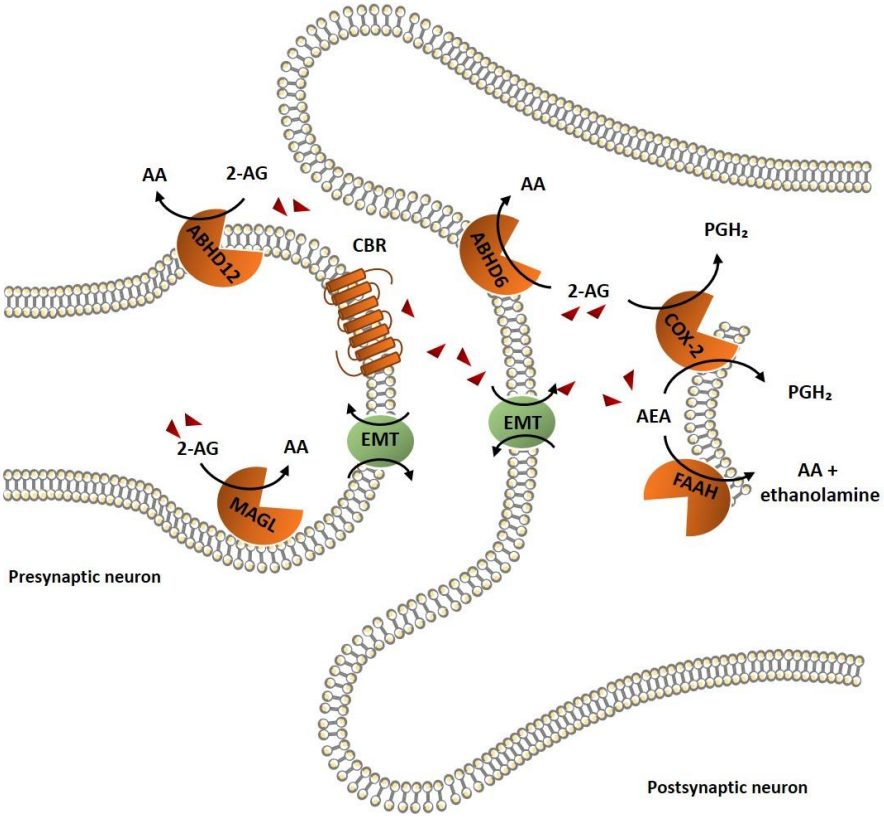

Figure 13. Enzymatic machinery for the degradation of AEA and 2-AG. Main 2-AG degradation in AA and glycerol is performed by MAGL, but ABHD6 and ABHD12 are responsible for a minor degradation. AEA is mainly degraded by FAAH in AA and ethanolamine. COX-2 oxidizes 2-AG into PG-AE and AEA in PG-G. FAAH=Fatty acid amide hydrolase; MAGL=monoacylglycerol lipase; COX-2=cyclooxygenase-2; ABHD6=α/β-Hydrolase 6; ABHD12= α/β-Hydrolase 12; AA=arachidonic acid; PGH_2=prostaglandin H_2.

Since my doctoral thesis is mainly focused on the endocannabinoid AEA, in the following section I will provide a more detailed description of the process of the degradation of AEA operated by FAAH.

1.2.4.1 Degradation of AEA

FAAH was originally purified and cloned from rat liver microsomes in 1996 (Cravatt et al., 1996). In rats, FAAH is present in the liver, the small intestine, the testis and in the brain (Katayama et al., 1997). In brain, FAAH is present in regions with strong endocannabinoid signalling such as cortex, hippocampus, cerebellum and amygdale (Tsou et al., 1998). Interestingly, the distribution of FAAH and CB receptors at the synapse is complementary: the enzyme is localized in post-synaptic neurons and the CB receptors are in pre-synaptic neurons (Egertova et al., 1998). The distribution in primary cells is variable, for instance, HeLa cells do not express FAAH, while it is present in rat basophilic leukaemia cells RBL-2H3 and rat C6 glioma cells (Bjorklund et al., 2014).

FAAH is an intracellular homodimeric enzyme with esterase and amidase properties, which catalyzes the hydrolysis of the AEA amide bond giving the corresponding AA and ethanolamine (Deutsch

and Chin, 1993) (Figure 14A). By using X-ray techniques, the structure of the enzyme, complexed with the inhibitor methoxy arachidonyl phosphonate (MAP) was elucidated (Bracey et al., 2002) (Figure 14B).

Three important pockets compose the active site: an acyl-chain binding pocket (ABP), a membrane access channel (MAC) and a cytosolic port (CP). In the ABP, aromatic and aliphatic residues allow the accommodation of the acyl-chain of AEA and others molecules. The MAC directs to a protein surface opening facing the membrane bilayer. The CP serves as the passageway for water molecules to access the catalytic centre as well as the exit route for the polar reaction products (Bracey et al., 2002). The enzyme possesses a catalytic triad different from the one of the common serine hydrolase, consisting of three amino acidic residues: Ser241, Ser217 and Lys142 (Patricelli and Cravatt, 1999, Patricelli et al., 1999, Bracey et al., 2002). Ser241 acts as nucleophile to form a tetrahedral intermediate with the carboxylic group of AEA. Lys142 acts as base to activate and stabilize Ser217 and Ser217 stabilizes the oxygen anion of the tetrahedral intermediate.

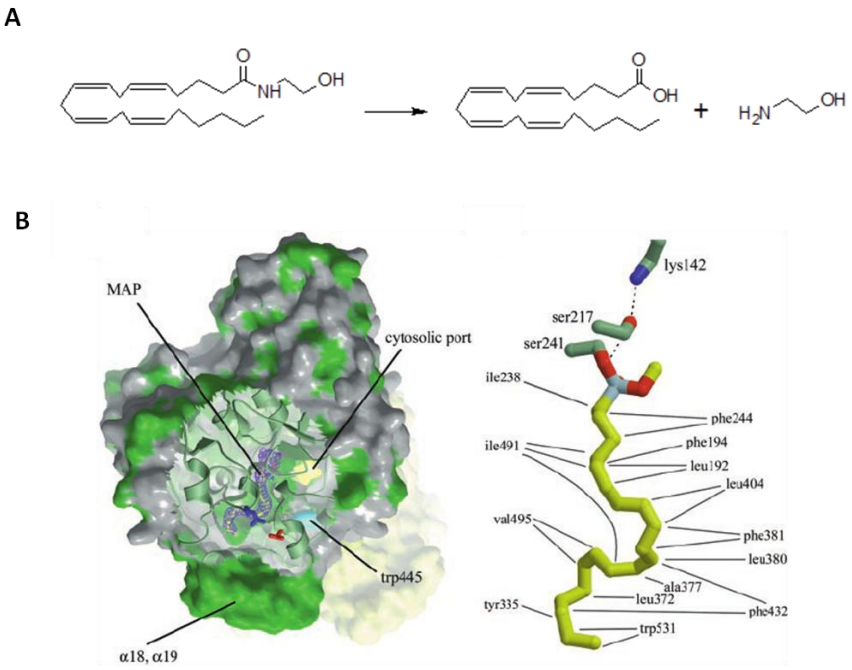

Figure 14. Hydrolysis of AEA by FAAH. (A) AEA is hydrolysed by FAAH into AA and ethanolamine. (B) The catalytic triad of FAAH consists in 3 amino acids: Ser241 acts as nucleophile to form a tetrahedral intermediate with the carboxylic group of AEA (or the phosphorus of MAP as shown in the figure). Lys142 acts as base to activate and stabilize Ser217. Ser217 stabilizes the oxygen anion of the tetrahedral intermediate. (From Bracey *et al.,* (2002)).

Since FAAH is the major enzyme involved in the degradation of AEA, and thus in the termination of its signalling, the inhibition of such enzyme represents a pharmacological strategy to enhance AEA levels and associated responses, with therapeutic effects. Several compounds act as FAAH inhibitors, either in an irreversible or reversible way (Figure 15). Irreversible inhibitors bind to the enzyme covalently and their effect cannot be reversed, while reversible inhibitors bind to the enzyme with non-covalent bonds such as

hydrogen bonds, ionic bonds and hydrophobic interactions. Early studies on the design of FAAH inhibitors were based on similarities with the endogenous enzyme substrate. These compounds include aldehydes, α-ketoamides, α-ketoesters and α-ketoheterocycles. The lead compound of this last class of molecule is the 7-phenyl-1-[5-(pyridin-2-yl)-1,3-oxazol-2-yl]heptan-1-one (OL-135) (Boger et al., 2005), which is able to reversibly inhibit FAAH and exert analgesic effects in animal models of pain (Lichtman et al., 2004). Moreover, the reversible inhibitor enolcarbamate ST-4070 was shown to be promising in the treatment of neuropathic pain (Caprioli et al., 2012). Also plant-derived compounds have been reported to inhibit FAAH (Russo, 2016). Usually they show reversible inhibition, such as the *N*-benzyloleamide "macamide" (Almukadi et al., 2013), *N*-alkylamides (Hajdu et al., 2014) and the flavonoids genistein, daidzein, kaempferol and biochanin A (Thors et al., 2007a, Thors et al., 2007b, Thors et al., 2008, Thors et al., 2010).

Among the irreversible inhibitors, the synthetic URB597 represents the lead compound of the carbamate-based inhibitors. Through FAAH inhibition, URB597 increases brain AEA levels and enhances AEA mediated responses (Fegley et al., 2005), such as anti-inflammatory and analgesic (Jayamanne et al., 2006) and antidepressant-like effects (Bortolato et al., 2007). Other irreversible FAAH inhibitors are the tetrazolium-based compound LY-2183240 and the sulphonyl fluoride AM3506. LY-2183240, initially developed as AEA uptake inhibitor, was after shown to irreversibly inhibit also FAAH and other serine hydrolase (Alexander and Cravatt, 2006). By inhibiting FAAH, AM3506 is able to normalizes cardiovascular function in hypertension (Godlewski et al., 2010) and endotoxin-induced gastrointestinal mobility in mice (Bashashati et al., 2012).

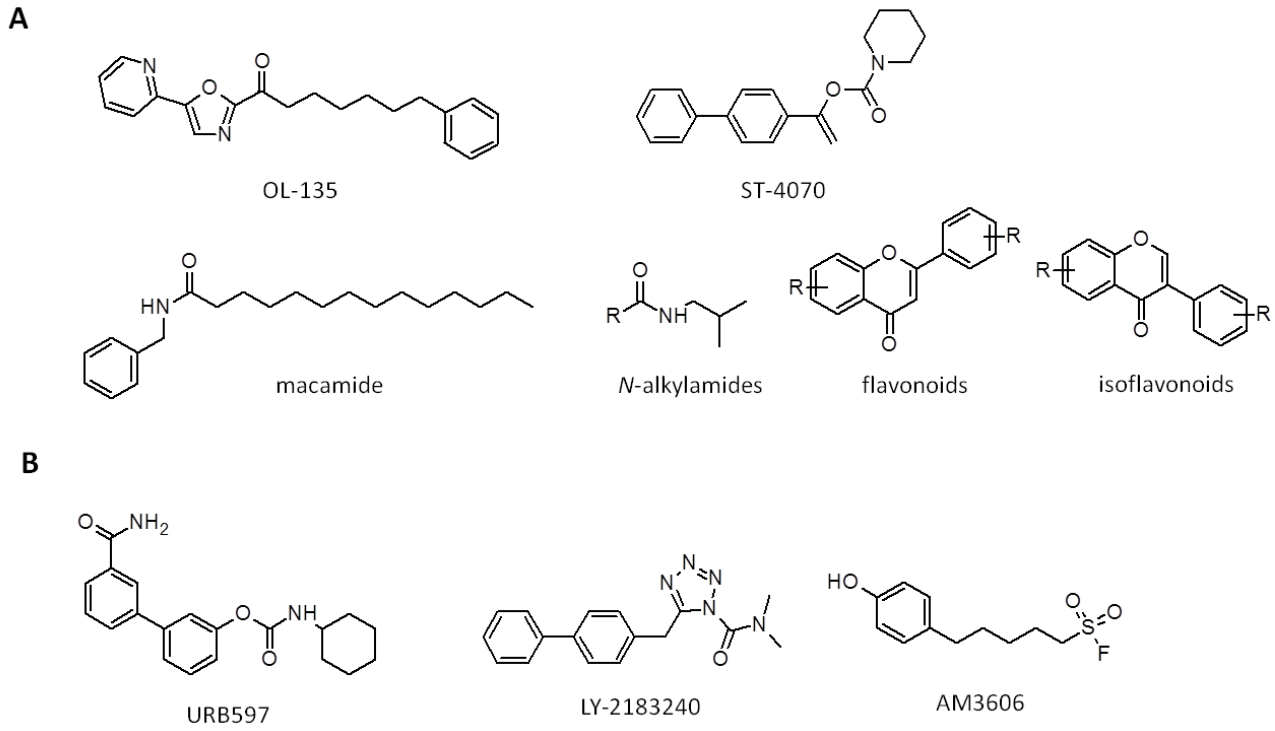

Figure 15. Reversible (A) and irreversible (B) FAAH inhibitors.

Thus, FAAH has become an attractive target in current drug discovery and it represents an interesting pharmacological tool for the treatment of conditions associated with imbalanced endocannabinoid signalling including anxiety, depression, pain, inflammation and a range of metabolic disorders. However, the identification of FAAH inhibitors with appropriate selectivity and potency, suitable for clinical studies remains the main challenge in the research on this target.

1.2.5 Pathophysiological role of the endocannabinoid system and pharmacological modulation

Since the discovery of the two major endocannabinoids and their receptors, enormous advances have been made in understanding the pathophysiological role of the endocannabinoid system and its therapeutic potential. As described before, CB_1 and CB_2 receptors, widespread in several cell-types in both central and peripheral nervous system as well in several other body tissues, are involved in the modulation of multiple functions. Endocannabinoids are synthesized and released "on demand" as an adaptive reaction to re-establish normal homeostasis when this is pathologically perturbed. However, chronic activation of the ECS also contributes to the progress or symptoms of the disorder (Di Marzo and Petrosino, 2007).

In the CNS, via their retrograde signalling, endocannabinoids are able to modulate γ-aminobutyric acid (GABA) and glutamatergic neurotransmission with implications for learning, memory and emotional responses (Wilson and Nicoll, 2001, Marsicano et al., 2002, Moreira and Lutz, 2008, Panlilio et al., 2016). CB_1 receptor activation in hippocampus promotes hippocampal cellular proliferation (Aguado et al., 2005). Peripheral activation of CB_1/CB_2 receptors leads to therapeutic responses in the autonomic nervous system such as normalization of gastrointestinal motility and blood pressure (Godlewski et al., 2010, Bashashati et al., 2012).

The ECS has also a homeostatic role in metabolic functions, such as regulation of energy storage and nutrient transport (Bellocchio et al., 2008, Bosier et al., 2013). Via activation of CB_1 receptors in the brain, the ECS stimulates appetite and food intake (Jamshidi and Taylor, 2001, Mazier et al., 2015, Lau et al., 2017). On the other hand, its excessive activation can lead to obesity (Mazier et al., 2015). Accordingly, new therapeutic drugs were designed as blockers of endocannabinoid action. CB_1 receptor antagonism has represented a therapeutic strategy against obesity, as documented with the first approved anti-obesity drug rimonabant (Rinaldi-Carmona et al., 1994). However, clinical studies with rimonabant revealed adverse events related to anxiety and depression in the treated patients, due to an excessive inhibition of CB_1 receptors.

Endocannabinoids are involved also in the regulation of mood and they have therapeutic effects in neuropsychiatric and mood disorders (Micale et al., 2013). For instance, some studies have demonstrated that the ECS modulates dopaminergic neurotransmission, whose excessive activation could be associated

to psychiatric disorders (van der Stelt and Di Marzo, 2003, Covey et al., 2017) and improves behavioural responses in animal models of depression (Umathe et al., 2011). In addition, anxiolytic effects are observed by enhancing the endocannabinoid tone, suggesting the role of this system in regulating pathologic conditions associated with anxiety (Bortolato et al., 2006).

Activation of CB_1 receptors in brain, spinal cord and peripheral sensory neurons induce analgesia (Calignano et al., 1998, Richardson et al., 1998, Martin et al., 1999). Also the NAE PEA, which is synthesized from a common phospholipid precursor of AEA, exerts analgesic effect similar to AEA by activating peripheral CB_2-like receptors (Calignano et al., 1998).

Activation of CB_2 receptors represents as well an interesting pharmacological approach to treat diverse disorders. For instance, a recent report by Verty and colleagues (2015) suggested a possible anti-obesity role of the CB_2 agonists JWH-015 by modulating energy homeostasis (Verty et al., 2015). Other studies showed that the CB_2 receptors are important for glucose homeostasis, suggesting it as target for the treatment of metabolic disorders associated with disrupted glucose homeostasis such as diabetes (Juan-Pico et al., 2006, Bermudez-Silva et al., 2007). CB_2 receptors may also be a promising target for neurodegenerative disorders such as multiple and amyotrophic lateral sclerosis, Parkinson´s and Alzheimer's disease. In fact, brain CB_2 receptors are important in the control of neuroinflammatory events associated with brain damage (Stella, 2004, Fernandez-Ruiz et al., 2008). For instance, the CB_2 agonist JWH-015 was shown to induce human macrophages to remove beta-amyloid protein *in vitro*, which form aggregates disrupting neural functioning leading to Alzheimer's disease (Tolon et al., 2009).

Enhanced AEA levels and related responses, represents an interesting pharmacological approach to treat several conditions characterized by a down-regulated endocannabinoid tone or in which its activation is beneficial. Enhanced AEA tone can be achieved through inhibition of its degradation, mediated by FAAH. In fact, FAAH exerts a key role in the termination of AEA signalling in the CNS and in peripheral tissues. A study by Cravatt and colleagues (2011) showed that FAAH knockout mice have brain AEA levels 15-fold higher compare to the wild-type and they display reduced pain sensation and CB_1-dependent behavioural responses (Cravatt et al., 2001). Inhibition of FAAH by natural and synthetic molecules thus represent a pharmacological tool for the treatment of conditions associated with imbalanced endocannabinoid signalling including anxiety, depression and a range of metabolic disorders. In fact, FAAH inhibitors have already shown promising results in acute, inflammatory and neuropathic pain (Jhaveri et al., 2006, Jhaveri et al., 2008, Naidu et al., 2010, Sasso et al., 2015, Lomazzo et al., 2015, Kinsey et al., 2011, Brindisi et al., 2018), anxiety and mood disorders (Gobbi et al., 2005, Micale et al., 2009, Greco et al., 2015, Bambico et al., 2016), nausea (Rock et al., 2008), hypertension (Batkai et al., 2004) and Parkinson's disease (Kreitzer and Malenka, 2007).

1.2.6 Endocannabinoid system in plants

Despite mammals, also plants possess an "endocannabinoid signalling network", composed by fatty acid amides signalling molecules (NAEs), their binding proteins and degrading enzymes (Shrestha et al., 2003, Chapman, 2004). Although some differences between mammal and plant ECS are evident, the formation, degradation and oxidation pathways of NAEs seem to be well conserved in both animal and plant systems.

Like in mammals, NAEs are fatty acid amides derived from the membrane lipid constituent NAPE. In plants, they have been identified and quantified in different species (Chapman et al., 1999, Chapman et al., 2003, Gachet et al., 2017). In the '50s, Kuehl and colleagues (1957) gave the first report of the identification of NAEs in plants, in particular of PEA in soybeans (Kuehl et al., 1957). Later on, several studies led to the identification and quantification of medium chain NAEs in plants. *N*-laurylethanolamine (12:0), *N*-myristylethanolamine (14:0), PEA (16:0), OEA (18:1), and LEA (18:2) were identified in the seeds of different plant species such as soy, corn, cotton, peanuts and tomatoes mostly by GC-MS analyses (Chapman et al., 1999, Chapman et al., 2003). In a recent study, NAEs were identified and quantified in plants species belonging to the major phylogenetic clades by LC-MS (Gachet et al., 2017). Higher levels of PEA, OEA and LEA were detected in angiosperms compared to gymnosperms and monilophytes. Moreover, a new endocannabinoid-like molecule derived from juniperonic acid (JuA) namely juniperonoylethanolamine (JEA) was also identified in lower plants. Interestingly, vascular plants seem to produce neither the two major mammalian endocannabinoids AEA and 2-AG, nor AA, with some exceptions (Kursat et al., 2015, Gachet et al., 2017).

In 2003, radioligand binding assays performed with [^{3}H]-NAE 14:0 leaded to the identification of a binding protein for NAEs in membranes of tobacco cells suspension and tobacco leaves (Tripathy et al., 2003). The [^{3}H]-NAE 14:0 bound to the protein with high affinity with a K_d of 75 nM and 35 nM respectively, comparable to the range of K_d values reported for the mammalian CB receptors. Interestingly, at the optimal conditions for NAE 14:0 binding, AEA and WIN55,212-2 were not able to bind with the protein, as well as LEA, suggesting a different selectivity for NAE types between plant and mammalian receptors. However, the binding was reversed in presence of mammalian CB receptors antagonists such as AM281 and SR144528, pointing out the presence of a CB receptor-like binding protein in plants which mediates NAEs signalling like in animals.

Endogenous NAE levels are regulated through their hydrolysis by a fatty acid amide hydrolase, homologue of the mammalian FAAH. A member of the serine hydrolase family, responsible for the degradation of NAEs was found in cottonseed microsomes (Shrestha et al., 2002), later identified as the plant FAAH in *Arabidopsis thaliana* (Shrestha et al., 2003). Comparisons of the primary amino acid sequence of rat and the putative plant FAAH, showed only 18% of identity, but those amino acids that are

important for the activity of mammalian FAAH were well conserved also in the plant enzyme. Also, mammalian and plant FAAH have similar molecular weight (around 66 kDa), similar topologies and subcellular localization (Shrestha et al., 2003). Coding sequences for FAAH were isolated from *A. thaliana* and expressed in *E. Coli* and the FAAH hydrolytic activity was evaluated with functional and kinetic assays, demonstrating that the resulting enzyme was able to hydrolyse different NAEs such as NAE 12:0, NAE 14:0, NAE 16:0, NAE 18:2 and AEA with good affinity (K_m of 13.6 µM) even if it is not present in higher plants (Shrestha et al., 2003).

Accordingly to the previous findings, Chapman (2004) proposes a model for NAEs signalling pathway in plant, similar to the endocannabinoid signalling in animals (Chapman, 2004). Like in mammals, NAEs act as lipid signalling molecules activating short and long-term cellular responses via the binding to such protein for NAEs. In addition, NAEs signalling is terminated by hydrolysis from a fatty acid amide hydrolase, homologue of the mammalian enzyme (Chapman, 2004), as illustrated in Figure 16. Different internal or external stimuli can favourite NAE biosynthesis from the NAPE precursor mediated by the Phospholipase D family enzymes PLD β and γ isoforms. *In vitro* experiments using radiolabeled NAEs showed that NAEs are synthesized in the microsomes of plant cells (Chapman et al., 1995b). Three recombinant plant PLD isoforms (α, β and γ) were expressed in *E.coli* to study their ability to synthesize NAES from NAPE showing that PLD β and γ isoforms, but not the α, are responsible for NAEs formation (Pappan et al., 1998). Once synthesized, NAEs diffuse to a transmembrane binding protein (NBP), in the same or nearby cells, and interact with it, leading to cellular responses such as modification of plasma membrane ion flux and alteration of nuclear gene expression. Finally, the NAEs signal is terminated by the action of a FAAH that hydrolyses them into ethanolamine and free fatty acids.

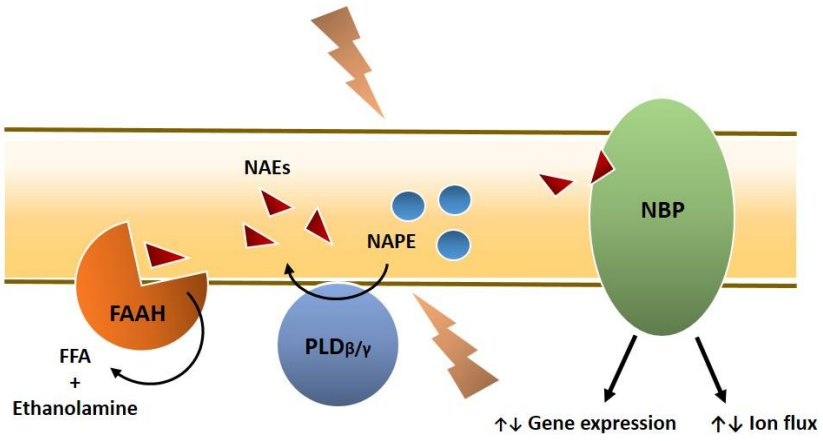

Figure 16. Schematic representation of NAEs signalling in plants. NAEs are synthesized from an *N*-acylphosphatidylethanolamine precursor, following intra or extracellular stimuli, by a Phospholipase D β and γ isoform. The activation of a NAEs binding protein leads to cellular responses such as changes in the ion flux or in the gene expression. NAEs signalling is terminated by the action of a Fatty acid amide hydrolase, which degrades them into free fatty acids and ethanolamine. NAEs=*N*-acylethanolamines; NAPE= *N*-

acylphosphatidylethanolamine; PLD=Phospholipase; NBP=NAE binding protein; FAAH=Fatty acid amide hydrolase; FFA=free fatty acids. (Readapted from Chapman (2004)).

Interestingly, functional and kinetic studies have demonstrated that the plant FAAH is inhibited by the mammalian FAAH inhibitor MAPF, but not by URB597 (Shrestha et al., 2006). This finding suggested the hypothesis that some structural difference between mammalian and plant FAAH occur, not allowing URB597 to bind to the active site of plant FAAH. However, structural modelling of rat and plant FAAH showed good similarities and a really well conserved catalytic site.

Like in mammals, plant NAEs act as signalling molecules, regulating different functions such as mediation of defence responses, inhibition of PLD α isoform and inhibitors of seedling root development (Chapman, 2004). While in animals AEA is the major responsible for the regulation of biological functions, medium chain NAEs (C14-C18) are usually responsible for such functions in plant tissues. Studies conducted in tobacco cells exposed to pathogen elicitors, revealed an increased production of C-14 NAEs from their NAPE precursor (Chapman et al., 1995a, Tripathy et al., 1999). Usually, in presence of elicitors, plant cells activate several responses such as changes in ion flux at the plasma membrane, change in the phosphorylation status of proteins, increase of ethylene production and phytoalexin defence compounds (Tripathy et al., 1999). These short-term responses are followed by an activation of the transcription of some defence genes such as the expression gene for Phenylalanine ammonia lyase 2 (PAL2), an enzyme involved in the biosynthesis of polyphenolic compounds such as flavonoids, phenylpropanoids, and which plays an important role of defence responses in plants (Tripathy et al., 1999). The study suggested that short- and long-term defence responses in plants are induced by increased NAE 14:0 levels, which might modulate ion flux at the plasma membrane and consequently attenuate the elicitor-induced alkalinisation, and activate PAL expression. A study of Austin-Brown and Chapman (2002), demonstrated that *N*-laurylethanolamine and *N*-myristylethanolamine were potent inhibitors of PLD α isoform with an IC_{50} of 150 nM (Austin-Brown and Chapman, 2002). PLD α isoform, which is not able to generate NAEs from NAPE precursors, has an important role in the degradation and reorganization of subcellular membranes of the cells and its activity needs to be regulated to avoid cell damage. In order to understand whether NAEs were able to inhibit PLD α *in vivo*, a process such as stomatal closure induced in epidermal cells treated with the plant hormone abscisic acid was studied. The study demonstrated that the stomatal closure is inhibited when plant tissues are treated with LEA, and it might be consequent to a PLD α inhibition mediated by NAEs. These findings suggested thus that the NAEs might be involved in the reorganization of subcellular membranes. In addition, some studies have demonstrated that plant NAEs are able to interfere with the normal seedling root cells development. Studies conducted on *A. thaliana* seedlings treated with exogenous LEA have revealed reduction of roots elongation, reduction of roots diameter and anomalous cells architecture (Blancaflor et al., 2003). Moreover, it has been shown that NAEs levels drop during germination and seedling growth (Chapman et al., 1999). Interestingly, Wang and co-workers (2006) have

found that when FAAH was overexpressed, seedlings were able to grow even when treated with high levels of exogenous NAEs (Wang et al., 2006). These studies suggested that during the normal growth process NAEs are extensively metabolized and that high NAE levels could lead to an abnormal development of the plant. Another evidence of the implication of NAEs in the abnormal seedling development is that the mammalian CB_2 antagonist SR144528 reverses these effects observed in presence of high levels of NAEs.

Even though research on the endocannabinoid signalling in plant tissues is relatively more recent than the one on mammalian, all these findings have brought evidence of a well conserved system in eukaryotic cells during evolution and of a crucial role of this lipid network in plant physiology. Therefore, in this doctoral project we also questioned whether plant-derived molecules able to modulate the mammalian endocannabinoid system might have a similar role in plant tissues, as will be discussed later (see Chapter 4 and Chapter 6 for further details).

CHAPTER 2 – RESEARCH OBJECTIVES

Plant-based medicines have important therapeutic applications. Since antiquity, the interest in understanding and using herbal drugs for the treatment of human pathologies can be traced across several societies. Therapeutic indications of plant-derived drugs are reported in a multitude of historical texts, spacing from Greek-Roman to the Indian and Chinese societies (Matthioli, 1568, Hoernle, 2011, Commission, 2015, Leonti and Verpoorte, 2017). The enormous phytochemical diversity produced by botanical species has been used as an invaluable source for drug discovery and as a source for tool compounds enabling advancements in medicine and pharmacology. Motivated by the early success in drug discovery from natural sources researchers of the twentieth century concentrated their effort on the isolation and characterization of bioactive plant secondary metabolites. One of the most noteworthy examples is arguably represented by the identification of the *Cannabis* component THC (Gaoni and Mechoulam, 1964, Hollman, 1996, Wall and Wani, 1996, Cragg, 1998). The identification of THC as the main psychoactive compound of *Cannabis sativa* L. triggered research activities, which were conductive to the elucidation of the ECS. The ECS is a major modulatory system involved in a variety of physiological functions including appetite regulation, pain perception, mood, learning and memory, motor function and immune responses (Di Marzo and Petrosino, 2007). The ECS comprises two main endogenous ligands (AEA and 2-AG), which interact with specific cannabinoid receptors (CB_1 and CB_2) as well as reuptake proteins and enzymes responsible for the degradation and inactivation of the endogenous ligands. Since the impairment of the ECS is frequently involved in pathological conditions, the targeting of the ECS by enhancing the endocannabinoid tone constitutes a promising approach for the development of novel therapeutic agents with anxiolytic, anti-depressant, anti-inflammatory and anti-nociceptive activity (Piomelli et al., 2000, Makriyannis et al., 2005, Di Marzo, 2009). In the course of such research activities several plant-derived compounds able to modulate the ECS have been characterized (Russo, 2016).

The aim of this doctoral thesis is to identify and characterize plant-derived compounds able to target and modulate the ECS. To address this objective, the starting point was the realization of a plant extract library based on a collection of drug samples associated with the herbal drugs described in the Dioscorides' *DMM* (see Staub et al., 2016 for further details). The treatise was selected as one of the most influent and comprehensive guide for the development of the modern knowledge on natural history, medicine and pharmacy in Europe. A collection of 670 herbal drugs was subjected to extraction, using a standardized process, described in detail in the *Materials and Methods* section. The obtained plant extract library was subjected to *in vitro* bioactivity screening in order to study the interaction of the extracts with the ECS, with particular focus on two biological targets: a) FAAH and b) CB_2 receptors. The hydrolytic activity of FAAH is one of the major processes responsible for the inactivation of the AEA. Thus,

pharmacological inhibition of FAAH is used as strategy to enhance the AEA signalling and produce associated therapeutic responses. Moreover, activation of CB_2 receptors represents an interesting pharmacological approach to treat diverse disorders such as diabetes, and neurodegenerative and immune diseases. In addition, in order to identify unspecific cytotoxic effects and to expand the information about the biological activities of the plant extracts of our library, the antiproliferative activity was evaluated.

For the identification of candidate herbal drugs and secondary metabolites for drug discovery, the data generated by the screening was combined with the information provided by the use of other approaches, such as phylogenetic and chemotaxonomic. With this strategy, some classes of secondary metabolites, known to be produced in the "active" herbal extracts, were selected as potential bioactive metabolites to subject to pharmacological investigation. The pharmacological profiling of the bioactive metabolites included functional *in vitro* assays aimed at the discrimination of selective versus multi-target interactions with the targets of the ECS, but also assessment of dose-response curves, kinetic profiling, cell-permeability studies and structure activity relationship (SAR) of the identified compounds.

The data generated from the *in vitro* FAAH inhibition screening of the *DDM* library were integrated with the data obtained from the screening of another extract library based on the Chinese Traditional Medicine (*Schwabe library*; see Chapter 3 for further details). The obtained results will be presented in a manuscript (Chapter 4), which is in preparation ("Identification of Prenylated Isoflavonoids as Potent, Selective and Reversible Fatty Acid Amide Hydrolase Inhibitors" Collu, M., Calarco, S., Nicolussi, S., Rau, M., Casu, L., Leonti, M., Gertsch, J.). The preliminary results obtained with the screening of the library for CB_2 receptors interaction and antiproliferative activity are presented in Chapter 5, Section 5.1.

Moreover, the Ayurvedic medicinal plant *Tinospora cordifolia* (Menispermaceae) was selected for pharmacological profiling towards the ECS, with particular focus on the inhibitory activity of the cellular uptake of AEA, based on broad ranging screening results and historical data presented in (Hoernle, 2011, Leonti and Casu, 2014). Leonti and Casu (2014) proposed that protoberberine alkaloids of *T. cordifolia* contributed to the psychoactive metabolites responsible for the psychedelic and euphoric effects associated with its consumption (Leonti and Casu, 2014), hypothesis which prompted the investigation of *T. Cordifolia* extract towards the ECS. The ethyl acetate extract of *T. cordifolia* was subjected to bio-guided fractionation with the help of chromatographic techniques with the aim to identify the secondary metabolites responsible for the inhibition of AEA uptake. The preliminary results obtained are presented in the Chapter 5, Section 5.2.

CHAPTER 3 - MATERIALS AND METHODS

3.1 Materials

Herbal drug samples extracted and screened in this study come from two different sources. One extract-library includes herbal drugs described and identified in Dioscorides' *DMM* (Matthioli, 1568). These were collected in different places around the Mediterranean area between 2014 and 2016 in an extensive botanical fieldwork, as part of the EU Project "*MedPlant"* (Staub et al., 2016). Plant specimens were identified and classified by Dr. P.O. Staub (Department of Biomedical Science, University of Cagliari). Botanical vouchers are deposited at the Herbarium of the Botanical Garden of Geneva (Switzerland) and at the Herbarium of the National and Kapodistrian University of Athens (ATHU). The collected herbal drug samples were dried at 40 – 60 °C and stored in plastic containers until extraction. The second extract library is based on the herbal drug collection obtained from the pharmaceutical company Dr. William Schwabe GmbH & Co. KG (Karlsruhe, Germany). *Psoralea corylifolia* fruits and *Tinospora cordifolia* stems were purchased from Kräuter Schulte (Germany).

Ethylacetate (EtOAc), hexane (Hex), acetonitrile (ACN), methanol (MeOH), ethanol (EtOH) dichloromethane (DCM) (99.8% purity), HPLC-grade MeOH, HPLC-grade ACN, ammonium acetate, dimethylsulfoxide (DMSO) and formic acid (FA) were purchased from Sigma Aldrich (Buchs, Switzerland). HPLC-grade EtOAc and Hex were obtained from Acros Organics (New Jersey, USA). Deionised water (18.2 MΩ × cm) was obtained from an ELGA Purelab Ultra Genetic system (VWS Ltd, ELGA LabWater, UK).

Sep-Pak® Vac 3 cc (500 mg) tC18 cartridges for Solid Phase Extraction (SPE), Silica gel 60 (0.040-0.063 mm) for Normal Phase chromatography, Silica gel 60 F_{254} Aluminium sheets and Silica gel C18 F_{254} glass sheets for Thin-Layer Chromatography (TLC) were purchased from VWR International (Milan, Italy).

Genistein (4',5,7-trihydroxyisoflavone), 7-hydroxyisoflavone, neobavaisoflavone (4',7-dihydroxy-3'-prenylisoflavone), daidzein (7,5'-dihydroxyisoflavone), auraptene (7-geranyloxycoumarin), farnesiferol A (7-[[(1S,4aS,6R,8aR)-6-hydroxy-5,5,8a-trimethyl-2-methylidene-3,4,4a,6,7,8-hexahydro-1H-naphthalen-1-yl]methoxy]chromen-2-one), 4',5,7-trihydroxy-6,8-diprenylisoflavone, berberine chloride hydrate (9,10-Dimethoxy-2,3-(methylenedioxy)-7,8,13,13a-tetrahydroberbinium), palmatine chloride hydrate (O,O-dimethyldemethyleneberberine), jatrorrhizine chloride (7,8,13,13a-tetradehydro-3-hydroxy-2,9,10-trimethoxyberbinium), 3-(4,5-dimethylthiazol-2-yl)-2,5-diphenyltetrazolium bromide (MTT), foetal bovine serum (FBS), RPMI 1640 medium, phosphate-buffered saline (PBS), trypsin, amphotericin B, Dulbecco's Modified Eagle Medium (1x) + Glutamax™-I, 2-[4-(2-hydroxyethyl)piperazin-1-yl]ethanesulfonic acid (HEPES), non-essential amino acids, sodium pyruvate, polyethylenimine (PEI) and G418 were purchased from Sigma Aldrich (Buchs, Switzerland). Biochanin A (5,7-dihydroxy-4'-methoxyisoflavone), farnesiferol B

(7-[(E)-5-[-3-hydroxy-2,2-dimethyl-6-methylidenecyclohexyl]-3-methylpent-2-enoxy] chromen-2-one), faselol (7-[[(1R,4aS,6R,8aR)-6-hydroxy-2,5,5,8a-tetramethyl-1,4,4a,6,7,8-hexahydronaphthalen-1-yl]methoxy]chromen-2-one) were purchased from InterBioScreen (Chernogolovka, Russia). Wighteone (5,7,4'-trihydroxy-6-prenylisoflavone), luteone (2',4',5,7-tetrahydroxy-6-prenylisoflavone), lupiwighteone (5,7,4'-trihydroxy-8-prenylisoflavone), licoisoflavone A (2',4',5,7-tetrahydroxy-3-prenylisoflavone) were purchased from Ambiter Green Pharma (Orléans, France). 8-Prenylluteone, barpisoflavone (2',4',7-trihydroxy-5-methoxyisoflavone), isolupialbigenina (4',5,7-trihydroxy-3',8-diprenylisoflavone), isoangustone A (4',5',5,7-tetrahydroxy-3',6-diprenylisoflavone) were purchased from AnalytiCon discovery GmbH (Postdam, Germany). [1-^{3}H]-ethanolamide ([^{3}H]-AEA) (specific activity 60 Ci/mmol) and [1,2,3-^{3}H]-2-monooleoyl glycerol ([^{3}H]-2-OG) (specific activity 60 Ci/mmol) were purchased from American Radiolabelled Chemicals Inc (Saint Louis, MO, US). AEA, UCM707, OMDM2, WWL70, THL, JZL184, URB597 and all the analytical and internal standards for LC-MS analyses (5*Z*,8*Z*,11*Z*,14*Z*-eicosatetraenoic acid (arachidonic acid, AA), 5*Z*,8*Z*,11*Z*,14*Z*-eicosatetraenoic-5,6,8,9,11,12,14,15-d_8 acid (AA-d_8), *N*-(2-hydroxyethyl)-5*Z*,8*Z*,11*Z*,14*Z*-eicosatetraenamide (AEA), *N*-(2- hydroxyethyl-1,1,2,2-d_4)- 5*Z*,8*Z*,11*Z*,14*Z*-eicosatetraenamide (AEA-d_4), 5*Z*,8*Z*,11*Z*,14*Z*-eicosatetraenoic acid, 2-glyceryl ester (2-arachidonoylglycerol, 2-AG), 5*Z*,8*Z*,11*Z*,14*Z*-eicosatetraenoic acid (2-AG-d_5), *N*-(2- hydroxyethyl)-9*Z*,12*Z*-octadecadienamide (*N*-linoleoylethanolamide, LEA), *N*-(2-hydroxyethyl-1,1,2,2-d_4)-9*Z*,12*Z*-octadecadienamide (LEA-d_4), *N*-(2-hydroxyethyl)-9*Z*-octadecenamide (*N*-oleoylethanlonamide, OEA), *N*-(2-hydroxyethyl-1,1,2,2-d_4)-9*Z*-octadecenamide (OEA-d_4), *N*-(2-hydroxyethyl)-hexadecanamide (*N*-palmitoylethanolamide, PEA), *N*-(2-hydroxyethyl)-hexadecanamide-15,15,16,16,16-d_5 (PEA-d_5)) were purchased from Cayman Chemical Company (Tallinn, Estonia). 2-OG was purchased from Santa Cruz Biotechnology (Dallas, Texas, US). CP55,940 [side chain-2,3,4-^{3}H(N)] (specific activity 164.9 Ci/mmol), Ultima Gold Scintillation cocktail and MicroScint20 scintillation liquid, Unifilter-92 GF/B plates were purchased from PerkinElmer. WIN 55,212-2 was purchased from PerkinElmer Life Science (Waltham, MA, USA). MercaChem Company (Nijmegen, The Netherlands) synthesized RX055. TAMRA-FP serine hydrolase probe was purchased from Thermo Fisher Scientific (Waltham, MA, US). Farnesiferol C (7-[(E)-3-methyl-5-[(1R,3R,4S)-2,2,4-trimethyl-7-oxabicyclo[2.2.1]heptan-3-yl]pent-2-enoxy]chromen-2-one), colladin ([(2R,4aR,5R,8aS)-1,1,4a-trimethyl-6-methylidene-5-[(2-oxochromen-7-yl)oxymethyl]-3,4,5,7,8,8a-hexahydro-2H-naphthalen-2-yl] acetate), samarcandin (7-[[(1S,2R,4aR,6R,8aS)-2,6-dihydroxy-2,5,5,8a-tetramethyl-3,4,4a,6,7,8-hexahydro-1H-naphthalen-1-yl]methoxy]chromen-2-one), kataravicinol (7-[(2E,6E)-10,11-dihydroxy-3,7,11-trimethyldodeca-2,6-dienoxy]chromen-2-one), colladonin (7-[[(1R,4aS,6R,8aR)-6-hydroxy-5,5,8a-trimethyl-2-methylidene-3,4,4a,6,7,8-hexahydro-1H-naphthalen-1-yl]methoxy]chromen-2-one) and umbelliprenin (7-[(2E,6E)-3,7,11-trimethyldodeca-2,6,10-trienoxy]chromen-2-one), isolated from *Ferula* species, were kindly given by Prof. Giovanni Appendino (Università del Piemonte Orientale, Faculty of Pharmacy, Novara , Italy).

Human monocytic leukaemia cells (U937), human embryonic kidney cells (HEK293), Chinese hamster ovary cells (CHO-K_1) and HeLa cells were purchased from the American Type Culture Collection, ATCC (Manassas, VA, US). C57BL76 male and female mice 9-10 weeks old, used for mouse brain membranes preparations, were obtained from Janvier Labs (Le Genest Saint Isle, France).

3.2 Methods

3.2.1 Plant extraction

In order to cover a wide range of secondary metabolites to extract, ethyl acetate was chosen as solvent for the extraction of the medicinal plants. Air-dried plant material was subjected to percolation with ethyl acetate at room temperature. After exhaustive percolation, the solvent was removed by using a rotary evaporator at 40 °C to obtain the crude extract from each sample. Extracts were stored at -20 °C until use.

3.2.2 Bio-guided fractionation of *Tinospora cordifolia* ethyl acetate extract

Vacuum Liquid Chromatography (VLC) and Liquid Chromatography (LC) were used for the fractionation of the EtOAc extract of *T. cordifolia*. Bioactivity (i.e. inhibition of the uptake of AEA) was used as a lead during the fractionation and isolation process. Chromatographic studies were conducted at the Department of Life and Environmental Sciences of the University of Cagliari (Italy) while the evaluation of the biological interaction with the ECS was conducted at the Institute of Biochemistry and Molecular Medicine of the University of Bern (Switzerland).

3.2.2.1 Vacuum Liquid Chromatography

Forty grams of crude EtOAc extract of dried *T. cordifolia* stems were subjected to a first fractionation through VLC in Normal Phase (NP-VLC), using 450 g of Silica gel 60 (0.040-0.063 mm) as stationary phase and DCM/EtOAc (9:1) with EtOAc step gradients as mobile phase. The fractionation was monitored by TLC observation. Sixteen fractions (1-16) were obtained from the VLC. Fractions 11 and 12 (810 mg in total), showing the highest AEA uptake inhibition, were selected for further processing. Fractions 11 and 12 were pooled in one fraction (to which I will refer as 11) and subjected to a further NP-VLC using 260 g of Silica gel 60 (0.040-0.063 mm) as stationary phase and a solvent system consisting of Hex/EtOAc (5:5) with EtOAc step gradients as mobile phase. The separation was monitored using TLC and finally thirteen fractions (11.1-11.13) were obtained.

3.2.2.2 Liquid Chromatography

Normal Phase liquid chromatography (NP-LC) was used for the study of the active fraction **11.5** (112 mg). 110 mg of Silica gel 60 (0.040-0.063 mm) were used as stationary phase, and a solvent system of

Hex/EtOAc (8:2) with EtOAc step gradient as mobile phase. The separation was monitored with TLC and seven fractions (11.5.1-11.5.7) were obtained.

3.2.2.3 Further Fractionation

Chromatographic purification by solid-liquid partition (Reverse Phase SPE (RP-SPE)) was used in the final fractionation steps of active fractions 11.5.3 (3), 11.5.4 (4), 11.5.5 (5), 11.6 (6), 11.7 (7) and 11.8 (8). Sep-Pak® Vac 3 cc tC 18 cartridges were pre-conditioned with ACN. The samples were dissolved in 1 ml of H_2O/ACN (5:5) and loaded on the cartridge. The elution of the samples was performed with H_2O/ACN (5:5) with ACN step gradient.

3.2.3 Cell culture

All cell types were grown in a humidified incubator at 37 °C and 5% CO_2. U937 cells and HeLa cells were cultured in RPMI 1640 medium supplemented with 10% FBS. *h*CB_1 and *h*CB_2-expressing CHO-K1 cells were cultured in RPMI 1640 medium supplemented with 1 g·ml^{-1} amphotericin B and 400 mg·ml^{-1} G418. HEK293 human embryonic kidney cells were cultured in Dulbecco's Modified Eagle Medium (1x) + Glutamax^{TM}-I supplemented with 1% HEPES, 1% non-essential amino acids, 1% sodium pyruvate, 10% FBS and 0.5% G418. *h*ABHD6 and *h*ABHD12 stably transfected HEK293 cells were transfected following a protocol previously described (Chicca et al., 2017) and cultured in the same media as wild type HEK293 cells (Raduner et al., 2006).

3.2.4 MTT assay

Colorimetric MTT method was used to evaluate the metabolic activity of HeLa cells treated with the plant extracts. A suspension of 20'000 cells·ml^{-1} in RPMI medium (supplemented with 10% of FBS) was prepared. The suspension was seeded in 96-well plates and incubated for 24 hours at 37 °C in 5% CO_2 atmosphere. After 24 hours, plant extracts at a concentration of 25 µg·ml^{-1} were added. Plates were incubated for 72 hours at 37 °C in 5% CO_2. After the 72 hours, the old medium was removed and fresh RPMI medium and the MTT solution (final concentration of 0.5 mg·ml^{-1}) were added and cells incubated for additional four hours. Finally, the purple formazan precipitate was solubilised by adding 200 µl of DMSO. The absorbance at 550 nm was determined by spectrophotometry. The results are expressed as percentage of cell viability compared to the DMSO control. Blank control was obtained by using the same conditions for the DMSO control without the cells. Each assay was carried out in triplicate.

3.2.5 Preparation of cell homogenates

3.2.5.1 Preparation U937 cell homogenates for the FAAH and MAGL assay

After culture until confluence, U937 cells were washed with cold sterile PBS and centrifuged at 1'200 rpm for 5 minutes at 4 °C. The supernatant was discarded and the pellet re-suspended in a proper

volume of 10 mM TRIS-HCl 1 mM EDTA buffer at pH 7.6 (the same used for the assay). The cell suspension was homogenized over ice with the Polytron at 30 rpm for about 30 seconds and the resulting homogenate was stored at -80 °C until further use.

3.2.5.2 Preparation of HEK293 cell homogenates for the ABHD assay

After culture until confluence, HEK293 cells were washed twice with cold sterile PBS and centrifuged at 1'200 rpm for 5 minutes. The supernatant was discarded and the pellet re-suspended in 10 mM TRIS-HCl 1 mM EDTA buffer at pH 7.6 (the same used for the assay). The cell suspension was homogenized over ice with the Polytron at 30 rpm for 30 seconds. The protein concentration was determined with the BCA protein assay method.

3.2.6 Membrane preparation

3.2.6.1 *h*CB_1 and *h*CB_2 transfected CHO-K_1 cell membranes

CHO-K_1 cells stably transfected with *h*CB_1 or *h*CB_2 receptors were cultured until confluence with RPMI 1640 medium supplemented with 400 $mg \cdot ml^{-1}$ of G418. The cells were washed twice with cold sterile PBS and centrifuged at 1'200 rpm for 5 minutes. The supernatant was discarded and the pellet re-suspended in 50 mM TRIS-HCl, 2.5 mM EDTA, 5 mM $MgCl_2$ buffer at pH 7.4, (the same used for the assay) and homogenized over ice with the Polytron at 30 rpm for a few minutes. The homogenate was centrifuged at 2'000 rpm for 7 minutes at 4 °C. The supernatant was collected and distributed in ultracentrifugation tubes and centrifuged at 32'000 rpm for 1 hour at 4 °C. The supernatant obtained after centrifugation was discharged and the pellet re-suspended in PBS and put in the ultrasonic bath for 5 minutes. The solution was passed through a syringe several times to disrupt the aggregates and homogenize the preparation. Protein concentration was measured using the BCA method and the aliquots frozen and stored at -80 °C until further use.

3.2.6.2 Mouse brain membranes

Fresh mouse brain tissue was homogenized over ice with the Polytron at 30 rpm for 2 minutes. The homogenates were then centrifuged at 2'000 rpm for 7 minutes at 4 °C. The supernatant was collected and distributed in ultracentrifugation tubes and centrifuged at 32000 rpm for 1 hour at 4 °C. The supernatant was discharged and the pellet was re-suspended in PBS and placed in the ultrasonic bath for 5 minutes. The solution was passed through a syringe several times to disrupt the aggregates and homogenize the preparation. Protein concentration was measured using the BCA method and the aliquots frozen and stored at -80 °C until further use.

3.2.7 AEA hydrolysis inhibition assay (FAAH assay)

The FAAH assay was used to evaluate the capability of plant extracts or pure compounds to inhibit the enzymatic degradation of AEA. The assay was performed using intact and homogenized U937 cells and mouse brain membranes, following a method previously described (Chicca et al., 2009) with some minor readjustments.

3.2.7.1 Assay in U937 cells

The assay was performed in 10 mM TRIS-HCl, 1 mM EDTA activity buffer at pH 8.0, supplemented with 0.1% (m/v) of fatty acid free BSA. Either cell homogenates or intact cells were suspended in the activity buffer (final concentration of 10^6 cells per sample) and 300 µl of the suspension distributed in AquaSil™ silanized tubes (Thermo Fisher Scientific, MA, USA). Controls, compounds or plant extracts were pre-incubated with either the homogenized or the intact cells for 15 and 30 minutes, respectively, at 37 °C and 400 rpm. 100 nM of AEA mixture (0.5 nM of [^{3}H]-AEA and 99.5 nM of AEA) was incubated for 15 minutes (at 37 °C and 400 rpm). The reaction was stopped by adding 600 µl of a mixture of CH_3Cl/MeOH (1:1). The samples were centrifuged at 0 °C and 13'000 rpm for 10 minutes and the aqueous phase (containing the [^{3}H]-ethanolamine) recovered and transferred into vials containing 3 ml of Ultima Gold Scintillation cocktail. The radioactivity of the phase was measured by liquid scintillation counting on a Tri-Carb 2100 TR liquid scintillation analyser. To ensure that our assay could effectively measure FAAH activity, the synthetic inhibitor URB597 was always used as positive control. As negative control (vehicle), we used DMSO 1% . This concentration was chosen based on previous published results indicating that it does not affect the measurements (Chicca et al., 2009, Nicolussi et al., 2014a, Nicolussi et al., 2014b, Chicca et al., 2017). The results were expressed as hydrolysis of [^{3}H]-AEA in percentage of the vehicle treated control (=100%). Blank values were obtained by the use of activity buffer without either the homogenate or the cells. Each assay was carried out in duplicate.

3.2.7.2 Assay in mouse brain membranes

The assay was performed with 10 mM TRIS-HCl, 1 mM EDTA activity buffer at pH 8.0, supplemented with 0.1% (m/v) of fatty acid free BSA. 20 µg of protein per sample was suspended in the activity buffer until the final volume of 300 µl. The protocol used is the same as previously described for U937 cell homogenates. DMSO 1% and URB597 100 nM were used as negative and positive control of FAAH inhiition, respectively. The results were expressed as hydrolysis of [^{3}H]-AEA in percentage of the vehicle treated control (=100%). Blank values were obtained by the use of activity buffer without membranes. Each assay was carried out in duplicate.

3.2.8 Kinetic experiments

The assays were performed using mouse brain membranes, following the protocol previously described for the FAAH assay. Mouse brain membranes were incubated with the endogenous substrate AEA at increasing concentrations (from 0.01 to 10 µM), either in absence or presence of inhibitors at two different concentrations. For the inhibitors, a concentration below and above their IC_{50} values was chosen (25 nM and 100 nM for neobavaisoflavone and 100 nM and 500 nM for luteone). Results were expressed as pmol of [^{3}H]-AEA hydrolysed·min^{-1}·mg^{-1} of protein. V_{max} and K_m values were calculated using the Michaelis-Menten function. Line Weaver-Burk plots were used to confirm the competitive nature of the inhibition. K_i values for the two inhibitors were calculated from the IC_{50} values and kinetic parameters, using the Cheng-Prusoff equation.

3.2.9 Rapid dilution assay

The rapid dilution assay was used to test whether the two isoflavonoids neobavaisoflavone and luteone bound to the FAAH enzyme in a reversible or irreversible way. The assay was performed using the protocol for the FAAH assay in mouse brain membranes described before, but with a 1:10 dilution of the reaction volume between the pre-incubation and the incubation steps. DMSO 1% and URB597 100 nM were used as negative and positive control for FAAH inhibition, respectively. Results were expressed as hydrolysis of [^{3}H]-AEA in percentage of the vehicle treated control (=100%). Blank values were obtained by the use of activity buffer without the membranes. Each assay was carried out in duplicate.

3.2.10 AEA uptake inhibition assay in U937 cells

AEA uptake inhibition assay was used as a lead in the investigation of the ethyl acetate extract of *T. cordifolia* and its fractions. The assay was performed following a protocol previously described (Chicca et al., 2012) with some adjustments. A suspension of 10^6 intact cells per sample was used in a final volume of 500 µl. The samples were screened at the concentration of 5 µg·ml^{-1}. Controls or samples were pre-incubated with the cells for 20 minutes at 37 °C and 400 rpm. 5 µl of AEA mixture (100 nM of AEA and 1 nM of [^{3}H]-AEA) was then added and incubated for 15 minutes at 37 °C and 400 rpm. The reaction was stopped by placing the tubes on ice and centrifuging them for 5 minutes at 10'000 rpm and 4 °C. The supernatant was discarded and the pellet re-suspended in 300 µl of cold 1% BSA in PBS (washing steps). The samples were centrifuged again for 5 minutes at 10'000 rpm and 4 °C, the supernatant discarded and the washing step was repeated. After discarding the supernatant, 250 µl of cold PBS and 1 ml of CH_3Cl/MeOH (1:1) were added and the samples were centrifuged at maximum speed for 10 minutes at 4 °C. The organic phase (containing the intracellular [^{3}H]-AEA) was recovered and transferred into vials with 3 ml of Ultima Gold Scintillation cocktail. The radioactivity of the phase was measured by liquid scintillation counting on Tri-

Carb 2100 TR liquid scintillation analyser. The results were expressed as [^{3}H]-AEA intracellular accumulation in percentage of the vehicle treated control (=100%). Each assay was carried out in triplicate.

3.2.11 *h*CB$_1$ and *h*CB$_2$ receptors radio-ligand binding assay

*h*CB$_1$ and *h*CB$_2$ receptors radio-ligand binding assay was used to test the ability of plant extracts or pure compounds to bind to CB$_1$/CB$_2$ receptors. To address it, the ability of the analyzed samples to displace the synthetic CB$_1$/CB$_2$ receptor ligand [^{3}H]-CP-55,940 from the binding site was evaluated. The assay was performed using a previously described protocol (Raduner et al., 2006, Gertsch et al., 2008). 10 µg of membranes of *h*CB$_1$ or *h*CB$_2$ receptors-transfected CHO-K1 cells per sample were used, re-suspended in the assay buffer (50 mM TRIS-HCl, 2.5 mM EDTA, 5 mM $MgCl_2$, 0.5% fatty acid free BSA, pH 7.4) together with the [^{3}H]-CP-55940 at the concentration of 0.25 nM per sample. The solution was distributed into AquaSil™ silanized glass tubes. Controls and compounds were incubated for 1 hour with the membrane preparation at 30 °C. After the incubation time, the solution was transferred in a Unifilter-92 GF/B plate and the filters (previously washed with a solution of 0.05% of PEI) were washed several times with 150 µl per well of ice-cold assay buffer supplemented with 0.5% fatty acid free BSA. 50 µl of MicroScint20 scintillation liquid was added and the radioactivity was measured with the 1450 MicroBeta Trilux top counter. DMSO was used as negative control and the ligand WIN 55,512-2 10 µM to determine the non-specific binding (around 3%). Non-specific binding was subtracted for each value and the results were expressed as percentage of [^{3}H]-CP-55940 bound to the receptors compared to the vehicle treated control (=100%). Each assay was carried out in triplicate.

3.2.12 2-OG hydrolysis inhibition assay (MAGL assay)

2-oleoylglycerol (2-OG) hydrolysis inhibition assay was used to evaluate the ability of the FAAH inhibitors neobavaisoflavone and luteone to inhibit also the enzyme MAGL in intact U937 cells.

The assay was performed using a procedure previously described with some modifications (Ghafouri et al., 2004, Bjorklund et al., 2010). A suspension of 10^6 cells per sample was added to the activity buffer (10 mM TRIS-HCl, 1 mM EDTA pH 8.0, 0.1% (m/v) of BSA) and distributed in silanized tubes, to a final volume of 500 µl. URB597 500 nM was added to each sample, to inhibit FAAH enzyme and to delete a potential radioactive signal given by its hydrolytic activity on 2-OG. Controls and compounds (final concentration of 10 µM) were pre-incubated with the cells for 30 minutes at 37 °C and 500 rpm. A 2-OG mixture (containing 1 nM of [^{3}H]-2-OG and 10 µM of 2-OG) was added and incubated for 15 minutes at 37 °C and 400 rpm. The enzymatic reaction was stopped by adding 1 ml of a CH_3Cl/MeOH (1:1) mixture. The samples were centrifuged at 0 °C and 10'000 rpm for 10 minutes. The aqueous phase (containing the [^{3}H]-2-OG) was recovered and transferred into vials with 3 ml of Ultima Gold Scintillation cocktail. The radioactivity of the phase was measured by liquid scintillation counting on a Tri-Carb 2100 TR liquid

scintillation analyser. DMSO and JZL184 10 µM were used as negative and positive control for MAGL inhibition, respectively. The results were expressed as hydrolysis of [^{3}H]-2-OG in percentage of the vehicle treated control (=100%). Blank values were obtained by the use of activity buffer without the cells. All experiments were performed in duplicate.

3.2.13 α/β-hydrolase 6 and α/β-hydrolase 12 inhibition assay

ABHD6 and ABHD12 inhibition assay was used to evaluate the ability of the FAAH inhibitors neobavaisoflavone and luteone to inhibit also the enzyme α/β-hydrolase 6 and α/β-hydrolase 12.

The assay was performed using ABHD12 or ABHD6 transfected HEK293T cell homogenates. 40 µg of protein per sample was suspended with the activity buffer (10mM TRIS-HCl, 1 mM EDTA pH 7.6, 0.4% (m/v) BSA, 46.5% PBS) to a final volume of 200 µl. 2 µl of compounds (at the concentration of 10 µM) or controls were pre-incubated with the homogenate for 30 minutes at 37 °C and 400 rpm. Afterwards a 2-OG mixture (1.25 nM of [^{3}H]-2-OG and 10 µM of 2-OG) was incubated for 5 minutes at 37 °C and 400 rpm. The reaction was stopped by adding 400 µl of a mixture of CH_3Cl/MeOH (1:1). The samples were centrifuged at 0 °C, and 13'000 rpm for 10 minutes. The aqueous phase (containing [^{3}H]-2OG) was recovered and transferred into vials with 3 ml of Ultima Gold Scintillation cocktail. The radioactivity of the phase was measured by liquid scintillation spectroscopy. Wild type HEK293T cells were used as blank, DMSO was used as negative control and THL 20 µM and WWL70 10 µM as positive controls for ABHD12 and ABHD6 inhibition, respectively. The results were expressed as percentage of [^{3}H]-OG hydrolysis in percentage of the vehicle treated control (=100%). Each assay was carried out in duplicate.

3.2.14 Activity-based protein profiling

Activity-based protein profiling (ABPP) was used to investigate the capability of the isoflavonoids to bind to serine hydrolase such as FAAH, MAGL and ABHDs. The protocol used was based on a previously described method (Baggelaar and Van der Stelt, 2017) with some modifications. Controls and compounds were pre-incubated with mouse brain membrane proteome (2 $mg \cdot ml^{-1}$) for 20 minutes at room temperature. Then, the TAMRA-FP Serine Hydrolase probe (125 nM) was incubated for 20 or 5 minutes (depending on the scope of the assay) at room temperature. The reaction was quenched by adding 3x loading buffer (150 mM Tris-HCl pH 6.8, 6% sodium dodecyl sulphate (SDS), 0.15% bromophenol blue, 30% glycerol, β-mercaptoethanol 7.5%, 10 µl per sample). The samples were boiled at 90 °C for 10 minutes to allow the denaturation of the proteins, cooled down and centrifuged at room temperature for 1 minute. Then the samples were loaded on a 12% SDS-PAGE gel and the proteins were resolved by electrophoresis at 150 Volt for about 150 minutes. The gels were scanned using a Typhoon FLA 9500 scanner. DMSO was used as negative control while URB597 4 µM, JZL184 1 µM, WWL70 10 µM, and THL 10 µM as positive controls

for FAAH, MAGL, ABHD6 and ABHD12 inhibition, respectively. The gels were processed and analysed with the image processing software ImageJ2.

3.2.15 LC-MS/MS analysis

LC-MS/MS analyses were performed to measure the content of *N*-acylethanolamines in sixteen selected plant extracts, following a previously published method with some adaptations (Gachet et al., 2017). For this purpose, known concentrations of calibration standards and a mix of IS were used to generate a calibration curve, which was used for the quantification of the analytes of interest in the sixteen plant extracts. An IS is a compound spiked to every sample that is analysed and that has to behave similarly to the analyte but provides a signal that can be distinguished from that of the analyte. Therefore, the used internal standard mixture contained a deuterated version of each analyte that is measured and quantified in the method. Additionally, the ISs were used to control the instrument performance, the extraction efficiency (e.g. recovery, matrix effect, ionization), the variation of the method and finally as reference in the analysed extracts for the quantification. Standard mixtures used as calibrants (calibration solutions) and IS were prepared in EtOH at concentrations of 0.01 $mg \cdot ml^{-1}$ and later diluted accordingly. The concentrations of the IS used for the analysis were 400 $pg \cdot ml^{-1}$ for AEA-d_4, LEA-d_4, OEA-d_4 and PEA-d_5, 1 $ng \cdot ml^{-1}$ for 2-AG-d_5, and 30 $ng \cdot ml^{-1}$ for AA-d_8. The reported concentrations were obtained upon spiking 5 µl of a 10-fold concentrated solution into the extraction solution and the final volume after concentration and reconstitution of the sample was 50 µl. Triplicate eleven points calibrations were prepared in the appropriate plant matrix. The ratio (peak area of each analyte/peak area of internal standard) was calculated and used to ensure linearity of the method. The slope, the intercept, and the regression coefficient of those calibration lines were determined.

3.2.15.1 LC-MS/MS conditions

Analyses were conducted on a LC-MS/MS system consisting of a 5500 QTrap mass spectrometer equipped with a TurboIonSpray probe (AB Sciex Concord, Ontario, Canada) connected to a ExionLC AC UHPLC (AB Sciex Concord, Ontario, Canada). Data were acquired and processed using Analyst software version 1.6.3 (AB Sciex Concord, Ontario, Canada). Samples temperature was maintained at 4 °C in the auto-sampler prior to analysis. A Reprosil-PUR C18 column (3 µm particle size; 2 × 50 mm, Dr. A. Maisch, High Performance LC-GmbH, Ammerbuch, Germany) was used, maintained at 40 °C. The analysis was performed in the negative ionisation mode for AA, and in the positive mode for AEA, 2-AG, LEA, OEA and PEA. The source used nitrogen as a curtain gas and was operated at a capillary ion spray voltage of -4250 V in the negative and +4500 V in the positive mode, respectively. The temperature was at 600 °C, curtain gas at 30 psi, GS1 at 50 psi, GS2 at 50 psi, entrance potential at 10 V. Analyses were performed in the multiple reaction monitoring (MRM) mode using one quantifier ion (Q) and at least one qualifier ion (q). The schedule MRM function was applied in both scan modes (target scan time of 1 sec and MRM detection

window of 60 sec). Two identical enhanced product ion scans (EPI) were recorded over a mass range of m/z 50-500 at a rate of 4000 amu/s using the linear ion trap with a fixed fill time of 50 ms, which enabled Q0 trapping and Q1 at unit resolutions. The system was operated in positive and negative mode with two different mobile phases and gradient methods. In positive mode the mobile phases were: water/ammonium acetate 2 mM/0.1% FA (solvent A) and MeOH/ammonium acetate 2 mM (solvent B). The gradient started at 15% B for 0.5 min, 15–70% B from 0.5 to 3.5 min, 70–99% B from 3.5 to 8.0 min and held at 99% from 8.0 to 12 min with subsequent re-equilibration at 15% for further 2.5 min. The flow rate was 0.35 ml·min^{-1}. In negative mode, the organic mobile phase (B) was substituted with ACN containing 0.1% formic acid. The gradient started at 5% B, increasing linearly to 40% at 3 min, then to 65% at 9 min and linearly again to 95% at 10 min; this was maintained until 14 min, with subsequent re-equilibration at 5% for further 3 min. The flow rate was 0.3 ml·min^{-1}. The following MRM transitions of the analytes and the IS were monitored: Positive mode: 2-AG m/z 379→287, 379→203 (IS: 2-AG-d5 384→287); AEA m/z 348→133, 348→62 (IS: AEA-d4 352→66); LEA m/z 324→109, 324→62 (IS: LEA-d4 328→66); OEA m/z 326→309, 326→62 (IS: OEA-d4 330→66), PEA m/z 300→283, 300→62 (IS: PEA-d5 305→62); Negative mode: AA m/z 303→259, 303→59 (IS: AA-d8 311→59).

3.2.15.2 Preparation of samples

100 µg of plant extracts were added to a 0.1 M FA solution in water and rapidly transferred to glass tubes on ice, containing 1.5 ml of a mixture of EtOAc/Hex (9:1) with 0.1% FA and 5 µl of the IS mixture. Samples were strongly vortex for 20 seconds, sonicated in a cold bath for 5 min, and subsequently centrifuged at 3'000 rpm for 10 min at 4°C. Samples were then kept for 10 min in dry ice to freeze the aqueous phase. The upper organic phase was transferred in plastic tubes, evaporated and the extracts reconstituted in 50 µl of ACN/water (8:2). 10 µl of the solution were injected in the LC-MS/MS system.

3.2.16 Statistical analysis

All graphs, calculations and analyses were made using GraphPad Prism 5.0 program (GraphPad Software, CA, US). Results were expressed as mean ± SEM and were calculated as percentage of vehicle control, if not mentioned otherwise. IC_{50} values were calculated using the Non-Linear regression and the log(inhibitor) vs. response -- Variable slope (four parameters) function. EC_{50} values were calculated using the log(agonist) vs. response -- Variable slope (four parameters) function. K_m and V_{max} values were calculated using the Michaelis-Menten function. K_i values were calculated using the Non-Linear regression plots of the K_m^{app}/V_{max} as a function of the inhibitor concentration.

3.2.17 Molecular docking experiments

Molecular docking experiments were performed to better study the inhibitory activity of neobavaisoflavone and luteone on FAAH-1. Molecular docking is a computational procedure able to predict

the putative binding mode of one or more compounds with respect to a specific target structure. In order to asses this study, it is necessary to prepare the 3D structure of the target and the ligands.

3.2.17.1 Characterization and analysis of the FAAH-1 protein

The FAAH-1 mouse protein sequence was obtained from UniProt (http://www.uniprot.org/) and submitted to NCBI-Protein Blast (https://blast.ncbi.nlm.nih.gov/Blast.cgi?PAGE=Proteins) (Altschul et al., 1990, Boratyn et al., 2012) in order to check the availability of a 3D structure in the Protein Data Bank (PDB) (Berman et al., 2002). The FASTA sequence of mouse FAAH-1 is represented in Supplementary Figure 1. From this analysis, it was possible to observe that in the PDB the 3D structure of the target is not available. However, there are several 3D structures for FAAH-1 rat and FAAH-1 humanized (a protein where some residues have been mutated in order to obtain a binding pocket similar to the human one). The FAAH-1 humanized shows the sensitivity profile of the human FAAH inhibitor but maintains the high expression of the rat enzyme. Moreover, the rat and humanized structure sequences share respectively the 92% and the 91% of identity with the query mouse sequence. Therefore, these were considered for multiple sequence alignment by means of Clustal Omega tool (https://www.ebi.ac.uk/Tools/msa/clustalo/) (Sievers et al., 2011) (Supplementary Figure 2). The amino acids in the binding pocket were compared to define the differences between them (Supplementary Figure 3). In this site, only one difference was found between rat and mouse enzymes: F194 is substituted by a tyrosine. Instead, four binding pocket residues are different in the humanized enzyme: i.e. L192F, A377T, I491V, V495M. Therefore, we concluded that the 3D model of the rat enzyme is suitable for docking experiments to reproduce the experimental conditions of the biological assay. Furthermore, the 3D structure alignment of rat (pdb code 3QK5) (Gustin et al., 2011) and humanized rat (pdb code 3PPM) (Mileni et al., 2011) shows that the mutations of L192F and I491V may affect the binding mode of inhibitors since they have a different steric hindrance.

3.2.17.2 Validation of the protocol

In order to validate the docking protocol, we have carried out self and cross docking experiments. Fourteen complexes available in the PDB were selected and prepared (Supplementary Table 1).

For the preparation of the ligand, theoretical 3D models of compounds have been downloaded from the PDB. Most of the compounds bind covalently FAAH-1. For these, the docked compound mimics the covalently bound ligand without the covalent bond with Serine241, with O-, or the hydrolyzed compound bound to the enzyme. Ligands were protonated at physiological pH by means of LigPrep protocol (LigPrep, Schrödinger, LLC, New York, NY, 2018) and docked in the global minimum energy conformation. The most stable conformation has been determined by molecular mechanics conformational analysis performed with Macromodel software version 9.2 (Mohamadi et al., 1990). In particular by applying MMFFs (Merck molecular force fields) (Halgren, 1996) and GB/SA water implicit solvation model

(Kollman et al., 2000) using Polak-Ribier Conjugate Gradient (PRCG) method, 5000 iterations and a convergence criterion of 0.05 kcal/mol·Å. All the other parameters were left as default. New ligands tested were designed and then submitted to the conformational search applying the same protocol described above.

Since rat and humanized rat binding pockets are slightly different, in the docking validation experiments both have been considered. Specifically, it was selected the crystal structure with the best resolution for the rat enzyme (pdb code 3QK5, 2.20 Å) and the humanized rat (pdb code 3PPM, 1.78 Å). Protein preparation (optimization and minimization) was performed starting from protein structure model (imported from PDB), using Protein Preparation Wizard module in Maestro Graphical User Interface (GUI) (2018). Hydrogen atoms were added, bond orders were assigned and all the water molecules were analyzed and then removed because not structural. The protein crystal structure was subjected to a minimization that was performed until the average root-mean-square-deviation (RMSD) of the non-hydrogen atoms reached 0.3 Å.

Docking experiments were performed using Glide-SP (Friesner et al., 2004), Glide-XP (Friesner et al., 2006), Quantum-mechanical polarized Docking (QMPL) (Cho et al., 2005) and leaving all the default parameters. RMSD between the crystallographic pose and the best binding pose of each compound ranked by Glide score were calculated. The validated protocol was then applied to dock the new compounds. For the post-docking experiments, the best two complexes for each selected ligand were generated using the Merge tool in Maestro GUI and energy minimized. For energy minimization, Optimized Potential for Liquid Simulations (OPLS)-2005 was considered as force field and water as a solvent. The simulation was performed using the PRCG method with a maximum of 10000 interactions and converge threshold of 0.1 kcal/mol·Å.

CHAPTER 4 – RESULTS

Identification of Prenylated Isoflavonoids as Potent, Selective and Reversible Fatty Acid Amide Hydrolase Inhibitors

Bioactivity screening of medicinal plant extracts shows a phylogenetic clustering for inhibition of FAAH activity in Fabaceae

Plant extracts were screened with respect to their capability to inhibit the hydrolysis of AEA by FAAH in U937 cell homogenates. The results of the screening were presented using a phylogenetic tree in order to highlight the relationships across the herbal species included in this study (Figure 17). The tree was created by using the online tree generator tools phyloT© 2018 and iTOL (Letunic and Bork, 2007) and by inserting the accepted Latin binomials of the respective plant species (The Plant List, 2013). For the generation of the tree, each specific plant species (Latin binomial) could be included only once. Therefore, when a botanical species was associated with more than one herbal drug type (e.g. roots and leaves), the one having the highest potency of FAAH inhibition was chosen. In the Supplementary Table 3, the results of the screening for all the extracts are shown. The results are expressed as percentage of FAAH inhibition exerted by the plant extract at the concentration of 10 $\mu g \cdot ml^{-1}$ (Figure 17). "Hits" were considered those plant extracts, which inhibit FAAH activity > 80% at the concentration of 10 $\mu g \cdot ml^{-1}$. Using these criteria, eleven hits were identified. Interestingly, six of the eleven herbal extracts were from the Fabaceae family: *Lupinus angustifolius*, *Glycyrrhiza glabra*, *Glycyrrhiza uralensis*, *Psoralea corylifolia*, *Anagyris foetida* and *Medicago arborea* (Figure 17 and Supplementary Table 3). This suggests a phylogenetic clustering of FAAH inhibition potential of Fabaceae extracts.

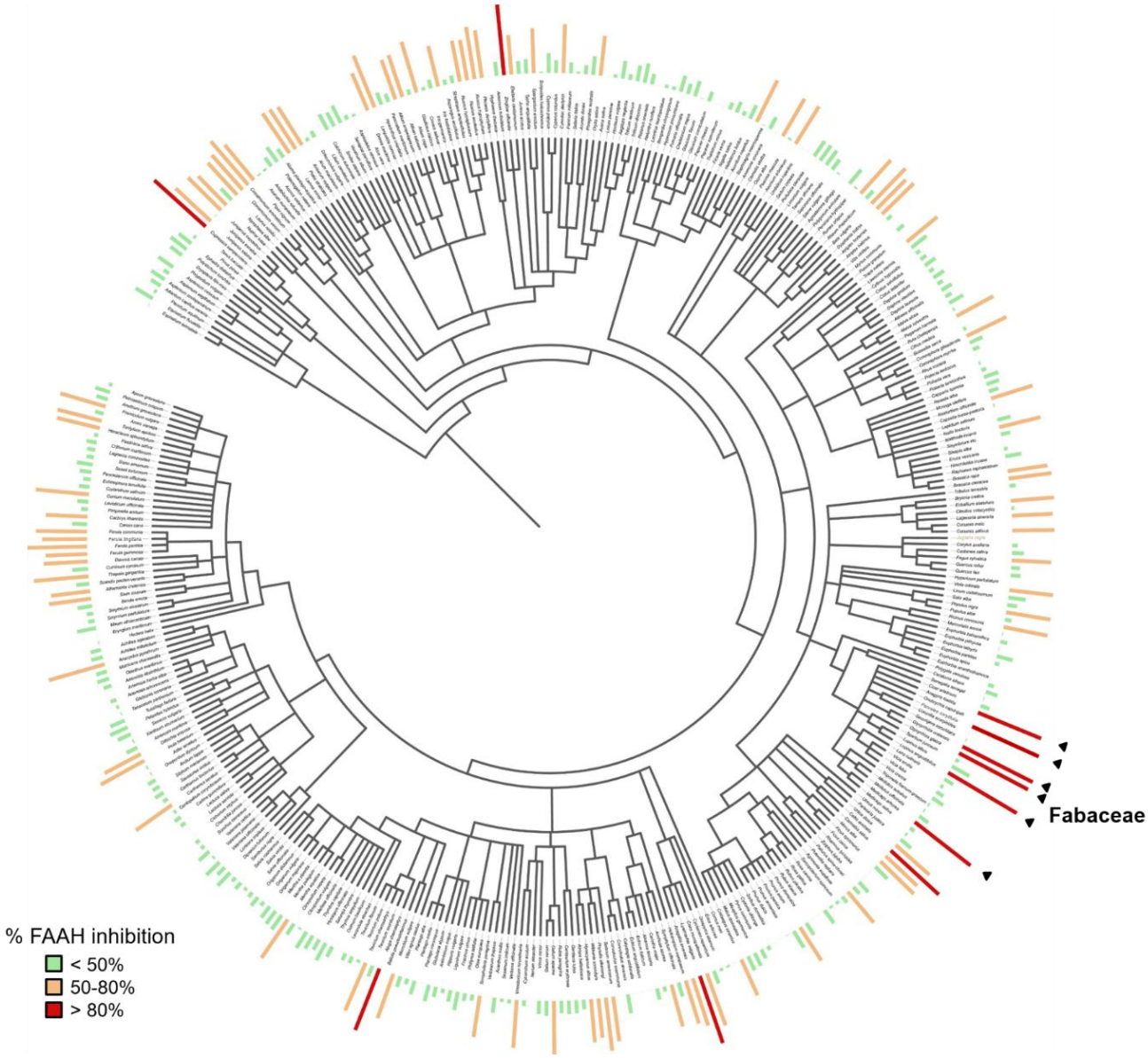

Figure 17. A phylogenetic distribution of FAAH inhibition is observed in the Fabaceae family. Representation of 450, out of 762 screened plant extracts of the two libraries, with corresponding percentage of FAAH inhibition. The ethyl acetate plant extracts were tested at 10 μg·ml^{-1} with respect to their ability to inhibit the hydrolysis of 100 nM of [^{3}H]-AEA mediated by FAAH in U937 cell homogenates. FAAH, Fatty acid amide hydrolase.

For the four most active plant extracts (*L. angustifolius*, *G. glabra*, *G. uralensis* and *P. corylifolia)*, a full concentration-dependent inhibition of FAAH activity was assessed resulting is the following IC_{50} values: 756.7 ng·ml^{-1} for *L. angustifolius*, 866.5 ng·ml^{-1} for *G. glabra*, 253.5 ng·ml^{-1} for *G. uralensis* and 502.5 ng·ml^{-1} for *P. corylifolia*.

LC-MS/MS quantification of N-acylethanolamines in plant extracts

Four potent FAAH inhibitor plant extracts plus other twelve, selected on the base of their different FAAH inhibition potency, were chosen for quantification of their NAE levels. With this quantification, the

hypothesis that FAAH inhibition potency may be correlated with the content of NAEs in the plant extracts, as consequence of an endogenous inhibition of NAEs hydrolysis, was tested. LC-MS/MS quantification indicated three major NAEs present in the plant extracts, i.e. LEA, OEA and PEA. Figure 18 shows the absence of relationship between the FAAH inhibition potency and the detected NAE levels in the extracts.

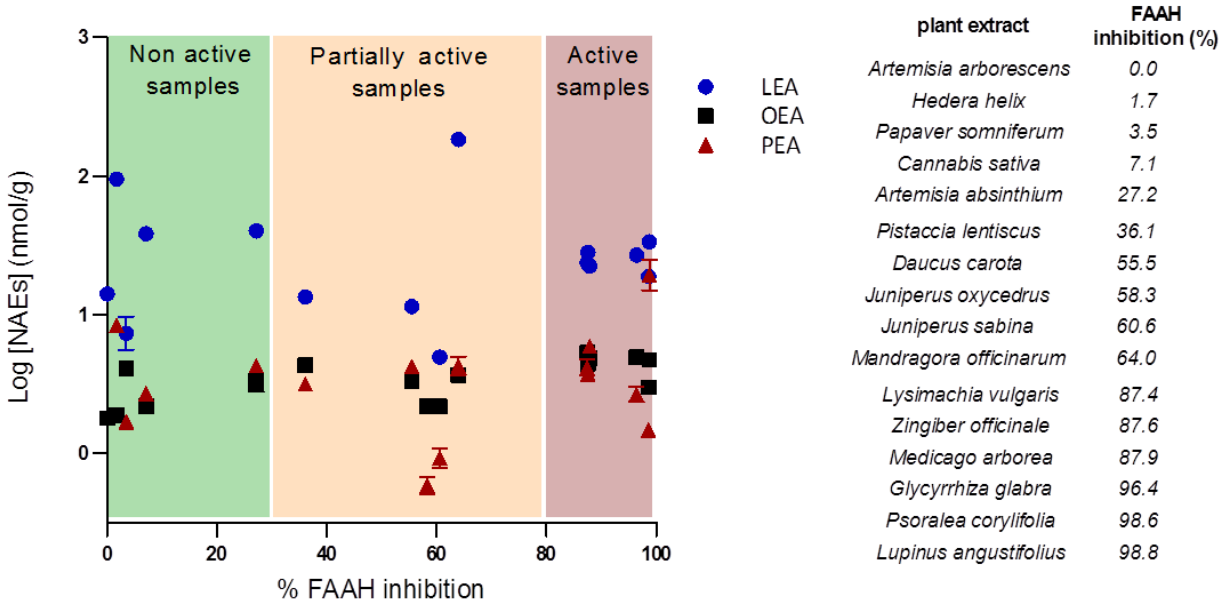

plant extract	FAAH inhibition (%)
Artemisia arborescens	0.0
Hedera helix	1.7
Papaver somniferum	3.5
Cannabis sativa	7.1
Artemisia absinthium	27.2
Pistaccia lentiscus	36.1
Daucus carota	55.5
Juniperus oxycedrus	58.3
Juniperus sabina	60.6
Mandragora officinarum	64.0
Lysimachia vulgaris	87.4
Zingiber officinale	87.6
Medicago arborea	87.9
Glycyrrhiza glabra	96.4
Psoralea corylifolia	98.6
Lupinus angustifolius	98.8

Figure 18. Relation between FAAH inhibition potency and *N*-acylethanolamine levels in plants extracts. The graph is generated from the data of the LC-MS/MS analysis of the 16 selected plant extracts for quantification of NAE levels. As shown, no relation exists between the FAAH inhibition of plant extracts and their NAE levels. A DMSO solution containing 100 µg of plant extract was added to a solution of water 0.1% FA, and extracted with a Hex/EtOAc (9:1) solution. NAE levels were quantified via LS-MS/MS analysis. Results are expressed as means ± SEM, from 2 independent experiments performed in duplicate (n=2, N=4). FAAH, Fatty acid amide hydrolase; LEA, *N*-laurylethanolamine; NAEs, *N*-acylethanolamines; OEA, *N*-oleoylethanolamine; PEA, *N*-palmitoylethanolamine.

Fabaceae are a source of bioactive isoflavonoids and prenylated derivatives

The accumulation of hits in the FAAH inhibition assay in extracts derived from Fabaceae prompted us to investigate these extracts in more detail. Besides the characteristic presence of quinolizidine and pyrrolizidine alkaloids, Fabaceae are known to be an abundant source of secondary metabolites such as isoflavonoids and their prenylated derivatives (Hashidoko et al., 1986, Lane et al., 1987, Yuldashev et al., 2000, Gafner et al., 2011, Wojakowska et al., 2013b, Aisyah et al., 2016, Araya-Cloutier et al., 2017). Notably, it has been shown that some isoflavonoids display FAAH inhibitory activity (Thors et al., 2007b, Thors et al., 2008, Thors et al., 2010). Isoflavonoids can undergo structural changes, for example prenylation, which has been suggested to increase their lipophilicity and, consequently, their interaction

with cellular membranes and biological activity (Barron and Ibrahim, 1996, Hatano et al., 2000, Chen et al., 2014).

Therefore, the possibility that the FAAH inhibition observed in the plant extracts from Fabaceae may correlate with the presence of such secondary metabolites was investigated. Based on chemotaxonomic analyses, we used similarity search algorithm provided in PubChem (https://pubchem.ncbi.nlm.nih.gov/) and in the open-access ZINC database (Shoichet Laboratory in the Department of Pharmaceutical Chemistry at the University of California, San Francisco (UCSF)) linked to high quality commercial available isoflavonoids and prenylated derivatives (at least 95% purity), which were then purchased (See *Materials* section).

The role of prenylated isoflavonoids as potential FAAH inhibitors, and whether and how prenylation may be responsible for such activity was explored. Fourteen isoflavonoid and prenylated isoflavonoid standards were tested for their ability to inhibit FAAH using mouse brain membrane preparations (Figure 19). The results of the screening showed that 7-hydroxyisoflavone (**1**), genistein (**2**), daidzein (**3**) and biochanin A (**4**) significantly inhibit FAAH activity at the concentration of 10 µM, in line with the literature (Thors et al., 2007b, Thors et al., 2008, Thors et al., 2010). Notably, the two prenylated isoflavonoids neobavaisoflavone (**10**) and luteone (**7**) fully inhibited FAAH activity at the concentration of 10 µM.

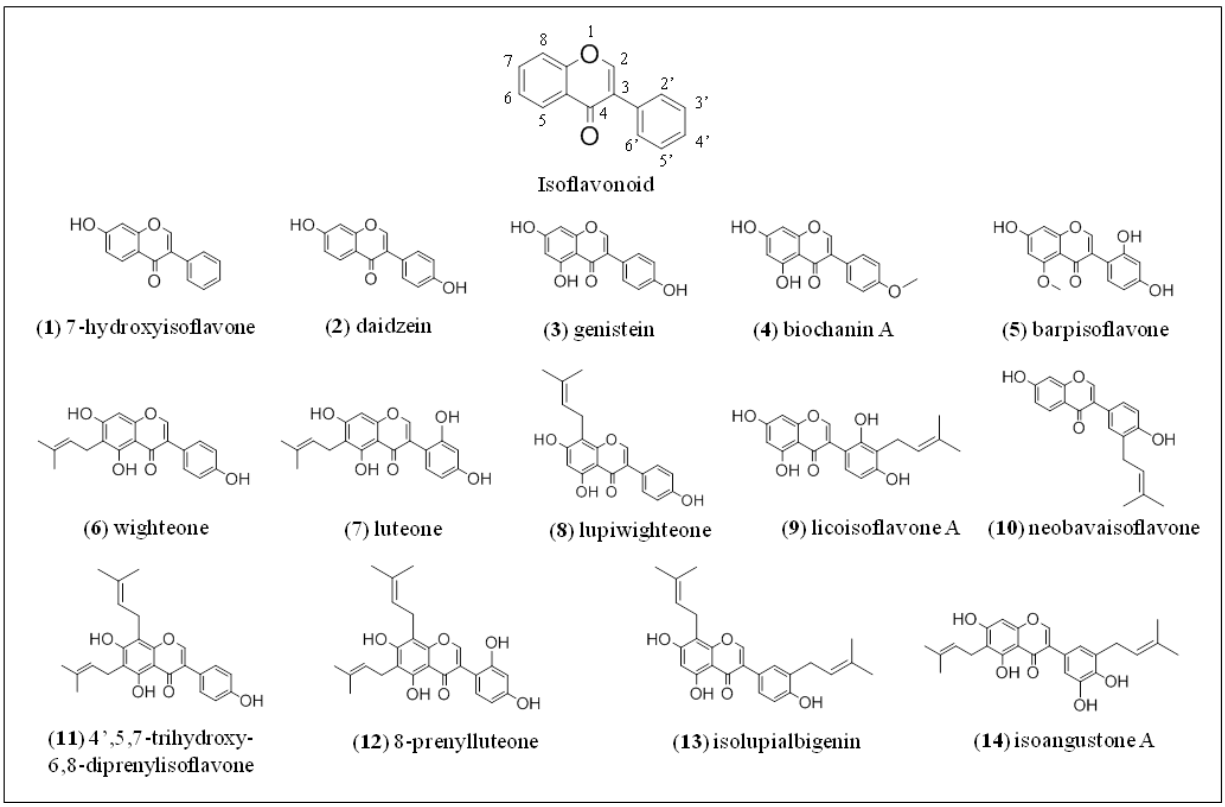

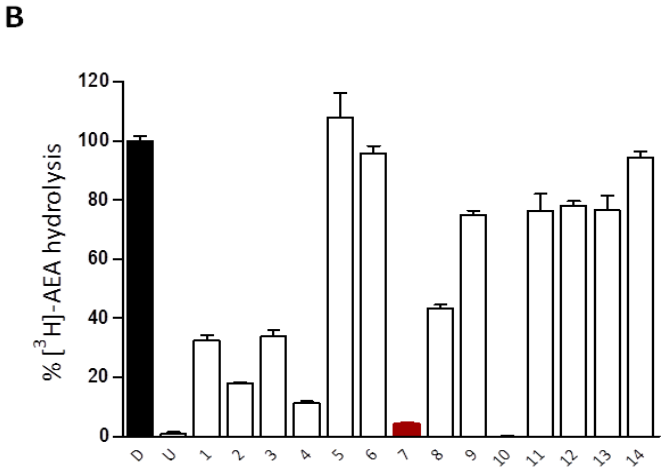

Figure 19. Chemical structure (A) and inhibition of AEA hydrolysis activity in mouse brain membranes preparations (B) of the studied isoflavonoids. The assay was performed using 20 µg of mouse brain membranes preparation per sample and 100 nM of AEA mixture. The samples were dissolved in DMSO and tested at the concentration of 10 µM. URB597 100 nM was used as positive control for FAAH inhibition. Shown are means ± SEM from 2 independent experiments performed in duplicate, n=2, N=4. AEA, anandamide; D, DMSO; U, URB597.

Since the phytochemical composition of *L. angustifolius*, *G. glabra*, *G. uralensis* and *P. corylifolia* extracts was unknown, mass spectrometry (MS) analyses of these extracts were performed and the resulting MS spectra were compared with the MS spectra of the standard isoflavonoids and prenylated derivatives. By comparing the MS spectra of the four plant extracts (Figure 20) with the spectra of the standard compounds (Supplementary Figure 4), it seems that some of the isoflavonoids are present in these plant extracts. The molecular weights and corresponding fragment ions $[M-H]^-$ of the analysed standards are provided in Supplementary Table 2.

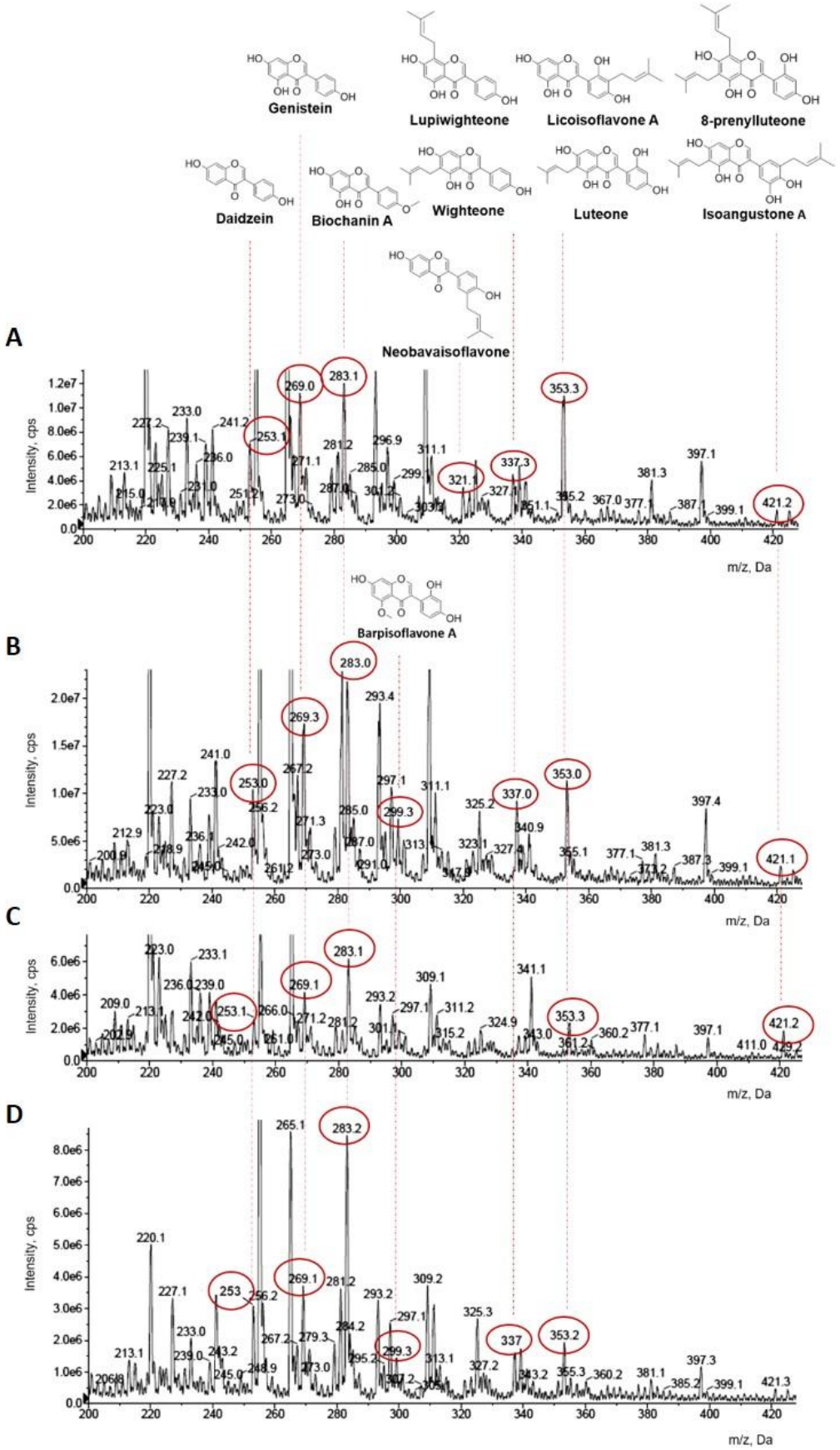

Figure 20. MS spectra of highly active plant extracts on FAAH inhibition suggest the presence of isoflavonoids and prenylated derivatives. Full scan spectra of *Lupinus angustifolius* (A), *Glycyrrhiza glabra* (B), *Psoralea corylifolia* (C) and *Glycyrrhiza uralensis* (D)

extracts. Plant extracts were infused at the concentration of 50 ng·ml^{-1}. Conditions of measurement: 37% ACN in water solution; flow rate 7 µl·min^{-1}; AB Sciex 5500 Q-Trap, negative mode.

In order to confirm that the extracts effectively contained the most active isoflavonoids (i.e. daidzein, genistein, biochanin A, luteone and neobavaisoflavone), the MS spectra of the extracts (Figure 20) were compared with those of the extracts spiked with the standards (Supplementary Figure 5). From this comparison, it is evident that the signals for these standards are increasing after their addition to the extracts. This observation thus indicates the presence of the active isoflavonoids in the four active plant extracts.

Characterisation of FAAH inhibitory activity by neobavaisoflavone and luteone in mouse brain membranes

First, the most potent FAAH inhibitors neobavaisoflavone and luteone were tested in full concentration-dependent experiments to assess their potency and investigate their mechanism of action. The results showed IC_{50} values of 63.2 nM for neobavaisoflavone and 391.6 nM for luteone (Figure 21A). For comparative purposes, we determined the IC_{50} value of the synthetic FAAH inhibitor URB597 and of the isoflavonoids daidzein (the corresponding non-prenylated backbone of neobavaisoflavone) and biochanin A, which were 2 nM, 3.7 µM and 1.2 µM, respectively (Table 1). Both neobavaisoflavone and luteone display higher inhibition than daidzein and biochanin A. Interstingly, neobavaisoflavone was 60-times more potent than its non prenylated analog daidzein (IC_{50} values of 63.2 nM and 3.7 µM for neobavaisoflavone and daidzein, respectively). In further experiments, we evaluated the time dependence of neobavaisoflavone and luteone effect. As shown in Fig. 21B, both compounds exhibited a time-independent inhibition of FAAH activity, as the rate of AEA hydrolysed did not change upon different pre-incubation times with the compounds (0-30 min).

Table 1. IC_{50} values for FAAH activity inhibition by the isoflavonoids neobavaisoflavone, luteone, daidzein, biochanin A and the synthetic inhibitor URB597

Compound	IC_{50} (nM)	95% CI (nM)
Neobavaisoflavone	63.2	55.7 – 71.6
Luteone	391.6	295.0 – 519.9
Daidzein	3742.0	1276.0 – 1097.1
Biochanin A	1220.3	970.2 - 1520.0
URB597	2.0	1.3 – 3.0

Values were calculated from 3 independent experiments using at least 7 concentrations of each compound. For comparative purposes, IC_{50} values of daidzein, biochanin A and of the irreversible inhibitor URB597 were determined. Compounds were dissolved in DMSO. Results are expressed as means and normalized to the vehicle (=100% of AEA hydrolysed). n=3, N=6

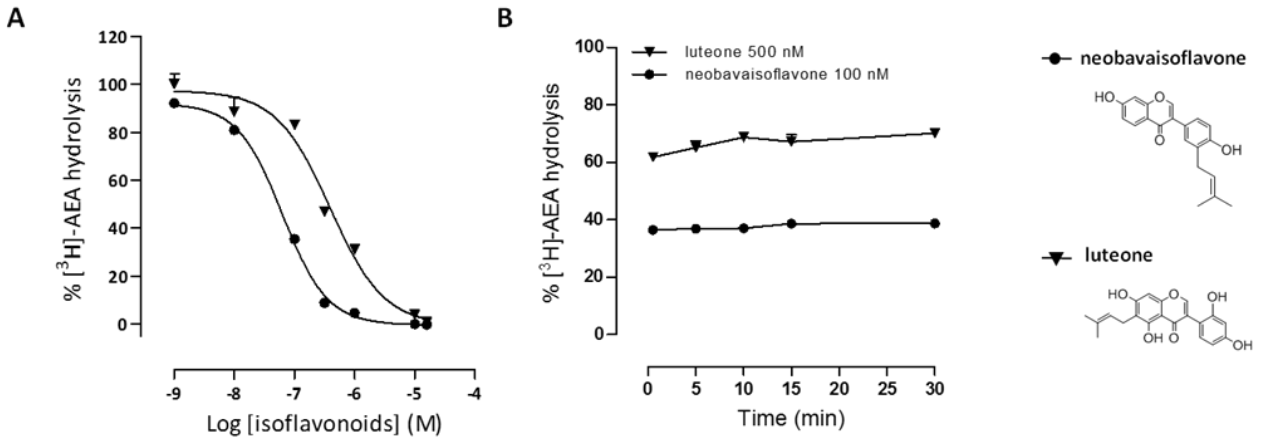

Figure 21. IC_{50} values (A) and time course (B) of FAAH inhibition by neobavaisoflavone and luteone in mouse brain membranes. (A) The assay was performed in mouse brain membrane preparations (20 µg per sample), with 15 minutes of pre-incubation of the enzyme with the inhibitors and 15 minutes of incubation with 100 nM of AEA mixture. IC_{50} values are 63.2 nM and 391.6 nM for neobavaisoflavone and luteone, respectively. n=3 independent experiments performed in duplicate (N=6) using 7 different concentrations of the compounds. Shown are means ± SEM and the IC_{50} was calculated using the log(inhibitor) vs. response -- Variable slope (four parameters) function. The samples were dissolved in DMSO. (B) The assay was performed in mouse brain membranes (20 µg per sample), with different times of pre-incubation of the inhibitors (0.5, 5, 10, 15 and 30 minutes) and 100 nM of AEA mixture. Shown are means ± SEM. The samples were dissolved in DMSO. n=3 independent experiments performed in duplicate (N=6). AEA, anandamide.

In a next step, ABPP assays were performed in order to assess the selectivity of neobavaisoflavone and luteone versus MAGL and ABHD6, the major enzymes involved in 2-AG hydrolysis. As expected, the positive control URB597 (4 µM) competes with the TAMRA-FP serine hydrolase probe for binding to FAAH (63 KDa) (Figure 22). The same behaviour was displayed by the two isoflavonoids, in particular at the concentration of 25 µM (Figure 22A). The inhibition of FAAH appears to be specific, as there was no significant binding to MAGL (double band at 31 and 33 kDa) and ABHD6 (30 kDa), which are instead selectively inhibited by the positive controls JZL184 (1 µM) and WWL70 (10 µM), respectively (Figure 22).

To test the reversibility of the FAAH inhibition, a second ABPP analysis was performed, by incubating the mouse brain proteome with the TAMRA-FP serine hydrolase probe for 20 minutes (Figure 22C). This gel was compared with the previous one, obtained by incubating the probe for 5 minutes (Figure 22B). The FAAH inhibitor biochanin A (Thors et al., 2010) was used for comparative purposes. As shown in the gel of Figure 22B, by incubating the probe for 5 minutes, the three isoflavonoids are able to effectively

compete with the probe and therefore the corresponding FAAH band (63 kDa) is nearly absent. In contrast, by incubating the probe for longer (20 minutes), the three isoflavonoids are competed away by the probe, and once the covalent bond enzyme-probe is formed, the isoflavonoids are no longer able to bind in the active site (Figure 22C). On the contrary, the irreversible FAAH inhibitor URB597 maintained the same potency in inhibiting FAAH after 5 and 20 min of incubation (Figure 22B and 22C). These results suggest that the isoflavonoids act as reversible FAAH inhibitors. In the case of neobavaisoflavone at the concentration of 10 µM, the intensity of the FAAH band is still very poor, probably due to the high potency of the compound as a FAAH inhibitor (IC_{50}=63.2 nM).

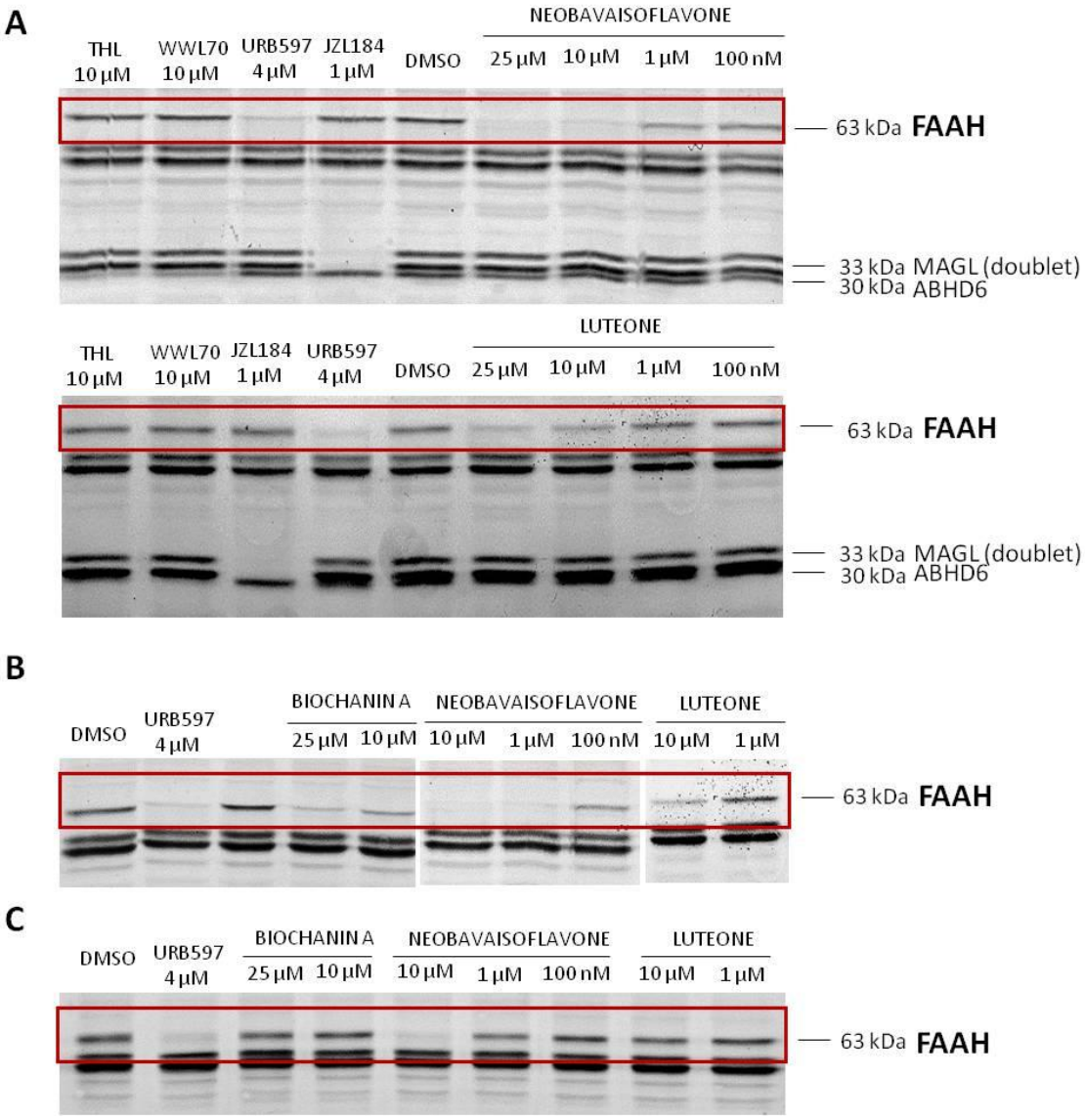

Figure 22. Activity-based protein profiling of neobavaisoflavone and luteone. (A) Gels are showing a concentration dependent FAAH inhibition (63 kDa), while no significant effect on other enzymes such as MAGL or ABHD6 (33, 31 and 30 kDa, respectively) is seen. Time of incubation with the TAMRA-FP serine hydrolase probe was 5 minutes. (B and C) The assay was performed with a time

of incubation with the probe of 5 and 20 minutes, respectively. The inhibitor biochanin A was used for comparative purposes. The irreversible FAAH inhibitor URB597 was used as positive control and DMSO as negative control. n=2.

As shown in Figure 22, the band corresponding to the other minor 2-AG hydrolytic enzyme ABHD12 (at 45 kDa) was not detected, suggesting a low expression of such enzyme in the mouse brain proteome used for the ABPP analysis. However, functional assay performed in HEK293 cells stably transfected with ABHD12 showed no inhibition of the hydrolytic activity by both isoflavonoids (see Supplementary Figure 7). In order to confirm the ABPP results, functional assays for ABHD6, and MAGL inhibition were performed for neobavaisoflavone and luteone. In addition, both isoflavonoids were assessed for binding to cannabinoid receptors CB_1 and CB_2 using radioactive-based assays. As shown in Supplementary Figure 7, both compounds did not significantly inhibit ABHD6, ABHD12 and MAGL, and did not bind to CB_1 and CB_2 receptors at the concentration of 10 μM.

In order to confirm the reversible FAAH inhibition exhibited by neobavaisoflavone and luteone in the ABPP assays, we performed functional rapid dilution assays for AEA hydrolysis (Figure 23). In this assay, mouse membrane preparations are incubated for 15 min with different concentration of the isoflavonoids and before adding AEA and starting the enzymatic hydrolysis, the reaction mixture is diluted 10x times. In case of irreversible inhibitors, the dilution of the reaction mixture does not affect the inhibitor. On the contrary, reversible inhibitors are displaced from the enzyme, leading to a significant loss in their inhibitory potency. As shown in Figure 23, after dilution, the percentage of AEA hydrolysis significantly increased for both compounds, unlike in non-diluted conditions, thus confirming that neobavaisoflavone and luteone act as reversible FAAH inhibitors. This difference was not observed for neobavaisoflavone at the concentration of 10 μM, because even with a 10x dilution of the reaction mixture this compound retains a concentration that is capable to fully inhibit FAAH.

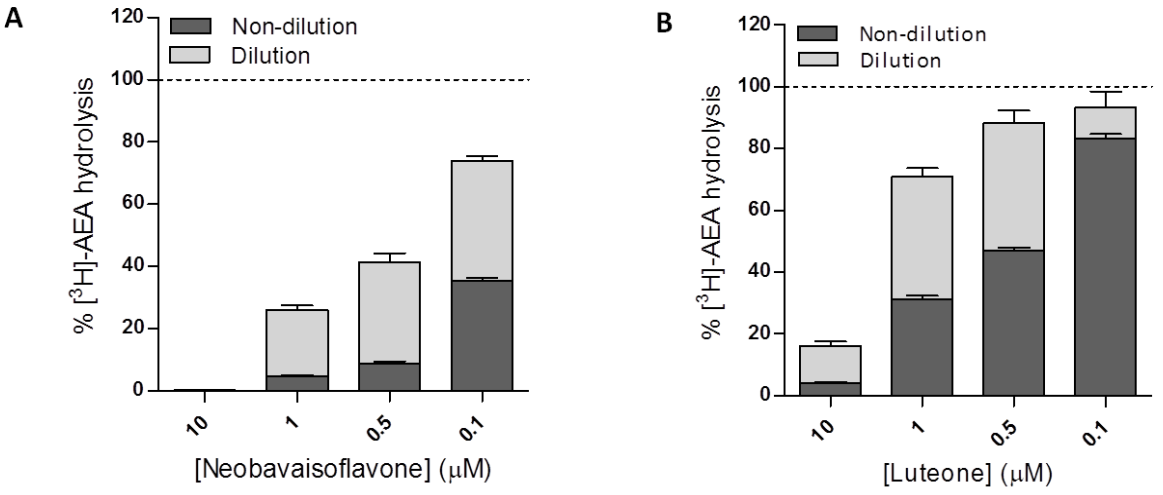

Figure 23. Reversible FAAH inhibition by neobavaisoflavone (A) and luteone (B). In the diluted conditions, the inhibitors were incubated with 20 μg of mouse brain membrane preparations in 30 μl of buffer solution, and then highly diluted immediately before the addition of the radiolabeled substrate. In the diluted condition, an increased percentage of AEA hydrolysed by FAAH is

observed compared with the one in the normal conditions at the same concentration of inhibitors, indicating a reversible binding. Results are expressed as means ± SEM and normalized to the vehicle control (=100% of AEA hydrolised). n=3, N=6.

In order to investigate the competitiveness of FAAH inhibition, additional *in vitro* kinetic experiments were performed. Both neobavaisoflavone and luteone showed a competitive mechanism of action (Figure 24, Table 2). In the absence of neobavaisoflavone the inhibition is saturable with a V_{max} value of 149.7 pmol·mg protein^{-1}·min^{-1} and K_m of 0.54 µM (Michaelis-Menten analysis). In the case of luteone, in absence of inhibitor, the inhibition is saturable with a V_{max} value of 149.4 pmol·mg protein^{-1}·min^{-1} and a K_m of 0.49 µM. In presence of both inhibitors V_{max}^{app} is nearly constant and the K_m^{app} is decreasing, thus indicating a competitive inhibition. On the right panel of Figure 24, Lineweaver-Burk plots are shown. For both isoflavonoids, the slope (K_m/V_{max}) increased in presence of the inhibitor as compared to the vehicle. The Y-intercept ($1/V_{max}$) did not change while the X-intercept ($-1/K_m$) decreased, in line with a reversible mechanism of action. The K_i values of FAAH inhibition of 53.3 nM for neobavaisoflavone and 325.7 nM for luteone were calculated using the Cheng-Prusoff equation for a competitive inhibition, where [S] was 0.1 µM, experimental IC_{50} were 63.2 nM and 391.6 nM and K_m were 0.54 µM and 0.49 µM respectively. K_i values obtained are similar to the experimental IC_{50} values , according to the Cheng-Prusoff equation for a competitive inhibition when [S] ≈ K_m (Cer et al., 2009).

Table 2. Kinetic parameters of neobavaisoflavone and luteone on FAAH inhibition in mouse brain membranes.

[neobavaisoflavone] (nM)	V_{max} (pmol·mg protein^{-1}·min^{-1})	K_m (µM)
0	149.7	0.54
25	148.9	1.18
100	148.9	2.30

[luteone] (nM)	V_{max} (pmol·mg protein^{-1}·min^{-1})	K_m (µM)
0	149.4	0.49
100	146.0	0.65
500	137.7	1.32

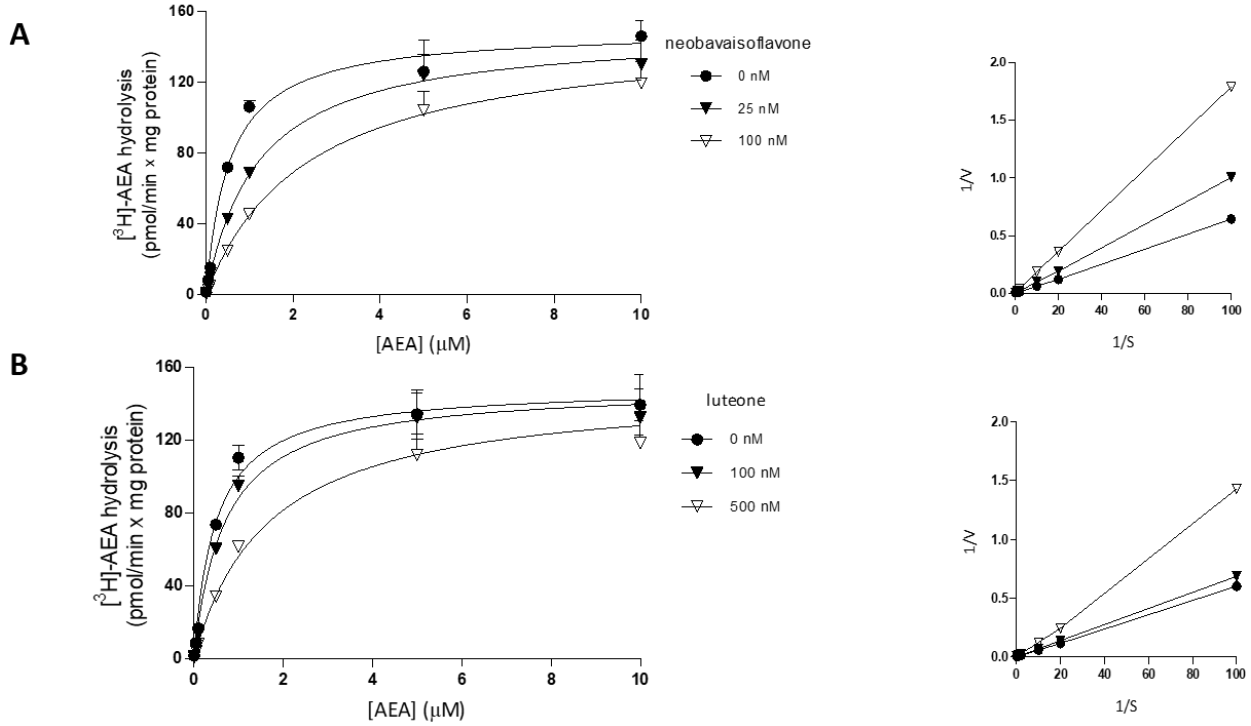

Figure 24. Mode of FAAH inhibition by neobavaisoflavone (A) and luteone (B). On the left, the curves are showing a competitive mode of inhibition: in absence of inhibitor, V_{max} calculated with nonlinear regression is 149.7 pmol·mg protein^{-1}·min^{-1} and 149.2 pmol·mg protein^{-1}·min^{-1} and the K_m 0.54 μM and 0.49 μM, respectively. In presence of inhibitors V_{max}^{app} is nearly constant and the K_m^{app} is increasing. On the right, the Lineweaver-Burk plots are also suggesting a competitive mode of inhibition, where the slope is increasing in presence of the inhibitor compared with the absence of it. Results are expressed as means ± SEM and n=3 (N=6). AEA, anandamide.

FAAH inhibition by neobavaisoflavone and luteone in living U937 cells

Since FAAH is an intracellular enzyme associated to the endoplasmatic reticulum (Deutsch and Chin, 1993), we tested the capacity of neobavaisoflavone and luteone to effectively cross the cell membrane by performing FAAH assays in living U937 cells. In this system, neobavaisoflavone still significantly inhibits FAAH with an IC_{50} value of 316 nM while minor effects are observed for luteone, with IC_{50} value of 2 μM (Figure 25A). In Figure 25B, comparison of the AEA hydrolysis rate in presence of neobavaisoflavone and daidzein at the concentration of 1 μM and 500 nM indicates once more a higher potency of the prenylated derivative.

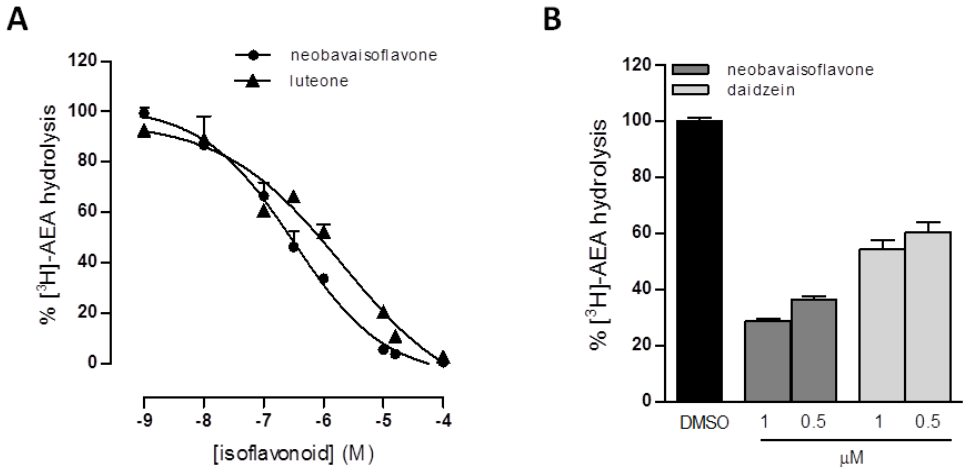

Figure 25. FAAH inhibition by neobavaisoflavone and luteone in living U937 cells. (A) IC_{50} values in intact U937 cells are 316 nM and 2 µM for neobavaisoflavone and luteone, respectively. (B) The prenylated neobavaisoflavone still shows higher potency than the corresponding non-prenylated compound daidzein and the highest potency among the four isoflavonoids tested. Luteone displays a potency comparable to daidzein and genistein. Results are expressed as means ± SEM and n=3 (N=6). AEA, anandamide.

Molecular docking studies for neobavaisoflavone and luteone

In order to rationalize the FAAH inhibitory activity of the most active isoflavonoids, molecular docking experiments have been carried out.

Before performing docking experiment, the protocol has been validated. This consists in finding a complex of a known inhibitor with target structure from the PDB and in docking the known inhibitor into the target (Re-docking). The comparison of docked pose and experimental (i.e. calculating the RMSD) can help to understand if the protocol is reliable. When this procedure is carried out considering different compounds available in different pdb entries of the same target, the validation is made through cross-docking. The second validation is preferable whenever is possible and the structure of the target allows it (i.e. target not too flexible) (Kirchmair et al., 2008, Moitessier et al., 2008).

Hence, re- and cross-docking experiments have been carried out. The best protocol turned out to be Glide-XP, and the results are reported in Table 3:

Table 3. Glide XP. Re- and cross-docking results considering the co-crystallized ligands reported in pdb complexes.

PDB crystals	Resolution	Type	Bound	3ppm/humanized RMSD Å	3qk5/rat RMSD Å
2VYA	2.75 Å	humanized	covalent	**1.142**	**1.776**
2WJ1	1.84 Å	humanized	covalent	**1.493**	7.248
2WJ2	2.55 Å	humanized	covalent	**1.284**	11.622

3K7F	1.95 Å	humanized	covalent	**1.417**	9.477
3K83	2.25 Å	humanized	covalent	3.542	8.623
3K84	2.25 Å	humanized	covalent	**1.095**	6.732
3LJ6	2.42 Å	humanized	covalent	6.367	6.366
3OJ8	1.90 Å	humanized	covalent	**2.337**	4.327
3PPM	1.78 Å	humanized	non-covalent	2.620	5.027
3PR0	2.20 Å	humanized	covalent	**1.863**	11.721
3QJ9	2.30 Å	rat	non-covalent	8.731	**0.233**
3QK5	2.20 Å	rat	non-covalent	5.721	**1.415**
3QKV	3.10 Å	rat	covalent	**2.317**	2.714
4HBP	2.91 Å	rat	covalent	**1.517**	2.959
4J5P	2.30 Å	humanized	covalent	**1.336**	11.46

Highlighted are the RMSD values < 2 Å. A RMSD value < 2 Å means that the docking was able to correctly predict the binding mode reported in the PDB. In yellow, the model used to study the activity of the isoflavonoids.

In particular, a RMSD value < 2 Å means that the docking was able to correctly predict the binding mode reported in the PDB. The re/cross-docking carried out considering the humanized model has given excellent results, as most of the compounds have been correctly positioned (RMSD < 2). This was not the case for cross docking in the rat enzyme, where most of co-crystallized ligands in the humanized enzyme are not correctly docked (RMSD > 2 Å). This can be explained because of the differences in the binding pocket and, in particular, the mutations L192F and I491V that do not make possible the correct positioning of the available ligands crystallized in the humanized. However, the re/cross-docking of the crystallized reversible ligands 3QJ9 and 3QK5 is correctly docked (Table 3). In addition, RMSD is calculated between the covalently bound compound (in most cases) and the unbound compound. This obviously affects the value of the RMSD. Furthermore, we must consider that most of docked ligands are bound covalently but we simulated a reversible docking, since the compounds to study are reversible ligands. Hence, the results obtained are outstanding and for this reason even a RMSD value slightly > 2 Å can be considered acceptable. Therefore, this protocol was considered reliable and applied for the subsequent docking experiments on the most active compounds.

Neobavaisoflavone, luteone, daidzein and biochanin A were docked in the PDB model 3QK5 to rationalize the activity. The best docking poses complexes were minimized and rescored and the most stable complexes were then analysed. Figure 26 shows the predicted binding mode and the interaction between the compounds and the active site of the enzyme.

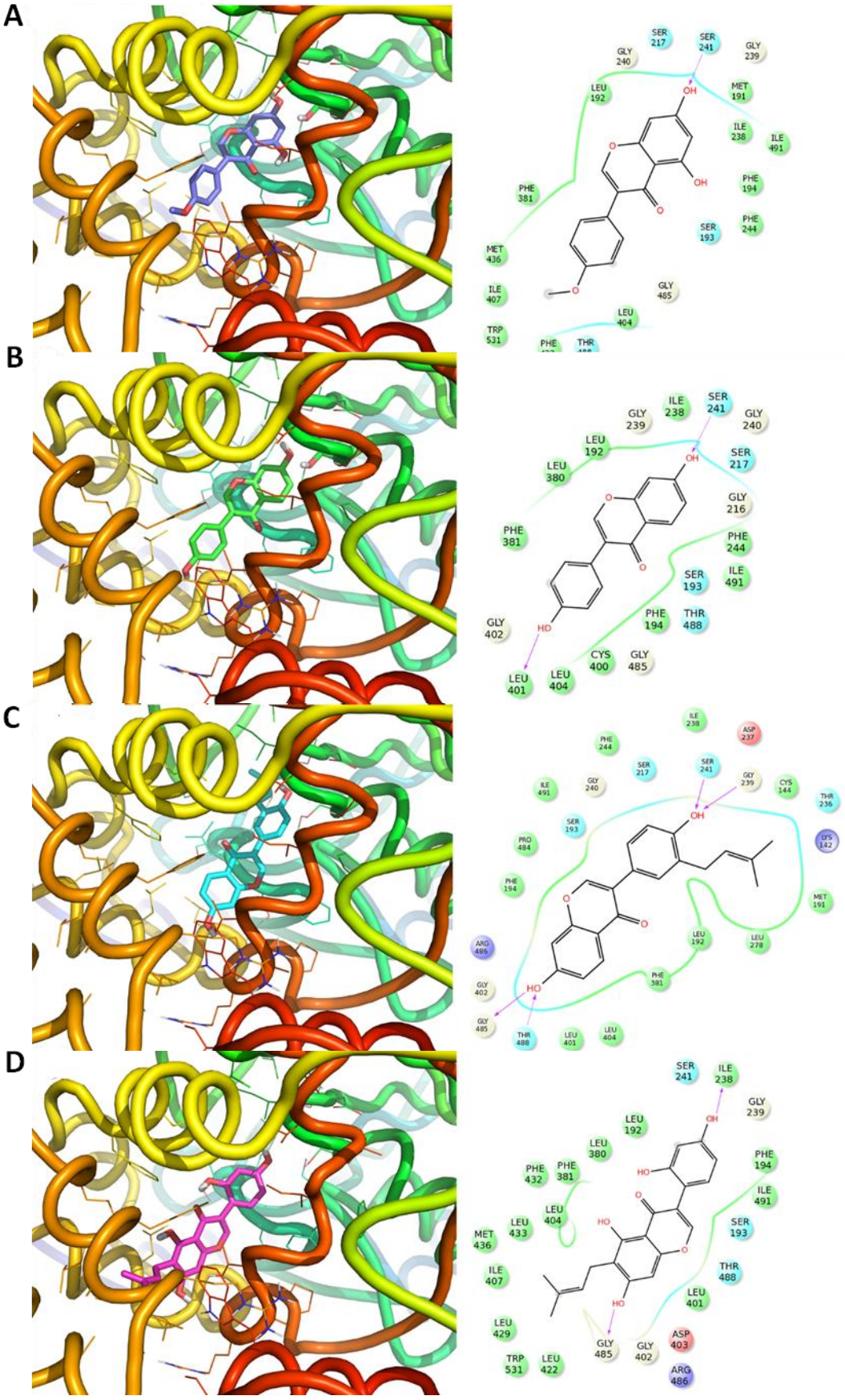

Figure 26. Predicted binding mode of biochanin A (A), daidzein (B), neobavaisoflavone (C) and luteone (D).

From the analysis of the binding mode is deductible the importance of the prenylated moiety. Notably, neobavaisoflavone is better able to fit into the active site than luteone, and it is stabilized both by hydrogen bonds and by numerous interactions with hydrophobic residues. In line with the experimental data, biochanin A and daidzein are less active than neobavaisoflavone and luteone.

Aknowledgements

We thank Daniele Pellagata (Insitute of Biochemistry and Molecular Medicine, Bern, Switzerland) to help in the mass spectrometry analyses, and Prof. Simona Distinto (Department of Life, Environmental and Drug Science, Cagliari, Italy) for the molecular docking studies.

CHAPTER 5 – SECONDARY PROJECTS: Preliminary results

5.1 Screening of Herbal Drug Extracts from the *De Materia Medica*: Antiproliferative activity and Cannabinoid Receptors Type-2 Binding

The extract library related to Dioscorides' *DMM* (Matthioli, 1568, Staub et al., 2016) was screened also for the binding to CB_2 receptors and potential non-CB receptor and non-FAAH mediated antiproliferative effect. The binding assays were performed using membrane preparations obtained from CHO-K1 cells stably transfected with *h*CB_2 receptors. The antiproliferative effect of the extract library was assessed using human HeLa cells, which do not express CB_1/CB_2 receptors and FAAH (Dickason-Chesterfield et al., 2006). Similar to the FAAH inhibition screening (Chapter 4), the results of the CB_2 binding and antiproliferative assays were represented using a phylogenetic tree (Figure 27). In addition, Supplementary Table 4 shows the results of CB_2 receptor binding and cytotoxicity screening for all extracts.

The results of the antiproliferative screening assays are expressed as percentage of non-viable cells (Figure 27A). By applying an arbitrary cut-off at 75% of cell viability inhibition at the concentration of 25 $\mu g \cdot ml^{-1}$, we identified 54 antiproliferative extracts out of the 660 screened (8.2%). As illustrated in Figure 27A, the antiproliferative effect did not show phylogenetic pattern. Therefore, we assume that a phylogenetic approach would not be a suitable criterion to find a correlation between general antiproliferative effect and the genetic pool of the plant kingdom. In addition, we used a Chi Square test for highlighting relationships between the cytotoxic activity of the extracts and the mode of application (internal, external, clyster, fumigation) of the associated herbal drugs described in the *DMM* (Matthioli, 1568). The statistical analysis (Supplementary Table 5) shows a significant relationship between cytotoxicity and the mode of therapeutic application as highly cytotoxic extracts (> 75% of non-viable cells) are most frequently associated with external applications while extracts showing moderate cytotoxicity (< 75% of non-viable cells) are most frequently associated with internal applications.

The results of the CB_2 receptor binding screening are expressed as percentage of binding to the CB_2 receptors. The extracts showing receptor binding higher than 80% at the concentration of 10 $\mu g \cdot ml^{-1}$ were considered "hits". The screening revealed only two plant extracts with significant activity i.e. *Ferula gummosa* and *Ferula persica* resin (Figure 27B), with 84.8% and 82.0% of CB_2 receptor binding, respectively, at the concentration of 10 $\mu g \cdot ml^{-1}$. Therefore, only 0.3% of the screened extracts of the *DMM* library showed significant binding to CB_2 receptors. Interestingly, only two of the four *Ferula* extracts included in this study display affinity to CB_2 receptors, as *Ferula tingitana* stalk and *Ferula communis* seed extracts

show only 27% and 20% of CB_2 binding, respectively. This observation might suggest that the secondary metabolites responsible for such activity are components of the *Ferula* resins.

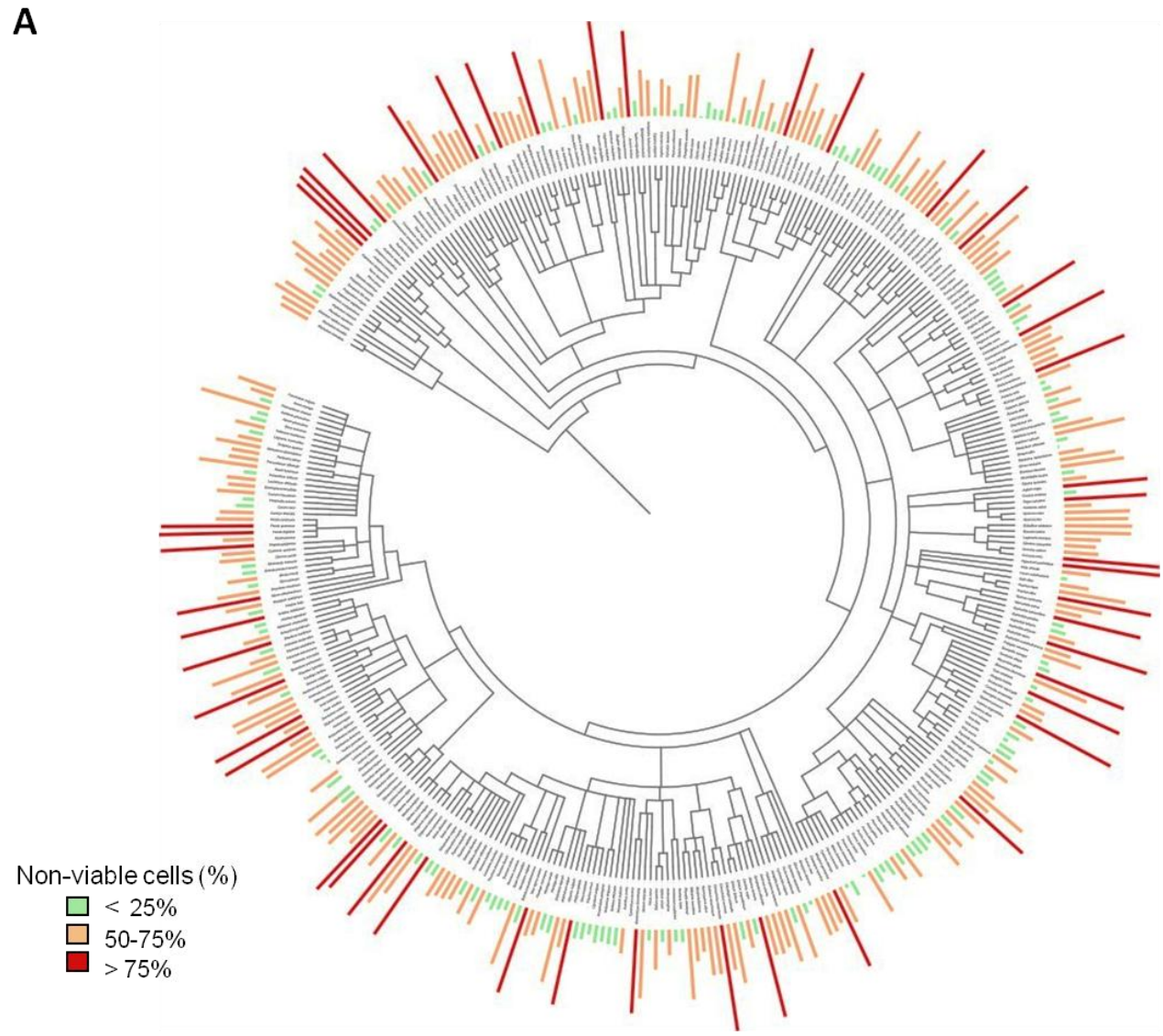

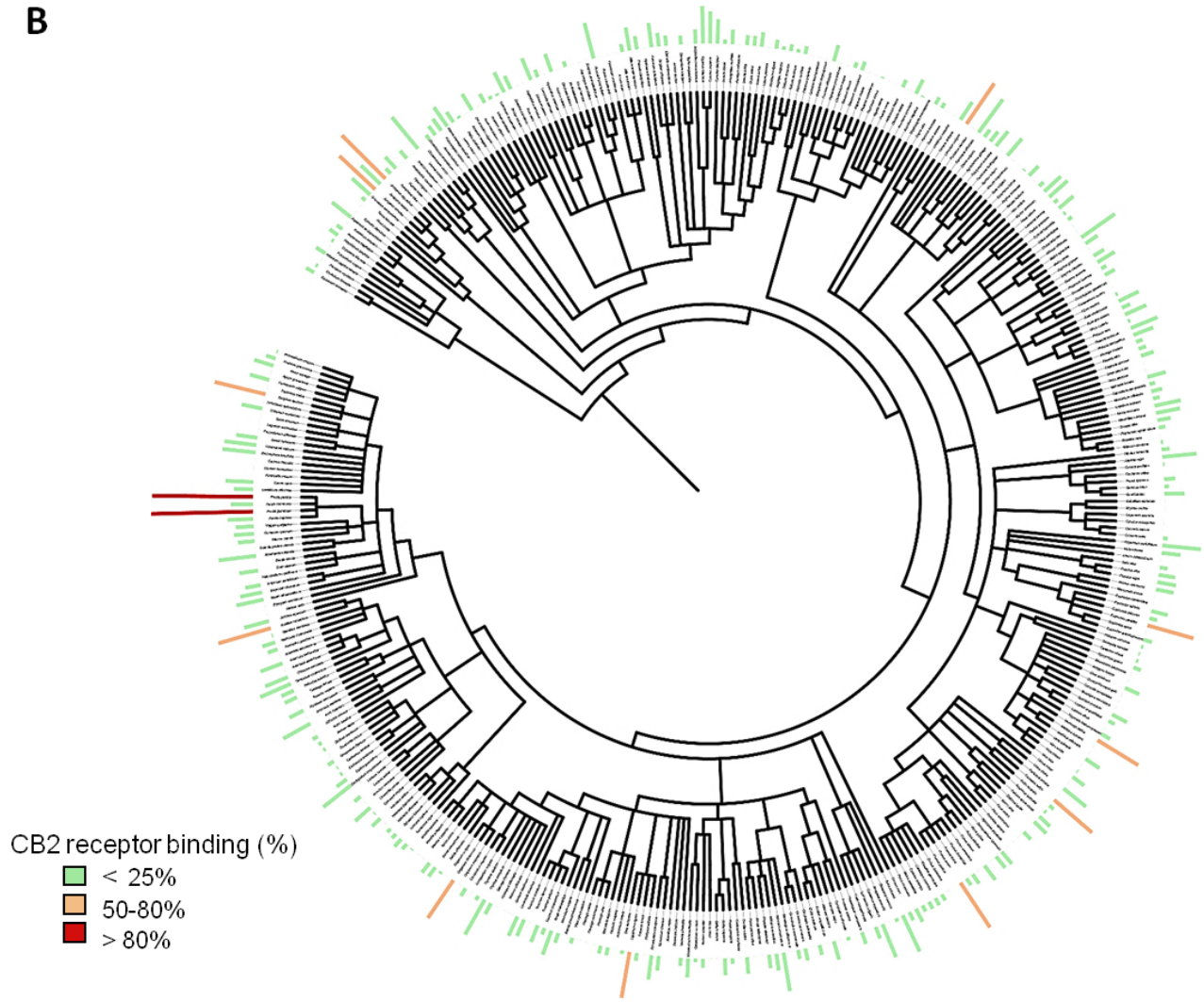

Figure 27. Results of the antiproliferative activity (A) and CB_2 receptor radioligand binding (B) screening of the *DMM* plant extract library. Representation of 450, out of 660 screened plant extracts, with corresponding percentage of non-viable cells (A) and binding to CB_2 receptors (B). The ethyl acetate plant extracts were tested at 25 $\mu g \cdot ml^{-1}$ for antiproliferative activity in HeLa cells and at 10 $\mu g \cdot ml^{-1}$ for binding to the CB_2 receptors in *h*CB_2 transfected CHO-K1 cells.

Further investigations were conducted with the extracts of *F. gummosa* and *F. persica* resin (Figure 28). First, in order to investigate the selectivity for CB_2 receptors, the ability to bind to CB_1 receptors as well was evaluated. As shown in Figure 28A and in Table 4, both extracts show significant binding to CB_2 receptors at the concentration of 10 $\mu g \cdot ml^{-1}$. The EC_{50} values for CB_2 receptor binding calculated from full concentration-dependent curves were 2.8 $\mu g \cdot ml^{-1}$ and 4.1 $\mu g \cdot ml^{-1}$ for *F. gummosa* and *F. persica* extract, respectively (Figure 28B and Table 4). At the concentration of 10 $\mu g \cdot ml^{-1}$, both extracts showed a 2/3-times lower affinity for CB_1 receptors. However, in order to properly evaluate the selectivity between CB_1 and CB_2 receptors, full concentration-dependent binding curves for *F. gummosa* and *F. persica* extracts to both cannabinoid receptors should be compared.

F. gummosa extract shows also antiproliferative effect in HeLa cells at the concentration of 25 µg·ml^{-1}. This property may be exerted by the presence of some sesquiterpene coumarins, which have been reported to have cytotoxic and anti-proliferative activity in cancer cell lines (Iranshahi et al., 2008, Iranshahi et al., 2010a).

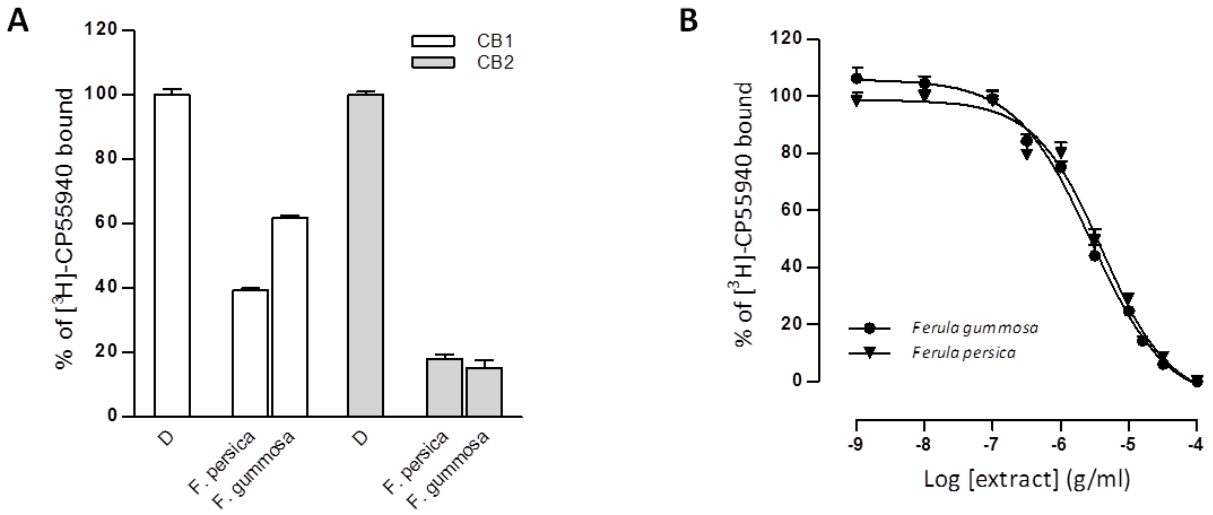

Figure 28. CB_1 and CB_2 receptor binding (A) and EC_{50} values for CB_2 binding (B) of *F. gummosa* and *F. persica* extracts. (A) *F. gummosa* and *F. persica* extracts show, at the concentration of 10 µg·ml^{-1}, significant binding to CB_2 receptors. At the same concentration, lower affinity for CB_1 receptors is observed for both extracts. DMSO (vehicle) was used as negative control. The results were expressed as percentage of [^{3}H]-CP-55940 bound to the receptors compared to the vehicle treated control (=100%). Shown are means ± SEM, from 2 independent experiments performed in triplicate (n=2, N=6). D, DMSO. (B) *F. gummosa* and *F. persica* extracts displace [^{3}H]-CP-55,940 from CB_2 receptors with an EC_{50} of 2.8 µg·ml^{-1} and 4.1 µg·ml^{-1}, respectively. Shown are means ± SEM, from 2 independent experiments performed in triplicate using 10 different concentrations of the plant extract (n=2, N=6). EC_{50} values were calculated using the log (agonist) vs. response -- Variable slope (four parameters) function.

Table 4. Summary of the investigations conducted on *F. gummosa* and *F. persica* extracts.

Plant extract	Non-viable cells (%) [a] (25 µg·ml^{-1})	CB_1 binding (%) [b] (10 µg·ml^{-1})	CB_2 binding (%) [b] (10 µg·ml^{-1})	EC_{50} (CB_2R) [c]
Ferula gummosa	83.6	38.2	84.8	2.8 µg·ml^{-1}
Ferula persica	31.8	60.7	82.0	4.1 µg·ml^{-1}

[a] antiproliferative activity was evaluated with the MTT assay method on HeLa cells. Results are expressed as percentage of non-viable cells compared to the vehicle treated cells (=0%). Assay was carried out in triplicate. Extracts were dissolved in DMSO.

[b] assay was performed in *h*CB_1 or *h*CB_2 transfected CHO-K1 cells. Results are expressed as percentage of binding to the receptors. Assay was carried out in triplicate. Extracts were dissolved in DMSO.

[c] assay was performed in *h*CB_2 transfected CHO-K1 cells. Extracts were dissolved in DMSO.

Several studies have investigated the phytochemistry of *Ferula* species, as discussed in Chapter 1. The *Ferula* genus is rich in sesquiterpenes (Iranshahi et al., 2003a, Appendino et al., 2006), sesquiterpene

coumarins and their glycosides (Abd El-Razek et al., 2001, Iranshahi et al., 2010b, Nazari and Iranshahi, 2011) and sulphur-containing compounds (Iranshahi et al., 2003b, Iranshahi et al., 2009b).

Notably, sesquiterpene coumarins received interest due to their different biological activities, which have been associated to many of the pharmacological properties of *Ferula* extracts (Nazari and Iranshahi, 2011, Sattar and Iranshahi, 2017) such as anti-inflammatory (Iranshahi et al., 2009a), cancer chemopreventive (Iranshahi et al., 2008, Iranshahi et al., 2009c) and anti-diabetic activity (Abu-Zaiton, 2010, Akhlaghi et al., 2012). Moreover, some terpenes are known for their interaction with CB_2 receptors and related therapeutic benefits (Sharma et al., 2015), with binding affinities spanning from the nanomolar to the micromolar concentrations. Among them, the sesquiterpene β-caryophyllene showed a K_i of 155 nM in *h*CB_2 receptors of HEK293 cells (Gertsch et al., 2008), and the triterpenes celastrol and euphol showed moderate CB_2 receptor interaction (Dutra et al., 2012, Yang et al., 2014).

Therefore, considering the ability of some terpenes to interact with CB_2 receptors and, the multitude of pharmacological features documented for sesquiterpene coumarins, which are abundant in *Ferula* genus, this class of secondary metabolites was selected as possible responsible for the observed interactions of *F. gummosa* and *F. persica* extracts with CB_2 receptors. Accordingly, the ability of sesquiterpene coumarins to interact with CB_2 receptors was investigated, testing 12 compounds among commercially available standards and pure compounds isolated from *Ferula* species (see *Materials* Section for more details), selected by using a similar approach described in Chapter 4. The interaction was assessed by performing radioligand binding assay in *h*CB_2-transfected CHO-K_1 cells. The chemical structures of the tested compounds as well as the results of the radioligand binding assay are represented in Figure 29.

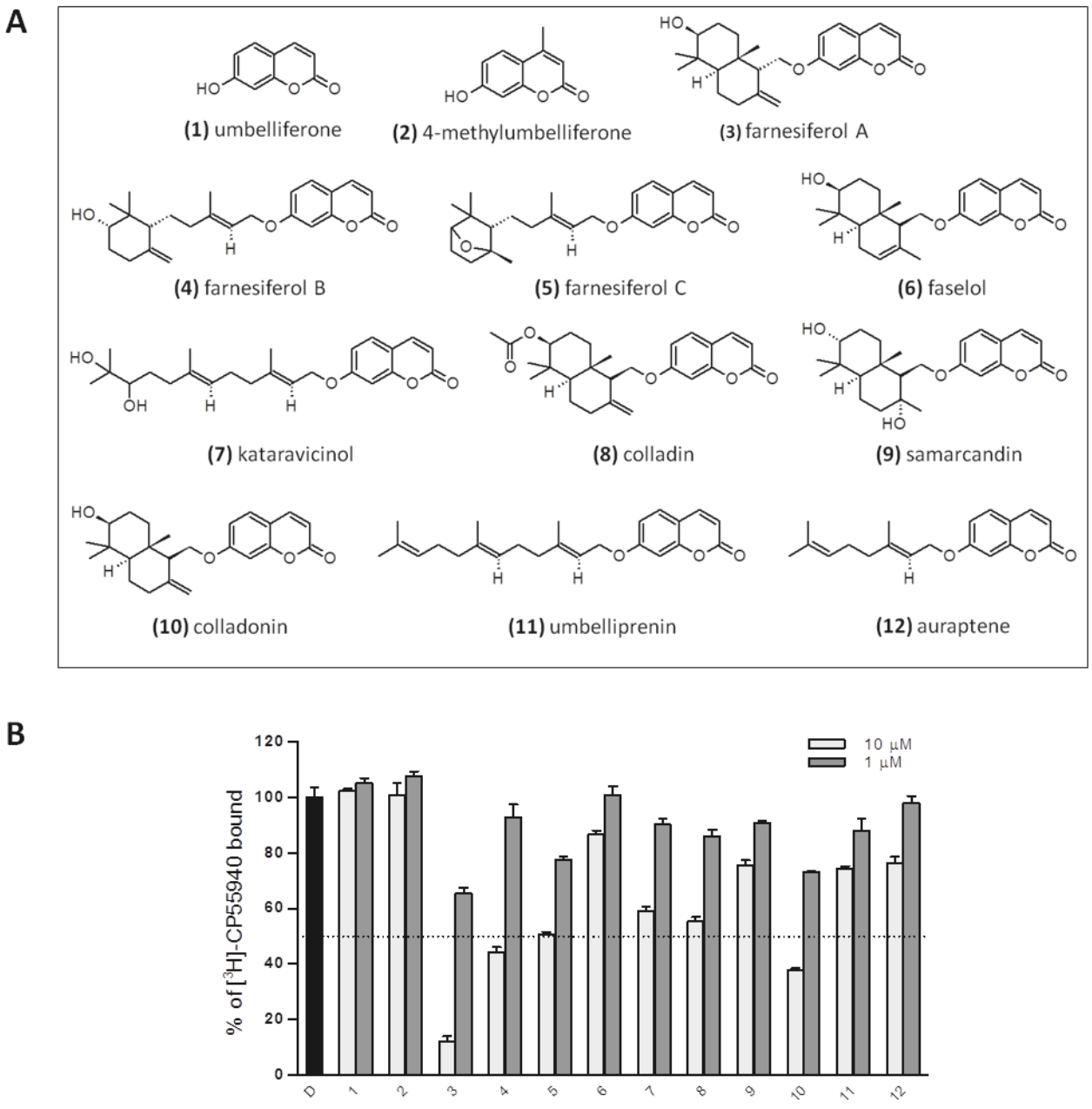

Figure 29. *h*CB_2 receptor radioligand binding assay of sesquiterpene coumarins. (A) Chemical structure of the tested compounds. (B) The assay was performed using 10 µg of CHO-K1 cell membranes, transfected with *h*CB_2 receptors, per sample. DMSO (vehicle) was used as negative control. The results were expressed as percentage of [^{3}H]-CP-55940 bound to the receptors compared to the vehicle treated control (=100%). Shown are means ± SEM from 2 independent experiments performed in triplicate, n=2, N=6.

As shown in Figure 29B, some of the tested sesquiterpene coumarins are able to interact with CB_2 receptors. In particular, farnesiferol A (**3**), displays good interaction at the concentration of 10 µM, along with colladonin (**10**), farnesiferol B (**4**) and farnesiferol C (**5**) though with less potency. The interaction of the simple coumarins umbelliferone (**1**) and 4-methylumbelliferone (**2**) was also evaluated. Neither of the compounds showed affinity for the receptor at the concentration of 10 µM, suggesting that the terpene moiety is responsible for the interaction.

Full concentration-dependent experiments to evaluate the potency of farnesiferol A, B and C and colladonin were assessed. EC_{50} values are 1.1 µM, 6.3 µM, 40.6 µM and 5.1 µM, respectively (Table 5). The EC_{50} value of the synthetic CB_2 agonist WIN55.212-2 in the same system and at the same experimental conditions was 14.4 nM. Interestingly, farnesiferol A (1S,4aS,6R,8aR) showed higher affinity for CB_2 receptors than its stereoisomer colladonin (1R,4aS,6R,8aR) (EC_{50} of 1.1 µM and 5.1 µM, respectively).

Table 5. EC_{50} values for CB_2 receptor binding of the sesquiterpene coumarins farnesiferol A, B, C, and colladonin and the synthetic agonist WIN55.212-2.

Compound	EC_{50} (µM)	95% CI (µM)
Farnesiferol A	1.1	0.9-1.4
Farnesiferol B	6.3	1.9-21.0
Farnesiferol C	40.6	3.2-508.7
Colladonin	5.1	2.9-9.1
WIN55.212-2	0.014	0.008-0.027

The assay was performed in *h*CB_1 or *h*CB_2 transfected CHO-K_1 cell membranes. EC_{50} values were calculated using the log(agonist) vs. response -- Variable slope (four parameters) function. Extracts were dissolved in DMSO. n=2 independent experiments performed in triplicate (N=6).

5.2 Inhibition of AEA Uptake by *Tinospora cordifolia* Ethyl Acetate Extract

The Ayurvedic medicinal plant *Tinospora cordifolia* was subjected to profiling towards the ECS. The rational for such investigation is based on broad ranging screening results and historical data presented in a work of Leonti and Casu (2014). The authors proposed that protoberberine alkaloids of *T. cordifolia* contributed to the psychoactive effects associated with its consumption (Leonti and Casu, 2014), hypothesis which prompted to hypothesize that such effects were mediated by an interaction with the ECS.

To address this objective, the pharmacological interactions of the ethyl acetate extract of *T. cordifolia* stems with the components of the ECS was investigated. Specifically, the affinity for CB_1 and CB_2 receptors, and the inhibition of the hydrolysis and of the cellular uptake of AEA were evaluated (Figure 30). As a general screening, a concentration of 5 $\mu g \cdot ml^{-1}$ was chosen.

As shown in Figure 30A, the extract did not show any significant binding to both CB_1 and CB_2 receptors at the concentration of 5 $\mu g \cdot ml^{-1}$. In U937 cell homogenates, the extract displayed only a modest inhibition of AEA hydrolysis, with around 60% of residual FAAH activity and a significant inhibition of AEA uptake in U937 cells (Figure 30B and 30C). The IC_{50} value for AEA uptake inhibition was 4.8 $\mu g \cdot ml^{-1}$.

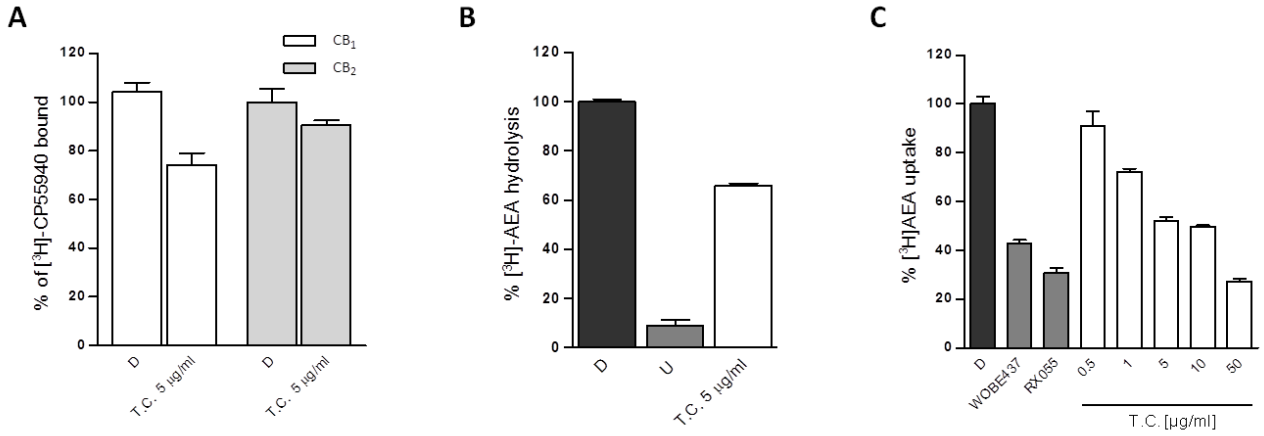

Figure 30. Profile of *T. cordifolia* ethyl acetate extract on the ECS. (A) The radioligand binding assay was performed using 10 µg of membranes of *h*CB_1 or *h*CB_2 receptors transfected CHO-K1 cells per sample. DMSO (vehicle) was used as negative control. The results were expressed as percentage of [^{3}H]-CP-55940 bound to the receptors compared to the vehicle treated control (=100%). Shown are means ± SEM, from 2 independent experiments performed in triplicate (n=2, N=6). (B) The FAAH inhibition assay was performed in U937 cell homogenates. URB597 100 nM was used as positive control for AEA hydrolysis inhibition and DMSO (vehicle) as negative control. The results are expressed as percentage of cellular [^{3}H]-AEA hydrolysed, compared to the vehicle treated control (=100%). Shown are means ± SEM, from 2 independent experiments performed in duplicate (n=2, N=4). (C) AEA uptake inhibition assay was performed in U937 cell homogenates. WOBE437 and RX055 1 µM were used as positive controls for AEA uptake inhibition and DMSO (vehicle) as negative control. The results are expressed as percentage of cellular [^{3}H]-AEA uptake, compared to the vehicle treated control (=100%). Shown are means ± SEM, from 3 independent experiments performed in triplicate (n=3, N=9). AEA, anandamide; D, DMSO; U, URB597; T.C., *Tinospora cordifolia*.

In addition, the antiproliferative activity of *T. cordifolia* extract was evaluated with the colorimetric MTT method in HeLa cells. Since the inhibition of cell viability was below 25% at the concentration of 25 $\mu g \cdot ml^{-1}$, the extract can be considered non-cytotoxic.

Focusing the attention on the inhibition of the uptake of AEA, we aimed at identifying the secondary metabolites responsible for such inhibition. In order to verify the hypothesis proposed by Leonti and Casu, commercially available protoberberine alkaloids (i.e. berberine, palmatine and jatrorrhizine) were tested for their ability to inhibit AEA uptake, with negative outcome (IC_{50}>100 µM) (Supplementary Figure 8). Therefore, we decided to subject the *T. cordifolia* extract to bio-guided fractionation. The bio-guided fractionation was assessed using chromatographic techniques. First, the ethyl acetate extract was subjected to NP-VLC, which yielded sixteen sub-fractions (1-16). These fractions were tested for AEA uptake inhibition (Figure 31). From the results of the assay, two most active fractions (**11** and **12**) were identified.

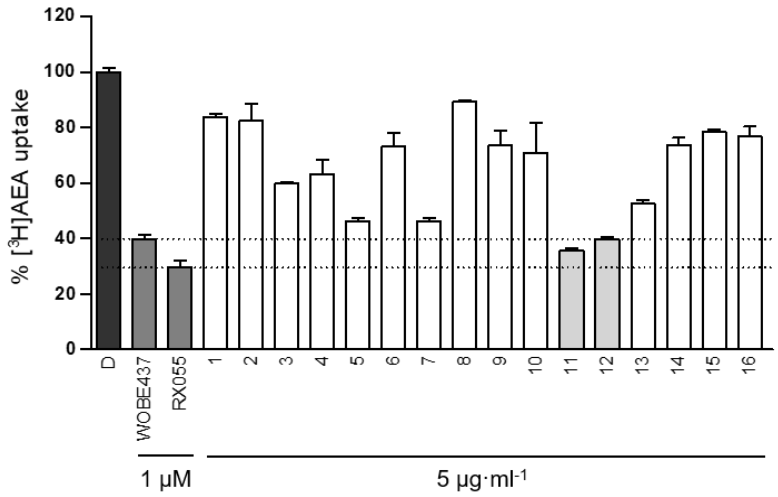

Figure 31. AEA uptake inhibition by the fractions of *T. cordifolia* ethyl acetate extract. Shown are the results of the screening of the fractions of *T. cordifolia* ethyl acetate extract obtained from the VLC. The assay was performed in U937 cell homogenates. WOBE437 and RX055 1 µM were used as positive controls for AEA uptake inhibition and DMSO (vehicle) as negative control. The results are expressed as percentage of cellular [^{3}H]-AEA uptake, compared to the vehicle treated control (=100%). Shown are means ± SEM, from 2 independent experiments performed in triplicate (n=2, N=6). Highlighted are the most active fractions, **11** and **12**. AEA, anandamide; D, DMSO.

Fractions 11 and 12, which were pulled together (**11**), were subjected to subsequent fractionations. After each step of separation, the activity of the obtained sub-fractions was assessed (at the concentration of 5 $\mu g \cdot ml^{-1}$) and the fractions with the highest inhibitory activity were selected for further processing. The Figure 32 provides a schematic overview of the bio-guided fractionation, which led to the most active fractions (**3.1**, **3.2**, **4.1**, **4.2**, **5.1**, **5.2**, **6.1**, **6.2**, **7.1**, **7.2**, **8.1** and **8.2**).

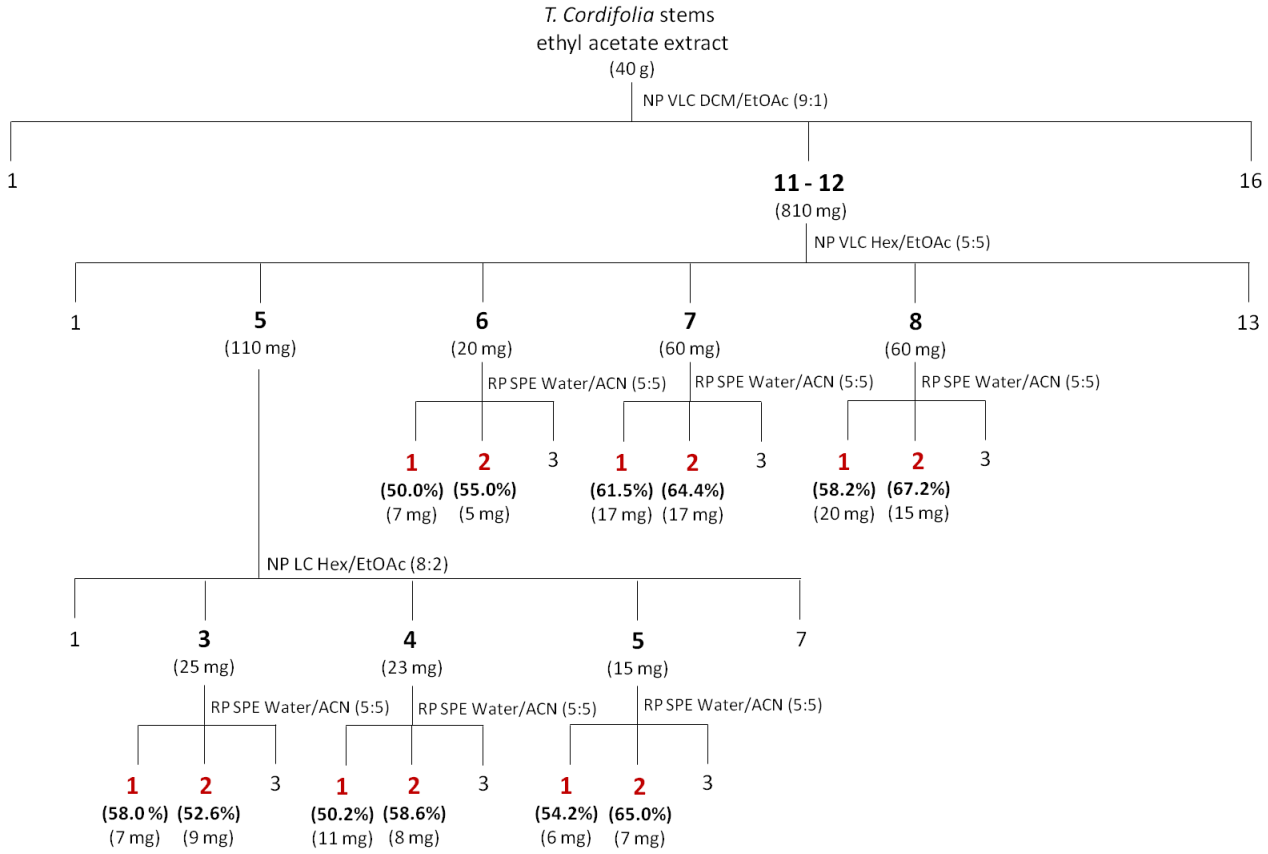

Figure 32. Bio-guided fractionation of *T. cordifolia* stems ethyl acetate extract. Forty grams of crude ethyl acetate extract of *T. cordifolia* stems were subjected to NP-VLC, using a mixture DCM/EtOAc (9:1) in EtOAc step gradient as mobile phase, which yielded to sixteen fractions (1-16). Fractions 11 and 12, which showed the highest AEA uptake inhibition activity, were subjected to a second NP-VLC, using a mixture of Hex/EtOAc (5:5) in EtOAc step gradient, as mobile phase, which yielded to thirteen subfractions (1-13). Fraction 11.5 was subjected to NP-LC, using a mixture of Hex/EtOAc (8:2) in EtOAc step gradient, as mobile phase, which yielded to seven subfractions (1-7). Active subfractions 3, 4, 5, 6, 7 and 8 were subjected to chromatographic purification by solid-liquid partition (RP-SPE), using a mixture of water/ACN (5:5) in ACN step gradient, which yielded to three subfractions. For the most active fractions, the activity expressed as percentage of inhibition of AEA uptake, is reported.

Qualitative TLC of the active fractions **3-8** showed similarities among the sub-fractions **3.1**, **4.1**, **5.1**, **6.1**, **7.1** and **8.1** and among **3.2**, **4.2**, **5.2**, **6.2**, **7.2**, and **8.2** in the chemical components. As example, Figure 33 provides a TLC chromatogram for the fractions **3, 4** and **7.**

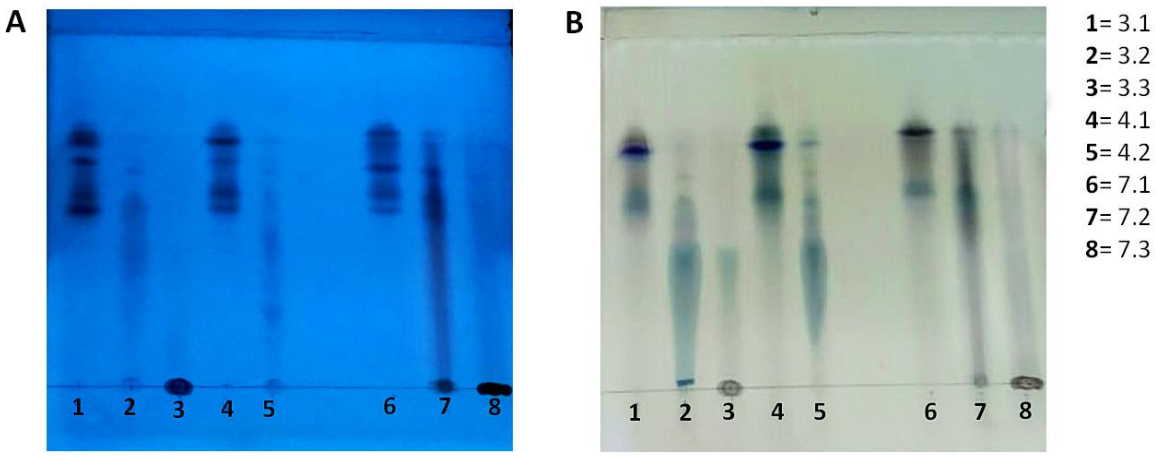

Figure 33. TLC chromatogram of active fractions of *T. cordifolia* extract before (A) and after (B) staining. Silica gel C18 F_{254}, mobile phase water/ACN (1:1), 0.1% TFA. (A) Fluorescence under 254 nm UV light. (B) Detection by visible light after vanillin staining (6 g vanillin, 1.5 ml conc. sulphuric acid, 95 ml 96% ethanol).

The most active fractions were also tested for their ability to inhibit the AEA hydrolysis mediated by FAAH (Figure 34). AEA uptake occurs via facilitated diffusion mediated by a membrane transporter and the driving force of this process is the inward concentration gradient maintained by FAAH-mediated hydrolysis (Chicca et al., 2012, Nicolussi et al., 2014a, Chicca et al., 2017). Therefore, we assessed this assay in order to understand whether the measured percentage of intracellular [^{3}H]-AEA was influenced by an inhibition of its degradation. Indeed, sub-fractions **3.2**, **4.2**, **5.2**, **6.2**, and **7.2**, along with **8.2** with less effectiveness, were able to inhibit AEA hydrolysis with high potency, and therefore, the AEA uptake inhibition displayed by such sub-fractions is FAAH-dependent. Despite, sub-fractions **3.1**, **4.1**, **5.1**, **6.1**, **7.1** and **8.1** did not show significant FAAH inhibition (Figure 34B).

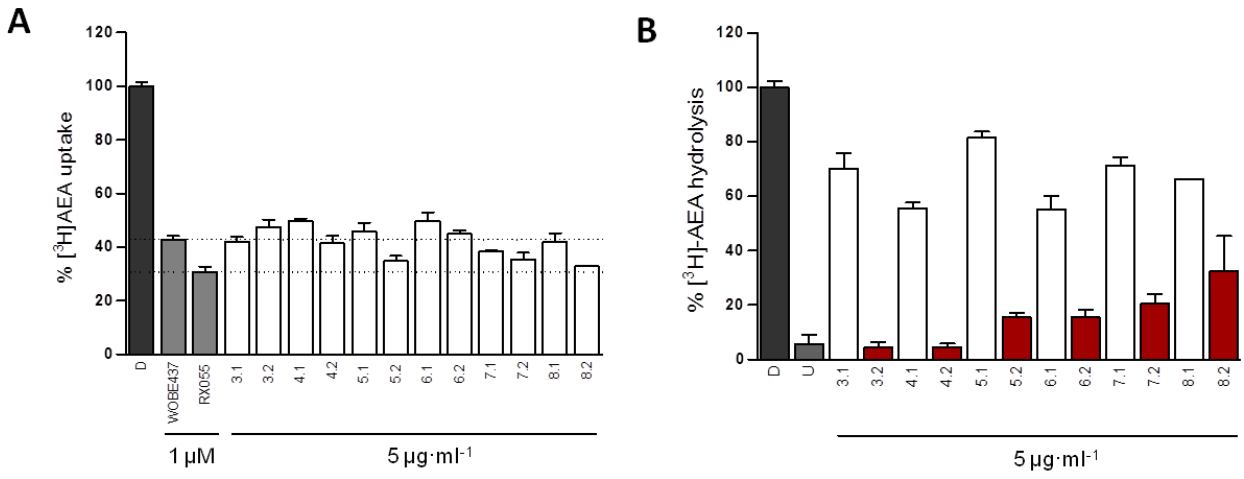

Figure 34. AEA hydrolysis inhibition by the most active fractions of *T. cordifolia* extract on AEA uptake inhibition. (A) Overview of the most active subfranctions for AEA uptake inhibition, deriving from the bioguided fractionation of **11** and **12**. (B) The AEA uptake

inhibition observed for some fractions is mostly driven by FAAH inhibition. The assay was performed in U937 cell homogenates, URB597 100 nM was used as positive control for AEA hydrolysis inhibition and DMSO as negative control. The results are expressed as percentage of cellular [^{3}H]-AEA hydrolysed, compared to the vehicle treated control (=100%). Shown are means ± SEM, from 2 independent experiments performed in duplicate (n=2, N=4). Extracts were dissolved in DMSO. AEA, anandamide; D, DMSO; U, URB597.

Acknowledgements

We thank Simon Nicolussi, Mark Rau and Patricia Schenker for helping in the *in vitro* assays of the *T. cordifolia* extract.

CHAPTER 6 – DISCUSSION AND OUTLOOKS

6.1 Identification of Prenylated Isoflavonoids as Potent, Selective and Reversible Fatty Acid Amide Hydrolase Inhibitors

In the present work, 762 medicinal plant extracts from the *DMM* and *Schwabe* libraries were tested for specific *in vitro* inhibition of FAAH in U937 cell homogenates. The data obtained from the screening were analysed under a phylogenetic approach, in order to find a relationship between plant phylogeny and the observed inhibitory activity. This phylogenetic perspective revealed an interesting clustering of FAAH inhibition within the Fabaceae family, where the extracts of *Lupinus angustifolius*, *Glycyrrhiza glabra*, *Glycyrrhiza uralensis*, *Psoralea corylifolia*, *Anagyris foetida*, and *Medicago arborea*, all belonging to these family, showed potent FAAH inhibition. Nevertheless, FAAH inhibition was also observed in some non-phylogenetically related plants, such as *Zingiber officinale* (Zingiberaceae), *Cupressus sempervirens* (Cupressaceae), *Celtis australis* (Cannabaceae), *Lysimachia vulgaris* (Myrsinaceae) and *Ajuga chamaepitys* (Lamiaceae).

In *DMM*, Fabaceae-derived extracts were recommended for the treatment of ulcers, abscesses, wounds and inflammations of the skin and of the gastrointestinal tract (Matthioli, 1568). In the traditional medicine, *Glycyrrhiza* extracts are generally used for the treatment of the ailments described above, in addition to their antimicrobial, antioxidant and anti-diabetic activities (Fiore et al., 2005, Hosseinzadeh and Nassiri-Asl, 2015). *Psoralea corylifolia* extracts and their bioactive compounds are known for their anti-inflammatory and anti-oxidant properties as well (Zhang et al., 2016). As FAAH inhibition has been shown to produce some of the effects described above (Oláh et al., 2016, Sasso et al., 2015, Naidu et al., 2010), we hypothesize that some of the effects of the medicinal plants from Fabaceae are exerted via FAAH inhibition. Thus, we searched for a possible link between bioactive Fabaceae-derived secondary metabolites and FAAH inhibition.

A multitude of studies about secondary metabolites of Fabaceae has shown similarities in the chemical composition, particularly highlighting the presence of isoflavonoids and their prenylated derivatives. Notably, the flavonoids and isoflavonoids 7-hydroxyisoflavone, genistein, daidzein, biochanin A and kaempferol have been previously reported as FAAH inhibitors (Thors et al., 2007b, Thors et al., 2007a, Thors et al., 2008, Thors et al., 2010). Despite being known that prenylated isoflavonoids have broad biological effects, (e.g. antibacterial, antioxidant, estrogenic and anti-inflammatory activity (Chen et al., 2014)), FAAH inhibitory activity has not been reported yet. Furthermore, it has been suggested that the

prenylation can increase the lipophilicity and, consequently, the interaction with cellular membranes and biological activity as compared to its backbone (Barron and Ibrahim, 1996, Hatano et al., 2000). Therefore, we proposed prenylated isoflavonoids, which are widely produced in Fabaceae, as potential FAAH inhibitors.

In order to test our hypothesis, the FAAH inhibitory activity of fourteen compounds was assessed at the concentration of 10 μM in mouse brain membrane preparations (Figure 19). FAAH inhibitory activity of 7-hydroxyisoflavone, daidzein, genistein and biochanin A was confirmed in our experiments, and these cmpounds are among the most active (Figure 19). By comparing the rate of AEA hydrolysed by FAAH in presence of genistein, biochanin A or barpisoflavone at the concentration of 10 μM, it is evident that genistein and biochanin A are more effective FAAH inhibitors than barpisoflavone (Figure 19). Although the calculation of IC_{50} values for those compounds is required to address their structure-activity relatioship (SAR), our results suggest that a free hydroxy group at C-5 might be a requirement for the interaction with the enzyme and, therfore, its inhibition. However, the presence of a C-5 hydroxyl group does not seem to be essential for the inhibition, since compounds such as neobavaisoflavone (IC_{50}=63.2 nM) and daidzein (IC_{50}=3.7 μM), which do not present such hydroxyl group, show significant FAAH inhibitory activity (Table 1). The prenylation and the position of the prenyl chain seems to affect the activity against FAAH. Indeed, prenylation of daidzein (IC_{50}=3.7 μM) at the C-5' leads to a very potent FAAH inhibitor (i.e. neobavaisoflavone, IC_{50}=63.2 nM). However, the corresponding prenylated derivative of genistein at the C-8 (i.e. lupiwighteone) has nearly no changes in the activity at the concentration of 10 μM, whereas the prenylated at the C-6 (i.e. wighteone), does not show FAAH inhbition at the same concentration. Prenylation of 2'-hydroxygenistein at the C-6 results in luteone, which showed to be a very active compund with an IC_{50} of 391.6 nM. At 10 μM, luteone displays almost a full inihibition of FAAH, while licoisoflavone A (3'-prenyl-2'hydroxygenistein) is inactive. Interestingly, wighteone is an inactive compound at 10 μM and only differs from luteone for the absence of the hydroxyl group in the C-2'. In addition, the presence of a second prenyl group seems to lead to inactive compounds (e.g. 8-prenylluteone and all the other di-prenylated isoflavonoids), suggesting that the addition of a second prenyl substituent may result in a bulky molecule unable to interact with the enzyme.

Considering that dose-response relationships were not determined for all compounds, we cannot properly discuss about the structure-activity relationships (SAR). Therefore, these are preliminar interpretations and IC_{50} values of all the studied compounds will be required in order to understand the real influence of the prenylation on FAAH inhibition. Therefore, an important outlook of my work is to determine the IC_{50} values for all the isoflavonoids tested, eventually including even additional compounds, in order to properly analyse a SAR and to identify the structural requirements for FAAH inhibition in this class of compounds. For instance, it would be relevant to compare the IC_{50} values of luteone and its

backbone 2'-hydroxygenistein, in order to verify wheather the prenylation is responsible for an increased FAAH inhibition, like in the case of neobavaisoflavone and daidzein.

Among the tested isoflavonoids, the prenylated neobavaisoflavone and luteone were the two most potent FAAH inhibitors, with IC_{50} values of 63.2 nM and 391.6 nM, respectively. Interestingly, these compounds are 10-20 times more potent than the known isoflavonoid FAAH inhibitors daidzein and biochanin A which showed in our assay conditions IC_{50} values of 3.7 µM and 1.2 µM, respectively, in agreement with the values reported in the literature (Thors et al., 2007b, Thors et al., 2010).

It has been reported that neobavaisoflavone and luteone are able to exert other *in vitro* effects, including antimicrobial, antioxidant, anti-inflammatory, anti-tumoral and estrogenic-receptor modulatory activity (Fukui et al., 1973, Bronikowska et al., 2010, Szliszka et al., 2011a, Szliszka et al., 2011b, Kuete et al., 2014, Akter et al., 2016). Remarkably, these effects occur at micromolar concentrations, with a factor >10 higher than the IC_{50} values for FAAH inhibition, which can be considered a new biological property of neobavaisoflavone and luteone. Thanks to the involvement of the ECS in many pathophysiological conditions, we could speculate that the inhibition of FAAH may be responsible, at least in part, of most of the reported biological effects observed in phenotypic assays *in vitro*.

A detailed assessment of the mechanism of action of FAAH inhibition indicated that neobavaisoflavone and luteone are potent, competitive, selective and reversible FAAH inhibitors (Figures 22, 23 and 24). The latter property can be explained by a series of non-covalent interactions between our polyphenolic compounds and the catalytic site of the enzyme such as hydrogen bonds, ionic bonds and hydrophobic interactions, as reported for other similar molecules (Bennick, 2002, Simon et al., 2003, Lo Piparo et al., 2008, Bordenave et al., 2014). Considering the reversible and non-covalent nature of the interactions with FAAH, along with the low nanomolar potency, neobavaisoflavone may represent a promising natural compound for further therapeutic applications.

Computational studies helped to clarify the interactions of these two isoflavonoids with the active site of FAAH and supported the experimental data obtained with the biological assays. The docking protocol validation has been successful and allowed a proper docking of the studied isoflavonoids. The results of the experiments (Figure 26) highlighted not only the importance of the prenyl moiety, but also the position. Indeed, the prenylated neobavaisoflavone and luteone resulted more active than daidzein and biochanin A, in line with the experimental results. However, while the substitution in the coumarin portion of the isoflavonoid (i.e. luteone) keeps the ligand in the entrance of the pocket, the substitution in the phenyl portion (i.e. neobavaisoflavone) allows the compound to reach the catalytic residues Ser241, Ser217 and Lys142. This results in neobavaisoflavone more active than luteone. Moreover, the results indicated that also the number and the position of the hydroxyl groups influence the activity, since in luteone multiple substitutions prevent the accommodation inside the pocket, resulting in a less active compound. Therefore,

docking experiments gave important insights about the interactions of these inhibitors with the active site of the enzyme and about the SAR of this class of FAAH inhibitors. Moreover, this information may help in the future to eventually modify the chemical scaffold with the aim to design and generate more drug-like derivatives .

Importantly, the results of our study indirectly demonstrated that neobavaisoflavone and luteone efficiently cross the cell membranes (Figure 25). Since FAAH has an intracellular localization, we investigated the real effectiveness of these compounds as FAAH inhibitors in living cells, as in membranes or homogenates preparations this physiological barrier is absent. In living cells, both compounds showed still good IC_{50} values for FAAH inhibition (316 nM for neobavaisoflavone and 2 µM for luteone). In this system, compared to the mouse brain membrane preparations, higher concentrations are required to inhibit FAAH, suggesting that the cell membrane may constitute a barrier for the compounds. However, other factors cannot be excluded, such as the stability of the compound in living cells, a partial segregation in the phospholipid bilayer and/or intracellular organelles, and the different origin of the biological matrices (brain vs. immune cells). Moreover, the differential involvement of other enzymes in the hydrolysis of AEA (e.g. FAAH-1 vs. FAAH-2, MAGL, COX-2) between mouse membrane preparations and U937 living cells should be considered. Furthermore, in luteone, the presence of four hydroxyl groups, which confer hydrophilic features to the compound, may represent a disadvantage for cell-permeability. On the other hand, the prenyl-moiety may facilitate cell-permeability, increasing the lipophilicity and the affinity for the cell membrane. This can partially explain the higher potency of neobavaisoflavone as compared with its non-prenylated analogue daidzein (Figure 25B).

Cell-permeability is an important feature for neobavaisoflavone and luteone. However, more information about pharmacokinetic, bioavailability and stability in body fluids of these isoflavonoids need to be investigated in order to further assess the therapeutic potential of these FAAH inhibitors in preclinical animal disease models. Moreover, the capacity of these compounds to cross the blood-brain barrier (BBB) is a critical factor for their potential *in vivo* effect on CNS related diseases. In 2016, Gao and colleagues reported the stability of neobavaisoflavone contained in *P. corylifolia* extract and its pharmacokinetic profile after oral administration in rats. The authors have shown that neobavaisoflavone is well absorbed at the gastrointestinal tract level and it has a good stability in plasma (Gao et al., 2016). More recently, Yang and colleagues (2018) investigated the peripheral and CNS concentrations of the major constituents of the *P. corylifolia* fruit extract, including neobavaisoflavone, after oral administration of the extract in rats. Eleven compounds, among coumarins and prenylflavonoids, were extracted at different time points from rat plasma and distinct brain areas, and quantified by LC–MS/MS method. The results showed that all the tested compounds were absorbed into the bloodstream and rapidly distributed into the brain (Yang et al., 2018). Compared to the coumarins, the prenylflavonoids could penetrate the BBB more easily and thus

rapidly accumulate in the brain. The authors concluded that the compounds are orally bioavailable and that efficiently reach the brain, thus supporting the potential clinical value of *P. corylifolia* extract and its major constituents.

The high potent inhibition of FAAH activity showed by neobavaisoflavone, in addition to its capacity to cross the BBB, suggests that this isoflavonoid could reach bioactive concentrations in the brain leading to potential therapeutic effects. Moreover, since FAAH is not only localized in the brain, but rather distributed ubiquitously in the body, it will be of particular interest to investigate the biodistribution of neobavaisoflavone in peripheral tissues. Therefore, future studies should be aimed at thoroughly assessing the therapeutic value of neobavaisoflavone and luteone by investigating their pharmacokinetics, metabolism and tissue distribution. A possible experiment to address this aim consist in a time-course quantification (0-24h) of these isoflavonoids in plasma, to evaluate parameters such as Cmax, Tmax, half-life, AUC and oral bioavailability, after intravenous or oral administration of a single dose in rodents. Furthermore, a quantification of the amount of the compound in brain and peripheral organs after single and repeated administrations could be assessed, to verify the tissue distribution and possible accumulation. Tissue levels of AEA could be also quantified, in order to evaluate the efficacy of FAAH inhibition displayed by the isoflavonoids.

The effect of neobavaisoflavone and luteone as potent FAAH inhibitors suggests that these compounds may be tested for several potential therapeutic applications. The pharmacological inhibition of the AEA degradation has promising therapeutic effects in the treatment of mood and anxiety disorders (Gobbi et al., 2005, Bedse et al., 2018), as well as in pain management, including the treatment of acute inflammatory and neuropathic pain (Jhaveri et al., 2006, Jhaveri et al., 2008, Kinsey et al., 2011). Nevertheless, no consistent correlation between the *in vivo* therapeutic effects exerted by flavonoids and isoflavonoids and FAAH inhibition has been directly reported yet. For instance, a previous study of Thors and colleagues (2010) attempted to investigate *in vivo* the effects of FAAH inhibition of the isoflavonoid biochanin A. The authors showed that biochanin A inhibits pain sensitisation in anesthetized mice treated with formalin (Thors et al., 2010). However, the authors did not directly address the link between these effects and FAAH inhibition. Toker *et al*., (2004) showed that the FAAH inhibitor kaempferol produces antinociceptive and anti-inflammatory effects in animal models of pain upon oral administration (Toker et al., 2004), but whether these effects were specifically mediated by FAAH inhibition it has not been confirmed.

Our results provide the molecular evidence for further investigations on the pharmacology of neobavaisoflavone and luteone *in vivo* under physiological and/or pathological conditions. Pharmacological inhibition of FAAH activity has been shown to produce analgesic and anxiolytic effects (see *Introduction*, Section 1.2.5). Thus, one way to test the effect of neobavaisoflavone and luteone in these conditions is to

combine pharmacology and experimental rodent models. For instance, models such as the hot plate test and the formalin test (Eddy and Leimbach, 1953, Tjolsen et al., 1992) could be used to evaluate analgesia and nociception, while anxiety could be evaluated under the elevated plus maze test (Pellow et al., 1985). Pathological conditions involving chronic inflammation often induce an increasing of the AEA levels in order to overcome the disease. However, increased or efficient FAAH activity mostly restricts these AEA effects (Sagar et al., 2009). Therefore, animal models of chronic pain or neuropathic pain will be useful to assess the potential of neobavaisoflavone and luteone against inflammation.

Some irreversible FAAH inhibitors reached phase I and II of clinical development for the treatment of inflammatory and anxiety disorders. Unfortunately, none of these inhibitors have proceeded in the clinical development so far mainly due to lack of efficacy. For instance, the compound PF-04457845 was assessed in a phase II trial in patients with osteoarthritic pain of the knee (Huggins et al., 2012). In line with the mechanism of action, PF-04457845 led to a 10-fold increase of the concentration of AEA and other NAEs in blood. However, the inhibitor failed to reduce pain and inflammation of the knee in the patients (Huggins et al., 2012). It was suggested that covalent and irreversible inhibition of FAAH can lead to an overflow of AEA which can be oxygenated by the COX-2. Indeed, in inflammatory conditions, COX-2 is overexpressed and can efficiently metabolize AEA generating a plethora of prostaglandin-like molecules, which exert different and not fully elucidated biological actions that can contrast the positive effects of AEA (Kozak et al., 2002, Glaser and Kaczocha, 2010, Maccarrone, 2017). Therefore, reversible and time-limited inhibition of FAAH may represent a better pharmacological approach and non-covalent FAAH inhibitors can be a new class of more efficient therapeutic agents. In the context of a proper drug discovery project, our results indicate that neobavaisoflavone and luteone can be used as templates to initiate proper medchem studies aimed at designing more drug-like reversible and non-covalent FAAH inhibitors.

In the present study, we also attempted to investigate the potential role of plant secondary metabolites in the modulation of the endogenous NAE levels in plant tissue. Eukaryotic cells have a well conserved endocannabinoid signalling system and thus plants and mammals share the archetypal components of this lipid network, namely endogenous signalling molecules, binding proteins and enzymes responsible for the termination of the signalling (Chapman, 2004). The ECS exerts different functions in plant tissues, primary directed towards the mediation of defence responses (Chapman, 2004). Therefore, the question was raised whether such secondary metabolites have an endogenous role in the modulation of the endocannabinoid levels in plant tissues. To investigate this possibility we quantified the NAEs in sixteen plant extracts with different FAAH inhibitory potencies (measured in human cell lines and mouse brain membrane preparations) by LC-MS/MS analysis (Figure 18). We hypothesized that plant extracts displaying the highest FAAH inhibition against human and rodent FAAH may contain higher amounts of NAE levels as the result of an endogenous inhibition of NAEs hydrolysis. Our analyses showed no correlation

between the FAAH inhibition and NAE levels in the extracts. However, these negative results are not enough to fully reject this hypothesis. In fact, detected NAE levels can depend on several factors. For instance, NAE levels can be influenced by the collection and the extraction of the plant material and by the studied plant part (e.g. leaves vs. roots). Therefore, quantification of NAE levels in fresh plant tissues can give a better idea.

Additionally, it remains to be investigated whether the identified plant-derived inhibitors targeting the mammalian FAAH (neobavaisoflavone and luteone), can also inhibit plant FAAH. This hypothesis can be tested by performing ABPP experiments and NAE hydrolysis assays using homogenized plant tissues expressing FAAH. Previous studies carried out in *A. thaliana* tissue homogenates expressing FAAH reported the kinetic profiling of plant FAAH and provided information about its functional hydrolytic activity (Shrestha et al., 2003, Shrestha et al., 2006, Kim et al., 2013). Thus, the interactions between plant FAAH and the inhibitors neobavaisoflavone and luteone can be established testing their ability to inhibit the hydrolysis of radiolabeled NAEs in plant tissue homogenates expressing FAAH. As previously stated, the plant ECS is involved in defence responses (Chapman, 2004). Therefore, it would be important to investigate the functional relevance of the inhibition of plant FAAH, by neobavaisoflavone and luteone, in plant tissues exposed to either elicitors or stress conditions. Complementary analysis should include the quantification of NAEs after the insult as well as relation between the resistance to the insult and the amount of neobavaisoflavone and luteone produced. Indeed, it has been demonstrated that NAE levels increase during pathogen elicitation and stress conditions (Chapman et al., 1995a, Chapman, 2004). Importantly, it has been shown that the total content of isoflavonoids and prenylated derivatives increase in some plants during the same events (Wojakowska et al., 2013a, Aisyah et al., 2016), as it is known that these secondary metabolites are involved in the primary defensive responses in plant tissues. Therefore, if successful, these experiments may reveal a novel mechanism through which such secondary metabolites mediate defensive responses in plants.

Given the consistent distribution of FAAH inhibitors in food plants (e.g. lupine and liquorice), it is also important to take in consideration the dietary relevance of phytocannabinoids. The ECS has a regulatory role on food intake and energy balance (Bellocchio et al., 2008, DiPatrizio and Piomelli, 2012, Lau et al., 2017) and there is an increasing evidence that dietary constituents are able to modulate the ECS (Thors et al., 2007b, Gertsch et al., 2008, Leonti et al., 2010, Nicolussi et al., 2014b). In a recent review, Gertsch (2017) provides an evolutionary perspective linking diet and the ECS with emphasis on the pathophysiological changes following the adoption of an agriculturalist lifestyle. A diet rich in phytocannabinoids might be able to counteract disorders associated with neolithization such as hyperlipidaemia, diabetes, hepatorenal inflammation and cardiometabolic risk (Gertsch, 2017). Interestingly, the considerable number of plants important for feeding and agriculture that display high

FAAH inhibitory activity highlights the beneficial implications of a diet rich in cannabimimetic agents for human health.

In conclusion, we have provided new evidence that the natural prenylated isoflavonoids neobavaisoflavone and luteone from Fabaceae are new potent and selective *in vitro* FAAH inhibitors. Molecular docking experiments rationalized the activity of the two compounds as reversible FAAH inhibitors and gave important insights about their interactions with the active site, which in the future may help in the design and identification of new potent FAAH inhibitors. Although further studies are necessary to assess the pharmacokinetics, the bioavailability and the *in vivo* efficacy of such compounds as FAAH inhibitors, they may nevertheless represent promising templates for the development of new anti-inflammatory, anti-nociceptive and anxiolytic agents. In addition, neobavaisoflavone and luteone may be used as scaffolds for the design of reversible and non-covalent FAAH inhibitors with better pharmacological and pharmacokinetic profile compared with current irreversible analogues.

6.2 Screening of Herbal Drug Extracts from the *De Materia Medica*: Antiproliferative Activity and Cannabinoid Type-2 Receptors Binding

The 660 medicinal plant extracts from the *DMM* library were tested for non-specific anti-proliferative effects in HeLa cells and for interactions with CB_2 receptors in membranes of *h*CB_2 receptor-transfected CHO-K1 cells. Unlike the FAAH screening, phylogenetic examination of the obtained data did not underline any relevant cluster. Indeed, non-specific cytotoxicity was found across extracts of different species and families without any significant phylogenetic association, and the CB_2 receptors binding screening revealed only two "hits", followed by few non-phylogenetically correlated plant species with moderate interaction with CB_2 receptors (see Figure 27 and Supplementary Table 4). Therefore, a phylogenetic approach is not suitable to find association between both plant genetic pool and general anti-proliferative activity or CB_2 receptors interaction.

Evaluation of the anti-proliferative potential is important for drug discovery, since a sample generating anti-proliferative responses may be eliminated from subsequent screening or may constitute a "hit" for cancer research. In our study, some of the plant extracts identified as "hits" either for FAAH inhibition or CB_2 receptor interaction showed also significant anti-proliferative effects at 25 $\mu g \cdot ml^{-1}$, *G. glabra* roots (85.5% of non-viable cells) and *F. gummosa* resin (83.6% of non-viable cells) (see Supplementary Table 4). Nevertheless, the general anti-proliferative activity of the secondary metabolites active towards the ECS was not verified. Thus, the evaluation of any anti-proliferative activity induced by the active prenylated isoflavonoids and sesquiterpene coumarins needs to be addressed, in order to complete the pharmacological profile of such compounds. In the case of farnesiferol A, which in our screening showed the best interaction towards CB_2 receptors, previous studies have shown cytotoxic and anti-proliferative activity in cancer cell lines (Iranshahi et al., 2008, Iranshahi et al., 2010a). Since the ECS seems to be a potential target for cancer therapy, it would be relevant to test whether any cytotoxic activity of the compound is related to its interaction with the ECS (Blazquez et al., 2003, Guindon and Hohmann, 2011, Khan et al., 2016).

Chi-square analysis pointed out that those herbal drugs whose extracts showed pronounced antiproliferative activity have a significantly different profile of administration in the *DMM*. In fact, the most frequently described way of administration for the 54 antiproliferative drugs in the *DMM* was related to external applications, whereas internal applications were less frequently associated with these herbal drugs. For the non cytotoxic drugs, the situation was reversed with the internal uses most frequently mentioned and external applications less important. Therefore, it seems that extracts derived from herbal drugs with topic applications have a higher probability to show cytotoxicity than those obtained from

herbal drugs with internal applications. In conclusion, the results may suggest that the cytotoxicity assay may be used to predict whether an herbal drug is rather applied externally or internally.

The results of the CB_2 receptor binding studies showed that *F. gummosa* and *F. persica* resin extracts interact with CB_2 receptors with EC_{50} of 2.8 $\mu g \cdot ml^{-1}$ and 4.1 $\mu g \cdot ml^{-1}$, respectively (Figure 28). The genus *Ferula* is a rich source of biologically active compounds (Nazari and Iranshahi, 2011). Among them, the presence of sesquiterpene coumarins have been associated with some of the pharmacological properties of *Ferula* extracts, such as anti-inflammatory, anti-nociceptive and cancer-chemopreventive activities (Nazari and Iranshahi, 2011, Sattar and Iranshahi, 2017). Notably, activation of CB_2 receptors leads to similar therapeutic effects. For instance, peripheral CB_2 receptor activation leads to anti-inflammatory and anti-nociceptive responses in animal models of inflammation (Ibrahim et al., 2003, Gertsch et al., 2008) and to anti-proliferative and pro-apoptotic effects in immortalized cell lines (Capozzi et al., 2018). Therefore, sesquiterpene-coumarins, secondary metabolites representative of *Ferula* species, were proposed as class of compounds potentially responsible for the observed CB_2 receptors affinity of the *Ferula* extracts.

Among the twelve screened compounds (Figure 29), farnesiferol A displayed the best interaction with CB_2 receptors with an EC_{50} of 1.1 µM, followed by colladonin and farnesiferol B, with EC_{50} of 5.1 and 6.3 µM, respectively (Table 5). In order to understand whether the terpene moiety was responsible for the activity, the simple coumarins umbelliferone and 4-methylumbelliferone were also tested. At the concentrations of 1 µM and 10 µM, both compounds did not show interaction with CB_2 receptors (Figure 29). These results suggest that the terpene moiety, rather than the coumarinic seems to be responsible for the interaction with the CB_2 receptors, and therefore, for the activity. Interestingly, colladonin, which differs from farnesiferol A only by the configuration of the chiral centre C-1, displayed a lower affinity for CB_2 receptors, suggesting that the configuration of the C-1 may influence this property. The double ring in the terpene moiety does not seem to be an essential requirement for the activity, since farnesiferol B has similar EC_{50} than farnesiferol A and colladonin (Figure 29 and Table 5). Unlike, it seems that a C=C double bond at C-2' and a free hydroxyl group at C-6 play an important role for the activity, since farnesiferol C, which lacks these structural requirements, has lower potency (EC_{50}=40.75 µM). Therefore, taking into account the chemical structure of the screened compounds and their affinity for CB_2 receptors, we hypothesize that a C=C double bond at C-2' may be important for a good interaction with the receptor, as well as the presence of a free hydroxyl group at C-6 and the configuration of the chiral centre C-1. However, further studies need to be carried out in order to properly understand the SAR of this class of chemical compounds.

Among the tested compounds, farnesiferol A showed the best interaction with CB_2 receptors (Figure 29 and Table 5). The reported biological activities of farnesiferol A space from the nanomolar range to the micromolar range (Nazari and Iranshahi, 2011). Therefore, the CB_2 receptor binding can be

considered as a new elucidated *in vitro* property of this compound. When compared to the potency of other known plant-derived CB_2 ligands (Raduner et al., 2006, Gertsch et al., 2008), the potency of farnesiferol A is rather modest. However, the compound may represent a starting point for structural modifications aimed to the development of more potent CB_2 receptor ligands.

In order to better characterize the pharmacological profile of the most active compounds farnesiferol A, farnesiferol B and colladonin, further studies must be designed to specifically address several issues. First, EC_{50} values for CB_1 receptors binding are required, in order to understand whether these compounds are selective for CB_2 receptors. Indeed, selective CB_2 receptor ligands devoid of the psychoactive side effects typically associated with CB_1 receptor activation are potential drug candidates for the treatment of inflammation, pain, atherosclerosis and arthritis (Gertsch et al., 2008, Ibrahim et al., 2003, Bermudez-Silva et al., 2007, Fukuda et al., 2014, Tolon et al., 2009). In addition, their behaviour as full agonist, partial agonist, antagonists or inverse agonists at CB_2 receptors must be properly addressed. The reported traditional uses and therapeutic properties of *Ferula* extracts as anti-inflammatory, anti-nociceptive and anti-diabetic remedy may suggests the presence of agonists of CB_2 receptors, rather than antagonist/inverse agonists (Abu-Zaiton, 2010, Mahboubi, 2016). One way to properly assess the behaviour of these ligands, is to perform [^{35}S]GTPγS functional assay (Chicca et al., 2017). Upon activation of a GPCR by an agonist, conformational changes in the receptor allow the Gα subunit to release guanosine diphosphate (GDP) and to bind guanosine-5'-tryphosphate (GTP) (Strange, 2010). The principle of the [^{35}S]GTPγS functional assay is that using a non-hydrolysable radiolabeled GTP analogue is possible to measure the activation of the GPCR by measuring the amount of radiolabeled GTP bound to the cell membranes. In addition, with this assay, is possible to differentiate agonist, antagonist, and inverse agonist activities (Harrison and Traynor, 2003, Strange, 2010).

In summary, in this study we have identified sesquiterpene coumarins farnesiferol A, farnesiferol B and colladonin as new *in vitro* CB_2 receptors ligands, with EC_{50} values in the low micromolar range. This biological activity let us speculate that these secondary metabolites can be responsible at least in part for the CB_2 receptor affinity observed in our *Ferula* extracts. This property may be related also to some of the reported therapeutic activities of *Ferula* species, which may be associated to an involvement of the ECS via CB_2 receptors. Moreover, the same class of compounds may be responsible for the anti-proliferative property in tumoral cells that we observed in *F. gummosa* extract. However, we cannot exclude the possibility that other classes of secondary metabolites of the genus *Ferula* are able to interact with CB_2 receptors and, therefore, being co-responsible for the observed biological activity.

Overall, these findings may open a new perspective in the medical use of *Ferula* resin and their secondary metabolites for the treatment of conditions or disorders where the modulation of CB_2 receptors is of therapeutic relevance.

6.3 Inhibition of AEA Uptake by *Tinospora cordifolia* Ethyl Acetate Extract

The pharmacological profiling of *T. cordifolia* extract towards the ECS was prompted by the hypothesis that the psychoactive effects exerted by this medicinal plant are associated with the presence of secondary metabolites able to modulate the ECS. Indeed, the profiling of *T. cordifolia* extract towards the components of the ECS revealed that it significantly inhibits the uptake of AEA in U937 cells (IC_{50}=4.8 µg·ml^{-1}) with limited effects over FAAH and not significant binding towards CB_1 or CB_2 receptors (Figure 30).

The protoberberine alkaloids berberine, palmatine and jatrorrhizine, initially proposed to contribute to such biological activity, were found to be inactive (Supplementary Figure 8). Therefore, bio-guided fractionation of the *T. cordifolia* extract was initiated to identify the secondary metabolites responsible for the AEA uptake inhibition (Figure 32). The chromatographic fractionation of the extract led to the identification of the sub-fractions 3-8 as the most active on the inhibition of the AEA uptake (Figure 32). Further chromatographic purification of these fractions by solid-liquid partition yielded to sub-fractions 1 and 2 as active, and subfractions 3 as inactive. This suggests that the purification step allowed first the elution of the active metabolites and the retention of the inactive ones, which were eluted in a second step, by increasing the lipophilicity of the elution solvent with a higher rate of ACN. This observation might indicate that the active compounds possess better hydrophilic properties than the inactive ones, since they eluted before.

Another interesting observation concerns the inhibition of FAAH possessed by some fractions (Figure 34B). Reuptake of signalling molecules is an essential step for the termination of signal transduction. In the specific case of AEA, cellular uptake is followed by intracellular hydrolysis, mainly mediated by FAAH (Di Marzo et al., 1994). FAAH activity maintains an inward concentration gradient across the plasma membrane that represents the driving force for AEA uptake (Fowler et al., 2004, Chicca et al., 2012). Accordingly, FAAH inhibitors should reduce the observed rate of cell association of AEA (Fowler, 2013). This is the case of the subfractions 3.2, 4.2, 5.2, 6.2, 7.2 and 8.2, where the observed reduced rate of AEA cellular uptake seems to be an effect of the inhibition of FAAH (Figure 34B). Although the compounds contained in those fractions have not been identified yet, the data suggest that subfractions 3.2, 4.2, 5.2, 6.2, 7.2 and 8.2 may contain secondary metabolites mainly acting as FAAH inhibitors, whereas subfractions 3.1, 4.1, 5.1, 6.1, 7.1 and 8.1 may contain compounds that specifically inhibit the cellular uptake of AEA, rather than the hydrolysis.

The most active fractions (Figure 34) at the concentration of 5 µg·ml^{-1}, inhibited the cellular uptake of AEA similarly to the synthetic selective AEA uptake inhibitors WOBE437 and RX055, used as positive controls at the concentration of 1 µM (Chicca et al., 2017). Since TLC chromatograms suggest that those

active fractions include several secondary metabolites (Figure 33), the effective concentration of the pure active compounds in the fractions is most likely lower than 5 $\mu g \cdot ml^{-1}$. Therefore, once isolated, the pure compounds might have much lower IC_{50} values, and therefore higher potency, than the one observed for the original fraction. However, synergistic effects among the compounds that constitute the fractions cannot be excluded.

All these observations prompted us to purify and identify the pure active compounds contained in the active fractions. Unfortunately, the complexity of the fractions, deductible also from the TLC chromatograms (Figure 33), and the small amount of material obtained during the bioguided fractionation (few milligrams of each active fraction) make difficult to apply further techniques aimed at purifying the active metabolites, along with the elucidation of their structure and their molecular mechanism involved in the potential effect. Therefore, we decided to interrupt the bioguided fractionation in search of the active metabolites, although their isolation would be achievable with a higher amount of material.

Nevertheless, our results showed that the AEA uptake inhibition property is a new *in vitro* biological property of *T. cordifolia* extract, which may be related to some of the multiple therapeutic effects associated to the use of this medicinal plant. Indeed, the immunomodulatory, anti-inflammatory, anti-diabetic properties of *T. cordifolia* may be linked to a modulatory action on the ECS (Patgiri et al., 2014, Gupta et al., 1967, Upadhyay et al., 2011).

An interesting observation concerns the chemical nature of the compounds that are expected to be found in the active fractions. For instance, stems of *T. cordifolia* are rich in clerodane diterpenes, mainly in the glycosilate form (Maurya et al., 1997, Maurya and Handa, 1997, Maurya et al., 2004). These secondary metabolites have attracted the interest in recent years due to their notable biological activities, including antitumor, anti-inflammatory, hypoglycaemic and hypolipidemic activity (Li et al., 2016). It has been demonstrated that some clerodane diterpenes are able to exert pharmacological actions towards the ECS components. For instance, the hallucinogenic clerodane salvinorin A (from *Salvia divinorum*) is a potent and selective agonist for *κ* opioid receptors (KOR). However, its multiple pharmacological effects are likely due to action on other targets, such as the CB_1 receptors. Indeed, Aviello and colleagues (2011) showed that by activating KOR and CB_1 receptors, salvinorin A exerts potent *in vivo* anti-inflammatory and antinociceptive effects (Aviello et al., 2011). Additionally, some clerodane diterpenes exert MAGL inhibition activity (De Leo et al., 2018). Therefore, clerodane diterpenes may represent suitable candidates to be the active secondary metabolites of *T. cordifolia* extract.

In conclusion, this part of the study identified the activity of *T. cordifolia* extract towards the inhibition of cell AEA uptake and attempted the identification of the secondary metabolites responsible for this effect. Unfortunately, the amount of material obtained during the bioguided fractionation only led to

the identification of the active subfractions, without achieving the final objective of purify and identify the active compounds. Nevertheless, we can report that inhibition of AEA uptake is a new *in vitro* biological activity of *T. cordifolia*, which may be associated to some of the therapeutic properties of this medicinal plant, such as anti-inflammatory, anti-diabetic and immunomodulatory action. Our work thus reinforces the therapeutic value of this medicinal plant and provides evidence about its interactions with the ECS.

REFERENCES

ABD EL-RAZEK, M. H., OHTA, S., AHMED, A. A. & HIRATA, T. 2001. Sesquiterpene coumarins from the roots of Ferula assa-foetida. *Phytochemistry,* 58**,** 1289-95.

ABIRAMASUNDARI, G., SUMALATHA, K. R. & SREEPRIYA, M. 2012. Effects of Tinospora cordifolia (Menispermaceae) on the proliferation, osteogenic differentiation and mineralization of osteoblast model systems in vitro. *J Ethnopharmacol,* 141**,** 474-80.

ABU-ZAITON, A. S. 2010. Anti-diabetic activity of Ferula assafoetida extract in normal and alloxan-induced diabetic rats. *Pak J Biol Sci,* 13**,** 97-100.

ADAMS, M., BERSET, C., KESSLER, M. & HAMBURGER, M. 2009. Medicinal herbs for the treatment of rheumatic disorders--a survey of European herbals from the 16th and 17th century. *J Ethnopharmacol,* 121**,** 343-59.

ADAMS, M., GMUNDER, F. & HAMBURGER, M. 2007. Plants traditionally used in age related brain disorders--a survey of ethnobotanical literature. *J Ethnopharmacol,* 113**,** 363-81.

ADAMS, M., GSCHWIND, S., ZIMMERMANN, S., KAISER, M. & HAMBURGER, M. 2011. Renaissance remedies: Antiplasmodial protostane triterpenoids from Alisma plantago-aquatica L. (Alismataceae). *J Ethnopharmacol,* 135**,** 43-7.

ADHAMI, H.-R., FITZ, V., LUBICH, A., KAEHLIG, H., ZEHL, M. & KRENN, L. 2014. Acetylcholinesterase inhibitors from galbanum, the oleo gum-resin of Ferula gummosa Boiss. *Phytochemistry Letters,* 10**,** lxxxii-lxxxvii.

AFNAN, Q., ADIL, M. D., NISSAR-UL, A., RAFIQ, A. R., AMIR, H. F., KAISER, P., GUPTA, V. K., VISHWAKARMA, R. & TASDUQ, S. A. 2012. Glycyrrhizic acid (GA), a triterpenoid saponin glycoside alleviates ultraviolet-B irradiation-induced photoaging in human dermal fibroblasts. *Phytomedicine,* 19**,** 658-64.

AGARWAL, A., MALINI, S., BAIRY, K. L. & RAO, M. S. 2002. Effect of Tinospora cordifolia on learning and memory in normal and memory deficit rats. *Indian Journal of Pharmacology,* 34**,** 339-349.

AGUADO, T., MONORY, K., PALAZUELOS, J., STELLA, N., CRAVATT, B., LUTZ, B., MARSICANO, G., KOKAIA, Z., GUZMAN, M. & GALVE-ROPERH, I. 2005. The endocannabinoid system drives neural progenitor proliferation. *FASEB J,* 19**,** 1704-6.

AISYAH, S., VINCKEN, J. P., ANDINI, S., MARDIAH, Z. & GRUPPEN, H. 2016. Compositional changes in (iso)flavonoids and estrogenic activity of three edible Lupinus species by germination and Rhizopus-elicitation. *Phytochemistry,* 122**,** 65-75.

AKHLAGHI, F., RAJAEI, Z., HADJZADEH, M. A. R., IRANSHAHI, M. & ALIZADEH, M. 2012. Antihyperglycemic effect of asafoetida (Ferula assafoetida oleo-gum-resin) in streptozotocin-induced diabetic rats. *World Applied Sciences Journal,* 17**,** 157-162.

AKTER, K., BARNES, E. C., LOA-KUM-CHEUNG, W. L., YIN, P., KICHU, M., BROPHY, J. J., BARROW, R. A., IMCHEN, I., VEMULPAD, S. R. & JAMIE, J. F. 2016. Antimicrobial and antioxidant activity and chemical characterisation of Erythrina stricta Roxb. (Fabaceae). *Journal of Ethnopharmacology,* 185**,** 171-181.

ALEXANDER, J. P. & CRAVATT, B. F. 2006. The putative endocannabinoid transport blocker LY2183240 is a potent inhibitor of FAAH and several other brain serine hydrolases. *J Am Chem Soc,* 128**,** 9699-704.

ALMUKADI, H., WU, H., BOHLKE, M., KELLEY, C. J., MAHER, T. J. & PINO-FIGUEROA, A. 2013. The macamide N-3-methoxybenzyl-linoleamide is a time-dependent fatty acid amide hydrolase (FAAH) inhibitor. *Mol Neurobiol,* 48**,** 333-9.

ALTSCHUL, S. F., GISH, W., MILLER, W., MYERS, E. W. & LIPMAN, D. J. 1990. Basic local alignment search tool. *J Mol Biol,* 215**,** 403-10.

AMERI, A. 1999. The effects of cannabinoids on the brain. *Prog Neurobiol,* 58**,** 315-48.

APPENDINO, G., MAXIA, L., BASCOPE, M., HOUGHTON, P. J., SANCHEZ-DUFFHUES, G., MUNOZ, E. & STERNER, O. 2006. A meroterpenoid NF-kappaB inhibitor and drimane sesquiterpenoids from Asafetida. *J Nat Prod,* 69**,** 1101-4.

ARAYA-CLOUTIER, C., DEN BESTEN, H. M., AISYAH, S., GRUPPEN, H. & VINCKEN, J. P. 2017. The position of prenylation of isoflavonoids and stilbenoids from legumes (Fabaceae) modulates the antimicrobial activity against Gram positive pathogens. *Food Chem,* 226**,** 193-201.

ASHA, M. K., DEBRAJ, D., PRASHANTH, D., EDWIN, J. R., SRIKANTH, H. S., MURUGANANTHAM, N., DETHE, S. M., ANIRBAN, B., JAYA, B., DEEPAK, M. & AGARWAL, A. 2013. In vitro anti-Helicobacter pylori activity of a flavonoid rich extract of Glycyrrhiza glabra and its probable mechanisms of action. *J Ethnopharmacol,* 145**,** 581-6.

AUSTIN-BROWN, S. L. & CHAPMAN, K. D. 2002. Inhibition of phospholipase D alpha by N-acylethanolamines. *Plant Physiol,* 129**,** 1892-8.

AVIELLO, G., BORRELLI, F., GUIDA, F., ROMANO, B., LEWELLYN, K., DE CHIARO, M., LUONGO, L., ZJAWIONY, J. K., MAIONE, S., IZZO, A. A. & CAPASSO, R. 2011. Ultrapotent effects of salvinorin A, a hallucinogenic compound from Salvia divinorum, on LPS-stimulated murine macrophages and its anti-inflammatory action in vivo. *J Mol Med (Berl),* 89**,** 891-902.

AYUSH 2001. *The Ayurvedic Pharmacopoeia of India. Part I Vol. I. New Delhi: Department of AYUSH, Ministry of Health and Family Welfare.*

BADAR, V. A., THAWANI, V. R., WAKODE, P. T., SHRIVASTAVA, M. P., GHARPURE, K. J., HINGORANI, L. L. & KHIYANI, R. M. 2005. Efficacy of Tinospora cordifolia in allergic rhinitis. *J Ethnopharmacol,* 96**,** 445-9.

BAFNA, P. A. & BALARAMAN, R. 2005. Anti-ulcer and anti-oxidant activity of pepticare, a herbomineral formulation. *Phytomedicine,* 12**,** 264-70.

BAGGELAAR, M. P., MACCARRONE, M. & VAN DER STELT, M. 2018. 2-Arachidonoylglycerol: A signaling lipid with manifold actions in the brain. *Prog Lipid Res,* 71**,** 1-17.

BAGGELAAR, M. P. & VAN DER STELT, M. 2017. Competitive ABPP of Serine Hydrolases: A Case Study on DAGL-Alpha. *Methods Mol Biol,* 1491**,** 161-169.

BAIRY, K. L., RAO, Y., KUMAR DAS, S. & KUMAR, K. B. 2004. Efficacy of Tinospora cordifolia on Learning and Memory in Healthy Volunteers: A Double-Blind, Randomized, Placebo Controlled Study. *2,* 3**,** 57-0.

BAMBICO, F. R., DURANTI, A., NOBREGA, J. N. & GOBBI, G. 2016. The fatty acid amide hydrolase inhibitor URB597 modulates serotonin-dependent emotional behaviour, and serotonin1A and serotonin2A/C activity in the hippocampus. *Eur Neuropsychopharmacol,* 26**,** 578-90.

BARANN, M., MOLDERINGS, G., BRUSS, M., BONISCH, H., URBAN, B. W. & GOTHERT, M. 2002. Direct inhibition by cannabinoids of human 5-HT3A receptors: probable involvement of an allosteric modulatory site. *Br J Pharmacol,* 137**,** 589-96.

BARRON, D. & IBRAHIM, R. K. 1996. Isoprenylated flavonoids—a survey. *Phytochemistry,* 43**,** 921-982.

BASHASHATI, M., STORR, M. A., NIKAS, S. P., WOOD, J. T., GODLEWSKI, G., LIU, J., HO, W., KEENAN, C. M., ZHANG, H., ALAPAFUJA, S. O., CRAVATT, B. F., LUTZ, B., MACKIE, K., KUNOS, G., PATEL, K. D., MAKRIYANNIS, A., DAVISON, J. S. & SHARKEY, K. A. 2012. Inhibiting fatty acid amide hydrolase normalizes endotoxin-induced enhanced gastrointestinal motility in mice. *Br J Pharmacol,* 165**,** 1556-71.

BATKAI, S., PACHER, P., OSEI-HYIAMAN, D., RADAEVA, S., LIU, J., HARVEY-WHITE, J., OFFERTALER, L., MACKIE, K., RUDD, M. A., BUKOSKI, R. D. & KUNOS, G. 2004. Endocannabinoids acting at cannabinoid-1 receptors regulate cardiovascular function in hypertension. *Circulation,* 110**,** 1996-2002.

BAUER, M., CHICCA, A., TAMBORRINI, M., EISEN, D., LERNER, R., LUTZ, B., POETZ, O., PLUSCHKE, G. & GERTSCH, J. 2012. Identification and quantification of a new family of peptide endocannabinoids (Pepcans) showing negative allosteric modulation at CB1 receptors. *J Biol Chem,* 287**,** 36944-67.

BEDSE, G., BLUETT, R. J., PATRICK, T. A., ROMNESS, N. K., GAULDEN, A. D., KINGSLEY, P. J., PLATH, N., MARNETT, L. J. & PATEL, S. 2018. Therapeutic endocannabinoid augmentation for mood and anxiety disorders: comparative profiling of FAAH, MAGL and dual inhibitors. *Translational Psychiatry,* 8**,** 92.

BELLOCCHIO, L., CERVINO, C., PASQUALI, R. & PAGOTTO, U. 2008. The endocannabinoid system and energy metabolism. *J Neuroendocrinol,* 20**,** 850-7.

BELTRAMO, M., STELLA, N., CALIGNANO, A., LIN, S. Y., MAKRIYANNIS, A. & PIOMELLI, D. 1997. Functional role of high-affinity anandamide transport, as revealed by selective inhibition. *Science,* 277**,** 1094-7.

BENARD, G., MASSA, F., PUENTE, N., LOURENCO, J., BELLOCCHIO, L., SORIA-GOMEZ, E., MATIAS, I., DELAMARRE, A., METNA-LAURENT, M., CANNICH, A., HEBERT-CHATELAIN, E., MULLE, C., ORTEGA-

GUTIERREZ, S., MARTIN-FONTECHA, M., KLUGMANN, M., GUGGENHUBER, S., LUTZ, B., GERTSCH, J., CHAOULOFF, F., LOPEZ-RODRIGUEZ, M. L., GRANDES, P., ROSSIGNOL, R. & MARSICANO, G. 2012. Mitochondrial CB(1) receptors regulate neuronal energy metabolism. *Nat Neurosci,* 15**,** 558-64.

BENNICK, A. 2002. Interaction of plant polyphenols with salivary proteins. *Crit Rev Oral Biol Med,* 13**,** 184-96.

BERMAN, H. M., BATTISTUZ, T., BHAT, T. N., BLUHM, W. F., BOURNE, P. E., BURKHARDT, K., FENG, Z., GILLILAND, G. L., IYPE, L., JAIN, S., FAGAN, P., MARVIN, J., PADILLA, D., RAVICHANDRAN, V., SCHNEIDER, B., THANKI, N., WEISSIG, H., WESTBROOK, J. D. & ZARDECKI, C. 2002. The Protein Data Bank. *Acta Crystallogr D Biol Crystallogr,* 58**,** 899-907.

BERMUDEZ-SILVA, F. J., SANCHEZ-VERA, I., SUAREZ, J., SERRANO, A., FUENTES, E., JUAN-PICO, P., NADAL, A. & RODRIGUEZ DE FONSECA, F. 2007. Role of cannabinoid CB2 receptors in glucose homeostasis in rats. *Eur J Pharmacol,* 565**,** 207-11.

BISOGNO, T., HOWELL, F., WILLIAMS, G., MINASSI, A., CASCIO, M. G., LIGRESTI, A., MATIAS, I., SCHIANO-MORIELLO, A., PAUL, P., WILLIAMS, E. J., GANGADHARAN, U., HOBBS, C., DI MARZO, V. & DOHERTY, P. 2003. Cloning of the first sn1-DAG lipases points to the spatial and temporal regulation of endocannabinoid signaling in the brain. *J Cell Biol,* 163**,** 463-8.

BISOGNO, T., LIGRESTI, A. & DI MARZO, V. 2005. The endocannabinoid signalling system: biochemical aspects. *Pharmacol Biochem Behav,* 81**,** 224-38.

BISOGNO, T., SEPE, N., MELCK, D., MAURELLI, S., DE PETROCELLIS, L. & DI MARZO, V. 1997. Biosynthesis, release and degradation of the novel endogenous cannabimimetic metabolite 2-arachidonoylglycerol in mouse neuroblastoma cells. *Biochem J,* 322 (Pt 2)**,** 671-7.

BISSET, N. G. & NWAIWU, J. 1983. Quaternary alkaloids of tinospora species. *Planta Med,* 48**,** 275-9.

BJORKLUND, E., BLOMQVIST, A., HEDLIN, J., PERSSON, E. & FOWLER, C. J. 2014. Involvement of fatty acid amide hydrolase and fatty acid binding protein 5 in the uptake of anandamide by cell lines with different levels of fatty acid amide hydrolase expression: a pharmacological study. *PLoS One,* 9**,** e103479.

BJORKLUND, E., NOREN, E., NILSSON, J. & FOWLER, C. J. 2010. Inhibition of monoacylglycerol lipase by troglitazone, N-arachidonoyl dopamine and the irreversible inhibitor JZL184: comparison of two different assays. *Br J Pharmacol,* 161**,** 1512-26.

BLANCAFLOR, E. B., HOU, G. & CHAPMAN, K. D. 2003. Elevated levels of N-lauroylethanolamine, an endogenous constituent of desiccated seeds, disrupt normal root development in Arabidopsis thaliana seedlings. *Planta,* 217**,** 206-17.

BLANKMAN, J. L., SIMON, G. M. & CRAVATT, B. F. 2007. A comprehensive profile of brain enzymes that hydrolyze the endocannabinoid 2-arachidonoylglycerol. *Chem Biol,* 14**,** 1347-56.

BLAZQUEZ, C., CASANOVA, M. L., PLANAS, A., GOMEZ DEL PULGAR, T., VILLANUEVA, C., FERNANDEZ-ACENERO, M. J., ARAGONES, J., HUFFMAN, J. W., JORCANO, J. L. & GUZMAN, M. 2003. Inhibition of tumor angiogenesis by cannabinoids. *FASEB J,* 17**,** 529-31.

BOGER, D. L., FECIK, R. A., PATTERSON, J. E., MIYAUCHI, H., PATRICELLI, M. P. & CRAVATT, B. F. 2000. Fatty acid amide hydrolase substrate specificity. *Bioorg Med Chem Lett,* 10**,** 2613-6.

BOGER, D. L., MIYAUCHI, H., DU, W., HARDOUIN, C., FECIK, R. A., CHENG, H., HWANG, I., HEDRICK, M. P., LEUNG, D., ACEVEDO, O., GUIMARAES, C. R., JORGENSEN, W. L. & CRAVATT, B. F. 2005. Discovery of a potent, selective, and efficacious class of reversible alpha-ketoheterocycle inhibitors of fatty acid amide hydrolase effective as analgesics. *J Med Chem,* 48**,** 1849-56.

BORATYN, G. M., SCHAFFER, A. A., AGARWALA, R., ALTSCHUL, S. F., LIPMAN, D. J. & MADDEN, T. L. 2012. Domain enhanced lookup time accelerated BLAST. *Biol Direct,* 7**,** 12.

BORDENAVE, N., HAMAKER, B. R. & FERRUZZI, M. G. 2014. Nature and consequences of non-covalent interactions between flavonoids and macronutrients in foods. *Food Funct,* 5**,** 18-34.

BORTOLATO, M., CAMPOLONGO, P., MANGIERI, R. A., SCATTONI, M. L., FRAU, R., TREZZA, V., LA RANA, G., RUSSO, R., CALIGNANO, A., GESSA, G. L., CUOMO, V. & PIOMELLI, D. 2006. Anxiolytic-like properties of the anandamide transport inhibitor AM404. *Neuropsychopharmacology,* 31**,** 2652-9.

BORTOLATO, M., MANGIERI, R. A., FU, J., KIM, J. H., ARGUELLO, O., DURANTI, A., TONTINI, A., MOR, M., TARZIA, G. & PIOMELLI, D. 2007. Antidepressant-like activity of the fatty acid amide hydrolase inhibitor URB597 in a rat model of chronic mild stress. *Biol Psychiatry,* 62**,** 1103-10.

BOSIER, B., BELLOCCHIO, L., METNA-LAURENT, M., SORIA-GOMEZ, E., MATIAS, I., HEBERT-CHATELAIN, E., CANNICH, A., MAITRE, M., LESTE-LASSERRE, T., CARDINAL, P., MENDIZABAL-ZUBIAGA, J., CANDUELA, M. J., REGUERO, L., HERMANS, E., GRANDES, P., COTA, D. & MARSICANO, G. 2013. Astroglial CB1 cannabinoid receptors regulate leptin signaling in mouse brain astrocytes. *Mol Metab,* 2**,** 393-404.

BRACEY, M. H., HANSON, M. A., MASUDA, K. R., STEVENS, R. C. & CRAVATT, B. F. 2002. Structural adaptations in a membrane enzyme that terminates endocannabinoid signaling. *Science,* 298**,** 1793-6.

BRINDISI, M., BORRELLI, G., BROGI, S., GRILLO, A., MARAMAI, S., PAOLINO, M., BENEDUSI, M., PECORELLI, A., VALACCHI, G., DI CESARE MANNELLI, L., GHELARDINI, C., ALLARA, M., LIGRESTI, A., MINETTI, P., CAMPIANI, G., BUTINI, S., DI MARZO, V. & GEMMA, S. 2018. Development of Potent Inhibitors of Fatty Acid Amide Hydrolase Useful for the Treatment of Neuropathic Pain. *ChemMedChem*.

BRONIKOWSKA, J., SZLISZKA, E., CZUBA, Z. P., ZWOLINSKI, D., SZMYDKI, D. & KROL, W. 2010. The combination of TRAIL and isoflavones enhances apoptosis in cancer cells. *Molecules,* 15**,** 2000-15.

BUENZ, E. J., SCHNEPPLE, D. J., BAUER, B. A., ELKIN, P. L., RIDDLE, J. M. & MOTLEY, T. J. 2004. Techniques: Bioprospecting historical herbal texts by hunting for new leads in old tomes. *Trends Pharmacol Sci,* 25**,** 494-8.

CALIGNANO, A., LA RANA, G., GIUFFRIDA, A. & PIOMELLI, D. 1998. Control of pain initiation by endogenous cannabinoids. *Nature,* 394**,** 277-81.

CAPOZZI, A., MATTEI, V., MARTELLUCCI, S., MANGANELLI, V., SACCOMANNI, G., GAROFALO, T., SORICE, M., MANERA, C. & MISASI, R. 2018. Anti-Proliferative Properties and Proapoptotic Function of New CB2 Selective Cannabinoid Receptor Agonist in Jurkat Leukemia Cells. *Int J Mol Sci,* 19.

CAPRIOLI, A., COCCURELLO, R., RAPINO, C., DI SERIO, S., DI TOMMASO, M., VERTECHY, M., VACCA, V., BATTISTA, N., PAVONE, F., MACCARRONE, M. & BORSINI, F. 2012. The novel reversible fatty acid amide hydrolase inhibitor ST4070 increases endocannabinoid brain levels and counteracts neuropathic pain in different animal models. *J Pharmacol Exp Ther,* 342**,** 188-95.

CER, R. Z., MUDUNURI, U., STEPHENS, R. & LEBEDA, F. J. 2009. IC50-to-Ki: a web-based tool for converting IC50 to Ki values for inhibitors of enzyme activity and ligand binding. *Nucleic Acids Res,* 37**,** W441-5.

CHAPMAN, K. D. 2004. Occurrence, metabolism, and prospective functions of N-acylethanolamines in plants. *Prog Lipid Res,* 43**,** 302-27.

CHAPMAN, K. D., CONYERS-JACKSON, A., MOREAU, A. & TRIPATHY, S. 1995a. Increased N-acylphosphatidylethanolamine biosynthesis in elicitor-treated tobacco cells. *Physiol Palnt,* 95**,** 120-126.

CHAPMAN, K. D., LIN, I. & DESOUZA, A. D. 1995b. Metabolism of cottonseed microsomal N-acylphosphatidylethanolamine. *Archives of Biochemistry and Biophysics,* 318**,** 401-407.

CHAPMAN, K. D., VENABLES, B., MARKOVIC, R., BLAIR, R. W. J. & BETTINGER, C. 1999. N-Acylethanolamines in Seeds. Quantification of Molecular Species and Their Degradation upon Imbibition. *Plant Physiology,* 120**,** 1157-1164.

CHAPMAN, K. D., VENABLES, B. J., DIAN, E. E. & GROSS, G. W. 2003. Identification and quantification of neuroactive N-acylethanolamines in cottonseed processing fractions. *Journal of the American Oil Chemists' Society,* 80**,** 223-229.

CHEN, X., MUKWAYA, E., WONG, M. S. & ZHANG, Y. 2014. A systematic review on biological activities of prenylated flavonoids. *Pharm Biol,* 52**,** 655-60.

CHICCA, A., MARAZZI, J., NICOLUSSI, S. & GERTSCH, J. 2012. Evidence for bidirectional endocannabinoid transport across cell membranes. *J Biol Chem,* 287**,** 34660-82.

CHICCA, A., NICOLUSSI, S., BARTHOLOMAUS, R., BLUNDER, M., APARISI REY, A., PETRUCCI, V., REYNOSO-MORENO, I. D. C., VIVEROS-PAREDES, J. M., DALGHI GENS, M., LUTZ, B., SCHIOTH, H. B., SOEBERDT, M., ABELS, C., CHARLES, R. P., ALTMANN, K. H. & GERTSCH, J. 2017. Chemical probes to potently

and selectively inhibit endocannabinoid cellular reuptake. *Proc Natl Acad Sci U S A,* 114**,** E5006-E5015.

CHICCA, A., RADUNER, S., PELLATI, F., STROMPEN, T., ALTMANN, K. H., SCHOOP, R. & GERTSCH, J. 2009. Synergistic immunomopharmacological effects of N-alkylamides in Echinacea purpurea herbal extracts. *Int Immunopharmacol,* 9**,** 850-8.

CHIURCHIU, V., RAPINO, C., TALAMONTI, E., LEUTI, A., LANUTI, M., GUENICHE, A., JOURDAIN, R., BRETON, L. & MACCARRONE, M. 2016. Anandamide Suppresses Proinflammatory T Cell Responses In Vitro through Type-1 Cannabinoid Receptor-Mediated mTOR Inhibition in Human Keratinocytes. *J Immunol,* 197**,** 3545-3553.

CHO, A. E., GUALLAR, V., BERNE, B. J. & FRIESNER, R. 2005. Importance of accurate charges in molecular docking: quantum mechanical/molecular mechanical (QM/MM) approach. *J Comput Chem,* 26**,** 915-31.

CHO, S., PARK, J. H., PAE, A. N., HAN, D., KIM, D., CHO, N. C., NO, K. T., YANG, H., YOON, M., LEE, C., SHIMIZU, M. & BAEK, N. I. 2012. Hypnotic effects and GABAergic mechanism of licorice (Glycyrrhiza glabra) ethanol extract and its major flavonoid constituent glabrol. *Bioorg Med Chem,* 20**,** 3493-501.

COMMISSION, C. P. 2015. *Pharmacopoeia of the People's Republic of China (2015 English Edition) Vol 1*, China Medical Science Press.

COVEY, D. P., MATEO, Y., SULZER, D., CHEER, J. F. & LOVINGER, D. M. 2017. Endocannabinoid modulation of dopamine neurotransmission. *Neuropharmacology,* 124**,** 52-61.

CRAGG, G. M. 1998. Paclitaxel (Taxol): a success story with valuable lessons for natural product drug discovery and development. *Med Res Rev,* 18**,** 315-31.

CRAGG, G. M. & NEWMAN, D. J. 2013. Natural products: a continuing source of novel drug leads. *Biochim Biophys Acta,* 1830**,** 3670-95.

CRAGG, G. M., NEWMAN, D. J. & SNADER, K. M. 1997. Natural Products in Drug Discovery and Development. *Journal of Natural Products,* 60**,** 52-60.

CRAVATT, B. F., DEMAREST, K., PATRICELLI, M. P., BRACEY, M. H., GIANG, D. K., MARTIN, B. R. & LICHTMAN, A. H. 2001. Supersensitivity to anandamide and enhanced endogenous cannabinoid signaling in mice lacking fatty acid amide hydrolase. *Proc Natl Acad Sci U S A,* 98**,** 9371-6.

CRAVATT, B. F., GIANG, D. K., MAYFIELD, S. P., BOGER, D. L., LERNER, R. A. & GILULA, N. B. 1996. Molecular characterization of an enzyme that degrades neuromodulatory fatty-acid amides. *Nature,* 384**,** 83-7.

DAAKA, Y., FRIEDMAN, H. & KLEIN, T. W. 1996. Cannabinoid receptor proteins are increased in Jurkat, human T-cell line after mitogen activation. *J Pharmacol Exp Ther,* 276**,** 776-83.

DAFNI, A., YANIV, Z. & PALEVITCH, D. 1984. Ethnobotanical survey of medicinal plants in northern Israel. *J Ethnopharmacol,* 10**,** 295-310.

DAY, T. A., RAKHSHAN, F., DEUTSCH, D. G. & BARKER, E. L. 2001. Role of fatty acid amide hydrolase in the transport of the endogenous cannabinoid anandamide. *Mol Pharmacol,* 59**,** 1369-75.

DE LEO, M., HUALLPA, C. G., ALVARADO, B., GRANCHI, C., POLI, G., DE TOMMASI, N. & BRACA, A. 2018. New diterpenes from Salvia pseudorosmarinus and their activity as inhibitors of monoacylglycerol lipase (MAGL). *Fitoterapia*.

DE PETROCELLIS, L., BISOGNO, T., DAVIS, J. B., PERTWEE, R. G. & DI MARZO, V. 2000. Overlap between the ligand recognition properties of the anandamide transporter and the VR1 vanilloid receptor: inhibitors of anandamide uptake with negligible capsaicin-like activity. *FEBS Lett,* 483**,** 52-6.

DEUTSCH, D. G. & CHIN, S. A. 1993. Enzymatic synthesis and degradation of anandamide, a cannabinoid receptor agonist. *Biochem Pharmacol,* 46**,** 791-6.

DEUTSCH, D. G., GLASER, S. T., HOWELL, J. M., KUNZ, J. S., PUFFENBARGER, R. A., HILLARD, C. J. & ABUMRAD, N. 2001. The cellular uptake of anandamide is coupled to its breakdown by fatty-acid amide hydrolase. *J Biol Chem,* 276**,** 6967-73.

DEVANE, W. A., DYSARZ, F. A., 3RD, JOHNSON, M. R., MELVIN, L. S. & HOWLETT, A. C. 1988. Determination and characterization of a cannabinoid receptor in rat brain. *Mol Pharmacol,* 34**,** 605-13.

DEVANE, W. A., HANUS, L., BREUER, A., PERTWEE, R. G., STEVENSON, L. A., GRIFFIN, G., GIBSON, D., MANDELBAUM, A., ETINGER, A. & MECHOULAM, R. 1992. Isolation and structure of a brain constituent that binds to the cannabinoid receptor. *Science,* 258**,** 1946-1949.

DHINGRA, D., PARLE, M. & KULKARNI, S. K. 2004. Memory enhancing activity of Glycyrrhiza glabra in mice. *J Ethnopharmacol,* 91**,** 361-5.

DI MARZO, V. 2009. The endocannabinoid system: its general strategy of action, tools for its pharmacological manipulation and potential therapeutic exploitation. *Pharmacol Res,* 60**,** 77-84.

DI MARZO, V., BISOGNO, T., SUGIURA, T., MELCK, D. & DE PETROCELLIS, L. 1998. The novel endogenous cannabinoid 2-arachidonoylglycerol is inactivated by neuronal- and basophil-like cells: connections with anandamide. *Biochem J,* 331 (Pt 1)**,** 15-9.

DI MARZO, V., FONTANA, A., CADAS, H., SCHINELLI, S., CIMINO, G., SCHWARTZ, J. C. & PIOMELLI, D. 1994. Formation and inactivation of endogenous cannabinoid anandamide in central neurons. *Nature,* 372**,** 686-91.

DI MARZO, V. & PETROSINO, S. 2007. Endocannabinoids and the regulation of their levels in health and disease. *Curr Opin Lipidol,* 18**,** 129-40.

DICKASON-CHESTERFIELD, A. K., KIDD, S. R., MOORE, S. A., SCHAUS, J. M., LIU, B., NOMIKOS, G. G. & FELDER, C. C. 2006. Pharmacological Characterization of Endocannabinoid Transport and Fatty Acid Amide Hydrolase Inhibitors. *Cellular and Molecular Neurobiology,* 26**,** 405-421.

DINH, T. P., FREUND, T. F. & PIOMELLI, D. 2002. A role for monoglyceride lipase in 2-arachidonoylglycerol inactivation. *Chem Phys Lipids,* 121**,** 149-58.

DIPATRIZIO, N. V. & PIOMELLI, D. 2012. The thrifty lipids: endocannabinoids and the neural control of energy conservation. *Trends Neurosci,* 35**,** 403-11.

DUTRA, R. C., SIMAO DA SILVA, K. A., BENTO, A. F., MARCON, R., PASZCUK, A. F., MEOTTI, F. C., PIANOWSKI, L. F. & CALIXTO, J. B. 2012. Euphol, a tetracyclic triterpene produces antinociceptive effects in inflammatory and neuropathic pain: the involvement of cannabinoid system. *Neuropharmacology,* 63**,** 593-605.

EDDY, N. B. & LEIMBACH, D. 1953. Synthetic analgesics. II. Dithienylbutenyl- and dithienylbutylamines. *J Pharmacol Exp Ther,* 107**,** 385-93.

EGERTOVA, M., GIANG, D. K., CRAVATT, B. F. & ELPHICK, M. R. 1998. A new perspective on cannabinoid signalling: complementary localization of fatty acid amide hydrolase and the CB1 receptor in rat brain. *Proc Biol Sci,* 265**,** 2081-5.

ESMAEILI, S., HAJIMEHDIPOOR, H., RAMEZANI, A. & MOSADDEGH, M. 2012. The Cytotoxic Effects of Ferula Persica var. Persica and Ferula Hezarlalehzarica against HepG2, A549, HT29, MCF7 and MDBK Cell Lines. *Iranian Journal of Pharmaceutical Sciences,* 8**,** 115-119.

FEGLEY, D., GAETANI, S., DURANTI, A., TONTINI, A., MOR, M., TARZIA, G. & PIOMELLI, D. 2005. Characterization of the fatty acid amide hydrolase inhibitor cyclohexyl carbamic acid 3'-carbamoyl-biphenyl-3-yl ester (URB597): effects on anandamide and oleoylethanolamide deactivation. *J Pharmacol Exp Ther,* 313**,** 352-8.

FEGLEY, D., KATHURIA, S., MERCIER, R., LI, C., GOUTOPOULOS, A., MAKRIYANNIS, A. & PIOMELLI, D. 2004. Anandamide transport is independent of fatty-acid amide hydrolase activity and is blocked by the hydrolysis-resistant inhibitor AM1172. *Proc Natl Acad Sci U S A,* 101**,** 8756-61.

FELDER, C. C., JOYCE, K. E., BRILEY, E. M., MANSOURI, J., MACKIE, K., BLOND, O., LAI, Y., MA, A. L. & MITCHELL, R. L. 1995. Comparison of the pharmacology and signal transduction of the human cannabinoid CB1 and CB2 receptors. *Mol Pharmacol,* 48**,** 443-50.

FERNANDEZ-RUIZ, J., PAZOS, M. R., GARCIA-ARENCIBIA, M., SAGREDO, O. & RAMOS, J. A. 2008. Role of CB2 receptors in neuroprotective effects of cannabinoids. *Mol Cell Endocrinol,* 286**,** S91-6.

FICHNA, J., DICAY, M., LEWELLYN, K., JANECKA, A., ZJAWIONY, J. K., MACNAUGHTON, W. K. & STORR, M. A. 2012. Salvinorin A has antiinflammatory and antinociceptive effects in experimental models of colitis in mice mediated by KOR and CB1 receptors. *Inflamm Bowel Dis,* 18**,** 1137-45.

FIORE, C., EISENHUT, M., RAGAZZI, E., ZANCHIN, G. & ARMANINI, D. 2005. A history of the therapeutic use of liquorice in Europe. *J Ethnopharmacol,* 99**,** 317-24.

FLOYD, C. D., LEBLANC, C. & WHITTAKER, M. 1999. Combinatorial chemistry as a tool for drug discovery. *Prog Med Chem,* 36**,** 91-168.

FOWLER, C. J. 2013. Transport of endocannabinoids across the plasma membrane and within the cell. *FEBS J,* 280**,** 1895-904.

FOWLER, C. J., TIGER, G., LIGRESTI, A., LOPEZ-RODRIGUEZ, M. L. & DI MARZO, V. 2004. Selective inhibition of anandamide cellular uptake versus enzymatic hydrolysis--a difficult issue to handle. *Eur J Pharmacol,* 492**,** 1-11.

FRIESNER, R. A., BANKS, J. L., MURPHY, R. B., HALGREN, T. A., KLICIC, J. J., MAINZ, D. T., REPASKY, M. P., KNOLL, E. H., SHELLEY, M., PERRY, J. K., SHAW, D. E., FRANCIS, P. & SHENKIN, P. S. 2004. Glide: a new approach for rapid, accurate docking and scoring. 1. Method and assessment of docking accuracy. *J Med Chem,* 47**,** 1739-49.

FRIESNER, R. A., MURPHY, R. B., REPASKY, M. P., FRYE, L. L., GREENWOOD, J. R., HALGREN, T. A., SANSCHAGRIN, P. C. & MAINZ, D. T. 2006. Extra precision glide: docking and scoring incorporating a model of hydrophobic enclosure for protein-ligand complexes. *J Med Chem,* 49**,** 6177-96.

FUKUDA, S., KOHSAKA, H., TAKAYASU, A., YOKOYAMA, W., MIYABE, C., MIYABE, Y., HARIGAI, M., MIYASAKA, N. & NANKI, T. 2014. Cannabinoid receptor 2 as a potential therapeutic target in rheumatoid arthritis. *BMC Musculoskelet Disord,* 15**,** 275.

FUKUI, H., EGAWA, H., KOSHIMIZU, K. & MITSUI, T. 1973. A New Isoflavone with Antifungal Activity from Immature Fruits of Lupinus luteus. *Agricultural and Biological Chemistry,* 37**,** 417-421.

GACHET, M. S., SCHUBERT, A., CALARCO, S., BOCCARD, J. & GERTSCH, J. 2017. Targeted metabolomics shows plasticity in the evolution of signaling lipids and uncovers old and new endocannabinoids in the plant kingdom. *Sci Rep,* 7**,** 41177.

GAFNER, S., BERGERON, C., VILLINSKI, J. R., GODEJOHANN, M., KESSLER, P., CARDELLINA, J. H., FERREIRA, D., FEGHALI, K. & GRENIER, D. 2011. Isoflavonoids and coumarins from Glycyrrhiza uralensis: antibacterial activity against oral pathogens and conversion of isoflavans into isoflavan-quinones during purification. *J Nat Prod,* 74**,** 2514-9.

GALIEGUE, S., MARY, S., MARCHAND, J., DUSSOSSOY, D., CARRIERE, D., CARAYON, P., BOUABOULA, M., SHIRE, D., LE FUR, G. & CASELLAS, P. 1995. Expression of central and peripheral cannabinoid receptors in human immune tissues and leukocyte subpopulations. *Eur J Biochem,* 232**,** 54-61.

GANGAN, V. D., PRADHAN, P., SIPAHIMALANI, A. T. & BANERJI, A. 1994. Cordifolisides A, B, C: norditerpene furan glycosides from Tinospora cordifolia. *Phytochemistry,* 37**,** 781-6.

GANGAN, V. D., PRADHAN, P., SIPAHIMALANI, A. T. & BANERJI, A. 1996. Palmatosides, C,F; Diterpene furann glucosides from Tinospora cordifolia – Structural elucidation by 2D NMR Spectroscopy. *Indian Journal of Chemistry,* 35**,** 630.

GAO, Q., XU, Z., ZHAO, G., WANG, H., WENG, Z., PEI, K., WU, L., CAI, B., CHEN, Z. & LI, W. 2016. Simultaneous quantification of 5 main components of Psoralea corylifolia L. in rats' plasma by

utilizing ultra high pressure liquid chromatography tandem mass spectrometry. *J Chromatogr B Analyt Technol Biomed Life Sci,* 1011**,** 128-35.

GAONI, Y. & MECHOULAM, R. 1964. Isolation, Structure, and Partial Synthesis of an Active Constituent of Hashish. *Journal of American Chemical Society,* 86**,** 1646-1647.

GAUR, R., YADAV, K. S., VERMA, R. K., YADAV, N. P. & BHAKUNI, R. S. 2014. In vivo anti-diabetic activity of derivatives of isoliquiritigenin and liquiritigenin. *Phytomedicine,* 21**,** 415-22.

GERTSCH, J. 2017. Cannabimimetic phytochemicals in the diet - an evolutionary link to food selection and metabolic stress adaptation? *Br J Pharmacol,* 174**,** 1464-1483.

GERTSCH, J., LEONTI, M., RADUNER, S., RACZ, I., CHEN, J. Z., XIE, X. Q., ALTMANN, K. H., KARSAK, M. & ZIMMER, A. 2008. Beta-caryophyllene is a dietary cannabinoid. *Proc Natl Acad Sci U S A,* 105**,** 9099-104.

GHAFOURI, N., TIGER, G., RAZDAN, R. K., MAHADEVAN, A., PERTWEE, R. G., MARTIN, B. R. & FOWLER, C. J. 2004. Inhibition of monoacylglycerol lipase and fatty acid amide hydrolase by analogues of 2-arachidonoylglycerol. *Br J Pharmacol,* 143**,** 774-84.

GIORGETTI, M., NEGRI, G. & RODRIGUES, E. 2007. Brazilian plants with possible action on the central nervous system: a study of historical sources from the 16th to 19th century. *J Ethnopharmacol,* 109**,** 338-47.

GLASER, S. T. & KACZOCHA, M. 2010. Cyclooxygenase-2 mediates anandamide metabolism in the mouse brain. *J Pharmacol Exp Ther,* 335**,** 380-8.

GOBBI, G., BAMBICO, F. R., MANGIERI, R., BORTOLATO, M., CAMPOLONGO, P., SOLINAS, M., CASSANO, T., MORGESE, M. G., DEBONNEL, G., DURANTI, A., TONTINI, A., TARZIA, G., MOR, M., TREZZA, V., GOLDBERG, S. R., CUOMO, V. & PIOMELLI, D. 2005. Antidepressant-like activity and modulation of brain monoaminergic transmission by blockade of anandamide hydrolysis. *Proc Natl Acad Sci U S A,* 102**,** 18620-5.

GODLEWSKI, G., ALAPAFUJA, S. O., BATKAI, S., NIKAS, S. P., CINAR, R., OFFERTALER, L., OSEI-HYIAMAN, D., LIU, J., MUKHOPADHYAY, B., HARVEY-WHITE, J., TAM, J., PACAK, K., BLANKMAN, J. L., CRAVATT, B. F., MAKRIYANNIS, A. & KUNOS, G. 2010. Inhibitor of fatty acid amide hydrolase normalizes cardiovascular function in hypertension without adverse metabolic effects. *Chem Biol,* 17**,** 1256-66.

GRAHAM, P. H. & VANCE, C. P. 2003. Legumes: importance and constraints to greater use. *Plant Physiol,* 131**,** 872-7.

GRECO, R., BANDIERA, T., MANGIONE, A. S., DEMARTINI, C., SIANI, F., NAPPI, G., SANDRINI, G., GUIJARRO, A., ARMIROTTI, A., PIOMELLI, D. & TASSORELLI, C. 2015. Effects of peripheral FAAH blockade on NTG-induced hyperalgesia--evaluation of URB937 in an animal model of migraine. *Cephalalgia,* 35**,** 1065-76.

GUINDON, J. & HOHMANN, A. G. 2011. The endocannabinoid system and cancer: therapeutic implication. *Br J Pharmacol,* 163**,** 1447-63.

GUPTA, S. S., VERMA, S. C., GARG, V. P. & RAI, M. 1967. Anti-diabetic effects of Tinospora cardifolia. I. Effect on fasting blood sugar level, glucose tolerance and adrenaline induced hyperglycaemia. *Indian J Med Res,* 55**,** 733-45.

GUSTIN, D. J., MA, Z., MIN, X., LI, Y., HEDBERG, C., GUIMARAES, C., PORTER, A. C., LINDSTROM, M., LESTER-ZEINER, D., XU, G., CARLSON, T. J., XIAO, S., MELEZA, C., CONNORS, R., WANG, Z. & KAYSER, F. 2011. Identification of potent, noncovalent fatty acid amide hydrolase (FAAH) inhibitors. *Bioorg Med Chem Lett,* 21**,** 2492-6.

HAJDU, Z., NICOLUSSI, S., RAU, M., LORANTFY, L., FORGO, P., HOHMANN, J., CSUPOR, D. & GERTSCH, J. 2014. Identification of endocannabinoid system-modulating N-alkylamides from Heliopsis helianthoides var. scabra and Lepidium meyenii. *J Nat Prod,* 77**,** 1663-9.

HALGREN, T. A. 1996. Merck molecular force field. II. MMFF94 van der Waals and electrostatic parameters for intermolecular interactions. *Journal of Computational Chemistry,* 17**,** 520-552.

HANUS, L., ABU-LAFI, S., FRIDE, E., BREUER, A., VOGEL, Z., SHALEV, D. E., KUSTANOVICH, I. & MECHOULAM, R. 2001. 2-arachidonyl glyceryl ether, an endogenous agonist of the cannabinoid CB1 receptor. *Proc Natl Acad Sci U S A,* 98**,** 3662-5.

HARRISON, C. & TRAYNOR, J. R. 2003. The [35S]GTPgammaS binding assay: approaches and applications in pharmacology. *Life Sci,* 74**,** 489-508.

HASHIDOKO, Y., S., T. & MIZUTANI, J. 1986. New complex Isoflavones in the roots of yellow lupin (Lupinus luteus L., cv. Barpine). *Agricultural and Biological Chemistry,* 50**,** 1797-1807.

HATANO, T., SHINTANI, Y., AGA, Y., SHIOTA, S., TSUCHIYA, T. & YOSHIDA, T. 2000. Phenolic constituents of licorice. VIII. Structures of glicophenone and glicoisoflavanone, and effects of licorice phenolics on methicillin-resistant Staphylococcus aureus. *Chem Pharm Bull (Tokyo),* 48**,** 1286-92.

HEBERT-CHATELAIN, E., DESPREZ, T., SERRAT, R., BELLOCCHIO, L., SORIA-GOMEZ, E., BUSQUETS-GARCIA, A., PAGANO ZOTTOLA, A. C., DELAMARRE, A., CANNICH, A., VINCENT, P., VARILH, M., ROBIN, L. M., TERRAL, G., GARCIA-FERNANDEZ, M. D., COLAVITA, M., MAZIER, W., DRAGO, F., PUENTE, N., REGUERO, L., ELEZGARAI, I., DUPUY, J. W., COTA, D., LOPEZ-RODRIGUEZ, M. L., BARREDA-GOMEZ, G., MASSA, F., GRANDES, P., BENARD, G. & MARSICANO, G. 2016. A cannabinoid link between mitochondria and memory. *Nature,* 539**,** 555-559.

HERRING, A. C., KOH, W. S. & KAMINSKI, N. E. 1998. Inhibition of the cyclic AMP signaling cascade and nuclear factor binding to CRE and kappaB elements by cannabinol, a minimally CNS-active cannabinoid. *Biochem Pharmacol,* 55**,** 1013-23.

HOERNLE, R. A. F. 2011. The Bower Manuscript. Facsimile leaves, Nagari transcript, romanised transliteration and English translation with notes. Calcutta, Superintendent Government Printing, India 1912. New Delhi: Reprint for Aditya Prakashan.

HOLLISTER, L. E. 1986. Health aspects of cannabis. *Pharmacol Rev,* 38**,** 1-20.

HOLLMAN, A. 1996. Drugs for atrial fibrillation. Digoxin comes from Digitalis lanata. *BMJ,* 312**,** 912.

HONG, Y. K., WU, H. T., MA, T., LIU, W. J. & HE, X. J. 2009. Effects of Glycyrrhiza glabra polysaccharides on immune and antioxidant activities in high-fat mice. *Int J Biol Macromol,* 45**,** 61-4.

HOSSEINZADEH, H. & NASSIRI-ASL, M. 2015. Pharmacological Effects of Glycyrrhiza spp. and Its Bioactive Constituents: Update and Review. *Phytotherapy Research,* 29**,** 1868-1886.

HOWLETT, A. C., BARTH, F., BONNER, T. I., CABRAL, G., CASELLAS, P., DEVANE, W. A., FELDER, C. C., HERKENHAM, M., MACKIE, K., MARTIN, B. R., MECHOULAM, R. & PERTWEE, R. G. 2002. International Union of Pharmacology. XXVII. Classification of cannabinoid receptors. *Pharmacol Rev,* 54**,** 161-202.

HOWLETT, A. C., JOHNSON, M. R., MELVIN, L. S. & MILNE, G. M. 1988. Nonclassical cannabinoid analgetics inhibit adenylate cyclase: development of a cannabinoid receptor model. *Mol Pharmacol,* 33**,** 297-302.

HUANG, S. M., BISOGNO, T., TREVISANI, M., AL-HAYANI, A., DE PETROCELLIS, L., FEZZA, F., TOGNETTO, M., PETROS, T. J., KREY, J. F., CHU, C. J., MILLER, J. D., DAVIES, S. N., GEPPETTI, P., WALKER, J. M. & DI MARZO, V. 2002. An endogenous capsaicin-like substance with high potency at recombinant and native vanilloid VR1 receptors. *Proc Natl Acad Sci U S A,* 99**,** 8400-5.

HUGGINS, J. P., SMART, T. S., LANGMAN, S., TAYLOR, L. & YOUNG, T. 2012. An efficient randomised, placebo-controlled clinical trial with the irreversible fatty acid amide hydrolase-1 inhibitor PF-04457845, which modulates endocannabinoids but fails to induce effective analgesia in patients with pain due to osteoarthritis of the knee. *Pain,* 153**,** 1837-46.

IBRAHIM, M. M., DENG, H., ZVONOK, A., COCKAYNE, D. A., KWAN, J., MATA, H. P., VANDERAH, T. W., LAI, J., PORRECA, F., MAKRIYANNIS, A. & MALAN, T. P., JR. 2003. Activation of CB2 cannabinoid receptors by AM1241 inhibits experimental neuropathic pain: pain inhibition by receptors not present in the CNS. *Proc Natl Acad Sci U S A,* 100**,** 10529-33.

IRANSHAHI, M., AMIN, G.-R., JALALIZADEH, H. & SHAFIEE, A. 2003a. New Germacrane Derivative from Ferula persica. *Pharmaceutical Biology,* 41**,** 431-433.

IRANSHAHI, M., AMIN, G. R., AMINI, M. & SHAFIEE, A. 2003b. Sulfur containing derivatives from Ferula persica var. latisecta. *Phytochemistry,* 63**,** 965-6.

IRANSHAHI, M., ASKARI, M., SAHEBKAR, A. & ADJIPAVLOU-LITINA, D. 2009a. Evaluation of antioxidant, anti-inflammatory and lipoxygenase inhibitory activities of the prenylated coumarin umbelliprenin. *DARU: Journal of Pharmaceutical Sciences,* 17**,** 99-103.

IRANSHAHI, M., KALATEGI, F., REZAEE, R., SHAHVERDI, A. R., ITO, C., FURUKAWA, H., TOKUDA, H. & ITOIGAWA, M. 2008. Cancer chemopreventive activity of terpenoid coumarins from Ferula species. *Planta Med,* 74**,** 147-50.

IRANSHAHI, M., MASULLO, M., ASILI, A., HAMEDZADEH, A., JAHANBIN, B., FESTA, M., CAPASSO, A. & PIACENTE, S. 2010a. Sesquiterpene Coumarins from Ferula gumosa. *Journal of Natural Products,* 73**,** 1958-1962.

IRANSHAHI, M., MASULLO, M., ASILI, A., HAMEDZADEH, A., JAHANBIN, B., FESTA, M., CAPASSO, A. & PIACENTE, S. 2010b. Sesquiterpene coumarins from Ferula gumosa. *J Nat Prod,* 73**,** 1958-62.

IRANSHAHI, M., NOROOZI, S., BEHRAVAN, J., KARIMI, G. & SCHNEIDER, B. 2009b. Persicasulphide C, a new sulphur-containing derivative from Ferula persica. *Nat Prod Res,* 23**,** 1584-8.

IRANSHAHI, M., SAHEBKAR, A., TAKASAKI, M., KONOSHIMA, T. & TOKUDA, H. 2009c. Cancer chemopreventive activity of the prenylated coumarin, umbelliprenin, in vivo. *Eur J Cancer Prev,* 18**,** 412-5.

IZZO, A. A. 2004. Cannabinoids and intestinal motility: welcome to CB2 receptors. *Br J Pharmacol,* 142**,** 1201-2.

JACOB, A. & TODD, A. R. 1940. Cannabis indica. Part II. Isolation of cannabidiol from Egyptian hashish. Observations on the structure of cannabinol. *J. Chem. Soc.***,** 649-653.

JALALI, H. T., EBRAHIMIAN, Z. J., EVTUGUIN, D. V. & PASCOAL NETO, C. 2011. Chemical composition of oleo-gum-resin from Ferula gummosa. *Industrial Crops and Products,* 33**,** 549-553.

JALALI, H. T., PETRONILHO, S., VILLAVERDE, J. J., COIMBRA, M. A., DOMINGUES, M. R. M., EBRAHIMIAN, Z. J., SILVESTRE, A. J. D. & ROCHA, S. M. 2013. Assessment of the sesquiterpenic profile of Ferula gummosa oleo-gum-resin (galbanum) from Iran. Contributes to its valuation as a potential source of sesquiterpenic compounds. *Industrial Crops and Products,* 44**,** 185-191.

JALILZADEH-AMIN, G., NAJARNEZHAD, V., ANASSORI, E., MOSTAFAVI, M. & KESHIPOUR, H. 2015. Antiulcer properties of Glycyrrhiza glabra L. extract on experimental models of gastric ulcer in mice. *Iran J Pharm Res,* 14**,** 1163-70.

JAMSHIDI, N. & TAYLOR, D. A. 2001. Anandamide administration into the ventromedial hypothalamus stimulates appetite in rats. *Br J Pharmacol,* 134**,** 1151-4.

JAYAMANNE, A., GREENWOOD, R., MITCHELL, V. A., ASLAN, S., PIOMELLI, D. & VAUGHAN, C. W. 2006. Actions of the FAAH inhibitor URB597 in neuropathic and inflammatory chronic pain models. *Br J Pharmacol,* 147**,** 281-8.

JHAVERI, M. D., RICHARDSON, D., KENDALL, D. A., BARRETT, D. A. & CHAPMAN, V. 2006. Analgesic effects of fatty acid amide hydrolase inhibition in a rat model of neuropathic pain. *J Neurosci,* 26**,** 13318-27.

JHAVERI, M. D., RICHARDSON, D., ROBINSON, I., GARLE, M. J., PATEL, A., SUN, Y., SAGAR, D. R., BENNETT, A. J., ALEXANDER, S. P., KENDALL, D. A., BARRETT, D. A. & CHAPMAN, V. 2008. Inhibition of fatty acid

amide hydrolase and cyclooxygenase-2 increases levels of endocannabinoid related molecules and produces analgesia via peroxisome proliferator-activated receptor-alpha in a model of inflammatory pain. *Neuropharmacology,* 55**,** 85-93.

JUAN-PICO, P., FUENTES, E., BERMUDEZ-SILVA, F. J., JAVIER DIAZ-MOLINA, F., RIPOLL, C., RODRIGUEZ DE FONSECA, F. & NADAL, A. 2006. Cannabinoid receptors regulate Ca(2+) signals and insulin secretion in pancreatic beta-cell. *Cell Calcium,* 39**,** 155-62.

JUDD, W. S., CAMPBELL, C. S., KELLOGG, E. A., STEVENS, P. F. & DONOGHUE, M. J. 2002. *Plant Systematics: A Phylogenetic Approach,* Sunderland, MA, Sinauer Associates.

KACZOCHA, M., GLASER, S. T. & DEUTSCH, D. G. 2009. Identification of intracellular carriers for the endocannabinoid anandamide. *Proc Natl Acad Sci U S A,* 106**,** 6375-80.

KAKKAR, A., VERMA, D. R., SURYAVANSHI, S. & DUBEY, P. 2013. Characterization of Chemical Constituents of *Tinospora cordifolia Chemistry of Natural Compounds,* 49**,** 155-156.

KAPIL, A. & SHARMA, S. 1997. Immunopotentiating compounds from Tinospora cordifolia. *J Ethnopharmacol,* 58**,** 89-95.

KAPLAN, B. L. 2013. The role of CB1 in immune modulation by cannabinoids. *Pharmacol Ther,* 137**,** 365-74.

KARLSSON, M., CONTRERAS, J. A., HELLMAN, U., TORNQVIST, H. & HOLM, C. 1997. cDNA cloning, tissue distribution, and identification of the catalytic triad of monoglyceride lipase. Evolutionary relationship to esterases, lysophospholipases, and haloperoxidases. *J Biol Chem,* 272**,** 27218-23.

KATAYAMA, K., UEDA, N., KURAHASHI, Y., SUZUKI, H., YAMAMOTO, S. & KATO, I. 1997. Distribution of anandamide amidohydrolase in rat tissues with special reference to small intestine. *Biochim Biophys Acta,* 1347**,** 212-8.

KAUFMAN, P. B., DUKE, J. A., BRIELMANN, H., BOIK, J. & HOYT, J. E. 1997. A comparative survey of leguminous plants as sources of the isoflavones, genistein and daidzein: implications for human nutrition and health. *J Altern Complement Med,* 3**,** 7-12.

KHAN, M. A., GRAY, A. I. & WATERMAN, P. G. 1989. Tinosporaside, an 18-norclerodane glucoside from Tinospora cordifolia. *Phytochemistry,* 28**,** 273-275.

KHAN, M. I., SOBOCINSKA, A. A., CZARNECKA, A. M., KROL, M., BOTTA, B. & SZCZYLIK, C. 2016. The Therapeutic Aspects of the Endocannabinoid System (ECS) for Cancer and their Development: From Nature to Laboratory. *Curr Pharm Des,* 22**,** 1756-66.

KIM, H. J., SEO, J. Y., SUH, H. J., LIM, S. S. & KIM, J. S. 2012. Antioxidant activities of licorice-derived prenylflavonoids. *Nutr Res Pract,* 6**,** 491-8.

KIM, K. R., JEONG, C. K., PARK, K. K., CHOI, J. H., PARK, J. H., LIM, S. S. & CHUNG, W. Y. 2010. Anti-inflammatory effects of licorice and roasted licorice extracts on TPA-induced acute inflammation and collagen-induced arthritis in mice. *J Biomed Biotechnol,* 2010**,** 709378.

KIM, S. C., FAURE, L. & CHAPMAN, K. D. 2013. Analysis of fatty acid amide hydrolase activity in plants. *Methods Mol Biol,* 1009**,** 115-27.

KINGSTON, D. G. 2000. Recent advances in the chemistry of taxol. *J Nat Prod,* 63**,** 726-34.

KINSEY, S. G., NAIDU, P. S., CRAVATT, B. F., DUDLEY, D. T. & LICHTMAN, A. H. 2011. Fatty acid amide hydrolase blockade attenuates the development of collagen-induced arthritis and related thermal hyperalgesia in mice. *Pharmacol Biochem Behav,* 99**,** 718-25.

KIRCHMAIR, J., DISTINTO, S., SCHUSTER, D., SPITZER, G., LANGER, T. & WOLBER, G. 2008. Enhancing Drug Discovery Through In Silico Screening: Strategies to Increase True Positives Retrieval Rates. *Current Medicinal Chemistry,* 15**,** 2040-2053.

KLAUKE, A. L., RACZ, I., PRADIER, B., MARKERT, A., ZIMMER, A. M., GERTSCH, J. & ZIMMER, A. 2014. The cannabinoid CB(2) receptor-selective phytocannabinoid beta-caryophyllene exerts analgesic effects in mouse models of inflammatory and neuropathic pain. *Eur Neuropsychopharmacol,* 24**,** 608-20.

KLEYER, J., NICOLUSSI, S., TAYLOR, P., SIMONELLI, D., FURGER, E., ANDERLE, P. & GERTSCH, J. 2012. Cannabinoid receptor trafficking in peripheral cells is dynamically regulated by a binary biochemical switch. *Biochem Pharmacol,* 83**,** 1393-412.

KOLLMAN, P. A., MASSOVA, I., REYES, C., KUHN, B., HUO, S., CHONG, L., LEE, M., LEE, T., DUAN, Y., WANG, W., DONINI, O., CIEPLAK, P., SRINIVASAN, J., CASE, D. A. & CHEATHAM, T. E., 3RD 2000. Calculating structures and free energies of complex molecules: combining molecular mechanics and continuum models. *Acc Chem Res,* 33**,** 889-97.

KOZAK, K. R., CREWS, B. C., MORROW, J. D., WANG, L. H., MA, Y. H., WEINANDER, R., JAKOBSSON, P. J. & MARNETT, L. J. 2002. Metabolism of the endocannabinoids, 2-arachidonylglycerol and anandamide, into prostaglandin, thromboxane, and prostacyclin glycerol esters and ethanolamides. *J Biol Chem,* 277**,** 44877-85.

KOZAK, K. R., ROWLINSON, S. W. & MARNETT, L. J. 2000. Oxygenation of the endocannabinoid, 2-arachidonylglycerol, to glyceryl prostaglandins by cyclooxygenase-2. *J Biol Chem,* 275**,** 33744-9.

KREITZER, A. C. & MALENKA, R. C. 2007. Endocannabinoid-mediated rescue of striatal LTD and motor deficits in Parkinson's disease models. *Nature,* 445**,** 643-7.

KUEHL, F. F., JACOB, T. A., GANLEY, O. H., ORMOND, R. E. & MEISINGER, M. A. P. 1957. The identification of N-(2-hydroxyethyl)-palmitamide as a naturally occurring anti-inflammatory agent. *J. Am. Chem. Soc.,* 79**,** 5577-5578.

KUETE, V., SANDJO, L. P., KWAMOU, G. M., WIENCH, B., NKENGFACK, A. E. & EFFERTH, T. 2014. Activity of three cytotoxic isoflavonoids from Erythrina excelsa and Erythrina senegalensis (neobavaisoflavone, sigmoidin H and isoneorautenol) toward multi-factorial drug resistant cancer cells. *Phytomedicine,* 21**,** 682-8.

KURSAT, M., EMRE, I., YILMAZ, O., CIVELEK, S., DEMIR, E. & TURKOGLU, I. 2015. Phytochemical Contents of Five *Artemisia* Species. *Not Sci Biol,* 7**,** 495-499.

LANE, G. A., O.R.W., S. & SKIPP, R. A. 1987. Isoflavonoids as insect feeding deterrents and sntifungal components from root of Lupinus angustifolius. *Journal of Chemical Ecology,* 13.

LARDOS, A., PRIETO-GARCIA, J. & HEINRICH, M. 2011. Resins and Gums in Historical Iatrosophia Texts from Cyprus - A Botanical and Medico-pharmacological Approach. *Front Pharmacol,* 2**,** 32.

LAU, B. K., COTA, D., CRISTINO, L. & BORGLAND, S. L. 2017. Endocannabinoid modulation of homeostatic and non-homeostatic feeding circuits. *Neuropharmacology,* 124**,** 38-51.

LEE, Y. S., KIM, S. H., JUNG, S. H., KIM, J. K., PAN, C. H. & LIM, S. S. 2010. Aldose reductase inhibitory compounds from Glycyrrhiza uralensis. *Biol Pharm Bull,* 33**,** 917-21.

LEONTI, M. 2011. The future is written: impact of scripts on the cognition, selection, knowledge and transmission of medicinal plant use and its implications for ethnobotany and ethnopharmacology. *J Ethnopharmacol,* 134**,** 542-55.

LEONTI, M. & CASU, L. 2014. Soma, food of the immortals according to the Bower Manuscript (Kashmir, 6th century A.D.). *J Ethnopharmacol,* 155**,** 373-86.

LEONTI, M., CASU, L., RADUNER, S., COTTIGLIA, F., FLORIS, C., ALTMANN, K. H. & GERTSCH, J. 2010. Falcarinol is a covalent cannabinoid CB1 receptor antagonist and induces pro-allergic effects in skin. *Biochem Pharmacol,* 79**,** 1815-26.

LEONTI, M. & VERPOORTE, R. 2017. Traditional Mediterranean and European herbal medicines. *J Ethnopharmacol,* 199**,** 161-167.

LETUNIC, I. & BORK, P. 2007. Interactive Tree Of Life (iTOL): an online tool for phylogenetic tree display and annotation. *Bioinformatics,* 23**,** 127-8.

LI, R., MORRIS-NATSCHKE, S. L. & LEE, K. H. 2016. Clerodane diterpenes: sources, structures, and biological activities. *Nat Prod Rep,* 33**,** 1166-226.

LI, W., BLANKMAN, J. L. & CRAVATT, B. F. 2007. A functional proteomic strategy to discover inhibitors for uncharacterized hydrolases. *J Am Chem Soc,* 129**,** 9594-5.

LI, W. L., ZHENG, H. C., BUKURU, J. & DE KIMPE, N. 2004. Natural medicines used in the traditional Chinese medical system for therapy of diabetes mellitus. *Journal of Ethnopharmacology,* 92**,** 1-21.

LICHTMAN, A. H., LEUNG, D., SHELTON, C. C., SAGHATELIAN, A., HARDOUIN, C., BOGER, D. L. & CRAVATT, B. F. 2004. Reversible inhibitors of fatty acid amide hydrolase that promote analgesia: evidence for an unprecedented combination of potency and selectivity. *J Pharmacol Exp Ther,* 311**,** 441-8.

LIGPREP, S., LLC, NEW YORK, NY, 2018, .

LIGRESTI, A., MORERA, E., VAN DER STELT, M., MONORY, K., LUTZ, B., ORTAR, G. & DI MARZO, V. 2004. Further evidence for the existence of a specific process for the membrane transport of anandamide. *Biochem J,* 380**,** 265-72.

LIGRESTI, A., VILLANO, R., ALLARA, M., UJVARY, I. & DI MARZO, V. 2012. Kavalactones and the endocannabinoid system: the plant-derived yangonin is a novel CB(1) receptor ligand. *Pharmacol Res,* 66**,** 163-9.

LIU, J., WANG, L., HARVEY-WHITE, J., OSEI-HYIAMAN, D., RAZDAN, R., GONG, Q., CHAN, A. C., ZHOU, Z., HUANG, B. X., KIM, H. Y. & KUNOS, G. 2006. A biosynthetic pathway for anandamide. *Proc Natl Acad Sci U S A,* 103**,** 13345-50.

LO PIPARO, E., SCHEIB, H., FREI, N., WILLIAMSON, G., GRIGOROV, M. & CHOU, C. J. 2008. Flavonoids for controlling starch digestion: structural requirements for inhibiting human alpha-amylase. *J Med Chem,* 51**,** 3555-61.

LOMAZZO, E., BINDILA, L., REMMERS, F., LERNER, R., SCHWITTER, C., HOHEISEL, U. & LUTZ, B. 2015. Therapeutic potential of inhibitors of endocannabinoid degradation for the treatment of stress-related hyperalgesia in an animal model of chronic pain. *Neuropsychopharmacology,* 40**,** 488-501.

LONG, J. Z., LI, W., BOOKER, L., BURSTON, J. J., KINSEY, S. G., SCHLOSBURG, J. E., PAVON, F. J., SERRANO, A. M., SELLEY, D. E., PARSONS, L. H., LICHTMAN, A. H. & CRAVATT, B. F. 2009. Selective blockade of 2-arachidonoylglycerol hydrolysis produces cannabinoid behavioral effects. *Nat Chem Biol,* 5**,** 37-44.

LOPEZ-RODRIGUEZ, M. L., VISO, A., ORTEGA-GUTIERREZ, S., FOWLER, C. J., TIGER, G., DE LAGO, E., FERNANDEZ-RUIZ, J. & RAMOS, J. A. 2003. Design, synthesis and biological evaluation of new endocannabinoid transporter inhibitors. *Eur J Med Chem,* 38**,** 403-12.

LOZOVAYA, N., YATSENKO, N., BEKETOV, A., TSINTSADZE, T. & BURNASHEV, N. 2005. Glycine receptors in CNS neurons as a target for nonretrograde action of cannabinoids. *J Neurosci,* 25**,** 7499-506.

MACCARRONE, M. 2017. Metabolism of the Endocannabinoid Anandamide: Open Questions after 25 Years. *Front Mol Neurosci,* 10**,** 166.

MACCOSS, M. & BAILLIE, T. A. 2004. Organic Chemistry in Drug Discovery. *Science,* 303**,** 1810-1813.

MAHBOUBI, M. 2016. Ferula gummosa, a Traditional Medicine with Novel Applications. *J Diet Suppl,* 13**,** 700-18.

MAKARA, J. K., MOR, M., FEGLEY, D., SZABO, S. I., KATHURIA, S., ASTARITA, G., DURANTI, A., TONTINI, A., TARZIA, G., RIVARA, S., FREUND, T. F. & PIOMELLI, D. 2005. Selective inhibition of 2-AG hydrolysis enhances endocannabinoid signaling in hippocampus. *Nat Neurosci,* 8**,** 1139-41.

MAKRIYANNIS, A., MECHOULAM, R. & PIOMELLI, D. 2005. Therapeutic opportunities through modulation of the endocannabinoid system. *Neuropharmacology,* 48**,** 1068-71.

MARRS, W. R., BLANKMAN, J. L., HORNE, E. A., THOMAZEAU, A., LIN, Y. H., COY, J., BODOR, A. L., MUCCIOLI, G. G., HU, S. S., WOODRUFF, G., FUNG, S., LAFOURCADE, M., ALEXANDER, J. P., LONG, J. Z., LI, W., XU, C., MOLLER, T., MACKIE, K., MANZONI, O. J., CRAVATT, B. F. & STELLA, N. 2010. The serine hydrolase ABHD6 controls the accumulation and efficacy of 2-AG at cannabinoid receptors. *Nat Neurosci,* 13**,** 951-7.

MARSICANO, G., GOODENOUGH, S., MONORY, K., HERMANN, H., EDER, M., CANNICH, A., AZAD, S. C., CASCIO, M. G., GUTIERREZ, S. O., VAN DER STELT, M., LOPEZ-RODRIGUEZ, M. L., CASANOVA, E., SCHUTZ, G., ZIEGLGANSBERGER, W., DI MARZO, V., BEHL, C. & LUTZ, B. 2003. CB1 cannabinoid receptors and on-demand defense against excitotoxicity. *Science,* 302**,** 84-8.

MARSICANO, G., WOTJAK, C. T., AZAD, S. C., BISOGNO, T., RAMMES, G., CASCIO, M. G., HERMANN, H., TANG, J., HOFMANN, C., ZIEGLGANSBERGER, W., DI MARZO, V. & LUTZ, B. 2002. The endogenous cannabinoid system controls extinction of aversive memories. *Nature,* 418**,** 530-4.

MARTIN, W. J., LOO, C. M. & BASBAUM, A. I. 1999. Spinal cannabinoids are anti-allodynic in rats with persistent inflammation. *Pain,* 82**,** 199-205.

MATSUDA, L. A., BONNER, T. I. & LOLAIT, S. J. 1993. Localization of cannabinoid receptor mRNA in rat brain. *J Comp Neurol,* 327**,** 535-50.

MATSUDA, L. A., LOLAIT, S. J., BROWNSTEIN, M. J., YOUNG, A. C. & BONNER, T. I. 1990. Structure of a cannabinoid receptor and functional expression of the cloned cDNA. *Nature,* 346**,** 561-4.

MATTHIOLI, A. 1568. I Discorsi di M. Pietro Andrea Matthioli. Sanese, Medico Cesareo, et del Serenissimo Principe Ferdinando Archiduca d'Austria & c.Nelli Sei Libri Di Pedacio Dioscoride Anazarbeo della Materia Medicale. Vincenzo Valgrisi, Venezia Reprinted in Facsimile, 1960-70. Stabilimento Tipografico Julia, Rome.

MAURYA, R., DHAR, K. L. & HANDA, S. S. 1997. A sesquiterpene glucoside from Tinospora cordifolia. *Phytochemistry,* 44**,** 749-750.

MAURYA, R. & HANDA, S. S. 1997. Tinocordifolin, a sesquiterpene from *Tinospora cordifolia Phytochemistry,* 49**,** 1343-1345.

MAURYA, R., MANHAS, L. R., GUPTA, P., MISHRA, P. K., SINGH, G. & YADAV, P. P. 2004. Amritosides A, B, C and D: clerodane furano diterpene glucosides from Tinospora cordifolia. *Phytochemistry,* 65**,** 2051-5.

MAURYA, R., WAZIR, V., KAPIL, A. & KAPIL, R. S. 1996. Cordifoliosides A and B, two New Phenylpropene Disaccharides from Tinospora cordifolia possessing Immunostimulant Activity. *Natural Product Letters,* 8**,** 7-10.

MAZIER, W., SAUCISSE, N., GATTA-CHERIFI, B. & COTA, D. 2015. The Endocannabinoid System: Pivotal Orchestrator of Obesity and Metabolic Disease. *Trends Endocrinol Metab,* 26**,** 524-537.

MAZZIO, E., DEIAB, S., PARK, K. & SOLIMAN, K. F. 2013. High throughput screening to identify natural human monoamine oxidase B inhibitors. *Phytother Res,* 27**,** 818-28.

MCFARLAND, M. J., PORTER, A. C., RAKHSHAN, F. R., RAWAT, D. S., GIBBS, R. A. & BARKER, E. L. 2004. A role for caveolae/lipid rafts in the uptake and recycling of the endogenous cannabinoid anandamide. *J Biol Chem,* 279**,** 41991-7.

MECHOULAM, R., BEN-SHABAT, S., HANUS, L., LIGUMSKY, M., KAMINSKI, N. E., SCHATZ, A. R., GOPHER, A., ALMOG, S., MARTIN, B. R., COMPTON, D. R., PERTWEE, R. G., GRIFFIN, G., BAYEWITCH, M., BARG, J. & VOGEL, Z. 1995. Identification of an endogenous 2-monoglyceride, present in canine gut, that binds to cannabinoid receptors. *Biochemical Pharmacology,* 50**,** 83-90.

MECHOULAM, R., HANUS, L. O., PERTWEE, R. & HOWLETT, A. C. 2014. Early phytocannabinoid chemistry to endocannabinoids and beyond. *Nat Rev Neurosci,* 15**,** 757-64.

MESSINA, M. J., PERSKY, V., SETCHELL, K. D. & BARNES, S. 1994. Soy intake and cancer risk: a review of the in vitro and in vivo data. *Nutr Cancer,* 21**,** 113-31.

MICALE, V., CRISTINO, L., TAMBURELLA, A., PETROSINO, S., LEGGIO, G. M., DRAGO, F. & DI MARZO, V. 2009. Anxiolytic effects in mice of a dual blocker of fatty acid amide hydrolase and transient receptor potential vanilloid type-1 channels. *Neuropsychopharmacology,* 34**,** 593-606.

MICALE, V., DI MARZO, V., SULCOVA, A., WOTJAK, C. T. & DRAGO, F. 2013. Endocannabinoid system and mood disorders: priming a target for new therapies. *Pharmacol Ther,* 138**,** 18-37.

MILENI, M., GARFUNKLE, J., EZZILI, C., CRAVATT, B. F., STEVENS, R. C. & BOGER, D. L. 2011. Fluoride-mediated capture of a noncovalent bound state of a reversible covalent enzyme inhibitor: X-ray crystallographic analysis of an exceptionally potent alpha-ketoheterocycle inhibitor of fatty acid amide hydrolase. *J Am Chem Soc,* 133**,** 4092-100.

MILLER, A. M. & STELLA, N. 2008. CB2 receptor-mediated migration of immune cells: it can go either way. *Br J Pharmacol,* 153**,** 299-308.

MOHAMADI, F., RICHARDS, N. G. J., GUIDA, W. C., LISKAMP, R., LIPTON, M., CAUFIELD, C., CHANG, G., HENDRICKSON, T. & STILL, W. C. 1990. Macromodel—an integrated software system for modeling organic and bioorganic molecules using molecular mechanics. *Journal of Computational Chemistry,* 11**,** 440-467.

MOITESSIER, N., ENGLEBIENNE, P., LEE, D., LAWANDI, J. & CORBEIL, C. R. 2008. Towards the development of universal, fast and highly accurate docking/scoring methods: a long way to go. *Br J Pharmacol,* 153 Suppl 1**,** S7-26.

MOREIRA, F. A. & LUTZ, B. 2008. The endocannabinoid system: emotion, learning and addiction. *Addict Biol,* 13**,** 196-212.

MUNRO, S., THOMAS, K. L. & ABU-SHAAR, M. 1993. Molecular characterization of a peripheral receptor for cannabinoids. *Nature,* 365**,** 61-5.

MUTALIK, M. & MUTALIK, M. 2011. Tinospora cordifolia: Role in depression, cognition and memory [online]. Australian Journal of Medical Herbalism, Vol. 23, No. 4, 2011: 168-173. Availability: <https://search.informit.com.au/documentSummary;dn=858453546766015;res=IELHEA> ISSN: 1033-8330. [cited 16 Sep 18]. .

NAIDU, P. S., KINSEY, S. G., GUO, T. L., CRAVATT, B. F. & LICHTMAN, A. H. 2010. Regulation of inflammatory pain by inhibition of fatty acid amide hydrolase. *J Pharmacol Exp Ther,* 334**,** 182-90.

NAVIA-PALDANIUS, D., SAVINAINEN, J. R. & LAITINEN, J. T. 2012. Biochemical and pharmacological characterization of human alpha/beta-hydrolase domain containing 6 (ABHD6) and 12 (ABHD12). *J Lipid Res,* 53**,** 2413-24.

NAZARI, Z. E. & IRANSHAHI, M. 2011. Biologically active sesquiterpene coumarins from Ferula species. *Phytother Res,* 25**,** 315-23.

NEWMAN, D. J. & CRAGG, G. M. 2016. Natural Products as Sources of New Drugs from 1981 to 2014. *Journal of Natural Products,* 79**,** 629-661.

NICOLUSSI, S., CHICCA, A., RAU, M., RIHS, S., SOEBERDT, M., ABELS, C. & GERTSCH, J. 2014a. Correlating FAAH and anandamide cellular uptake inhibition using N-alkylcarbamate inhibitors: from ultrapotent to hyperpotent. *Biochem Pharmacol,* 92**,** 669-89.

NICOLUSSI, S. & GERTSCH, J. 2015. Endocannabinoid transport revisited. *Vitam Horm,* 98**,** 441-85.

NICOLUSSI, S., VIVEROS-PAREDES, J. M., GACHET, M. S., RAU, M., FLORES-SOTO, M. E., BLUNDER, M. & GERTSCH, J. 2014b. Guineensine is a novel inhibitor of endocannabinoid uptake showing cannabimimetic behavioral effects in BALB/c mice. *Pharmacol Res,* 80**,** 52-65.

NOSALOVA, G., FLESKOVA, D., JURECEK, L., SADLONOVA, V. & RAY, B. 2013. Herbal polysaccharides and cough reflex. *Respir Physiol Neurobiol,* 187**,** 47-51.

O'SHAUGNESSY, W. B. 1841. The Bengal Dispensatory and Pharmacopoeia 579 (Bishop's College Press, 1841).

ODDI, S., FEZZA, F., PASQUARIELLO, N., D'AGOSTINO, A., CATANZARO, G., DE SIMONE, C., RAPINO, C., FINAZZI-AGRO, A. & MACCARRONE, M. 2009. Molecular identification of albumin and Hsp70 as cytosolic anandamide-binding proteins. *Chem Biol,* 16**,** 624-32.

OKAMOTO, Y., TSUBOI, K. & UEDA, N. 2009. Enzymatic formation of anandamide. *Vitam Horm,* 81**,** 1-24.

OLÁH, A., AMBRUS, L., NICOLUSSI, S., GERTSCH, J., TUBAK, V., KEMÉNY, L., SOEBERDT, M., ABELS, C. & BÍRÓ, T. 2016. Inhibition of fatty acid amide hydrolase exerts cutaneous anti-inflammatory effects both in vitro and in vivo. *Experimental Dermatology,* 25**,** 328-330.

ORTAR, G., LIGRESTI, A., DE PETROCELLIS, L., MORERA, E. & DI MARZO, V. 2003. Novel selective and metabolically stable inhibitors of anandamide cellular uptake. *Biochem Pharmacol,* 65**,** 1473-81.

ORTEGA-GUTIERREZ, S., HAWKINS, E. G., VISO, A., LOPEZ-RODRIGUEZ, M. L. & CRAVATT, B. F. 2004. Comparison of anandamide transport in FAAH wild-type and knockout neurons: evidence for contributions by both FAAH and the CB1 receptor to anandamide uptake. *Biochemistry,* 43**,** 8184-90.

OZ, M. 2006. Receptor-independent actions of cannabinoids on cell membranes: focus on endocannabinoids. *Pharmacol Ther,* 111**,** 114-44.

OZ, M., ZHANG, L. & MORALES, M. 2002. Endogenous cannabinoid, anandamide, acts as a noncompetitive inhibitor on 5-HT3 receptor-mediated responses in Xenopus oocytes. *Synapse,* 46**,** 150-6.

PAGOTTO, U., MARSICANO, G., COTA, D., LUTZ, B. & PASQUALI, R. 2006. The emerging role of the endocannabinoid system in endocrine regulation and energy balance. *Endocr Rev,* 27**,** 73-100.

PANLILIO, L. V., THORNDIKE, E. B., NIKAS, S. P., ALAPAFUJA, S. O., BANDIERA, T., CRAVATT, B. F., MAKRIYANNIS, A., PIOMELLI, D., GOLDBERG, S. R. & JUSTINOVA, Z. 2016. Effects of fatty acid amide hydrolase (FAAH) inhibitors on working memory in rats. *Psychopharmacology (Berl),* 233**,** 1879-88.

PAPPAN, K., AUSTIN-BROWN, S., CHAPMAN, K. D. & WANG, X. 1998. Substrate selectivities and lipid modulation of plant phospholipase D alpha, -beta, and -gamma. *Arch Biochem Biophys,* 353**,** 131-40.

PATEL, M. B. & MISHRA, S. 2011. Hypoglycemic activity of alkaloidal fraction of Tinospora cordifolia. *Phytomedicine,* 18**,** 1045-52.

PATGIRI, B., UMRETIA, B. L., VAISHNAV, P. U., PRAJAPATI, P. K., SHUKLA, V. J. & RAVISHANKAR, B. 2014. Anti-inflammatory activity of Guduchi Ghana (aqueous extract of Tinospora Cordifolia Miers.). *Ayu,* 35**,** 108-10.

PATRICELLI, M. P. & CRAVATT, B. F. 1999. Fatty acid amide hydrolase competitively degrades bioactive amides and esters through a nonconventional catalytic mechanism. *Biochemistry,* 38**,** 14125-30.

PATRICELLI, M. P., LOVATO, M. A. & CRAVATT, B. F. 1999. Chemical and mutagenic investigations of fatty acid amide hydrolase: evidence for a family of serine hydrolases with distinct catalytic properties. *Biochemistry,* 38**,** 9804-12.

PELLOW, S., CHOPIN, P., FILE, S. E. & BRILEY, M. 1985. Validation of open:closed arm entries in an elevated plus-maze as a measure of anxiety in the rat. *J Neurosci Methods,* 14**,** 149-67.

PERTWEE, R. G. 2005. Pharmacological actions of cannabinoids. *Handb Exp Pharmacol***,** 1-51.

PERTWEE, R. G. 2008. The diverse CB1 and CB2 receptor pharmacology of three plant cannabinoids: delta9-tetrahydrocannabinol, cannabidiol and delta9-tetrahydrocannabivarin. *Br J Pharmacol,* 153**,** 199-215.

PERTWEE, R. G., FERNANDO, S. R., NASH, J. E. & COUTTS, A. A. 1996. Further evidence for the presence of cannabinoid CB1 receptors in guinea-pig small intestine. *Br J Pharmacol,* 118**,** 2199-205.

PERTWEE, R. G., HOWLETT, A. C., ABOOD, M. E., ALEXANDER, S. P., DI MARZO, V., ELPHICK, M. R., GREASLEY, P. J., HANSEN, H. S., KUNOS, G., MACKIE, K., MECHOULAM, R. & ROSS, R. A. 2010. International Union of Basic and Clinical Pharmacology. LXXIX. Cannabinoid receptors and their ligands: beyond CB(1) and CB(2). *Pharmacol Rev,* 62**,** 588-631.

PETRUCCI, V., CHICCA, A., GLASMACHER, S., PALOCZI, J., CAO, Z., PACHER, P. & GERTSCH, J. 2017. Pepcan-12 (RVD-hemopressin) is a CB2 receptor positive allosteric modulator constitutively secreted by adrenals and in liver upon tissue damage. *Sci Rep,* 7**,** 9560.

PIOMELLI, D., GIUFFRIDA, A., CALIGNANO, A. & RODRIGUEZ DE FONSECA, F. 2000. The endocannabinoid system as a target for therapeutic drugs. *Trends Pharmacol Sci,* 21**,** 218-24.

PORTER, A. C., SAUER, J. M., KNIERMAN, M. D., BECKER, G. W., BERNA, M. J., BAO, J., NOMIKOS, G. G., CARTER, P., BYMASTER, F. P., LEESE, A. B. & FELDER, C. C. 2002. Characterization of a novel endocannabinoid, virodhamine, with antagonist activity at the CB1 receptor. *J Pharmacol Exp Ther,* 301**,** 1020-4.

RADUNER, S., MAJEWSKA, A., CHEN, J. Z., XIE, X. Q., HAMON, J., FALLER, B., ALTMANN, K. H. & GERTSCH, J. 2006. Alkylamides from Echinacea are a new class of cannabinomimetics. Cannabinoid type 2 receptor-dependent and -independent immunomodulatory effects. *J Biol Chem,* 281**,** 14192-206.

RAMESHA, B. T., GERTSCH, J., RAVIKANTH, G., PRITI, V., GANESHAIAH, K. N. & UMA SHAANKER, R. 2011. Biodiversity and chemodiversity: future perspectives in bioprospecting. *Curr Drug Targets,* 12**,** 1515-30.

REYNOSO-MORENO, I., CHICCA, A., FLORES-SOTO, M. E., VIVEROS-PAREDES, J. M. & GERTSCH, J. 2018. The Endocannabinoid Reuptake Inhibitor WOBE437 Is Orally Bioavailable and Exerts Indirect Polypharmacological Effects via Different Endocannabinoid Receptors. *Front Mol Neurosci,* 11**,** 180.

RICHARDSON, J. D., AANONSEN, L. & HARGREAVES, K. M. 1998. Hypoactivity of the spinal cannabinoid system results in NMDA-dependent hyperalgesia. *J Neurosci,* 18**,** 451-7.

RIDDLE, J. M. 1971. Dioscorides. *Dictionary of Scientific Biography,* 4**,** 119-123.

RIDDLE, J. M. 1980. Dioscorides. F.O. Cranz, P.O. Kristeller (Eds.), Catalogus translationum et commentariorum, 4. Medieval and Renaissance Latin Translations and Commentaries, Washington D.C., pp. 1-145.

RINALDI-CARMONA, M., BARTH, F., HEAULME, M., SHIRE, D., CALANDRA, B., CONGY, C., MARTINEZ, S., MARUANI, J., NELIAT, G., CAPUT, D. & ET AL. 1994. SR141716A, a potent and selective antagonist of the brain cannabinoid receptor. *FEBS Lett,* 350**,** 240-4.

ROCK, E. M., LIMEBEER, C. L., MECHOULAM, R., PIOMELLI, D. & PARKER, L. A. 2008. The effect of cannabidiol and URB597 on conditioned gaping (a model of nausea) elicited by a lithium-paired context in the rat. *Psychopharmacology (Berl),* 196**,** 389-95.

RØNSTED, N., SAVOLAINEN, V., MØLGAARD, P. & JÄGER, A. K. 2008. Phylogenetic selection of Narcissus species for drug discovery. *Biochemical Systematics and Ecology,* 36**,** 417-422.

RØNSTED, N., SYMONDS, M. R., BIRKHOLM, T., CHRISTENSEN, S. B., MEEROW, A. W., MOLANDER, M., MOLGAARD, P., PETERSEN, G., RASMUSSEN, N., VAN STADEN, J., STAFFORD, G. I. & JAGER, A. K. 2012. Can phylogeny predict chemical diversity and potential medicinal activity of plants? A case study of Amaryllidaceae. *BMC Evol Biol,* 12**,** 182.

ROSSI, F., SINISCALCO, D., LUONGO, L., DE PETROCELLIS, L., BELLINI, G., PETROSINO, S., TORELLA, M., SANTORO, C., NOBILI, B., PERROTTA, S., DI MARZO, V. & MAIONE, S. 2009. The

endovanilloid/endocannabinoid system in human osteoclasts: possible involvement in bone formation and resorption. *Bone,* 44**,** 476-84.

RUSSO, E. B. 2007. History of cannabis and its preparations in saga, science, and sobriquet. *Chem Biodivers,* 4**,** 1614-48.

RUSSO, E. B. 2016. Beyond Cannabis: Plants and the Endocannabinoid System. *Trends Pharmacol Sci,* 37**,** 594-605.

RYBERG, E., LARSSON, N., SJOGREN, S., HJORTH, S., HERMANSSON, N. O., LEONOVA, J., ELEBRING, T., NILSSON, K., DRMOTA, T. & GREASLEY, P. J. 2007. The orphan receptor GPR55 is a novel cannabinoid receptor. *Br J Pharmacol,* 152**,** 1092-101.

SADRAEI, H., ASGHARI, G. R., HAJHASHEMI, V., KOLAGAR, A. & EBRAHIMI, M. 2001. Spasmolytic activity of essential oil and various extracts of Ferula gummosa Boiss. on ileum contractions. *Phytomedicine,* 8**,** 370-6.

SAGAR, D. R., GAW, A. G., OKINE, B. N., WOODHAMS, S. G., WONG, A., KENDALL, D. A. & CHAPMAN, V. 2009. Dynamic regulation of the endocannabinoid system: implications for analgesia. *Mol Pain,* 5**,** 59.

SAHA, S. & GHOSH, S. 2012. Tinospora cordifolia: One plant, many roles. *Anc Sci Life,* 31**,** 151-9.

SANDER, L. 1987. Origin and date of the Bower Manuscript, a new approach. M. Yaldiz, W. Lobo (Eds.), Investigating the Indian Arts, Museum für Indische Kunst, Berlin (1987), pp. 313-323.

SARMA, D. N. K., KHOSA, R. L. & SAHAI, M. 1995. Isolation of Jatrorrhizine from Tinospora cordifolia Roots. *Planta Med,* 61**,** 98-99.

SASSO, O., MIGLIORE, M., HABRANT, D., ARMIROTTI, A., ALBANI, C., SUMMA, M., MORENO-SANZ, G., SCARPELLI, R. & PIOMELLI, D. 2015. Multitarget fatty acid amide hydrolase/cyclooxygenase blockade suppresses intestinal inflammation and protects against nonsteroidal anti-inflammatory drug-dependent gastrointestinal damage. *FASEB J,* 29**,** 2616-27.

SATTAR, Z. & IRANSHAHI, M. 2017. Phytochemistry and pharmacology of Ferula persica Boiss.: A review. *Iran J Basic Med Sci,* 20**,** 1-8.

SAVINAINEN, J. R., SAARIO, S. M. & LAITINEN, J. T. 2012. The serine hydrolases MAGL, ABHD6 and ABHD12 as guardians of 2-arachidonoylglycerol signalling through cannabinoid receptors. *Acta Physiol (Oxf),* 204**,** 267-76.

SCHMID, H. H., SCHMID, P. C. & NATARAJAN, V. 1996. The N-acylation-phosphodiesterase pathway and cell signalling. *Chem Phys Lipids,* 80**,** 133-42.

SCHMID, P. C., REDDY, P. V., NATARAJAN, V. & SCHMID, H. H. 1983. Metabolism of N-acylethanolamine phospholipids by a mammalian phosphodiesterase of the phospholipase D type. *J Biol Chem,* 258**,** 9302-6.

SEN, S., ROY, M. & CHAKRABORTI, A. S. 2011. Ameliorative effects of glycyrrhizin on streptozotocin-induced diabetes in rats. *J Pharm Pharmacol,* 63**,** 287-96.

SHARMA, C., SADEK, B., GOYAL, S. N., SINHA, S., KAMAL, M. A. & OJHA, S. 2015. Small Molecules from Nature Targeting G-Protein Coupled Cannabinoid Receptors: Potential Leads for Drug Discovery and Development. *Evid Based Complement Alternat Med,* 2015**,** 238482.

SHARMA, U., BALA, M., KUMAR, N., SINGH, B., MUNSHI, R. K. & BHALERAO, S. 2012. Immunomodulatory active compounds from Tinospora cordifolia. *J Ethnopharmacol,* 141**,** 918-26.

SHRESTHA, R., DIXON, R. A. & CHAPMAN, K. D. 2003. Molecular identification of a functional homologue of the mammalian FAAH in *Arabidopsis thaliana*. *Journal of Biological Chemistry,* 278**,** 34990-34997.

SHRESTHA, R., KIM, S. C., DYER, J. M., DIXON, R. A. & CHAPMAN, K. D. 2006. Plant fatty acid (ethanol) amide hydrolases. *Biochim Biophys Acta,* 1761**,** 324-34.

SHRESTHA, R., NOORDERMEER, M. A., VAN DER STELT, M., VELDINK, G. A. & CHAPMAN, K. D. 2002. N-acylethanolamines are metabolized by lipoxygenase and amidohydrolase in competing pathways during cottonseed imbibition. *Plant Physiol,* 130**,** 391-401.

SIEVERS, F., WILM, A., DINEEN, D., GIBSON, T. J., KARPLUS, K., LI, W., LOPEZ, R., MCWILLIAM, H., REMMERT, M., SODING, J., THOMPSON, J. D. & HIGGINS, D. G. 2011. Fast, scalable generation of high-quality protein multiple sequence alignments using Clustal Omega. *Mol Syst Biol,* 7**,** 539.

SIMON, C., BARATHIEU, K., LAGUERRE, M., SCHMITTER, J. M., FOUQUET, E., PIANET, I. & DUFOURC, E. J. 2003. Three-dimensional structure and dynamics of wine tannin-saliva protein complexes. A multitechnique approach. *Biochemistry,* 42**,** 10385-95.

SIMON, G. M. & CRAVATT, B. F. 2006. Endocannabinoid biosynthesis proceeding through glycerophospho-N-acyl ethanolamine and a role for alpha/beta-hydrolase 4 in this pathway. *J Biol Chem,* 281**,** 26465-72.

SIMONS, R., VINCKEN, J. P., MOL, L. A., THE, S. A., BOVEE, T. F., LUIJENDIJK, T. J., VERBRUGGEN, M. A. & GRUPPEN, H. 2011. Agonistic and antagonistic estrogens in licorice root (Glycyrrhiza glabra). *Anal Bioanal Chem,* 401**,** 305-13.

SINGH, S. S., PANDEY, S. C., SRIVASTAVA, S., GUPTA, V. S. & PATRO, B. 2003. Chemistry and medicinal properties of tinospora cordifolia (GUDUCHI). *Indian Journal of Pharmacology,* 35**,** 83-91.

SINHA, D., BONNER, T. I., BHAT, N. R. & MATSUDA, L. A. 1998. Expression of the CB1 cannabinoid receptor in macrophage-like cells from brain tissue: immunochemical characterization by fusion protein antibodies. *J Neuroimmunol,* 82**,** 13-21.

SMART, D., GUNTHORPE, M. J., JERMAN, J. C., NASIR, S., GRAY, J., MUIR, A. I., CHAMBERS, J. K., RANDALL, A. D. & DAVIS, J. B. 2000. The endogenous lipid anandamide is a full agonist at the human vanilloid receptor (hVR1). *Br J Pharmacol,* 129**,** 227-30.

SOUTHON, I. W. 1994. Phytochemical Dictionary of the Leguminosae. Chapman & Hall, London (1994).

SRINIVASAN, G., UNNIKRISHNAN, K., REMA SHREE, A. & BALACHANDRAN, I. 2008. HPLC estimation of berberine in Tinospora cordifolia and Tinospora sinensis. *Indian Journal of Pharmaceutical Sciences,* 70**,** 96-99.

STANELY, P., PRINCE, M. & MENON, V. P. 2000. Hypoglycaemic and other related actions of Tinospora cordifolia roots in alloxan-induced diabetic rats. *J Ethnopharmacol,* 70**,** 9-15.

STAUB, P. O., CASU, L. & LEONTI, M. 2016. Back to the roots: A quantitative survey of herbal drugs in Dioscorides' De Materia Medica (ex Matthioli, 1568). *Phytomedicine,* 23**,** 1043-52.

STELLA, N. 2004. Cannabinoid signaling in glial cells. *Glia,* 48**,** 267-77.

STEMPEL, A. V., STUMPF, A., ZHANG, H. Y., OZDOGAN, T., PANNASCH, U., THEIS, A. K., OTTE, D. M., WOJTALLA, A., RACZ, I., PONOMARENKO, A., XI, Z. X., ZIMMER, A. & SCHMITZ, D. 2016. Cannabinoid Type 2 Receptors Mediate a Cell Type-Specific Plasticity in the Hippocampus. *Neuron,* 90**,** 795-809.

STRANGE, P. G. 2010. Use of the GTPgammaS ([35S]GTPgammaS and Eu-GTPgammaS) binding assay for analysis of ligand potency and efficacy at G protein-coupled receptors. *Br J Pharmacol,* 161**,** 1238-49.

SUN, N. J., WOO, S. H., CASSADY, J. M. & SNAPKA, R. M. 1998. DNA Polymerase and Topoisomerase II Inhibitors from Psoralea corylifolia. *Journal of Natural Products,* 61**,** 362-366.

SUN, Y. X., TSUBOI, K., OKAMOTO, Y., TONAI, T., MURAKAMI, M., KUDO, I. & UEDA, N. 2004. Biosynthesis of anandamide and N-palmitoylethanolamine by sequential actions of phospholipase A2 and lysophospholipase D. *Biochem J,* 380**,** 749-56.

SZLISZKA, E., CZUBA, Z. P., SEDEK, L., PARADYSZ, A. & KROL, W. 2011a. Enhanced TRAIL-mediated apoptosis in prostate cancer cells by the bioactive compounds neobavaisoflavone and psoralidin isolated from Psoralea corylifolia. *Pharmacol Rep,* 63**,** 139-48.

SZLISZKA, E., SKABA, D., CZUBA, Z. P. & KROL, W. 2011b. Inhibition of inflammatory mediators by neobavaisoflavone in activated RAW264.7 macrophages. *Molecules,* 16**,** 3701-12.

TAM, J., HINDEN, L., DRORI, A., UDI, S., AZAR, S. & BARAGHITHY, S. 2018. The therapeutic potential of targeting the peripheral endocannabinoid/CB1 receptor system. *Eur J Intern Med,* 49**,** 23-29.

THE PLANT LIST 2013. Version 1.1. online, http://www.theplantlist.org/ (accessed 1st January 2015).

THORS, L., ALAJAKKU, K. & FOWLER, C. J. 2007a. The 'specific' tyrosine kinase inhibitor genistein inhibits the enzymic hydrolysis of anandamide: implications for anandamide uptake. *Br J Pharmacol,* 150**,** 951-60.

THORS, L., BELGHITI, M. & FOWLER, C. J. 2008. Inhibition of fatty acid amide hydrolase by kaempferol and related naturally occurring flavonoids. *Br J Pharmacol,* 155**,** 244-52.

THORS, L., BURSTON, J. J., ALTER, B. J., MCKINNEY, M. K., CRAVATT, B. F., ROSS, R. A., PERTWEE, R. G., GEREAU, R. W. T., WILEY, J. L. & FOWLER, C. J. 2010. Biochanin A, a naturally occurring inhibitor of fatty acid amide hydrolase. *Br J Pharmacol,* 160**,** 549-60.

THORS, L., ERIKSSON, J. & FOWLER, C. J. 2007b. Inhibition of the cellular uptake of anandamide by genistein and its analogue daidzein in cells with different levels of fatty acid amide hydrolase-driven uptake. *Br J Pharmacol,* 152**,** 744-50.

THYAGARAJAN, S., JAYARAM, S., GOPALAKRISHNAN, V., HARI, R., JEYAKUMAR, P. & SRIPATHI, M. 2002. Herbal medicines for liver diseases in India. *Journal of Gastroenterology and Hepatology,* 17**,** S370-S376.

TJOLSEN, A., BERGE, O. G., HUNSKAAR, S., ROSLAND, J. H. & HOLE, K. 1992. The formalin test: an evaluation of the method. *Pain,* 51**,** 5-17.

TOKER, G., KUPELI, E., MEMISOGLU, M. & YESILADA, E. 2004. Flavonoids with antinociceptive and anti-inflammatory activities from the leaves of Tilia argentea (silver linden). *J Ethnopharmacol,* 95**,** 393-7.

TOLON, R. M., NUNEZ, E., PAZOS, M. R., BENITO, C., CASTILLO, A. I., MARTINEZ-ORGADO, J. A. & ROMERO, J. 2009. The activation of cannabinoid CB2 receptors stimulates in situ and in vitro beta-amyloid removal by human macrophages. *Brain Res,* 1283**,** 148-54.

TRIPATHY, S., KLEPPINGER-SPARACE, K., DIXON, R. A. & CHAPMAN, K. D. 2003. Identification and characterization of a binding protein for N_acylethanolamines in membranes of tabacco cells *N. Murata et al. (eds.), Advanced Research on Plant Lipids***,** 315-318.

TRIPATHY, S., VENABLES, B. J. & CHAPMAN, K. D. 1999. N-Acylethanolamines in signal transduction of elicitor perception. Attenuation Of alkalinization response and activation of defense gene expression. *Plant Physiol,* 121**,** 1299-308.

TSOU, K., NOGUERON, M. I., MUTHIAN, S., SANUDO-PENA, M. C., HILLARD, C. J., DEUTSCH, D. G. & WALKER, J. M. 1998. Fatty acid amide hydrolase is located preferentially in large neurons in the rat central nervous system as revealed by immunohistochemistry. *Neurosci Lett,* 254**,** 137-40.

UMATHE, S. N., MANNA, S. S. & JAIN, N. S. 2011. Involvement of endocannabinoids in antidepressant and anti-compulsive effect of fluoxetine in mice. *Behav Brain Res,* 223**,** 125-34.

UPADHYAY, A. K., KUMAR, K., KUMAR, A. & MISHRA, H. S. 2010. Tinospora cordifolia (Willd.) Hook. f. and Thoms. (Guduchi) - validation of the Ayurvedic pharmacology through experimental and clinical studies. *Int J Ayurveda Res,* 1**,** 112-21.

UPADHYAY, R., PANDEY, R. P., SHARMA, V. & K., V. A. 2011. Assessment of the Multifaceted Immonomodulatory Potential of the Aqueous Extract of Tinospora Cordifolia. *Res J Chem Sci,* 1**,** 71-79.

VALIAKOS, E., MARSELOS, M., SAKELLARIDIS, N., CONSTANTINIDIS, T. & SKALTSA, H. 2015. Ethnopharmacological approach to the herbal medicines of the "Antidotes" in Nikolaos Myrepsos Dynameron. *J Ethnopharmacol,* 163**,** 68-82.

VALLEE, M., VITIELLO, S., BELLOCCHIO, L., HEBERT-CHATELAIN, E., MONLEZUN, S., MARTIN-GARCIA, E., KASANETZ, F., BAILLIE, G. L., PANIN, F., CATHALA, A., ROULLOT-LACARRIERE, V., FABRE, S., HURST, D. P., LYNCH, D. L., SHORE, D. M., DEROCHE-GAMONET, V., SPAMPINATO, U., REVEST, J. M., MALDONADO, R., REGGIO, P. H., ROSS, R. A., MARSICANO, G. & PIAZZA, P. V. 2014. Pregnenolone can protect the brain from cannabis intoxication. *Science,* 343**,** 94-8.

VAN DER STELT, M. & DI MARZO, V. 2003. The endocannabinoid system in the basal ganglia and in the mesolimbic reward system: implications for neurological and psychiatric disorders. *Eur J Pharmacol,* 480**,** 133-50.

VAN KIEM, P., VAN MINH, C., DAT, N. T., VAN KINH, L., HANG, D. T., NAM, N. H., CUONG, N. X., HUONG, H. T. & VAN LAU, T. 2010. Aporphine alkaloids, clerodane diterpenes, and other constituents from Tinospora cordifolia. *Fitoterapia,* 81**,** 485-489.

VANDEVOORDE, S. & FOWLER, C. J. 2005. Inhibition of fatty acid amide hydrolase and monoacylglycerol lipase by the anandamide uptake inhibitor VDM11: evidence that VDM11 acts as an FAAH substrate. *Br J Pharmacol,* 145**,** 885-93.

VERTY, A. N., STEFANIDIS, A., MCAINCH, A. J., HRYCIW, D. H. & OLDFIELD, B. 2015. Anti-Obesity Effect of the CB2 Receptor Agonist JWH-015 in Diet-Induced Obese Mice. *PLoS One,* 10**,** e0140592.

WADOOD, N., WADOOD, A. & SHAH, S. A. 1992. Effect of Tinospora cordifolia on blood glucose and total lipid levels of normal and alloxan-diabetic rabbits. *Planta Med,* 58**,** 131-6.

WALL, M. E. & WANI, M. C. 1996. Camptothecin and taxol: from discovery to clinic. *J Ethnopharmacol,* 51**,** 239-53; discussion 253-4.

WANG, L., YANG, R., YUAN, B., LIU, Y. & LIU, C. 2015. The antiviral and antimicrobial activities of licorice, a widely-used Chinese herb. *Acta Pharm Sin B,* 5**,** 310-5.

WANG, Y. S., SHRESTHA, R., KILARU, A., WIANT, W., VENABLES, B. J., CHAPMAN, K. D. & BLANCAFLOR, E. B. 2006. Manipulation of Arabidopsis fatty acid amide hydrolase expression modifies plant growth and sensitivity to N-acylethanolamines. *Proc Natl Acad Sci U S A,* 103**,** 12197-202.

WAZIR, V., MAURYA, R. & KAPIL, R. S. 1995. Cordioside, a clerodane furano diterpene glucoside from Tinospora cordifolia. *Phytochemistry,* 38**,** 447-449.

WEI, B. Q., MIKKELSEN, T. S., MCKINNEY, M. K., LANDER, E. S. & CRAVATT, B. F. 2006. A second fatty acid amide hydrolase with variable distribution among placental mammals. *J Biol Chem,* 281**,** 36569-78.

WHYTE, L. S., FORD, L., RIDGE, S. A., CAMERON, G. A., ROGERS, M. J. & ROSS, R. A. 2012. Cannabinoids and bone: endocannabinoids modulate human osteoclast function in vitro. *Br J Pharmacol,* 165**,** 2584-97.

WILLIAMSON, E. 2002. Major Herbs of Ayurveda. Churchill Livingstone, UK

WILSON, R. I. & NICOLL, R. A. 2001. Endogenous cannabinoids mediate retrograde signalling at hippocampal synapses. *Nature,* 410**,** 588-92.

WINK, M. 2003. Evolution of secondary metabolites from an ecological and molecular phylogenetic perspective. *Phytochemistry,* 64**,** 3-19.

WINK, M. 2013. Evolution of secondary metabolites in legumes (Fabaceae). *South African Journal of Botany,* 89**,** 164-175.

WINK, M. & MOHAMED, G. I. A. 2003. Evolution of chemical defense traits in the Leguminosae: mapping of distribution patterns of secondary metabolites on a molecular phylogeny inferred from nucleotide sequences of the rbcL gene. *Biochemical Systematics and Ecology,* 31**,** 897-917.

WINK, M. & WITTE, L. 1984. Turnover and transport of quinolizidine alkaloids. Diurnal fluctuations of lupanine in the phloem sap, leaves and fruits of Lupinus albus L. *Planta,* 161**,** 519-524.

WOJAKOWSKA, A., MUTH, D., NAROZNA, D., MADRZAK, C., STOBIECKI, M. & KACHLICKI, P. 2013a. Changes of phenolic secondary metabolite profiles in the reaction of narrow leaf lupin (Lupinus angustifolius) plants to infections with Colletotrichum lupini fungus or treatment with its toxin. *Metabolomics,* 9**,** 575-589.

WOJAKOWSKA, A., PIASECKA, A., GARCIA-LOPEZ, P. M., ZAMORA-NATERA, F., KRAJEWSKI, P., MARCZAK, L., KACHLICKI, P. & STOBIECKI, M. 2013b. Structural analysis and profiling of phenolic secondary metabolites of Mexican lupine species using LC-MS techniques. *Phytochemistry,* 92**,** 71-86.

WUJASTYK, D. 2003. The Roots of Ayurveda. Selections from Sanskrit. Medical Writings. Penguin Books Ltd., London.

YANG, L., LI, Y., REN, J., ZHU, C., FU, J., LIN, D. & QIU, Y. 2014. Celastrol attenuates inflammatory and neuropathic pain mediated by cannabinoid receptor type 2. *Int J Mol Sci,* 15**,** 13637-48.

YANG, Y.-F., ZHANG, Y.-B., CHEN, Z.-J., ZHANG, Y.-T. & YANG, X.-W. 2018. Plasma pharmacokinetics and cerebral nuclei distribution of major constituents of Psoraleae fructus in rats after oral administration. *Phytomedicine,* 38**,** 166-174.

YU, M., IVES, D. & RAMESHA, C. S. 1997. Synthesis of prostaglandin E2 ethanolamide from anandamide by cyclooxygenase-2. *J Biol Chem,* 272**,** 21181-6.

YULDASHEV, M. P., BATIROV, E. K., VDOVIN, A. D. & ABDULLAEV, N. D. 2000. Structural Study of Glabrisoflavone, a novel isoflavone from Glycyrrhiza glabra L. *Russian Journal of Bioorganic Chemistry,* 26**,** 784-786.

ZARGARI, A. 1989. Medicinal plants. Tehran: Tehran University Press.

ZARIFKAR, A., KARAMI-KHEIRABAD, M., EDJTEHADI, M., RASTGAR, K. & GHALJE, M. 2007. Evaluation of Antinociceptive Effect of Galbanum by Formalin Test in Mice. *Armaghane danesh,* 12**,** 19-27.

ZHANG, X., ZHAO, W., WANG, Y., LU, J. & CHEN, X. 2016. The Chemical Constituents and Bioactivities of Psoralea corylifolia Linn.: A Review. *Am J Chin Med,* 44**,** 35-60.

ZYGMUNT, P. M., PETERSSON, J., ANDERSSON, D. A., CHUANG, H., SORGARD, M., DI MARZO, V., JULIUS, D. & HOGESTATT, E. D. 1999. Vanilloid receptors on sensory nerves mediate the vasodilator action of anandamide. *Nature,* 400**,** 452-7.

LIST OF PUBLICATIONS

IN PREPARATION

Identification of Prenylated Isoflavonoids as Potent, Selective and Reversible Fatty Acid Amide Hydrolase Inhibitors

Collu, M.[1,2], Calarco, S.[1], Nicolussi, S.[1], Rau, M.[1], Casu, L.[2], Leonti, M.[3], Gertsch, J.[1]

[1]Institute of Biochemistry and Molecular Medicine, University of Bern, 3012 Bern, Switzerland

[2]Department of Life and Environmental Sciences, University of Cagliari, 09124 Cagliari, Italy

[3]Department of Biomedical Sciences, University of Cagliari, 09124 Cagliari, Italy

LIST OF COMUNICATIONS

Poster communications

2017 – 7th SWISS PHARMA SCIENCE DAY (Bern, Switzerland)

Bioprospecting for Anti-Chagas Medicinal Plants in Bolivia and Biological Evaluation

Salm, A., Collu, M., Calarco, S., Almanza, G., Gertsch, J.

2018 – 8th SWISS PHARMA SCIENCE DAY (Bern, Switzerland)

Targeting the Endocannabinoid System: Screening of Medicinal Plants Extracts Reveals Potent Fatty Acid Amide Hydrolase Inhibitors

Collu, M., Calarco, S., Casu, L., Leonti, M., Gertsch, J.

SUPPLEMENTARY DATA

>sp|O08914|FAAH1_MOUSE Fatty-acid amide hydrolase 1 OS=Mus musculus OX=10090 GN=Faah PE=1 SV=1

MVLSEVWTALSGLSGVCLACSLLSAAVVLRWTRSQTARGAVTRARQKQRAGLETMDKAVQRFRLQNPDLDSEALLALPLLQ
LVQKLQSGELSPEAVLFTYLGKAWEVNKGTNCVTSYLTDCETQLSQAPRQGLLYGVPVSLKECFSYKGHASTLGLSLNEGVTSE
SDCVVVQVLKLQGAVPFVHTNVPQSMLSYDCSNPLFGQTMNPWKPSKSPGGSSGGEGALIGSGGSPLGLGTDIGGSIRFPSA
FCGICGLKPTGNRLSKSGLKSCVYGQTAVQLSVGPMARDVDSLALCMKALLCEDLFRLDSTIPPLPFREEIYRSSRPLRVGYYET
DNYTMPTPAMRRAVMETKQSLEAAGHTLVPFLPNNIPYALEVLSAGGLFSDGGCSFLQNFKGDFVDPCLGDLVLVLKLPRWF
KKLLSFLLKPLFPRLAAFLNSMCPRSAEKLWELQHEIEMYRQSVIAQWKAMNLDVVLTPMLGPALDLNTPGRATGAISYTVLY
NCLDFPAGVVPVTTVTAEDDAQMEHYKGYFGDMWDNILKKGMKKGIGLPVAVQCVALPWQEELCLRFMREVERLMTPEK
RPS

Supplementary Figure 1. FASTA sequence of mouse FAAH-1 protein (UniProt code: O08914).

```
sp|O08914|FAAH1_MOUSE          MVLS--EVWTA-LSGLSGVCLACSLLSAAVVLRWT-----RSQTARGAVTRARQKQRAGL   52
3QK5:A|PDBID|CHAIN|SEQUENCE    MGGSHHHHHHGMASMTGGQQMGRDLYDDDDKDRWGSELETGRQKARGAATRARQKQRASL   60
3PPM:A|PDBID|CHAIN|SEQUENCE    ---------MGSSHHHHHHSSGLVPRGSHMASR-----WTGRQKARGAATRARQKQRASL   46
                                         .         .   .    *        *.****.*********.*

sp|O08914|FAAH1_MOUSE          ETMDKAVQRFRLQNPDLDSEALLALPLLQLVQKLQSGELSPEAVLFTYLGKAWEVNKGTN   112
3QK5:A|PDBID|CHAIN|SEQUENCE    ETMDKAVQRFRLQNPDLDSEALLTLPLLQLVQKLQSGELSPEAVFFTYLGKAWEVNKGTN   120
3PPM:A|PDBID|CHAIN|SEQUENCE    ETMDKAVQRFRLQNPDLDSEALLTLPLLQLVQKLQSGELSPEAVFFTYLGKAWEVNKGTN   106
                               **********************:********************:***************

sp|O08914|FAAH1_MOUSE          CVTSYLTDCETQLSQAPRQGLLYGVPVSLKECFSYKGHASTLGLSLNEGVTSESDCVVVQ   172
3QK5:A|PDBID|CHAIN|SEQUENCE    CVTSYLTDCETQLSQAPRQGLLYGVPVSLKECFSYKGHDSTLGLSLNEGMPSESDCVVVQ   180
3PPM:A|PDBID|CHAIN|SEQUENCE    CVTSYLTDCETQLSQAPRQGLLYGVPVSLKECFSYKGHDSTLGLSLNEGMPSESDCVVVQ   166
                               ************************************ **********: *********

sp|O08914|FAAH1_MOUSE          VLKLQGAVPFVHTNVPQSMLSYDCSNPLFGQTMNPWKPSKSPGGSSGGEGALIGSGGSPL   232
3QK5:A|PDBID|CHAIN|SEQUENCE    VLKLQGAVPFVHTNVPQSMLSFDCSNPLFGQTMNPWKSSKSPGGSSGGEGALIGSGGSPL   240
3PPM:A|PDBID|CHAIN|SEQUENCE    VLKLQGAVPFVHTNVPQSMFSYDCSNPLFGQTMNPWKSSKSPGGSSGGEGALIGSGGSPL   226
                               ********************:*:*************** **********************

sp|O08914|FAAH1_MOUSE          GLGTDIGGSIRFPSAFCGICGLKPTGNRLSKSGLKSCVYGQTAVQLSVGPMARDVDSLAL   292
3QK5:A|PDBID|CHAIN|SEQUENCE    GLGTDIGGSIRFPSAFCGICGLKPTGNRLSKSGLKGCVYGQTAVQLSLGPMARDVESLAL   300
3PPM:A|PDBID|CHAIN|SEQUENCE    GLGTDIGGSIRFPSAFCGICGLKPTGNRLSKSGLKGCVYGQTAVQLSLGPMARDVESLAL   286
                               ***********************************.**********:*******:****

sp|O08914|FAAH1_MOUSE          CMKALLCEDLFRLDSTIPPLPFREEIYRSSRPLRVGYYETDNYTMPTPAMRRAVMETKQS   352
3QK5:A|PDBID|CHAIN|SEQUENCE    CLKALLCEHLFTLDPTVPPLPFREEVYRSSRPLRVGYYETDNYTMPSPAMRRALIETKQR   360
3PPM:A|PDBID|CHAIN|SEQUENCE    CLKALLCEHLFTLDPTVPPLPFREEVYRSSRPLRVGYYETDNYTMPSPAMRRALIETKQR   346
                               *:******.** ** *:********:********************:******::****

sp|O08914|FAAH1_MOUSE          LEAAGHTLVPFLPNNIPYALEVLSAGGLFSDGGCSFLQNFKGDFVDPCLGDLVLVLKLPR   412
3QK5:A|PDBID|CHAIN|SEQUENCE    LEAAGHTLIPFLPNNIPYALEVLSAGGLFSDGGRSFLQNFKGDFVDPCLGDLILILRLPS   420
3PPM:A|PDBID|CHAIN|SEQUENCE    LEAAGHTLIPFLPNNIPYALEVLSTGGLFSDGGRSFLQNFKGDFVDPCLGDLILILRLPS   406
                               ********:***************:******** ******************:*:*:**

sp|O08914|FAAH1_MOUSE          WFKKLLSFLLKPLFPRLAAFLNSMCPRSAEKLWELQHEIEMYRQSVIAQWKAMNLDVVLT   472
3QK5:A|PDBID|CHAIN|SEQUENCE    WFKRLLSLLLKPLFPRLAAFLNSMRPRSAEKLWKLQHEIEMYRQSVIAQWKAMNLDVLLT   480
3PPM:A|PDBID|CHAIN|SEQUENCE    WFKRLLSLLLKPLFPRLAAFLNNMRPRSAEKLWKLQHEIEMYRQSVIAQWKAMNLDVLLT   466
                               ***:***:**************.* ********:**********************:**

sp|O08914|FAAH1_MOUSE          PMLGPALDLNTPGRATGAISYTVLYNCLDFPAGVVPVTTVTAEDDAQMEHYKGYFGDMWD   532
3QK5:A|PDBID|CHAIN|SEQUENCE    PMLGPALDLNTPGRATGAISYTVLYNCLDFPAGVVPVTTVTAEDDAQMELYKGYFGDIWD   540
3PPM:A|PDBID|CHAIN|SEQUENCE    PMLGPALDLNTPGRATGAVSYTMLYNCLDFPAGVVPVTTVTAEDDAQMELYKGYFGDIWD   526
                               ************************:*:************************************:**

sp|O08914|FAAH1_MOUSE          NILKKGMKKGIGLPVAVQCVALPWQEELCLRFMREVERLMTPEKRPS        579
3QK5:A|PDBID|CHAIN|SEQUENCE    IILKKAMKNSVGLPVAVQCVALPWQEELCLRFMREVEQLMTPQKQPS        587
3PPM:A|PDBID|CHAIN|SEQUENCE    IILKKAMKNSVGLPVAVQCVALPWQEELCLRFMREVEQLMTPQKQPS        573
                                ****.**:.:**************************:****:*:**
```

Supplementary Figure 2. Multiple sequences alignment. A comparison between the mouse FAAH-1 and the 3D model sequences. For the alignment it has been considered the crystal structure with the best resolution: rat FAAH-1 (pdb code 3QK5) (Gustin et al., 2011) and humanized rat FAAH-1 (pdb code 3PPM) (Mileni et al., 2011).

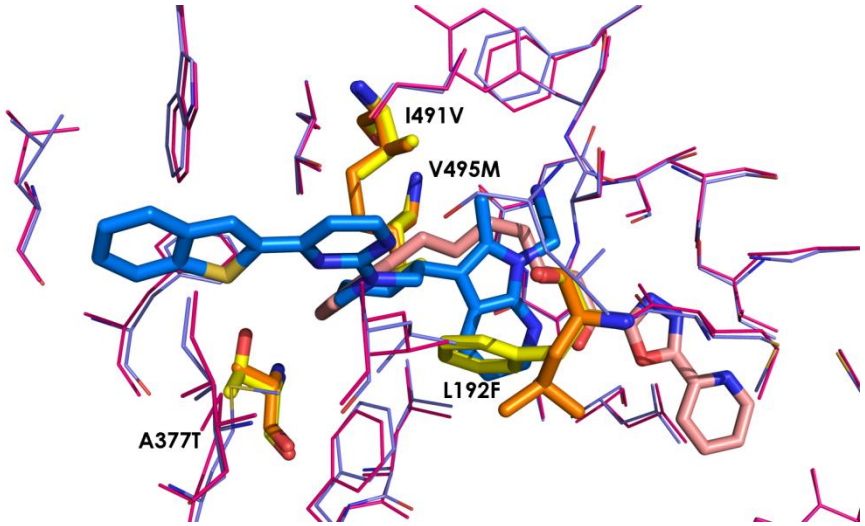

Supplementary Figure 3. Binding site residues alignment of FAAH-1 crystal structures. In magenta and orange the rat (PDB code 3QK5) residues, in violet and yellow the humanized rat (PDB code 3PPM) residues. The inhibitors are represented in sticks: in blue the 3QK5 ligand and in pink the 3PPM ligand.

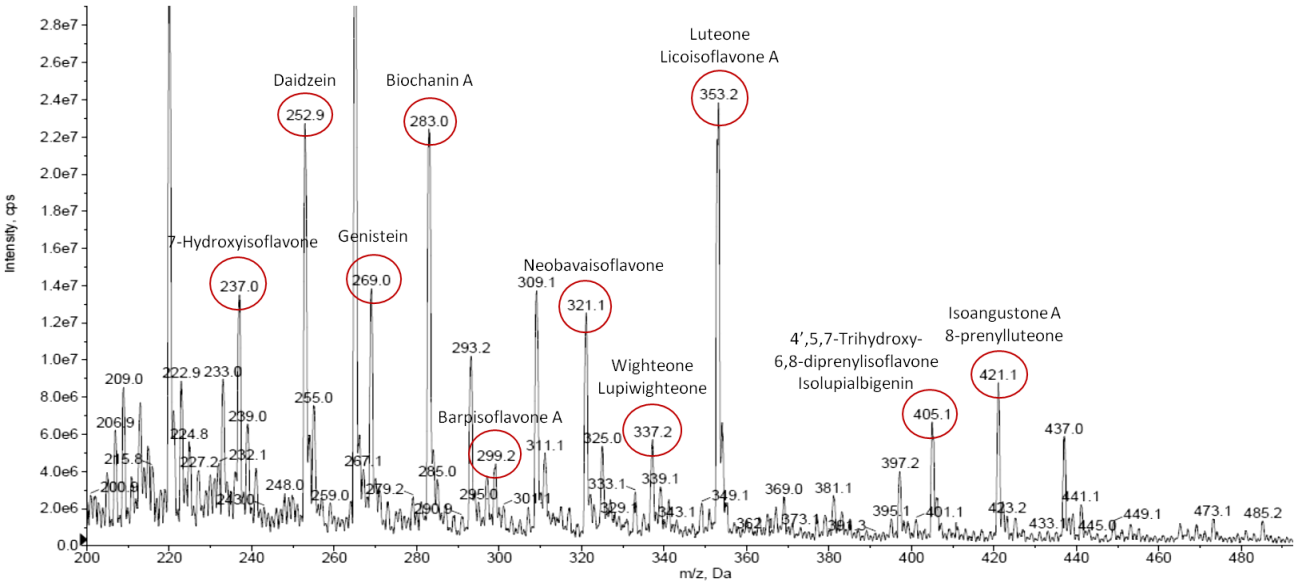

Supplementary Figure 4. Full scan MS spectra of the fourteen screened isoflavonoid standards. Conditions for the measurement: 37% ACN in water solution, standards at the final concentration of 50 ng·ml^{-1}, flow rate 7 µl·min^{-1}, AB Sciex 5500 Q-Trap, negative mode.

A

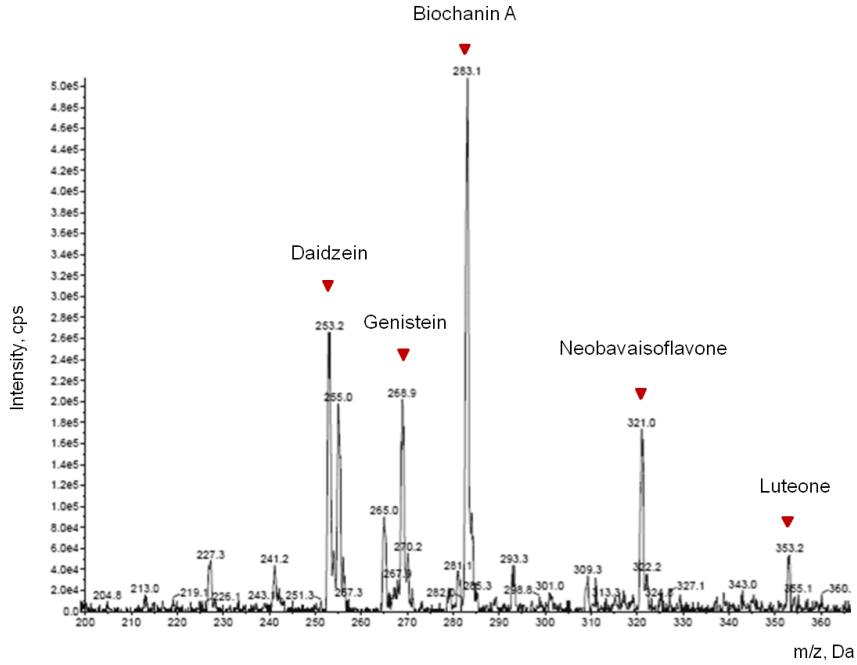
Biochanin A
283.1
Daidzein
253.2
Genistein
268.9
Neobavaisoflavone
321.0
Luteone
353.2
Intensity, cps
m/z, Da

B

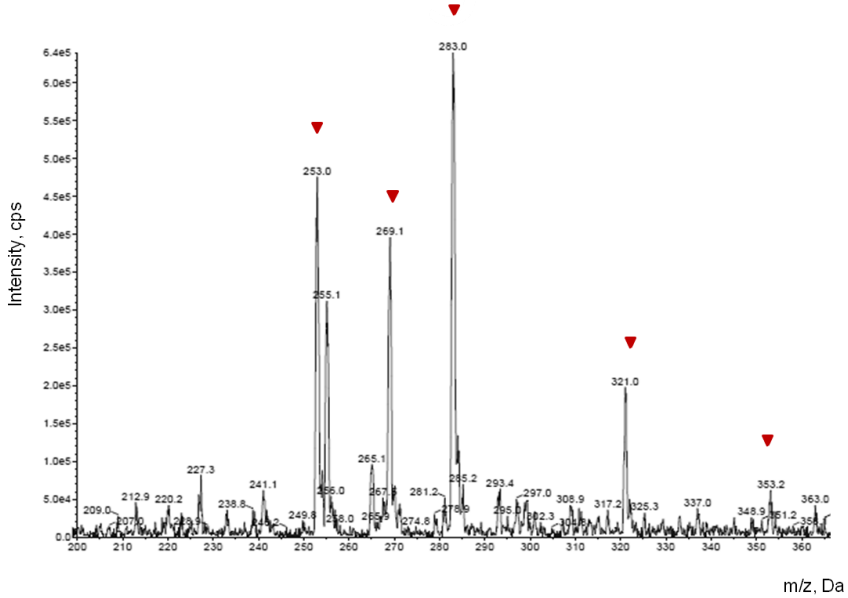
283.0
253.0
269.1
255.1
321.0
Intensity, cps
m/z, Da

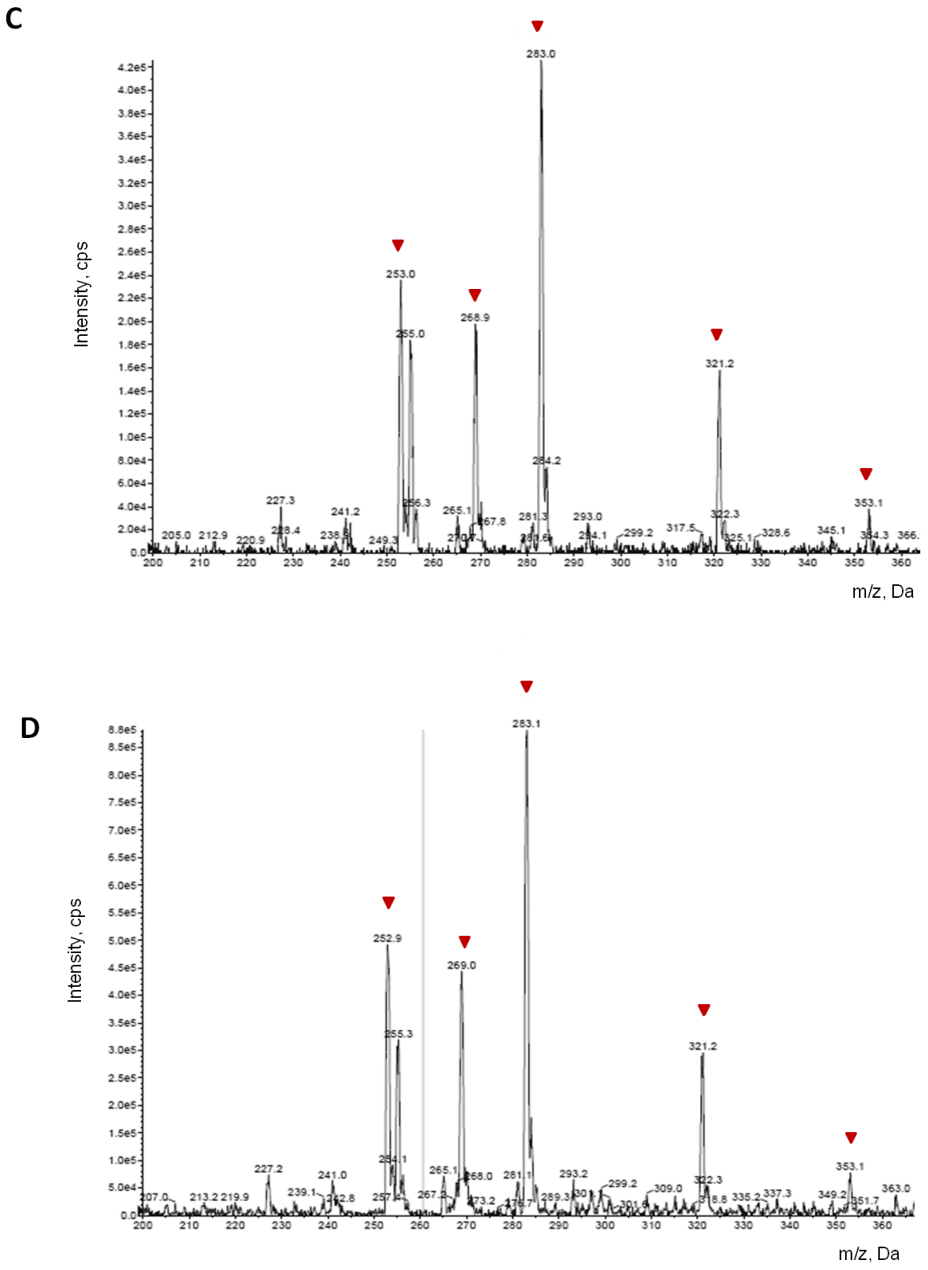

Supplementary Figure 5. Full scan MS spectra of *L. angustifolius* (A), *G. glabra* (B), *P. corylifolia* (C) and *G. uralensis* (D) extracts spiked with a solution containing the active isoflavonoids. Daidzein, genistein, biochanin A, neobavaisoflavone and luteone 100 ng·ml^{-1} were spiked in the plant extract matrix. Plant extracts were then infused at the concentration of 50 ng·ml^{-1}. Conditions of measurement: 37% ACN in water solution; flow rate 7 µl·min^{-1}; AB Sciex 5500 Q-Trap, negative mode.

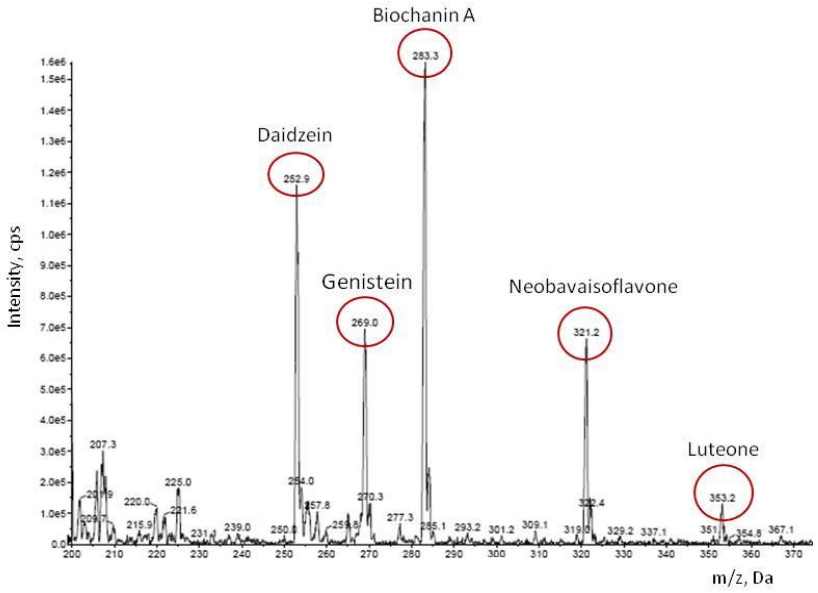

Supplementary Figure 6. Full scan MS spectra of the spiked solution containing daidzein, genistein, biochanin A, neobavaisoflavone and luteone. Conditions for the measurement: 37% ACN in water solution, standards at the final concentration of 100 ng/ml, flow rate 7 µl/min, AB Sciex 5500 Q-Trap, negative mode.

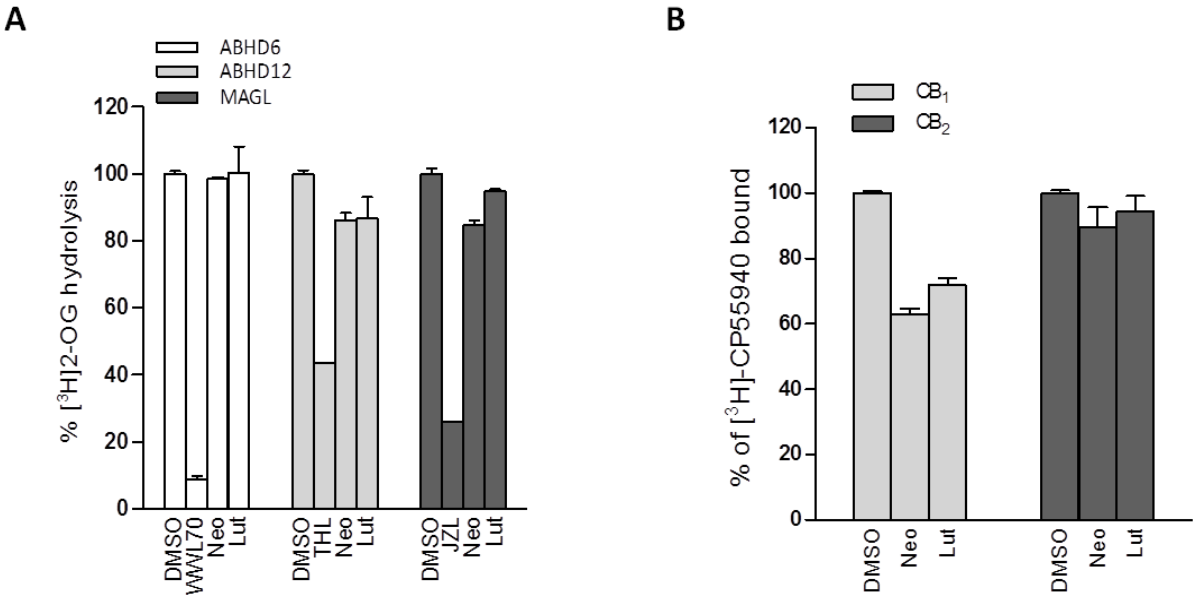

Supplementary Figure 7. ABHD6, ABHD12 and MAGL assay (A) and radioligand CB1 and CB2 receptors binding assay (B) for neobavaisoflavone and luteone. (A) MAGL assay was performed in U937, ABHDs assay in ABHD6 or ABHD12 transfected HEK923T cells. DMSO was used as negative control and WWL70, THL and JZL184 as positive controls for ABHD6, ABHD12 and MAGL inhibition, respectively. Results were expressed as percentage of [^{3}H]-2-OG hydrolysed compared to the vehicle control (=100%). (B) Radioligand binding assay was performed using 10 µg of CB_1/CB_2 receptors transfected CHO-K_1 cell membranes per sample. Results were expressed as percentage of [^{3}H]-CP55940 bound to the enzyme, compared to the vehicle control (=100%). DMSO was used as negative control. Both neobavaisoflavone and luteone (10 µM) did not show significant binding on both CB_1 and CB_2 receptors, neither significant inhibitory activity on MAGL and ABHD enzymes.

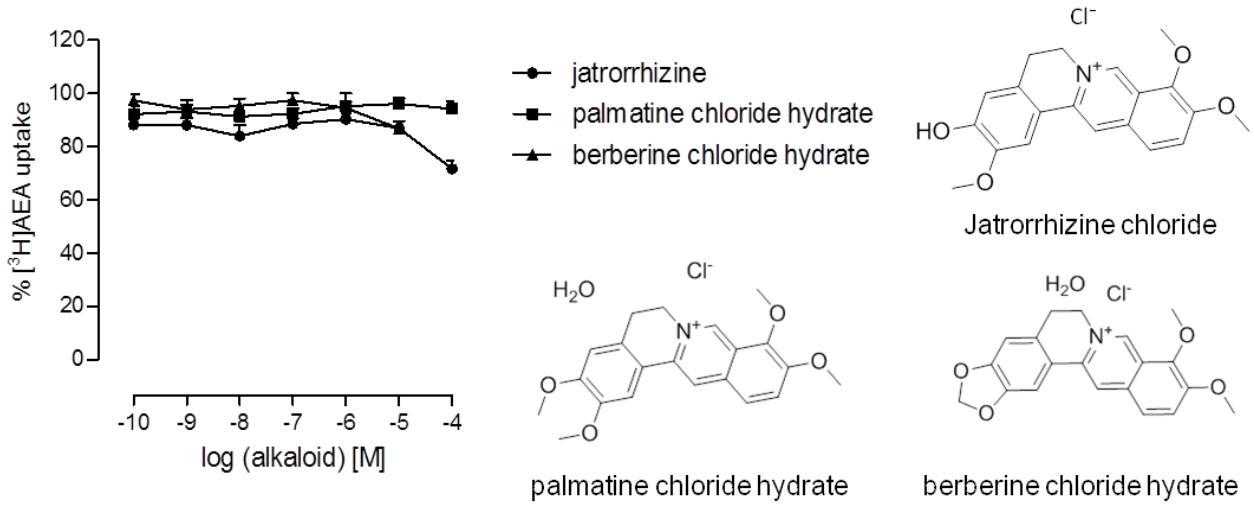

Supplementary Figure 8. AEA uptake inhibition assay of jatrorrhizine, palmatine and berberine in U937 cell homogenates. WOBE437 and RX055 1 µM were used as positive controls for AEA uptake inhibition and DMSO (vehicle) as negative control. The results are expressed as percentage of cellular [^{3}H]-AEA uptake, compared to the vehicle treated control (=100%). Shown are means ± SEM, from 3 independent experiments performed in triplicate (n=3, N=9).

Supplementary Table 1. PDB complexes considered for the docking protocol validation.

PDB	Method	Resolution	Type	Bound
2VYA	X-ray	2.75 Å	humanized	covalent
2WJ1	X-ray	1.84 Å	humanized	covalent
2WJ2	X-ray	2.55 Å	humanized	covalent
3K7F	X-ray	1.95 Å	humanized	covalent
3K83	X-ray	2.25 Å	humanized	covalent
3K84	X-ray	2.25 Å	humanized	covalent
3LJ6	X-ray	2.42 Å	humanized	covalent
3OJ8	X-ray	1.90 Å	humanized	covalent
3PPM	X-ray	1.78 Å	humanized	noncovalent
3PR0	X-ray	2.20 Å	humanized	covalent
3QJ9	X-ray	2.30 Å	rat	noncovalent
3QK5	X-ray	2.20 Å	rat	noncovalent
3QKV	X-ray	3.10 Å	rat	covalent
4HBP	X-ray	2.91 Å	rat	covalent
4J5P	X-ray	2.30 Å	humanized	covalent

Supplementary Table 2. Molecular weight and ion fragment $[M-H]^-$ of the isoflavonoid standards

Name	Molecular weight	$[M-H]^-$
7-Hydroxyisoflavone	238.2 g/mol	237 Da
Genistein	270.2 g/mol	269 Da
Daidzein	254.2 g/mol	253 Da
Barpisoflavone A	300.3 g/mol	299 Da
Biochanin A	284.3 g/mol	283 Da
Wighteone	338.4 g/mol	337 Da
Luteone	354.4 g/mol	353 Da
Isoangustone A	422.5 g/mol	421 Da
Lupiwighteone	338.4 g/mol	337 Da
Licoisoflavone A	354.4 g/mol	353 Da
Neobavaisoflavone	322.2 g/mol	321 Da
4',5,7-trihydroxy-6,8-diprenylisoflavone	406.5 g/mol	405 Da
Isolupialbigenin	406.5 g/mol	405 Da
8-Prenylluteone	422.5 g/mol	421 Da

Supplementary Table 3. Results of the FAAH screening for the plant extract of the *DMM* and Schwabe libraries in U937 cells.

Plant name	Part	FAAH inhibition (%)
	DMM library [a]	
Acanthus mollis	root/rhiz	36.0
Achillea ageratum	herb	25.6
Achillea millefolium	herb	28.7
Aconitum napellus	root/rhiz	58.0
Acorus calamus	root/rhiz	25.1
Adiantum capillus-veneris	herb	27.6
Aegilops neglecta	herb	13.6
Aeonium arboreum	leaf	55.3
Agrimonia eupatoria	herb	47.2
Agrimonia eupatoria	seed	18.8
Agrostemma githago	herb	0
Agrostemma githago	seed	2.1
Ajuga chamaepitys	**herb**	**82.0**
Alisma plantago	herb	36.2
Alisma plantago-aquatica	root/rhiz	24.4
Alkanna tinctoria	root/rhiz	42.4
Alkanna tinctoria	leaf	27.8

Allium ampeloprasum	seed	3.9
Allium ampeloprasum	leaf	52.9
Allium cepa	bulb	12.4
Allium sativum	leaf	29.4
Alliu sativum	bulb	55.3
Aloe vera	resin	11.7
Althaea officinalis	seed	39.1
Althaea officinalis	leaf	45.6
Althaea officinalis	root/rhiz	28.4
Ambrosia maritima	herb	28.2
Ammi visnaga	seed	20.8
Amomum subulatum	fruit	34.6
Anacyclus pyrethrum	root/rhiz	73.4
Anagallis arvensis	herb	62.6
Anagyris foetida	root/rhiz	72.3
Anagyris foetida	seed	32.7
Anagyris foetida	**leaf**	**84.8**
Anchusa azurea	seeds	0
Anchusa azurea	herb	55.0
Anchusa azurea	root/rhiz	56.2
Anemone coronaria	root/rhiz	31.8
Anethum graveolens	seed	28.8
Anethum graveolens	leaf	28.0
Antirrhinum majus	flower	24.5
Apium graveolens	leaf	36.1
Apium graveolens	root/rhiz	46.4
Apium graveolens	seeds	8.2
Aquilaria sp.	wood	59.3
Arctium lappa	leaf	20.8
Arctium lappa	root/rhiz	47.6
Arisarum vulgare	root/rhiz	56.4
Aristolochia rotunda	tuber	4.4
Artemisia absinthium	herb	19.2
Artemisia arborescens	herb	14.2
Artemisia arborescens	flower	34.3
Artemisia arborescens	herb	20.1
Artemisia herba	herb	0
Arum maculatum	leaf	42.2
Arum maculatum	seed	23.6
Arum maculatum	root/rhiz	8.3
Arundo donax	root/rhiz	38.2
Arundo donax	leaf	21.4
Arundo donax	leaf	3.0
Asarum europaeum	root/rhiz	31.5
Asparagus acutifolius	root/rhiz	45.5

Asparagus acutifolius	seeds	12.2
Asparagus sp.	stalk/shoot	60.3
Asphodelus ramosus	flower	36.0
Asphodelus ramosus	seed	5.3
Asphodelus ramosus	leaf	10.9
Asphodelus ramosus	root/rhiz	11.9
Asplenium ceterach	leaf	43.4
Asplenium sagittatum	leaf	14.6
Asplenium scolopendrium	leaf	38.2
Aster amellus	leaf	3.7
Astragalus gummifer	exudate	65.9
Athamanta cretensis	seed	49.3
Atriplex halimus	root/rhiz	37.7
Atriplex halimus	leaf	13.9
Atriplex hortensis	leaf	55.1
Atropa belladonna	root/rhiz	22.7
Avena sativa	seed	0
Ballota pseudodictamnus	herb	0
Ballota pseudodictamnus	root/rhiz	5.2
Berula erecta	leaf	35.7
Beta vulgaris	root/rhiz	0
Beta vulgaris	leaf	61.4
Bituminaria bituminosa	seeds	1.4
Bituminaria bituminosa	root/rhiz	49.1
Bituminaria bituminosa	leaf	45.7
Bongardia chrysogonum	root/rhiz	7.6
Boswellia sacra	exudate	6.8
Brassica oleracea	root/rhiz	34.2
Brassica oleracea	flower	8.7
Brassica oleracea	seeds	6.7
Brassica oleracea	leaf	54.4
Brassica rapa	herb	50.1
Brassica rapa	tuber	23.4
Brassica rapa	seeds	0.9
Bryonia cretica	stalk/shoot+leaf	0
Bryonia cretica	fruit+seed	0
Bryonia cretica	root/rhiz	14.7
Cachrys libanotis	root/rhiz	42.9
Cachrys libanotis	herb	47.5
Cachrys libanotis	seeds	53.0
Calystegia soldanella	herb	0
Cannabis sativa	leaf	54.4
Cannabis sativa	seed	7.1
Capparis spinosa	flower	36.2
Capparis spinosa	leaf	48.2

Capparis spinosa	root/rhiz	43.6
Capsella bursa	seed	2.2
Cardopatium corymbosum	roots	6.7
Carlina gummifera	root/rhiz	17.4
Carthamus lanatus	flowers	0
Carthamus lanatus	seed	55.9
Carthamus lanatus	leaf	21.2
Carthamus tinctorius	seed	12.4
Carum carvi	seed	36.9
Castanea sativa	seed	29.3
Castanea sativa	fruit	28.8
Celtis australis	fruit	10.8
Celtis australis	**wood**	**80.8**
Centaurium erythraea	herb	32.5
Ceratonia siliqua	fruit	29.1
Cerinthe major	leaf	11.4
Chelidonium majus	herb	38.9
Chelidonium majus	root/rhiz	42.1
Chondrilla juncea	root/rhiz	10.0
Cicer arietinum	seed	22.0
Cichorium intybus	leaf	41.3
Cichorium intybus	root/rhiz	0
Cinnamomum aromaticum	bark	72.8
Cinnamomum verum	bark	58.7
Cistus ladanifer	resin	30.3
Cistus salviifolius	flower	16.7
Citrullus colocynthis	fruit	6.6
Citrus medica	seed	0.6
Citrus medica	fruit	0
Clematis vitalba	root/rhiz	39.7
Clematis vitalba	seed	33.2
Clematis vitalba	stalk/shoot	0
Clinopodium nepeta	leaf	31.0
Clinopodium vulgare	herb	3.3
Colchicum autumnale	bulb	42.4
Commiphora gileadensis	wood	55.2
Commiphora gileadensis	exudate	39.8
Commiphora myrrha	exudate	33.6
Conium maculatum	seed	27.2
Conium maculatum	herb	67.4
Convolvulus arvensis	leaf	46.3
Convolvulus scammonia	latex	20.8
Convolvulus scammonia	root/rhiz	0
Coriandrum sativum	seed	25.9
Coriandrum sativum	leaf	48.5

Coris monspeliensis	root/rhiz	70.0
Cornus mas	leaf	33.8
Cornus mas	fruit	0
Coronilla scorpioides	herb	0
Corylus avellana	seed	12.9
Crataegus azarolus	fruit	16.3
Crataegus azarolus	fruit	49.4
Crithmum maritimum	leaf	24.1
Crithmum maritimum	seed	45.9
Crithmum maritimum	root/rhiz	28.4
Crocus sativus	stigma	22.3
Crocus sativus	bulb	7.7
Cucumis melo	fruit	5.5
Cucumis melo	seed	0
Cucumis melo	root/rhiz	28.3
Cucumis sativus	leaf	26.4
Cucumis sativus	seed	12.1
Cucumis sativus	fruit	53.6
Cuminum cyminum	seed	38.1
Cupressus sempervirens	fruit	27.0
Cupressus sempervirens	**leaf**	**85.8**
Cyclamen repandum	tuber	32.4
Cydonia oblonga	fruit	14.4
Cydonia oblonga	flower	9.4
Cynanchum acutum	leaf	13.5
Cynara scolytus	root/rhiz	41.6
Cynara scolytus	stalk/shoot	0
Cynodon dactylon	root/rhiz	61.4
Cyperus papyrus	herb	47.6
Cyperus rotundus	root/rhiz	30.7
Cytinus hypocistis	herb	11.9
Daphne gnidium	seed	12.6
Daphne gnidium	leaf	29.3
Daphne laureola	fruit	14.7
Daphne laureola	leaf	40.5
Daphne oleoides	leaf	30.9
Daucus carota	seed	55.5
Daucus carota	root/rhiz	35.0
Daucus carota	leaf	27.3
Diospyros ebenum	wood	6.1
Dipsacus fullonum	root/rhiz	43.7
Dittrichia viscosa	herb	63.3
Dittrichia viscosa	leaf	52.0
Dracunculus vulgaris	leaf	38.5
Dracunculus vulgaris	flower	16.3

Dracunculus vulgaris	seed	44.8
Dracunculus vulgaris	root/rhiz	17.4
Drimia maritima	bulb	58.5
Drimia maritima	seed	50.3
Dryopteris filix	root/rhiz	34.2
Dysphania botrys	herb	51.9
Ecballium elaterium	leaf	54.2
Ecballium elaterium	fruit	2.8
Ecballium elaterium	root/rhiz	27.3
Echinophora tenuifolia	flower	34.5
Echinophora tenuifolia	seed	17.1
Echium angustifolium	root/rhiz	0
Echium angustifolium	leaf	4.7
Echium italicum	leaf	0
Echium italicum	root/rhiz	9.9
Echium italicum	seed	0
Elettaria cardamomum	fruit	49.4
Ephedra distachya	fruit	38.3
Equisetum fluviatile	herb	48.3
Equisetum telmateia	herb	9.0
Equisetum telmateia	root/rhiz	0.4
Erica arborea	flower	5.0
Erica arborea	leaf	9.2
Eruca vesicaria	seed	8.2
Eruca vesicaria	leaf	29.3
Eryngium maritimum	leaf	0
Eryngium maritimum	root/rhiz	39.1
Euphorbia acanthothamnos	root/rhiz	3.8
Euphorbia acanthothamnos	herb	0
Euphorbia apios	root/rhiz	0
Euphorbia balsamifera	latex	16.1
Euphorbia lathyris	herb	39.4
Euphorbia paralias	root/rhiz	36.3
Euphorbia paralias	leaf	10.8
Euphorbia paralias	seeds	16.6
Euphorbia pithyusa	herb	0.1
Euphorbia pithyusa	root/rhiz	25.0
Fagus sylvatica	leaf	49.9
Fagus sylvatica	fruit	19.4
Fagus sylvatica	seed	0
Fagus sylvatica	bark	29.2
Ferula communis	seed	64.6
Ferula communis	stalk/shoot	37.6
Ferula gummosa	resin	52.4
Ferula persica	resin	75.3

Ferula tingitana	stalk	56.2
Ficaria verna	herb	27.5
Ficus carica	latex	0.0
Ficus carica	leaf	42.2
Ficus carica	fruit	18.5
Ficus sycomorus	fruit	42.0
Foeniculum vulgare	seed	31.7
Foeniculum vulgare	root/rhiz	59.4
Foeniculum vulgare	leaf	34.3
Fraxinus ornus	leaf	44.1
Fumaria officinalis	herb	25.4
Galium aparine	herb	68.8
Galium aparine	seed	9.5
Galium verum	flowers	35.0
Gentiana lutea	root/rhiz	31.1
Gladiolus italicus	bulb	66.8
Glaucium corniculatum	herb	23.5
Glaucium flavum	root/rhiz	33.3
Glaucium flavum	flower	13.9
Glaucium flavum	leaf	15.8
Glaucium flavum	seed	0.7
Glebionis coronaria	flower	29.4
Glebionis coronaria	stalk/shoot	6.4
Globularia alypum	seeds	40.8
Glycyrrhiza glabra	**roots**	**96.4**
Hedera helix	herb	43.5
Hedera helix	flower	35.9
Hedera helix	root	1.7
Hedera helix	leaf	46.3
Hedera helix	fruit	25.9
Heliotropium europaeum	seed	4.1
Heliotropium europaeum	herb	56.1
Helleborus lividus	shoots	35.2
Helosciadium nodiflorum	seeds	57.8
Helosciadium nodiflorum	leaf	38.8
Helosciadium nodiflorum	root/rhiz	21.3
Heracleum sphondylium	root/rhiz	55.1
Heracleum sphondylium	flower	47.3
Heracleum sphondylium	seeds	36.1
Hippuris vulgaris	herb	10.1
Hirschfeldia incana	herb	39.5
Hordeum vulgare	seed	43.3
Hyacinthus orientalis	bulb	30.8
Hyoscyamus albus	seeds	16.3
Hyoscyamus albus	root/rhiz	54.3

Hyoscyamus albus	herb	73.1
Hypecoum procumbens	herb	40.8
Hypericum perfoliatum	seed	0
Hypericum perfoliatum	herb	23.5
Hypericum perforatum	seed	25.8
Hyphaene thebaica	fruit	0
Hyssopus officinalis	herb	28.3
Inula helenium	root/rhiz	62.6
Inula helenium	leaf	37.4
Iris foetidissima	root/rhiz	0
Iris foetidissima	seed	52.4
Iris germanica	roots	21.3
Isatis tinctoria	leaf	32.5
Juglans regia	fruits	10.5
Juglans regia	seed	0
Juglans regia	oil	0
Juncus acutus	leaf	30.3
Juncus acutus	seeds	43.8
Juniperus excelsa	fruit	0.1
Juniperus excelsa	resin	3.8
Juniperus oxycedrus	bark	20.9
Juniperus oxycedrus	leaf	58.3
Juniperus oxycedrus	fruit	26.5
Junperus sabina	leaf	60.6
Lactuca sativa	seed	12.6
Lactuca sativa	leaf	15.8
Lactuca serriola	leaf	38.0
Lactuga sativa	leaf	0
Lagenaria siceraria	fruit	51.4
Lagoecia cuminoides	seed	19.8
Laurus nobilis	fruit	0
Laurus nobilis	root/rhiz	30.0
Laurus nobilis	leaf	54.5
Laurus nobilis	fruit	5.5
Lavandula stoechas	herb	17.6
Lawsonia inermis	leaf	46.3
Lemna minor	herb	60.6
Lens culinaris	seed	24.5
Leontice leontopetalum	root/rhiz	7.3
Leopoldia comosa	tuber	70.8
Lepidium sativum	seed	0
Lepidium sativum	herb	37.1
Lepidium sativum	leaf	40.3
Levisticum officinale	seed	26.5
Levisticum officinale	root/rhiz	44.1

Ligustrum vulgare	leaf	27.4
Lilium candidum	root/rhiz	11.7
Lilium candidum	leaf	0
Limonium vulgare	root/rhiz	44.8
Linum usitatissimum	seed	42.9
Lolium perenne	herb	7.7
Lonicera implexa	leaf	48.5
Lonicera implexa	seed	24.6
Lupinus albus	root/rhiz	48.7
Lupinus angustifolius	seed	28.5
Lupinus angustifolius	**root/rhiz**	**98.8**
Lysimachia vulgaris	**herb**	**87.4**
Malus domestica	fruit	37.4
Malva alcea	root/rhiz	16.3
Malva sylvestris	seed	39.5
Malva sylvestris	leaf	47.0
Malva sylvestris	root/rhiz	38.5
Mandragora officinarum	leaf	66.0
Mandragora officinarum	roots	64.0
Mandragora officinarum	fruit	9.3
Marrubium vulgare	leaf	59.4
Marrubium vulgare	seed	44.6
Matricaria chamomilla	flower	26.8
Matricaria chamomilla	herb	31.0
Matthiola incana	root/rhiz	53.5
Matthiola incana	herb	9.1
Matthiola incana	seed	0
Medicago arborea	**leaf**	**87.9**
Medicago sativa	seed	12.6
Melilotus officinalis	herb	26.9
Melilotus sulcatus	herb	2.4
Melissa officinalis	leaf	46.2
Mentha x piperita	herb	58.2
Mentha aquatica	seed	19.8
Mentha aquatica	herb	41.3
Mentha pulegium	herb	38.3
Mercurialis annua	herb	42.5
Mercurialis annua	seed	1.6
Mespilus germanica	fruit	34.9
Meum athamanticum	root/rhiz	46.7
Moringa oleifera	oil	23.7
Moringa oleifera	seed	23.8
Morus alba	fruit	17.4
Morus alba	latex	10.9
Morus alba	leaf	58.4

Morus alba	bark	22.6
Myriophyllum species	herb	21.2
Myrtus communis	leaf	29.6
Myrtus communis	fruit	20.9
Nasturtium officinale	leaf	54.7
Nelumbo nucifera	seed	40.9
Nelumbo nucifera	root/rhiz	0
Nerium oleander	leaf	32.0
Nerium oleander	flower	0
Nigella sativa	seeds	10.3
Nuphar lutea	root/rhiz	50.0
Nymphaea alba	root/rhiz	37.8
Ocimum basilicum	seed	0
Ocimum basilicum	leaf	32.4
Olea europaea	oil	16.1
Olea europaea	leaf	14.9
Olea europaea	fruit	43.8
Onobrychis caput	herb	0
Onopordum illyricum	leaf	2.3
Onopordum illyricum	root/rhiz	17.2
Opopanax chironium	root/rhiz	56.3
Opopanax chironium	seed	57.3
Origanum dictamnus	herb	25.6
Origanum dictamnus	root/rhiz	39.8
Origanum majorana	herb	34.0
Origanum vulgare	herb	10.3
Orobanche species	herb	24.7
Oryza sativa	seed	50.4
Osyris alba	herb	54.9
Otanthus maritimus	herb	29.7
Paeonia mascula	seeds	4.7
Paeonia mascula	root/rhiz	39.0
Paliurus spina-christi	leaf	21.6
Pancratium maritimum	seed	20.6
Panicum miliaceum	seeds	26.3
Papaver rhoeas	seed	0
Papaver rhoeas	leaf	32.9
Papaver rhoeas	fruit	32.9
Papaver somniferum	leaf	38.6
Papaver somniferum	latex	3.5
Papaver somniferum	fruit	17.1
Papaver somniferum	seeds	0
Parietaria judaica	herb	32.6
Pastinaca sativa	seed	44.2
Pastinaca sativa	root/rhiz	9.8

Pastinaca sativa	stalk/shoot	45.2
Peganum harmala	seed	3.5
Persicaria hydropiper	leaf	3.5
Petasites hybridus	herb	46.2
Petroselinum crispum	seed	37.1
Peucedanum officinale	root+resin	28.2
Phillyrea latifolia	leaf	18.3
Phoenix dactylifera	fruit	60.8
Phoenix dactylifera	flower	0
Phoenix dactylifera	leaf	25.2
Phragmites australis	root/rhiz	45.9
Phragmites australis	leaf	45.5
Physalis alkekengi	fruit	17.7
Physalis alkekengi	leaf	67.3
Pimpinella anisum	seeds	15.2
Pinus pinea	seed	6.3
Pinus pinea	bark	34.2
Pinus pinea	leaf	43.7
Piper nigrum	seeds	57.8
Pistacia lentiscus	exudate	25.7
Pistacia lentiscus	bark	30.4
Pistacia lentiscus	fruit	0
Pistacia lentiscus	root/rhiz	36.1
Pistacia lentiscus	herb	8.9
Pistacia lentiscus	leaf	39.2
Pistacia terebinthus	fruit	35.2
Pistacia terebinthus	resin	11.4
Pistacia terebinthus	leaf	43.3
Pistacia terebinthus	bark	32.3
Pistacia vera	seed	3.6
Pistia stratiotes	herb	59.9
Plantago afra	seeds	13.6
Plantago coronopus	root/rhiz	20.4
Plantago coronopus	herb	0
Plantago media	seed	34.0
Plantago media	root/rhiz	37.1
Plantago media	leaf	39.7
Platanus orientalis	leaf	25.3
Platanus orientalis	fruit	37.9
Platanus orientalis	bark	45.9
Polygala venulosa	herb	13.5
Polygonum aviculare	herb	44.0
Polypodium vulgare	root/rhiz	0
Polystichum lonchitis	leaf	48.9
Populus alba	leaf	29.4

Populus alba	bark	15.3
Populus nigra	leaf	63.7
Populus nigra	seeds	56.8
Portulaca oleracea	herb	44.6
Potamogeton natans	leaf	43.5
Potentilla reptans	root/rhiz	21.8
Potentilla reptans	herb	50.7
Poterium sanguisorba	leaf	61.4
Prunus armeniaca	fruit	0.7
Prunus avium	exudate	49.2
Prunus avium	fruit	17.2
Prunus domestica	exudate	45.4
Prunus domestica	fruit	39.8
Prunus domestica	leaf	33.6
Prunus dulcis	fruit	22.1
Prunus dulcis	root/rhiz	14.8
Prunus dulcis	exudate	22.9
Prunus dulcis	oil	23.7
Prunus dulcis	seeds	0
Prunus persica	fruit	46.1
Psoralea corylifolia	**fruits**	**92.5**
Pteridium aquilinum	root/rhiz	32.7
Pteridium aquilinum	leaf	6.8
Punica granatum	root/rhiz	43.5
Punica granatum	seed	0
Punica granatum	fruit	36.2
Punica granatum	flower	6.1
Pyrus communis	fruit	23.5
Quercus ilex	leaf	35.3
Quercus ilex	bark	39.8
Quercus ilex	seed+fruit	23.8
Quercus robur	leaf	25.8
Quercus robur	bark	26.1
Quercus robur	fruit	23.0
Quercus robur	seed	20.3
Raphanus raphanistrum	root/rhiz	46.9
Raphanus raphanistrum	seed	0
Reseda alba	seed	31.1
Rhamnus lycioides	herb	-3.2
Rheum rhaponticum	roots	25.0
Rhodiola rosea	roots	46.0
Rhus coriaria	leaf	44.5
Rhus coriaria	fruit	16.2
Ricinus communis	oil	0
Ricinus communis	leaf	56.3

Ricinus communis	seed	0
Ricinus communis	oil	0
Rosa canina	fruit	6.0
Rosa gallica	leaf	47.4
Rosa gallica	flower	38.3
Rubia peregrina	fruit	29.1
Rubia peregrina	roots	44.9
Rubia peregrina	herb	37.6
Rubus idaeus	flower	1.7
Rubus idaeus	leaf	26.1
Rubus idaeus	stalk/shoot	30.2
Rubus idaeus	fruit	0
Rubus plicatus	fruit	13.5
Rubus plicatus	stalk/shoot	0
Rubus plicatus	leaf	0
Rumex crispus	root/rhiz	76.6
Rumex crispus	seed	8.7
Rumex crispus	leaf	56.7
Ruscus aculeatus	fruit	37.0
Ruscus aculeatus	roots	51.1
Ruscus aculeatus	herb	69.2
Ruscus hypoglossum	root/rhiz	40.4
Ruscus hypoglossum	herb	52.2
Ruscus hypophyllum	leaf	67.0
Ruta chalepensis	herb	57.9
Ruta chalepensis	seed	21.7
Ruta graveolens	root/rhiz	52.4
Salix alba	bark	23.5
Salix alba	leaf	48.7
Salvia rosmarinus	herb	13.2
Salvia officinalis	leaf	19.6
Salvia viridis	seed	36.6
Salvia viridis	herb	7.3
Sambucus nigra	fruit	37.3
Sambucus nigra	leaf	18.6
Sambucus nigra	root/rhiz	11.7
Saponaria officinalis	root/rhiz	29.6
Sarcopoterium spinosum	seed	7.5
Sarcopoterium spinosum	leaf	26.8
Satureja thymbra	herb	47.6
Saussurea costus	root/rhiz	23.4
Scandix pecten-veneris	herb	31.7
Scirpoides holoschoenus	herb	2.5
Scirpoides holoschoenus	seed	25.9
Scrophularia peregrina	herb	52.0

Scrophularia peregrina	seed	21.7
Securigera securidaca	seed	1.5
Sedum cepaea	leaf	0
Senecio vulgaris	herb	34.8
Senegalia senegal	exudate	1.8
Serapias parviflora	tuber	11.4
Sesamum indicum	herb	34.5
Sesamum indicum	seeds	7.9
Sesamum indicum	oil	25.2
Seseli tortuosum	seeds	41.7
Seseli tortuosum	root/rhiz	38.8
Setaria italica	seeds	5.0
Silene vulgaris	seeds	2.0
Silybum marianum	stalk/shoot	18.2
Silybum marianum	root/rhiz	38.1
Sinapis alba	seeds	0
Sison amomum	seeds	17.2
Sisymbrium irio	seed	22.4
Sium sisarum	root/rhiz	53.9
Smilax aspera	fruit	44.8
Smilax aspera	leaf	37.5
Smyrnium olusatrum	root/rhiz	26.4
Smyrnium olusatrum	leaf	38.8
Smyrnium olusatrum	seeds	15.9
Smyrnium perfoliatum	leaf	15.7
Smyrnium perfoliatum	seed	33.9
Smyrnium perfoliatum	root/rhiz	35.6
Solanum americanum	leaf	56.4
Sonchus oleraceus	leaf	34.9
Sonchus oleraceus	root/rhiz	9.8
Sorbus domestica	fruit	0
Sparganium erectum	root/rhiz	57.0
Sparganium erectum	seed	42.9
Spartium junceum	flower	26.9
Spartium junceum	seed	8.5
Spartium junceum	herb	10.4
Staphisagria macrosperma	seeds	0.1
Streptopus amplexifolius	root/rhiz	18.3
Symphytum officinale	root/rhiz	34.3
Tamarix africana	herb	42.8
Tamarix species	fruit	20.4
Tamarix species	bark	31.7
Tanacetum parthenium	herb	1.2
Tanacetum parthenium	flowers	14.5
Taxus baccata	herb	0

Teucrium chamaedrys	herb	65.8
Teucrium flavum	herb	16.1
Teucrium polium	herb	6.4
Teucrium scordium	herb	27.1
Thalictrum minus	leaf	17.8
Thapsia garganica	root/rhiz	69.5
Thapsia garganica	herb	37.3
Thymbra capitata	herb	36.7
Thymus serpyllum	herb	27.4
Tordylium apulum	root/rhiz	57.2
Tordylium apulum	seed	16.9
Tordylium apulum	herb	40.2
Trapa natans	herb	49.2
Trapa natans	fruit	34.7
Tribulus terrestris	fruit	14.4
Tribulus terrestris	herb	45.9
Trigonella foenum-graecum	seed	3.7
Triticum aestivum	seed	38.1
Triticum dicoccon	seed	47.1
Tussilago farfara	root/rhiz	37.4
Tussilago farfara	leaf	46.0
Typha angustifolia	seed	34.3
Ulmus minor	root/rhiz	10.6
Ulmus minor	bark	17.2
Ulmus minor	leaf	4.9
Umbilicus rupestris	leaf	0
Urtica dioica	seed	56.2
Urtica dioica	herb	25.7
Valeriana celtica	root/rhiz+stalk	33.9
Valeriana jatamansi	root/rhiz	4.7
Valeriana officinalis	root/rhiz	44.2
Veratrum album	root/rhiz	46.7
Verbascum thapsus	leaf	22.4
Verbascum thapsus	root/rhiz	0
Verbena officinalis	root/rhiz	23.2
Verbena officinalis	leaf+herb	10.0
Vicia cracca	seed	31.3
Vicia ervilia	seed	7.3
Vicia faba	seed	19.0
Vinca minor	herb	31.1
Vincetoxicum hirundinaria	leaf	60.0
Vincetoxicum hirundinaria	root/rhiz	24.4
Viola odorata	leaf	55.8
Vitex agnus-castus	seeds	26.8
Vitex agnus-castus	leaf	43.4

Vitis vinifera	seed	0
Vitis vinifera	leaf	43.8
Vitis vinifera	fruit	6.9
Withania somnifera	root/rhiz	49.8
Withania somnifera	seeds+fruit	11.0
Xanthium strumarium	fruit	3.4
Zingiber officinale	**root/rhiz**	**87.6**
Zingiber officinale	leaf	37.9
Ziziphus jujuba	leaf	39.9
Ziziphus jujuba	root/rhiz	32.2
Ziziphus jujuba	fruit	33.8
	Schwabe library [b]	
Acanthopanax senticosus	bark	6.4
Achillea millefolium	-	3.5
Aesculus hippocastanum	leaves	0.0
Aframomum melegueta	fruits	61.4
Albizia julibrissin	bark	0.0
Amomum villosum	fruits	0.0
Anemarrhena asphodeloides	roots	0.0
Anethum graveolens	herb	0.0
Angelica archangelica	roots	6.4
Angelica archangelica	herb	9.2
Angelica dahurica	roots	0.0
Arctostaphylos uva-ursi	leaves	6.8
Artemisia scoparia	herb	32.1
Asclepias tuberosa	root/rhiz	12.2
Asparagus officinalis	rhiz	23.3
Asparagus racemosus	roots	0.0
Atractylodes lancea	rhiz	0.0
Atractylodes macrocephala	rhiz	3.2
Belamcanda chinensis	herb	0.0
Berberis vulgaris	herb	3.1
Betula pubescens	leaves	12.5
Borago officinalis	tot?	5.5
Capsicum annuum	fruits	21.3
Carex arenaria	rhiz	21.1
Cassia angustifolia	fruits	0.0
Castanea sativa	leaves	0.0
Chamomilla recutita	flowers	26.0
Citrullus colocynthis	fruits	5.2
Convallaria majalis	leaves	2.5
Curcuma longa	rhiz	48.8
Curcuma zanthorrhiza	rhiz	12.7
Cymbopogon citratus	-	2.3
Cymbopogon flexuosus	-	0.0

Cytisus scoparius	herb	62.7
Echinacea pallida	roots	52.6
Evodia ruticarpa	fruits	0.0
Fragaria vesca	leaves	0.0
Galeopsis segetum	herb	1.4
Glycyrrhiza uralensis	**roots**	**82.2**
***Glycyrrhiza uralensis* (10 µg·ml^{-1})**	**roots**	**98.3**
Guaiacum sanctum	bark	21.2
Hyoscyamus niger	leaves	40.0
Hypericum perforatum	herb	0.0
Illicium verum	fruits	6.4
Iris pallida	rhiz	0.0
Juncus effusus	medulla	7.3
Lamium album	herb	6.0
Levisticum officinale	roots	6.5
Lonicera japonica	flowers	5.4
Magnolia biondii	flowers	4.8
Marrubium vulgare	herb	7.5
Marrubium vulgare	herb	32.8
Mentha piperita	herb	11.8
Menyanthes trifoliata	leaves	16.3
Morus nigra	fruits	38.5
Paeonia lactiflora	root	0.0
Panax notoginseng	root/rhiz	0.0
Petroselinum crispum	herb	2.8
Phellodendron chinense	bark	0.0
Picea abies	-	0.0
Pimpinella major	roots	0.0
Pimpinella major	herb	8.6
Pinus sylvestris	-	0.0
Pinus sylvestris	-	0.0
Piper cubeba	-	2.5
Piper nigrum	seeds	1.9
Piper nigrum	seeds	4.0
Piper retrofractum	seeds	45.5
Plantago lanceolata	leaves	0.0
Podophyllum peltatum	rhiz	8.9
Potentilla anserina	herb	9.6
Primula veris	flowers	0.0
Primula veris	roots	0.0
Ptychopetalum olacoides	bark	10.7
Rehmannia glutinosa	roots	61.0
Rhododendron ferrugineum	leaves	0.0
Salvia miltiorrhiza	root/rhiz	65.9
Salvia officinalis	leaves	0.0

Santalum album	bark	25.8
Schisandra chinensis	fruits	1.3
Serenoa repens	fruits	3.1
Solidago virgaurea	herb	0.0
Sophora flavescens	roots	9.8
Sophora japonica	flowers	0.0
Stachys officinalis	herb	0.0
Symphytum officinale	herb	23.1
Taraxacum mongolicum	herb	0.0
Tilia cordata	flowers	7.6
Tilia tomentosa	flowers	0.0
Tussilago farfara	leaves	0.0
Urtica dioica	herb	39.7
Verbena officinalis	herb	32.1
Withania somnifera	roots	2.0
Xanthium sibiricum	fruits	0.0
Zingiber officinale	rhiz	59.7

[a]All the ethyl acetate extracts were screened for FAAH inhibition at the concentration of 10 μg·ml^{-1}.

[b]All the ethyl acetate extracts were screened for FAAH inhibition at the concentration of 5 μg·ml^{-1}, if not differently specified.

Highlighted are the eleven most active extracts, in red the extracts belonging to the Fabaceae family.

Supplementary Table 4. Results of the radioligand CB_2 receptors screening for the plant extracts of the *DMM* library in *h*CB_2 transfected CHO cells at 10 μg·ml^{-1} and of the cytotoxicity screening in HeLa cells at 25 μg·ml^{-1}.

Plant name	Part	Cell mortality (%)	CB_2 binding (%)
Acanthus mollis	root/rhiz	25.2	0.0
Achillea ageratum	herb	16.0	22.3
Achillea millefolium	herb	**77.3**	47.9
Aconitum napellus	root/rhiz	8.1	0.0
Acorus calamus	root/rhiz	18.0	9.6
Adiantum capillus-veneris	herb	47.6	9.5
Aegilops neglecta	herb	71.9	3.0
Aeonium arboreum	leaf	16.8	0.0
Agrimonia eupatoria	herb	7.2	0.0
Agrimonia eupatoria	seed	21.9	0.2
Agrostemma githago	herb	18.3	10.9
Agrostemma githago	seed	56.1	11.6
Ajuga chamaepitys	herb	12.5	22.2
Alisma plantago	herb	25.1	0.0
Alisma plantago-aquatica	root/rhiz	32.6	20.8
Alkanna tinctoria	root/rhiz	25.8	5.8
Alkanna tinctoria	leaf	**92.3**	16.0
Allium ampeloprasum	seed	14.7	13.6
Allium ampeloprasum	leaf	12.9	20.5

Allium cepa	bulb	36.7	0.0
Allium sativum	leaf	47.5	6.9
Allium sativum	bulb	4.6	6.9
Aloe vera	resin	12.0	5.7
Althaea officinalis	seed	18.7	7.2
Althaea officinalis	leaf	20.3	14.0
Althaea officinalis	root/rhiz	14.2	0.0
Ambrosia maritima	herb	67.3	0.0
Ammi visnaga	seed	24.3	17.8
Amomum subulatum	fruit	8.4	21.9
Anacyclus pyrethrum	root/rhiz	27.4	8.9
Anagallis arvensis	herb	55.2	0.0
Anagyris foetida	root/rhiz	10.4	0.0
Anagyris foetida	seed	**91.1**	37.2
Anagyris foetida	leaf	22.6	0.0
Anchusa azurea	seeds	15.0	23.6
Anchusa azurea	herb	18.1	0.0
Anchusa azurea	root/rhiz	42.3	0.0
Anemone coronaria	root/rhiz	23.9	13.1
Anethum graveolens	seed	73.0	0.0
Anethum graveolens	leaf	22.8	8.4
Antirrhinum majus	flower	68.6	0.0
Apium graveolens	leaf	26.1	0.0
Apium graveolens	root/rhiz	20.9	5.3
Apium graveolens	seeds	14.7	0.0
Aquilaria sp.	wood	**88.4**	28.6
Arctium lappa	leaf	11.2	0.0
Arctium lappa	root/rhiz	64.4	3.0
Arisarum vulgare	root/rhiz	**81.5**	0.0
Aristolochia rotunda	tuber	38.4	8.1
Artemisia absinthium	herb	27.7	0.0
Artemisia arborescens	herb	17.0	0.0
Artemisia arborescens	flower	0	0.0
Artemisia arborescens	herb	71.3	0.0
Artemisia herba	herb	18.6	20.6
Arum maculatum	leaf	43.8	0.0
Arum maculatum	seed	34.3	0.0
Arum maculatum	root/rhiz	20.7	0.0
Arundo donax	root/rhiz	23.0	0.0
Arundo donax	leaf	43.9	0.0
Arundo donax	leaf	16.4	3.9
Asarum europaeum	root/rhiz	29.4	0.0
Asparagus acutifolius	root/rhiz	14.4	0.0
Asparagus acutifolius	seeds	13.1	0.0
Asparagus sp.	stalk/shoot	32.0	6.9

Asphodelus ramosus	flower	16.9	0.0
Asphodelus ramosus	seed	0	0.0
Asphodelus ramosus	leaf	32.1	7.5
Asphodelus ramosus	root/rhiz	24.0	0.0
Asplenium ceterach	leaf	13.2	0.0
Asplenium sagittatum	leaf	30.2	5.2
Asplenium scolopendrium	leaf	14.4	21.4
Aster amellus	leaf	24.3	4.8
Astragalus gummifer	exudate	25.3	9.7
Athamanta cretensis	seed	18.6	33.9
Atriplex halimus	root/rhiz	25.0	0.0
Atriplex halimus	leaf	19.2	0.0
Atriplex hortensis	leaf	50.0	11.3
Atropa belladonna	root/rhiz	25.0	0.0
Avena sativa	seed	21.4	12.6
Ballota pseudodictamnus	herb	24.0	0.0
Ballota pseudodictamnus	root/rhiz	0	0.0
Berula erecta	leaf	30.1	0.0
Beta vulgaris	root/rhiz	14.4	0.0
Beta vulgaris	leaf	30.1	0.0
Bituminaria bituminosa	seeds	17.9	0.0
Bituminaria bituminosa	root/rhiz	17.9	6.6
Bituminaria bituminosa	leaf	59.8	0.0
Bongardia chrysogonum	root/rhiz	22.5	0.0
Boswellia sacra	exudate	4.4	9.5
Brassica oleracea	root/rhiz	24.1	0.0
Brassica oleracea	flower	65.2	0.0
Brassica oleracea	seeds	34.7	1.1
Brassica oleracea	leaf	30.2	0.0
Brassica rapa	herb	20.8	0.0
Brassica rapa	tuber	55.6	0.0
Brassica rapa	seeds	10.8	0.0
Bryonia cretica	stalk/shoot+leaf	8.4	0.0
Bryonia cretica	fruit+seed	0	0.0
Bryonia cretica	root/rhiz	68.6	0.0
Cachrys libanotis	root/rhiz	24.9	36.2
Cachrys libanotis	herb	24.2	36.9
Cachrys libanotis	seeds	34.7	0.0
Calystegia soldanella	herb	62.5	0.0
Cannabis sativa	leaf	**76.3**	0.0
Cannabis sativa	seed	**76.2**	43.0
Capparis spinosa	flower	28.8	11.2
Capparis spinosa	leaf	36.4	0.0
Capparis spinosa	root/rhiz	20.0	0.0
Capsella bursa	seed	21.5	4.8

Cardopatium corymbosum	roots	0	31.7
Carlina gummifera	root/rhiz	2.1	10.2
Carthamus lanatus	flowers	9.3	0.0
Carthamus lanatus	seed	15.8	0.0
Carthamus lanatus	leaf	0.3	0.9
Carthamus tinctorius	seed	8.4	1.5
Carum carvi	seed	23.4	24.6
Castanea sativa	seed	22.2	0.0
Castanea sativa	fruit	27.2	0.0
Celtis australis	fruit	33.5	0.0
Celtis australis	wood	15.6	4.6
Centaurium erythraea	herb	15.1	0.0
Ceratonia siliqua	fruit	15.8	1.6
Cerinthe major	leaf	20.0	0.0
Chelidonium majus	herb	82.5	0.0
Chelidonium majus	root/rhiz	77.6	0.0
Chondrilla juncea	root/rhiz	0	17.8
Cicer arietinum	seed	8.9	13.8
Cichorium intybus	leaf	55.6	0.0
Cichorium intybus	root/rhiz	21.6	1.0
Cinnamomum aromaticum	bark	30.6	4.1
Cinnamomum verum	bark	17.8	0.0
Cistus ladanifer	resin	20.0	0.0
Cistus salviifolius	flower	18.8	3.8
Citrullus colocynthis	fruit	32.1	0.0
Citrus medica	seed	29.5	0.0
Citrus medica	fruit	19.7	1.4
Clematis vitalba	root/rhiz	44.5	0.0
Clematis vitalba	seed	34.7	11.8
Clematis vitalba	stalk/shoot	27.4	11.8
Clinopodium nepeta	leaf	16.4	7.1
Clinopodium vulgare	herb	17.3	0.0
Colchicum autumnale	bulb	**83.5**	1.4
Commiphora gileadensis	wood	33.6	4.3
Commiphora gileadensis	exudate	21.9	0.0
Commiphora myrrha	exudate	**86.0**	0.0
Conium maculatum	seed	5.8	12.6
Conium maculatum	herb	38.7	0.0
Convolvulus arvensis	leaf	48.0	10.3
Convolvulus scammonia	latex	21.2	3.4
Convolvulus scammonia	root/rhiz	96.9	7.1
Coriandrum sativum	seed	14.7	15.4
Coriandrum sativum	leaf	16.7	28.5
Coris monspeliensis	root/rhiz	56.8	0.0
Cornus mas	leaf	24.5	6.1

Cornus mas	fruit	39.9	7.6
Coronilla scorpioides	herb	24.5	0.0
Corylus avellana	seed	16.7	0.2
Crataegus azarolus	fruit	33.4	5.6
Crataegus azarolus	fruit	27.5	6.7
Crithmum maritimum	leaf	10.0	0.0
Crithmum maritimum	seed	30.5	11.3
Crithmum maritimum	root/rhiz	17.8	18.9
Crocus sativus	stigma	3.3	0.8
Crocus sativus	bulb	11.5	16.3
Cucumis melo	fruit	**87.1**	0.0
Cucumis melo	seed	20.5	0.0
Cucumis melo	root/rhiz	23.0	3.6
Cucumis sativus	leaf	14.9	0.0
Cucumis sativus	seed	17.5	0.0
Cucumis sativus	fruit	35.1	0.0
Cuminum cyminum	seed	33.9	17.1
Cupressus sempervirens	fruit	30.2	0.0
Cupressus sempervirens	leaf	19.4	21.8
Cyclamen repandum	tuber	13.9	31.6
Cydonia oblonga	fruit	7.9	0.0
Cydonia oblonga	flower	39.2	6.1
Cynanchum acutum	leaf	0	2.8
Cynara scolytus	root/rhiz	34.6	0.0
Cynara scolytus	stalk/shoot	27.9	4.8
Cynodon dactylon	root/rhiz	30.2	21.7
Cyperus papyrus	herb	10.5	28.7
Cyperus rotundus	root/rhiz	37.7	34.0
Cytinus hypocistis	herb	38.1	1.4
Daphne gnidium	seed	21.9	0.0
Daphne gnidium	leaf	19.9	0.0
Daphne laureola	fruit	25.6	0.7
Daphne laureola	leaf	33.3	17.2
Daphne oleoides	leaf	**76.1**	10.2
Daucus carota	seed	36.4	0.0
Daucus carota	root/rhiz	16.9	0.0
Daucus carota	leaf	32.4	14.6
Diospyros ebenum	wood	40.6	2.1
Dipsacus fullonum	root/rhiz	30.2	4.3
Dittrichia viscosa	herb	31.9	0.0
Dittrichia viscosa	leaf	38.1	2.3
Dracunculus vulgaris	leaf	13.5	0.0
Dracunculus vulgaris	flower	24.9	7.4
Dracunculus vulgaris	seed	24.8	12.4
Dracunculus vulgaris	root/rhiz	9.4	16.2

Drimia maritima	bulb	**82.1**	13.9
Drimia maritima	seed	**79.3**	21.0
Dryopteris filix	root/rhiz	57.4	1.8
Dysphania botrys	herb	**79.0**	0.8
Ecballium elaterium	leaf	31.7	7.8
Ecballium elaterium	fruit	69.2	0.0
Ecballium elaterium	root/rhiz	70.0	0.0
Echinophora tenuifolia	flower	19.7	17.7
Echinophora tenuifolia	seed	27.8	29.6
Echium angustifolium	root/rhiz	29.0	0.0
Echium angustifolium	leaf	26.0	0.0
Echium italicum	leaf	13.1	0.0
Echium italicum	root/rhiz	16.7	0.0
Echium italicum	seed	23.8	8.7
Elettaria cardamomum	fruit	30.9	8.6
Ephedra distachya	fruit	24.6	0.0
Equisetum fluviatile	herb	34.8	1.3
Equisetum telmateia	herb	0	0.0
Equisetum telmateia	root/rhiz	31.2	7.3
Erica arborea	flower	0.4	0.0
Erica arborea	leaf	4.0	35.5
Eruca vesicaria	seed	57.7	11.3
Eruca vesicaria	leaf	0	24.0
Eryngium maritimum	leaf	24.5	3.8
Eryngium maritimum	root/rhiz	37.4	0.0
Euphorbia acanthothamnos	root/rhiz	10.5	3.6
Euphorbia acanthothamnos	herb	27.6	7.5
Euphorbia apios	root/rhiz	**97.4**	0.0
Euphorbia balsamifera	latex	**80.3**	0.0
Euphorbia lathyris	herb	20.0	14.6
Euphorbia paralias	root/rhiz	15.8	41.1
Euphorbia paralias	leaf	0.6	0.0
Euphorbia paralias	seeds	13.2	0.0
Euphorbia pithyusa	herb	27.1	0.0
Euphorbia pithyusa	root/rhiz	18.9	6.2
Fagus sylvatica	leaf	5.5	0.0
Fagus sylvatica	fruit	15.0	2.1
Fagus sylvatica	seed	28.6	6.3
Fagus sylvatica	bark	74.5	9.0
Ferula communis	seed	38.7	5.6
Ferula communis	stalk/shoot	22.7	19.3
Ferula gummosa	**resin**	**83.6**	**84.8**
Ferula persica	**resin**	31.8	**82**
Ferula tingitana	stalk	**85.6**	22.7
Ficaria verna	herb	39.4	0.0

Ficus carica	latex	39.0	3.4
Ficus carica	leaf	11.4	8.6
Ficus carica	fruit	20.2	0.0
Ficus sycomorus	fruit	18.2	0.0
Foeniculum vulgare	seed	40.3	11.4
Foeniculum vulgare	root/rhiz	17.0	13.9
Foeniculum vulgare	leaf	16.7	17.3
Fraxinus ornus	leaf	21.9	6.2
Fumaria officinalis	herb	13.3	0.0
Galium aparine	herb	13.5	0.0
Galium aparine	seed	40.1	14.2
Galium verum	flowers	15.8	0.0
Gentiana lutea	root/rhiz	16.8	14.2
Gladiolus italicus	bulb	13.0	0.0
Glaucium corniculatum	herb	29.9	7.1
Glaucium flavum	root/rhiz	8.0	0.0
Glaucium flavum	flower	61.3	0.0
Glaucium flavum	leaf	25.8	0.0
Glaucium flavum	seed	37.5	5.0
Glebionis coronaria	flower	23.0	0.0
Glebionis coronaria	stalk/shoot	22.8	22.0
Globularia alypum	seeds	23.8	6.1
Glycyrrhiza glabra	roots	**85.5**	6.3
Hedera helix	herb	18.6	0.0
Hedera helix	flower	17.4	0.5
Hedera helix	root	20.0	2.3
Hedera helix	leaf	18.8	0.0
Hedera helix	fruit	16.2	0.0
Heliotropium europaeum	seed	37.1	8.8
Heliotropium europaeum	herb	20.0	10.8
Helleborus lividus	shoots	**78.6**	6.3
Helosciadium nodiflorum	seeds	41.6	0.0
Helosciadium nodiflorum	leaf	44.2	15.0
Helosciadium nodiflorum	root/rhiz	29.4	0.0
Heracleum sphondylium	root/rhiz	11.7	0.0
Heracleum sphondylium	flower	46.4	13.3
Heracleum sphondylium	seeds	34.3	0.0
Hippuris vulgaris	herb	29.2	6.8
Hirschfeldia incana	herb	16.6	21.8
Hordeum vulgare	seed	13.7	7.6
Hyacinthus orientalis	bulb	32.9	0.0
Hyoscyamus albus	seeds	14.7	0.0
Hyoscyamus albus	root/rhiz	46.3	0.0
Hyoscyamus albus	herb	49.7	0.0
Hypecoum procumbens	herb	33.4	0.0

Hypericum perfoliatum	seed	24.4	0.0
Hypericum perfoliatum	herb	**89.1**	34.9
Hypericum perforatum	seed	49.8	9.4
Hyphaene thebaica	fruit	**89.7**	0.0
Hyssopus officinalis	herb	20.4	0.0
Inula helenium	root/rhiz	**86.0**	0.0
Inula helenium	leaf	**88.4**	28.0
Iris foetidissima	root/rhiz	54.0	0.0
Iris foetidissima	seed	73.8	4.5
Iris germanica	roots	2.1	0.0
Isatis tinctoria	leaf	34.7	0.0
Juglans regia	fruits	7.1	2.9
Juglans regia	seed	24.1	21.0
Juglans regia	oil	**76.9**	30.8
Juncus acutus	leaf	48.8	0.0
Juncus acutus	seeds	**77.4**	0.0
Juniperus excelsa	fruit	52.0	42.2
Juniperus excelsa	resin	**80.2**	0.0
Juniperus oxycedrus	bark	31.7	22.6
Juniperus oxycedrus	leaf	**80.8**	24.2
Juniperus oxycedrus	fruit	**83.7**	53.9
Junperus sabina	leaf	**86.7**	23.9
Lactuca sativa	seed	11.8	6.1
Lactuca sativa	leaf	23.3	0.0
Lactuca serriola	leaf	15.6	0.0
Lactuga sativa	leaf	34.1	25.2
Lagenaria siceraria	fruit	37.6	0.0
Lagoecia cuminoides	seed	18.7	0.0
Laurus nobilis	fruit	48.6	0.0
Laurus nobilis	root/rhiz	**83.2**	19.0
Laurus nobilis	leaf	12.4	36.0
Laurus nobilis	fruit	60.7	0.0
Lavandula stoechas	herb	21.1	18.5
Lawsonia inermis	leaf	68.5	3.5
Lemna minor	herb	22.2	10.3
Lens culinaris	seed	18.8	14.4
Leontice leontopetalum	root/rhiz	28.5	0.0
Leopoldia comosa	tuber	36.8	6.9
Lepidium sativum	seed	19.2	5.1
Lepidium sativum	herb	73.1	0.0
Lepidium sativum	leaf	30.9	0.9
Levisticum officinale	seed	12.9	5.7
Levisticum officinale	root/rhiz	29.6	17.0
Ligustrum vulgare	leaf	13.9	40.9
Lilium candidum	root/rhiz	13.9	0.0

Lilium candidum	leaf	36.1	2.4
Limonium vulgare	root/rhiz	15.4	42.8
Linum usitatissimum	seed	7.6	0.0
Lolium perenne	herb	13.6	0.0
Loniceraimplexa	leaf	28.5	0.0
Lonicera implexa	seed	39.3	8.3
Lupinus albus	root/rhiz	26.9	0.0
Lupinus angustifolius	seed	10.3	0.0
Lupinus angustifolius	root/rhiz	18.1	5.4
Lysimachia vulgaris	herb	20.2	10.8
Malus domestica	fruit	20.1	5.1
Malva alcea	root/rhiz	16.5	12.2
Malva sylvestris	seed	11.7	0.0
Malva sylvestris	leaf	29.0	8.0
Malva sylvestris	root/rhiz	12.5	36.6
Mandragora officinarum	leaf	14.8	16.8
Mandragora officinarum	roots	8.9	0.0
Mandragora officinarum	fruit	16.7	0.0
Marrubium vulgare	leaf	66.2	6.7
Marrubium vulgare	seed	20.6	8.5
Matricaria chamomilla	flower	12.1	0.0
Matricaria chamomilla	herb	2.7	11.6
Matthiola incana	root/rhiz	4.3	0.0
Matthiola incana	herb	21.5	12.4
Matthiola incana	seed	41.3	16.8
Medicago arborea	leaf	28.9	10.7
Medicago sativa	seed	6.1	41.5
Melilotus officinalis	herb	19.0	0.0
Melilotus sulcatus	herb	20.8	0.0
Melissa officinalis	leaf	24.1	0.0
Mentha x piperita	herb	43.3	0.0
Mentha aquatica	seed	28.8	0.1
Mentha aquatica	herb	76.9	0.0
Mentha pulegium	herb	22.8	0.0
Mercurialis annua	herb	17.6	0.0
Mercurialis annua	seed	27.5	0.0
Mespilus germanica	fruit	**75.4**	5.9
Meum athamanticum	root/rhiz	**76.3**	24.2
Moringa oleifera	oil	11.4	4.1
Moringa oleifera	seed	6.6	5.5
Morus alba	fruit	5.4	1.5
Morus alba	latex	12.8	3.2
Morus alba	leaf	23.4	0.0
Morus alba	bark	9.5	0.0
Myriophyllum species	herb	65.0	0.0

Myrtus communis	leaf	25.8	1.3
Myrtus communis	fruit	28.9	19.8
Nasturtium officinale	leaf	14.6	9.0
Nelumbo nucifera	seed	20.8	0.0
Nelumbo nucifera	root/rhiz	20.6	6.4
Nerium oleander	leaf	27.7	0.0
Nerium oleander	flower	70.1	7.9
Nigella sativa	seeds	12.5	0.0
Nuphar lutea	root/rhiz	13.1	13.9
Nymphaea alba	root/rhiz	9.5	5.6
Ocimum basilicum	seed	15.9	0.0
Ocimum basilicum	leaf	33.1	0.0
Olea europaea	oil	22.2	0.0
Olea europaea	leaf	8.9	2.0
Olea europaea	fruit	7.2	0.0
Onobrychis caput	herb	10.3	0.0
Onopordum illyricum	leaf	10.3	0.0
Onopordum illyricum	root/rhiz	63.6	5.2
Opopanax chironium	root/rhiz	25.1	12.5
Opopanax chironium	seed	48.5	26.2
Origanum dictamnus	herb	73.5	19.1
Origanum dictamnus	root/rhiz	18.1	39.8
Origanum majorana	herb	**84.2**	0.0
Origanum vulgare	herb	17.9	0.0
Orobanche species	herb	10.8	0.0
Oryza sativa	seed	1.9	8.8
Osyris alba	herb	37.4	6.1
Otanthus maritimus	herb	**83.7**	0.7
Paeonia mascula	seeds	19.9	0.7
Paeonia mascula	root/rhiz	16.0	4.1
Paliurus spina-christi	leaf	27.8	12.4
Pancratium maritimum	seed	29.3	0.0
Panicum miliaceum	seeds	7.6	0.0
Papaver rhoeas	seed	40.1	0.0
Papaver rhoeas	leaf	33.9	0.0
Papaver rhoeas	fruit	29.6	0.0
Papaver somniferum	leaf	33.1	0.0
Papaver somniferum	latex	29.1	0.0
Papaver somniferum	fruit	28.9	0.0
Papaver somniferum	seeds	12.9	0.0
Parietaria judaica	herb	32.8	0.0
Pastinaca sativa	seed	28.5	0.0
Pastinaca sativa	root/rhiz	6.5	0.0
Pastinaca sativa	stalk/shoot	24.2	0.0
Peganum harmala	seed	22.1	4.5

Persicaria hydropiper	leaf	47.1	0.0
Petasites hybridus	herb	**88.6**	11.2
Petroselinum crispum	seed	15.7	0.6
Peucedanum officinale	root+resin	30.2	0.0
Phillyrea latifolia	leaf	**77.6**	0.0
Phoenix dactylifera	fruit	25.1	2.6
Phoenix dactylifera	flower	18.4	7.6
Phoenix dactylifera	leaf	52.7	11.8
Phragmites australis	root/rhiz	4.7	3.7
Phragmites australis	leaf	42.8	12.8
Physalis alkekengi	fruit	72.6	4.8
Physalis alkekengi	leaf	9.3	12.0
Pimpinella anisum	seeds	14.6	0.0
Pinus pinea	seed	15.6	15.5
Pinus pinea	bark	12.3	21.7
Pinus pinea	leaf	41.0	0.0
Piper nigrum	seeds	37.7	0.0
Pistacia lentiscus	exudate	**86.3**	0.0
Pistacia lentiscus	bark	26.7	0.7
Pistacia lentiscus	fruit	1.5	1.1
Pistacia lentiscus	root/rhiz	20.6	2.6
Pistacia lentiscus	herb	23.2	3.3
Pistacia lentiscus	leaf	15.0	25.4
Pistacia terebinthus	fruit	11.0	7.4
Pistacia terebinthus	resin	5.9	14.6
Pistacia terebinthus	leaf	35.4	14.9
Pistacia terebinthus	bark	21.0	18.0
Pistacia vera	seed	6.4	1.2
Pistia stratiotes	herb	69.4	1.8
Plantago afra	seeds	21.6	0.0
Plantago coronopus	root/rhiz	25.4	0.0
Plantago coronopus	herb	27.2	0.0
Plantago media	seed	15.7	2.5
Plantago media	root/rhiz	24.6	0.0
Plantago media	leaf	18.3	0.0
Platanus orientalis	leaf	32.0	11.2
Platanus orientalis	fruit	25.2	20.1
Platanus orientalis	bark	49.8	0.0
Polygala venulosa	herb	41.4	1.3
Polygonum aviculare	herb	21.6	17.0
Polypodium vulgare	root/rhiz	47.9	0.0
Polystichum lonchitis	leaf	27.4	8.5
Populus alba	leaf	22.1	0.0
Populus alba	bark	**86.0**	14.9
Populus nigra	leaf	27.9	9.9

Populus nigra	seeds	69.2	16.4
Portulaca oleracea	herb	20.0	0.0
Potamogeton natans	leaf	26.6	13.0
Potentilla reptans	root/rhiz	16.8	0.0
Potentilla reptans	herb	4.6	0.0
Poterium sanguisorba	leaf	43.3	13.4
Prunus armeniaca	fruit	2.5	0.0
Prunus avium	exudate	11.5	9.3
Prunus avium	fruit	5.7	46.4
Prunus domestica	exudate	21.4	0.4
Prunus domestica	fruit	19.9	1.0
Prunus domestica	leaf	11.4	9.0
Prunus dulcis	fruit	12.0	0.0
Prunus dulcis	root/rhiz	1.3	0.0
Prunus dulcis	exudate	24.2	1.3
Prunus dulcis	oil	47.8	5.6
Prunus dulcis	seeds	4.3	6.4
Prunus persica	fruit	21.1	10.2
Pteridium aquilinum	root/rhiz	22.1	0.0
Pteridium aquilinum	leaf	39.6	0.0
Punica granatum	root/rhiz	23.3	0.0
Punica granatum	seed	28.0	4.1
Punica granatum	fruit	22.1	6.4
Punica granatum	flower	16.7	16.0
Pyrus communis	fruit	4.9	12.1
Quercus ilex	leaf	18.9	0.0
Quercus ilex	bark	13.4	6.8
Quercus ilex	seed+fruit	65.2	17.4
Quercus robur	leaf	26.4	0.0
Quercus robur	bark	26.6	0.0
Quercus robur	fruit	16.8	0.8
Quercus robur	seed	67.1	3.2
Raphanus raphanistrum	root/rhiz	16.4	0.0
Raphanus raphanistrum	seed	25.1	5.4
Reseda alba	seed	16.9	6.8
Rhamnus lycioides	herb	37.0	1.3
Rheum rhaponticum	roots	14.2	0.0
Rhodiola rosea	roots	**80.2**	0.0
Rhus coriaria	leaf	16.1	0.0
Rhus coriaria	fruit	27.1	20.4
Ricinus communis	oil	27.4	0.0
Ricinus communis	leaf	48.0	14.2
Ricinus communis	seed	3.0	15.4
Ricinus communis	oil	70.0	0.0
Rosa canina	fruit	17.9	2.5

Rosa gallica	leaf	5.8	0.0
Rosa gallica	flower	27.5	12.1
Rubia peregrina	fruit	25.9	0.0
Rubia peregrina	roots	22.6	0.0
Rubia peregrina	herb	17.3	4.7
Rubus idaeus	flower	20.5	0.0
Rubus idaeus	leaf	34.1	1.0
Rubus idaeus	stalk/shoot	25.1	4.6
Rubus idaeus	fruit	24.0	15.3
Rubus plicatus	fruit	18.0	0.0
Rubus plicatus	stalk/shoot	11.6	0.0
Rubus plicatus	leaf	12.7	0.0
Rumex crispus	root/rhiz	46.7	2.9
Rumex crispus	seed	5.0	7.3
Rumex crispus	leaf	25.6	19.3
Ruscus aculeatus	fruit	18.1	0.0
Ruscus aculeatus	roots	42.3	0.0
Ruscus aculeatus	herb	14.7	0.0
Ruscus hypoglossum	root/rhiz	48.0	1.5
Ruscus hypoglossum	herb	2.1	23.7
Ruscus hypophyllum	leaf	**77.4**	32.9
Ruta chalepensis	herb	27.7	6.1
Ruta chalepensis	seed	39.3	19.9
Ruta graveolens	root/rhiz	27.7	7.2
Salix alba	bark	24.1	1.6
Salix alba	leaf	29.4	6.1
Salvia rosmarinus	herb	55.2	1.4
Salvia officinalis	leaf	16.7	9.3
Salvia viridis	seed	16.0	0.0
Salvia viridis	herb	**84.2**	10.3
Sambucus nigra	fruit	26.7	0.0
Sambucus nigra	leaf	**85.9**	1.4
Sambucus nigra	root/rhiz	8.3	5.8
Saponaria officinalis	root/rhiz	38.2	36.7
Sarcopoterium spinosum	seed	23.8	0.0
Sarcopoterium spinosum	leaf	20.0	0.0
Satureja thymbra	herb	27.1	13.0
Saussurea costus	root/rhiz	**86.3**	0.0
Scandix pecten-veneris	herb	18.4	0.0
Scirpoides holoschoenus	herb	36.1	0.0
Scirpoides holoschoenus	seed	20.3	12.6
Scrophularia peregrina	herb	9.2	0.0
Scrophularia peregrina	seed	23.4	21.7
Securigera securidaca	seed	25.1	0.0
Sedum cepaea	leaf	65.5	0.0

Senecio vulgaris	herb	13.1	0.0
Senegalia senegal	exudate	10.9	0.2
Serapias parviflora	tuber	15.4	13.0
Sesamum indicum	herb	7.7	0.0
Sesamum indicum	seeds	23.3	0.0
Sesamum indicum	oil	10.8	0.0
Seseli tortuosum	seeds	60.7	13.8
Seseli tortuosum	root/rhiz	15.6	18.5
Setaria italica	seeds	16.2	8.4
Silene vulgaris	seeds	34.3	7.8
Silybum marianum	stalk/shoot	25.8	0.0
Silybum marianum	root/rhiz	21.4	1.6
Sinapis alba	seeds	1.3	11.3
Sison amomum	seeds	21.1	0.0
Sisymbrium irio	seed	12.1	0.0
Sium sisarum	root/rhiz	13.1	16.2
Smilax aspera	fruit	43.2	-0.9
Smilax aspera	leaf	22.2	16.0
Smyrnium olusatrum	root/rhiz	26.8	16.0
Smyrnium olusatrum	leaf	43.3	18.0
Smyrnium olusatrum	seeds	20.2	19.4
Smyrnium perfoliatum	leaf	14.1	0.0
Smyrnium perfoliatum	seed	25.1	13.1
Smyrnium perfoliatum	root/rhiz	34.3	13.1
Solanum americanum	leaf	49.7	34.1
Sonchus oleraceus	leaf	21.0	0.0
Sonchus oleraceus	root/rhiz	20.9	0.0
Sorbus domestica	fruit	0	0.0
Sparganium erectum	root/rhiz	47.5	0.1
Sparganium erectum	seed	19.2	7.6
Spartium junceum	flower	6.6	0.0
Spartium junceum	seed	6.6	6.7
Spartium junceum	herb	**96.9**	14.7
Staphisagria macrosperma	seeds	18.0	0.0
Streptopus amplexifolius	root/rhiz	25.3	0.0
Symphytum officinale	root/rhiz	41.4	2.8
Tamarix africana	herb	46.3	18.4
Tamarix species	fruit	34.3	0.0
Tamarix species	bark	37.9	2.1
Tanacetum parthenium	herb	53.7	0.0
Tanacetum parthenium	flowers	14.7	29.9
Taxus baccata	herb	52.4	3.9
Teucrium chamaedrys	herb	38.2	5.5
Teucrium flavum	herb	12.2	0.0
Teucrium polium	herb	19.7	15.8

Teucrium scordium	herb	15.2	15.8
Thalictrum minus	leaf	18.0	0.6
Thapsia garganica	root/rhiz	**85.1**	0.0
Thapsia garganica	herb	**86.8**	15.3
Thymbra capitata	herb	28.4	3.9
Thymus serpyllum	herb	33.4	35.4
Tordylium apulum	root/rhiz	19.1	1.7
Tordylium apulum	seed	24.5	11.5
Tordylium apulum	herb	24.5	45.3
Trapa natans	herb	35.5	3.6
Trapa natans	fruit	16.6	21.7
Tribulus terrestris	fruit	41.0	2.1
Tribulus terrestris	herb	24.6	6.0
Trigonella foenum-graecum	seed	30.2	8.3
Triticum aestivum	seed	27.1	2.4
Triticum dicoccon	seed	5.0	5.5
Tussilago farfara	root/rhiz	24.0	0.0
Tussilago farfara	leaf	44.1	11.3
Typha angustifolia	seed	20.7	0.0
Ulmus minor	root/rhiz	16.2	0.0
Ulmus minor	bark	4.3	0.0
Ulmus minor	leaf	28.8	0.0
Umbilicus rupestris	leaf	19.6	0.0
Urtica dioica	seed	35.1	0.0
Urtica dioica	herb	72.7	25.2
Valeriana celtica	root/rhiz+stalk/shoot	47.2	9.4
Valeriana jatamansi	root/rhiz	55.5	0.0
Valeriana officinalis	root/rhiz	59.8	3.5
Veratrum album	root/rhiz	36.3	8.6
Verbascum thapsus	leaf	11.8	0.0
Verbascum thapsus	root/rhiz	20.4	12.7
Verbena officinalis	root/rhiz	21.0	6.3
Verbena officinalis	leaf+herb	22.1	6.7
Vicia cracca	seed	22.8	0.6
Vicia ervilia	seed	23.5	0.0
Vicia faba	seed	6.9	12.9
Vinca minor	herb	13.2	0.0
Vincetoxicum hirundinaria	leaf	**75.6**	16.4
Vincetoxicum hirundinaria	root/rhiz	31.3	16.8
Viola odorata	leaf	29.1	16.4
Vitex agnus-castus	seeds	**80.7**	0.0
Vitex agnus-castus	leaf	0.6	4.7
Vitis vinifera	seed	16.1	0.0
Vitis vinifera	leaf	**83.6**	0.5
Vitis vinifera	fruit	20.2	4.3

Withania somnifera	root/rhiz	33.9	10.0
Withania somnifera	seeds+fruit	28.1	14.6
Xanthium strumarium	fruit	68.4	13.3
Zingiber officinale	root/rhiz	13.3	6.9
Zingiber officinale	leaf	14.0	11.7
Ziziphus jujuba	leaf	27.6	1.9
Ziziphus jujuba	root/rhiz	49.5	7.4
Ziziphus jujuba	fruit	34.4	14.6

Supplementary Table 5. Contingency table from Chi-Square analysis of *DMM* plant extracts screened for cytotoxicity.

	Clyster	**External application**	**Fumigation**	**Internal application**	***Row Totals***
Cytotoxic drugs	20 (16.77) [0.62]	**180** (164.49) [1.46]	13 (5.62) [9.71]	157 (183.13) [3.73]	370
Non-cytotoxic drugs	186 (189.23) [0.06]	1841 (1856.51) [0.13]	56 (63.38) [0.86]	**2093** (2066.87) [0.33]	4176
Column Totals	206	2021	69	2250	**4546 (Grand Total)**

Cytotoxic drugs: cell mortality higher than 75%, n=54; Non-cytotoxic drugs: cell mortality lower than 75%, n=606.

The contingency table provides the following information: the observed cell totals, (the expected cell totals) and [the chi-square statistic for each cell]. The chi-square statistic is 16.8983. The *p*-value is .000742. The result is significant at $p < .01$.